NASA/TM—1999–209573

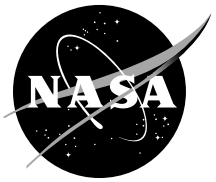

International Space Station ECLSS Technical Task Agreement Summary Report

Compiled by
C.D. Ray
Marshall Space Flight Center, Marshall Space Flight Center, Alabama

B.H. Salyer
ION Corporation, Huntsville, Alabama

August 1999

The NASA STI Program Office…in Profile

Since its founding, NASA has been dedicated to the advancement of aeronautics and space science. The NASA Scientific and Technical Information (STI) Program Office plays a key part in helping NASA maintain this important role.

The NASA STI Program Office is operated by Langley Research Center, the lead center for NASA's scientific and technical information. The NASA STI Program Office provides access to the NASA STI Database, the largest collection of aeronautical and space science STI in the world. The Program Office is also NASA's institutional mechanism for disseminating the results of its research and development activities. These results are published by NASA in the NASA STI Report Series, which includes the following report types:

- TECHNICAL PUBLICATION. Reports of completed research or a major significant phase of research that present the results of NASA programs and include extensive data or theoretical analysis. Includes compilations of significant scientific and technical data and information deemed to be of continuing reference value. NASA's counterpart of peer-reviewed formal professional papers but has less stringent limitations on manuscript length and extent of graphic presentations.

- TECHNICAL MEMORANDUM. Scientific and technical findings that are preliminary or of specialized interest, e.g., quick release reports, working papers, and bibliographies that contain minimal annotation. Does not contain extensive analysis.

- CONTRACTOR REPORT. Scientific and technical findings by NASA-sponsored contractors and grantees.

- CONFERENCE PUBLICATION. Collected papers from scientific and technical conferences, symposia, seminars, or other meetings sponsored or cosponsored by NASA.

- SPECIAL PUBLICATION. Scientific, technical, or historical information from NASA programs, projects, and mission, often concerned with subjects having substantial public interest.

- TECHNICAL TRANSLATION. English-language translations of foreign scientific and technical material pertinent to NASA's mission.

Specialized services that complement the STI Program Office's diverse offerings include creating custom thesauri, building customized databases, organizing and publishing research results…even providing videos.

For more information about the NASA STI Program Office, see the following:

- Access the NASA STI Program Home Page at ***http://www.sti.nasa.gov***

- E-mail your question via the Internet to help@sti.nasa.gov

- Fax your question to the NASA Access Help Desk at (301) 621–0134

- Telephone the NASA Access Help Desk at (301) 621–0390

- Write to:
  NASA Access Help Desk
  NASA Center for AeroSpace Information
  800 Elkridge Landing Road
  Linthicum Heights, MD 21090–2934

NASA/TM—1999–209573

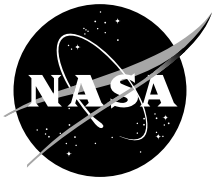

International Space Station ECLSS Technical Task Agreement Summary Report

Compiled by
C.D. Ray
Marshall Space Flight Center, Marshall Space Flight Center, Alabama

B.H. Salyer
ION Corporation, Huntsville, Alabama

National Aeronautics and
Space Administration

Marshall Space Flight Center • MSFC, Alabama 35812

August 1999

Acknowledgments

The authors would like to acknowledge the assistance of those individuals who aided in the preparation of this document. William James was instrumental in obtaining source data, J.D. DeMarcos edited and critiqued the text, Doris Bailey typed the manuscripts, the staffs of the NASA Headquarters Library and the Scientific and Technical Information Program provided assistance in locating bibliographic references, and the NASA Headquarters Printing and Graphics office developed the layout and handled printing.

Available from:

NASA Center for AeroSpace Information
800 Elkridge Landing Road
Linthicum Heights, MD 21090–2934
(301) 621–0390

National Technical Information Service
5285 Port Royal Road
Springfield, VA 22161
(703) 487–4650

TABLE OF CONTENTS

TABLE OF CONTENTS (Continued)

LIST OF FIGURES

LIST OF FIGURES (Continued)

LIST OF FIGURES (Continued)

LIST OF FIGURES (Continued)

LIST OF TABLES

LIST OF TABLES (Continued)

LIST OF TABLES (Continued)

LIST OF ACRONYMS

Δ	delta, change
4BMS	four-bed molecular sieve
ac	alternating current
AG	application generator
AMS	acoustic measurement system
AR	air revitalization
ARS	atmosphere revitalization subsystem
C_2	carbon
C&DH	command and data handling subsystem
CDR	critical design review
CDRA	carbon dioxide removal assembly
CE	conducted emissions
CFU	colony-forming unit
CH_4	methane
CHeCS	crew health care system
CHX	condensing heat exchanger
CMI	control monitor instrumentation
CMS	core module simulator
CO	carbon monoxide
CO_2	carbon dioxide
CPU	central processing unit
CRES	corrosion-resistant steel
CS	conducted susceptibility
CSC	Computer Sciences Corporation
DAS	Data Acquisition System
dc	direct current
DI	deionized
D/N	day/night
DOE/RD	design of experiments/robust design
DVB	divinylbenzene
ECLS	Environmental Control and Life Support

LIST OF ACRONYMS (Continued)

ECLSS	Environmental Control and Life Support System
EDO	extended duration orbiter
EEF	end-use equipment facility
EET	expendables evaluation test
EG&G	EG&G Rotron Custom Design Company
EMI	electromagnetic interference
EPA	Environmental Protection Agency
FC	fictive component
FCA	fictive component analysis
FID	flame ionization detector
FORTAN	formula translator
FTIR	Fourier transform infrared
GAC	granular activated carbon
GC	gas chromatograph
G/LS	gas/liquid separator
GN_2	gaseous nitrogen
GUI	graphical user interface
H_2	hydrogen
H_2O	water
H_2SO_4	sulfuric acid
HP	Hewlette Packard
HS	Hamilton Standard (Space Systems Company Inc.)
HTCO	high-temperature catalytic oxidizer
HWQM	hygiene water quality monitor
HX	heatexchanger
I_2	Iodine
IART	integrated air revitalization test
IAST	ideal adsorbed solution theory
ICD	interface control document
ICES	Intersociety Conference on Environmental Systems
ION	ION Corporation
IMV	intermodule ventilation
IR	infrared

LIST OF ACRONYMS (Continued)

IR–45	sorbent material
IR&D	internal research and development
ISS	*International Space Station*
IWP	interim water processor
JSC	Johnson Space Center
K1	conductivity sensor (VCD)
LABVIEW	computer program
LCT	life cycle test
LED	light-emitting diode
LiOH	lithium hydroxide
LSI	Life Systems, Inc.
LSTC	Life Sciences Technology Center, Boeing
Lucas	Lucas Aerospace
MAC	maximum allowable concentration
MCA	major constituent analyzer
MCV	microbial check valve
M/DM	multiplexer/demultiplexer
MFB	multifiltration bed
MGC	microbial growth chamber
MINS2	MSFC Information Network System
MLS	mostly liquid separator
mohm	microhms
mmHg	millimeters of Mercury
MS	mass spectrometer
MSFC	Marshall Space Flight Center
MUX	multiplexer
N_2	nitrogen
NH_3	ammonia
NO_2	nitrogen dioxide
NASA	National Aeronautics and Space Administration
NC40	noise criteria (level)
O_2	oxygen
OD	outer diametere

LIST OF ACRONYMS (Continued)

OGA	oxygen generation assembly
OSC	Orbital Science Corporation
P	Pressure
PDMR2P	two-phase pore diffusion model with reaction
PDMR3P	three-phase pore diffusion model with reaction
PACRATS	payload and components remote automated test system
PC	personal computer
PCA	pressure control assembly
PCI	Precision Combustion, Inc.
PCWQM	process control water quality monitor
PDC	power distribution and control
PDU	performance display unit
PET	performance enhancement test
PFA	portable fan assembly
PFU	plaque-forming unit
PLV	postlanding ventilation
POST	preoperational systems test
$ppCO_2$	carbon dioxide partial pressure
ppmv	parts per million by volume
pp	partial pressure
PRR	preliminary requirements review
PVC	poly-vinylchloride
QA	quality assurance
QC	quality control
QFD	quality function deployment
R2A	microbial growth media
RFP	request for proposal
Rid	review item discrepancies
rms	root mean square
rpm	revolution per minute
RTD	resistance temperature device
SAC	strong acid cation
SAE	Society of Automotive Engineers

LIST OF ACRONYMS (Continued)

SBA	strong base anion
SCMT	sodium-n-coconut acid-n-methyl taurate
SDS	sample distribution system
SFE	static feed electrolyzer
SMAC	spacecraft maximum allowable concentration
SO_3	sulfur trioxide
SPDFR	surface to pore diffusion flux ratio
SPE	solid polymer electrolysis
SRS	Sabatier reactor subsystem
SS	stainless steel
SS*F*	Space Station *Freedom*
SSP	Space Station Program (document)
SVSK	Hamilton Standard drawing number prefix
T	temperature
TC	thermocouple
TCB	trichlorobenzene
TCCA	trace contaminant control assembly (Russian)
TCCS	trace contaminant control subassembly
TCD	thermal conductivity detector
TCE	trichloroethylene
TCIT	trace contaminant injection test
TCL	thermal control and contamination control loop
THC	temperature and humidity control
TIMES	thermoelectric integrated membrane evaporation system
TOC	total organic carbon
TPCT	TCCS performance confirmation test
TTA	technical task agreement
UCS	urine collection system
μmhos	micromhos (inverse conductivity)
UP	urine processor
UPA	urine processor assembly
UPN	unique program numbers
UPPA	urine pretreatment prefilter assembly

LIST OF ACRONYMS (Continued)

UPS	urine pretreat injection
U.S. Hab	U.S. Habitat (module)
USOS	United States on-orbit segment (ISS)
Vac	volts alternating current
VCD	vapor compression distillation
UPAVCD-VA	VCD unit VA (life test)
VCD-IV	VCD unit IV (comparative test)
VCDS	vapor compression distillation system
Vdc	volts direct current
VRA	volatile removal assembly
WA–25	sorbent material
WAC	weak acid cation
WBA	weak base anion
WDS	water degradation study
WM	waste management
WP	water processor
WRM	water recovery management
WRT	water recovery test
WWORU	wastewater orbital replacement unit

TECHNICAL MEMORANDUM

INTERNATIONAL SPACE STATION ECLSS TECHNICAL TASK AGREEMENT SUMMARY REPORT

1. INTRODUCTION

This document provides a summary of current work accomplished under Technical Task Agreement (TTA) by the National Aeronautics and Space Administration (NASA) Marshall Space Flight Center (MSFC) regarding the *International Space Station* (*ISS*) Environmental Control and Life Support System (ECLSS). Current activities include ECLSS component design and development, computer model development, subsystem/integrated system testing, life testing, and general test support provided to the *ISS* program.

MSFC was assigned responsibility for Space Station ECLSS design and development in 1984. Activities completed during Space Station phases B and C/D included ECLSS design, analysis, and in-house testing. Under ECLSS design, MSFC was responsible for the six major ECLSS functions, specifications and standards, component design and development, and was the architectural control agent for the Space Station ECLSS. MSFC was responsible for ECLSS analytical model development and conducted subsystem and system level analyses. In-house subsystem and system level testing was conducted in support of the design process. This included testing of air revitalization (AR), water (H_2O) reclamation and management hardware, and certain nonregenerative systems.

All the activities described in this report were approved in task agreements between the MSFC and NASA Headquarters Space Station Program Management Office located at Johnson Space Center (JSC) and their prime contractor for the *ISS*, Boeing. These MSFC activities are in-line to the designing, development, testing, and flight of ECLSS equipment planned by the Boeing Company, Huntsville, Alabama, supporting Ion Corporation (ION), Huntsville Division, Boeing, Houston, Texas. MSFC's unique capabilities for performing integrated systems testing and analyses and its ability to perform some tasks cheaper and faster to support *ISS* program needs are the basis for the TTA activities.

Tasks were completed in the H_2O recovery and AR systems areas, and were divided into analytical model development, component design and development, subsystem and integrated systems testing, life testing, and general test support. The results of each of these tasks are described in this Technical Memorandum (TM). More detailed reports are referenced and are available on request from ION, or MSFC's Environmental Control and Life Support System (ECLSS) Group (FD21). A summary of earlier work accomplished under TTA's has been documented in reference 1.

2. TASK AGREEMENTS

MSFC initiated supporting development task agreements with the NASA Headquarters Space Station Program Office in fiscal year 1994 (FY 1994) and they cover projected activities through FY 2000. In addition, some FY 1993 ECLSS-funded tasks were also approved by the Program Office in 1993. Results of the FY 1996, FY 1997, and FY 1998 activities are summarized in this ECLSS report. Although MSFC has many tasks with the Program Office, only the ECLSS activities are summarized in this TM.

The current ECLSS activities are managed under two Program Office task agreement unique program numbers (UPN's), 478–31–34 and 478–31–41. Those agreements provide a task summary description, cost by fiscal year, and civil service manpower to accomplish the work.

3. ORGANIZATION

Organizations which support TTA activities and the interfaces are shown in figure 1. The ECLS Branch (ED62) of the Structures and Dynamics Laboratory within the Science and Engineering (S&E) directorate of MSFC managed the overall ECLSS TTA work. Within the ECLS Branch, engineers were assigned responsibilities to develop test requirements, perform analyses of test results, support actual testing, and manage special tasks performed under the ECLSS test services contract. The Development and Environmental Test Branch of the Systems Analysis and Integration Laboratory in S&E provided the test facilities and performed the ECLSS testing at MSFC. Test subjects from various organizations exercised in the end-use equipment facility (EEF) to generate metabolic waste products for H_2O reclamation testing. The test services contractor, ION, provided test support, analytical modeling of the integrated test configurations, test support and studies from the ECLSS subcontractors, and analytical model development. Various analytical laboratories support MSFC testing in the chemical and microbial analysis of air and H_2O samples. Overall results of the chemical/microbial laboratory analyses and the sensor data are maintained in a database developed by MSFC and utilized by all Space Station participants. Products provided to the *ISS* program include computer models, reports, and test reports/findings.

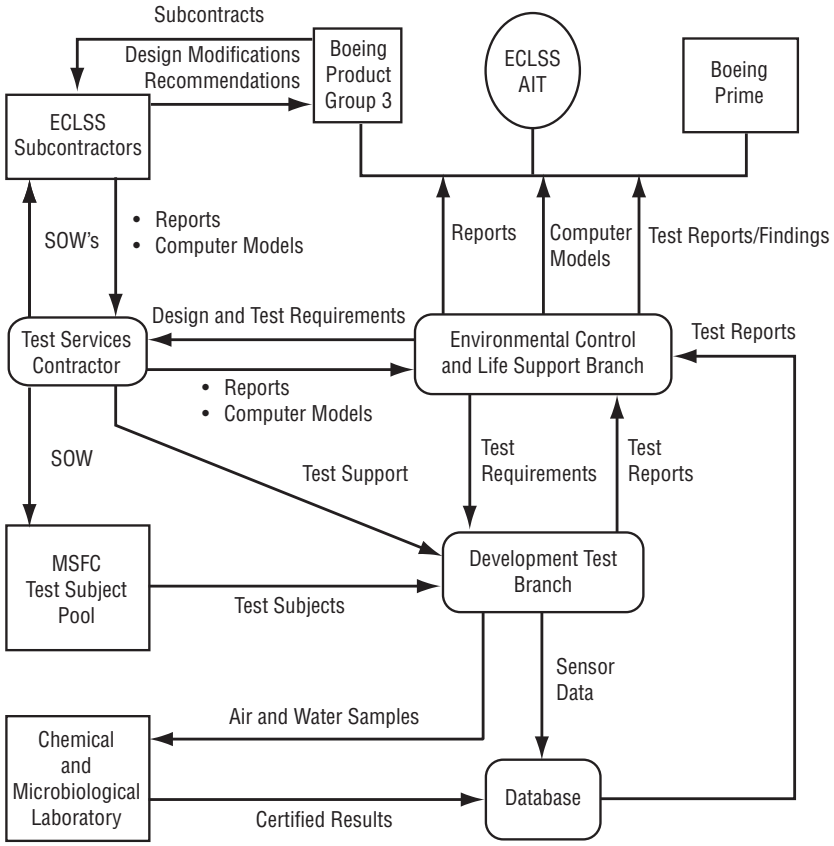

Figure 1. ECLSS TTA organizational interface.

4. COMPONENT DESIGN AND DEVELOPMENT

Component design and development activities include addressing design issues related to components in the *ISS* water processor (WP) and urine pretreatment, development of a portable fan assembly (PFA), delivery of flight-like condensing heat exchangers (CHX's), and refurbishment of a Sabatier carbon dioxide (CO_2) reduction system. Development work was done on the WP mostly liquid separator (MLS), process pump, gas/liquid separator (G/LS), and prefilter. No further development work will be done on the WP components under supporting development. Any subsequent work will be implemented and managed under the ECLSS Government-furnished equipment program. Urine pretreatment development responsibility has been transferred to JSC.

4.1 Mostly Liquid Separator[2]

The *ISS* will utilize a WP to provide potable H_2O from an input waste stream, partly consisting of reclaimed urine distillate; free gas; and used shower, handwash, and oral hygiene H_2O. The successful operation of the WP, particularly in a microgravity environment, requires that any free gas be separated from the liquid prior to processing. This requirement dictates the use of a G/LS. However, the presence of soaps in the input wastewater stream presents a unique challenge to the use of conventional pitot G/LS's, in that they are prone to foaming during operation, yielding unacceptable performance.

The MLS is an integral component in the wastewater orbital replacement unit (WWORU) of the WP. The WWORU schematic is shown in figure 2. This ORU is responsible for receiving, degassing, and storage of the Space Station wastewater. It also provides the system flow and pressure. The MLS is responsible for removing the free gas from wastewater and must be capable of handling up to a 960-lb/hr inlet flow rate.

A cross section of the first-generation design concept can be seen in figure 3. Prototype MLS units built and tested in the previous development program contained all of the features of the depicted flight unit except for a flight-style motor, which was replaced with a variable-speed, external direct-drive motor.

In operation, a constant-speed motor spins a hollow center shaft mounted on journal bearings. A series of disks is attached to the shaft extending radially outward to a diameter that is ≈0.25 in. from the inside diameter of a cylindrical housing. Each disk has a series of slotted holes extending through the disk near its center. The shaft has slots cut into its OD so that the space between some of the disks near the center of the stack is vented to the center of the shaft. The end of the shaft is open to a level control valve arrangement that connects to the gas vent. In operation, a mixture of H_2O and air enters the unit tangentially at a point near the motor end of the housing. This mixture is forced to spin around the housing with the H_2O moving to the outside and the air bubbles moving toward the centerline. The partially separated mixture then enters the disk portion of the housing where centrifugal action of the spinning disks forces the H_2O to the housing wall, forming an H_2O ring that is maintained in motion by contact with the outer edge of the spinning disks. The air moves to the centerline and flows through holes in the disks toward the slots that connect to the center of the shaft. As the control valve opens, gas is vented from the separator. The H_2O moves along the outer wall of the housing and exits tangentially, allowing recovery of some pressure head. The H_2O level in the H_2O ring is maintained by the action of the control valve.

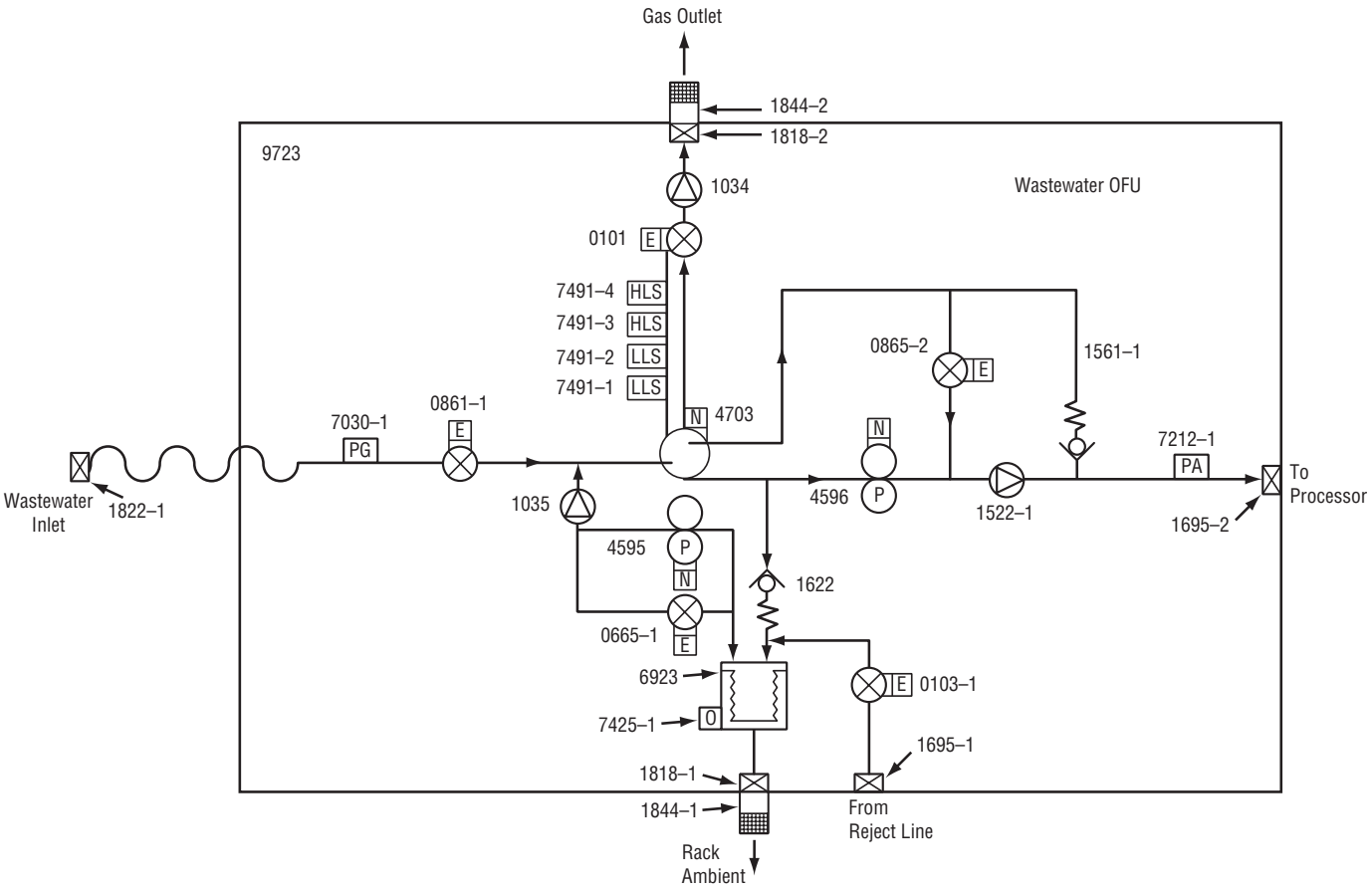

Figure 2. Water processor WW ORU.

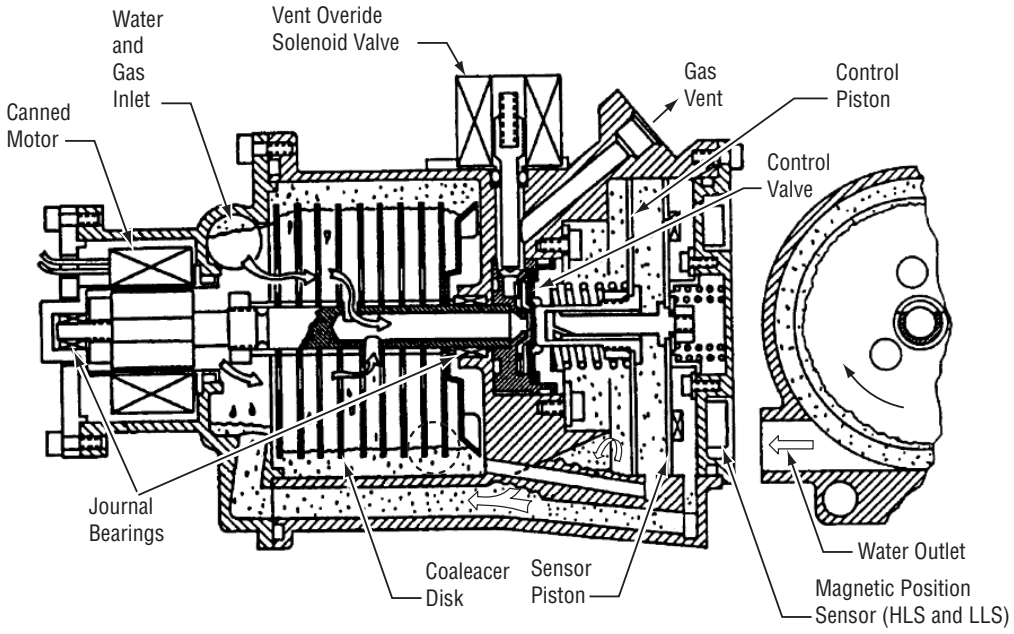

Figure 3. First-generation MLS design cross section.

An override mechanism is provided to enable the MLS to function in conditions where a suitable air/H_2O boundary has not been established; i.e., during startup, in a level control malfunction, or when input with either 100-percent air or H_2O for extended periods of time. The mechanism consists of a solenoid valve that overrides the vent function. A sensor piston, parallel to the control piston and sensing the same pressure differential, is magnetically coupled to two magnetic switches that signal when appropriate override actions need to occur. One switch closes the solenoid, and hence the air vent pathway, when H_2O is about to flood into the gas vent. The second override switch turns off the process pump and opens a recycle valve to recirculate H_2O back into the MLS in cases where insufficient H_2O exists within the MLS. This mode is also used during system startup.

A test program was designed to establish an operating speed for the motor (1,900 rpm), assess the operational performance of the MLS, and conduct an extended performance test to help assess if and how microbial growth would affect performance. The majority of testing was conducted using plastic MLS, allowing visual observation of its internal operation. Performance was measured using three H_2O conditions: deionized (DI) H_2O, fresh soap and DI H_2O, and collected shower H_2O.

Several observations were made during the course of testing, many of which affected subsequent MLS design. The major ones can be summarized as follows:

- Leakage of H_2O into the gas vent passageway caused H_2O carryover. Leakage was occurring past the journal bearing into the end of the hollow shaft (through which the gas vents), showing up as H_2O carryover.
- Several changes were made relative to sizing. Disk air holes were enlarged, and different front disks (closest to the inlet) were used to remove restrictions to air and H_2O flow, respectively.
- Agitation of the air/H_2O mixture needed to be reduced. Paddles that were part of the last disk (furthest from the inlet) needed to be removed. They were intended to help compensate for the additional drag the end of the internal chamber imparts to the rotating H_2O; instead, these paddles were found to be pumping air into the H_2O, elevating air carryover percentages. In addition, the inlet chamber, designed to preswirl the inlet stream, was found to cause elevated air carryover percentages at certain flow ranges.
- Instability was frequently noted during testing when using H_2O containing soap. This unstable operation was characterized by gas venting occurring in discrete intervals and by rotational speed variation under load. It was concluded that by using a constant-speed motor under steady-state conditions, gas venting would occur in a continuous manner, and not oscillate, as was being witnessed.

The first MLS development program had the following conclusions:

- The MLS performance met the *ISS* design requirements.
- Higher input flow rates required a higher rpm to prevent H_2O carryover into the gas vent line.
- The percentage of air carried over into the H_2O outlet line increased with increasing rpm and inlet flow.
- Backpressure instability will adversely affect air carryover performance.

The previous development program refined the design of the MLS but also indicated that additional development was required. The next program began in November 1995 to create and substantiate an improved MLS design and to further reduce technical risk.

A cross section of this second-generation design is shown in figure 4. Its design addresses the observations made during the previous development program.

This MLS operated in the same manner as in the previous design. Major design improvements included the placement of the control valves deep within the expanded-diameter shaft, which located the valve seat in the driest possible location.

Sizing issues were also addressed. Additional disk air holes were provided to reduce any restrictions in air flow. A new inlet chamber was provided to reduce agitation, and the overall length of the chamber was increased to provide additional residence time. The diameter of the outlet H_2O pipe was increased to minimize H_2O flow restrictions.

Instability issues were addressed in two significant ways. First, a test rig was designed that placed the inlet fluid reservoir, outlet fluid reservoir, and MLS each at different relative heights from each other, thereby utilizing gravity to set and provide constant inlet and outlet pressures. Second, a constant-speed motor was incorporated.

The override control was redesigned to utilize the same sensor piston as the preceding design but now used mechanical linkages to transmit piston position to the outside of the MLS. There, two mechanical microswitches were provided to signal when appropriate overrides were necessary.

The objective of this final program accomplished under MSFC TTA's was to utilize the knowledge gained from the prior MLS development programs to develop the next-generation MLS, improve upon its performance, and further investigate its capabilities. The development program was divided into a design/fabrication phase and a test phase.

Both test plan and test rig were devised to further develop the MLS technology, characterize its performance, and define its operating requirements. All testing was performed in the Hamilton Standard (HS) Advanced Engineering Laboratory.

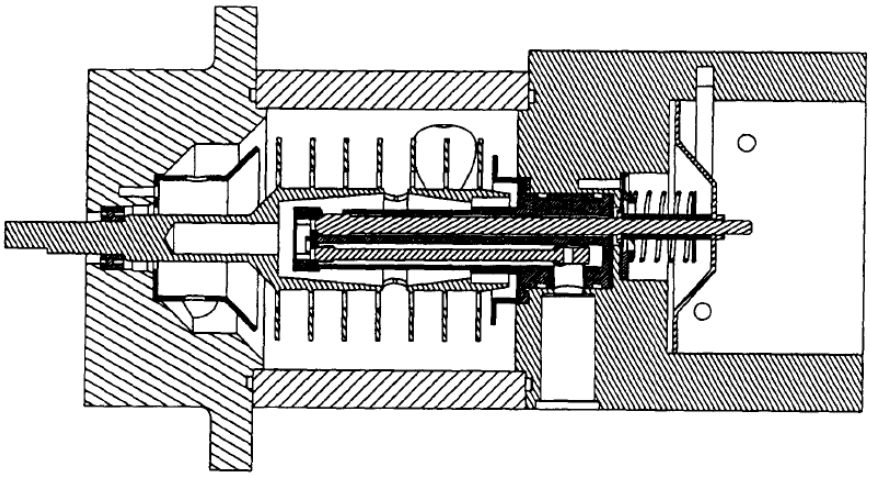

Figure 4. Second-generation MLS design cross section.

There were four testing phases:

1. Benchmarking the benefits provided by the new constant-speed motor and constant backpressure features of the test rig using the MLS unit from the previous development program.

2. Check out the new MLS unit.

3. Performance testing of the newly designed MLS. This testing progressed through three subphases of testing, each subphase assessing performance in different types of H_2O (DI, a mixture of soap and H_2O, and collected shower H_2O).

4. An extended performance test using collected shower H_2O to assess any sensitivity to biofilm formation.

In the earlier MLS development program, one of the final observations was that the MLS (at that time) primarily vented gas at discrete times rather than continuously. When this occurred, the depth of the H_2O ring within the MLS would increase in response to the venting gas. As the H_2O depth increased, so did the load applied to the motor, thereby reducing speed, and thus affecting the H_2O ring depth. It was concluded that the interaction of each of these responses resulted in the relative instability seen at times in the operation of the MLS unit, and that this instability affected the carryover performance. Consequently, it was concluded that the motor speed fluctuations and backpressure instability adversely affect air carryover performance.

The air carryover performance of the previous MLS was mapped using a distilled H_2O and air mixture. The MLS was tested in a horizontal orientation. Figure 5 shows the effects of constant backpressure on performance, and figure 6 shows the effect of using a constant-speed motor. As can be seen, air carryover performance of the previous MLS unit was significantly improved when tested using a constant-speed motor and when tested in an environment providing constant backpressure.

The new MLS unit was manufactured out of clear polycarbonate plastic to facilitate observation during testing. After assembly, the unit was installed on the test rig and checked out for proper operation. Initial performance testing was then conducted using distilled H_2O and air, with the MLS oriented horizontally.

The first tests conducted were meant to establish an operating speed for the motor. From past experience, it was known that there existed a minimum rpm for the MLS to operate at for a given inlet flow rate and air inlet percentage; going below this number would result in H_2O being carried over into the air outlet line. Before these tests were completed, however, some problems were experienced. Although relatively minor, they bear mentioning because of their effects later in the development program.

One operational difficulty experienced at the time was attributed to a failure to provide a mechanical limit to the length of control piston travel. The unrestricted travel caused the control valve stem to enlarge the hole in the flexible seal through which it passes, enabling H_2O from within the control housing to pass into the gas vent line. Modifications were made to prevent this from happening

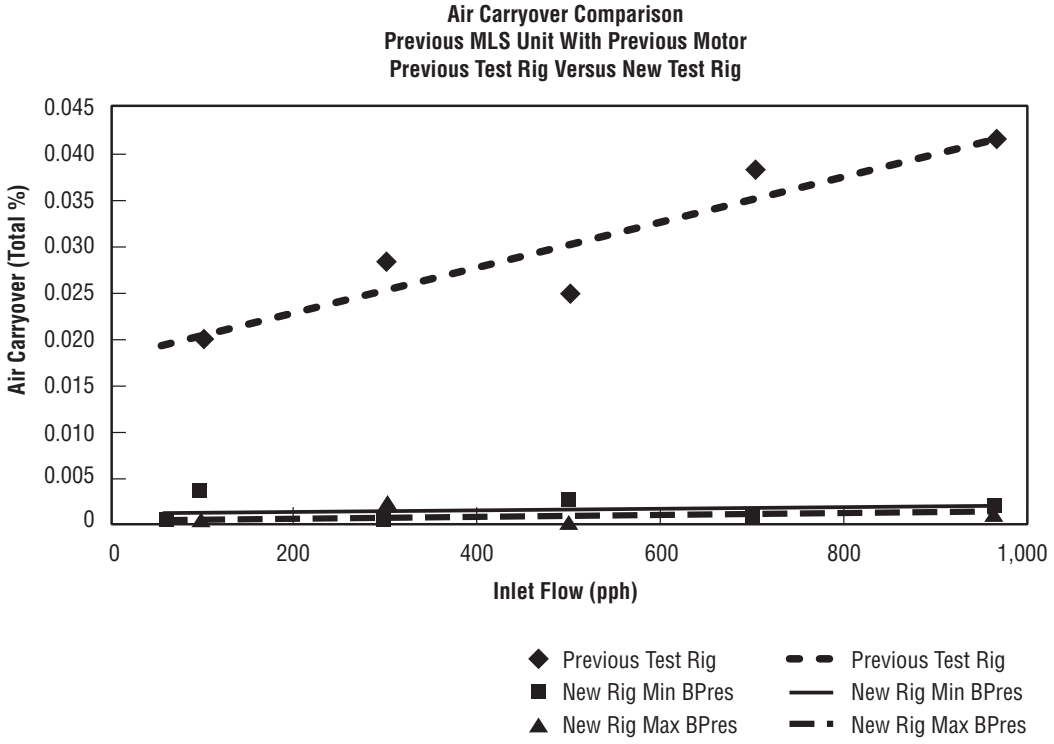

Figure 5. Constant backpressure performance improvement.

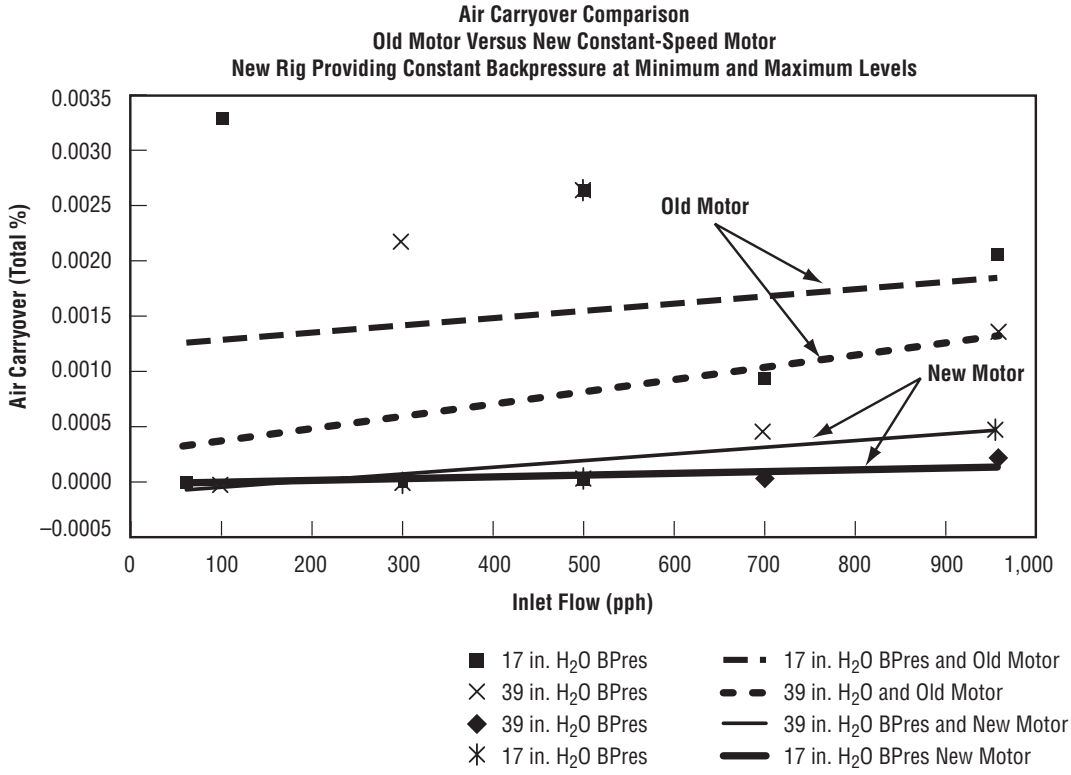

Figure 6. Constant-speed motor performance improvement.

again. The seal was reused as it seemed to still be performing its intended function. A second operational difficulty was found in the alignment of the control and override valves to their respective valve seats. The valve seat consisted of a flat disc of Viton® elastomer in which two properly located holes were placed. Incorrect alignment of components in this area was preventing the control valve from performing its proper function. Careful reassembly seemed to solve this problem.

Having benchmarked the performance of the MLS in clean H_2O, testing began using a mixture of DI H_2O and Igepon® soap. From past experience, it was known that this fluid provided the biggest challenge to the MLS due to the potential formation of foam within the unit.

Initial testing revealed poor performance that was due to leakage of air past the control valve seat. Since this problem had already been seen earlier in the program, the control and override valve seats were redesigned and new hardware was retrofit onto the MLS. Although performance was then improved, there was a tendency for the MLS to generate foam within it, adversely affecting performance. Because the success of the MLS to date was largely due to its ability to not produce excessive foam, this new observation was significant. Continued observation and testing of this condition revealed that recirculation of the air/H_2O mixture was occurring between each disk, and that the air flow holes in the first disk (nearest the inlet) were generating foam.

The revised design of the MLS was concluded to be the cause of these conditions. In contrast to the previous MLS design, the new design extended the length of the interior chamber but did not change the number of disks used, thus increasing the space between disks. When tested using a soap and H_2O mixture, it was noted that air and H_2O adjacent to a disk would not only travel radially outward as expected but would travel radially inward at the midpoint between disks, as shown in figure 7. This local recirculation flow carried foam and air bubbles from the air/H_2O interface deep into the H_2O ring and elevated air carryover percentages. Rather than change the disk spacing back to what it had been in the previous program, it was decided to instead correct the condition using the existing disk spacing, as it was believed that the recirculation flow was occurring in the previous MLS design.

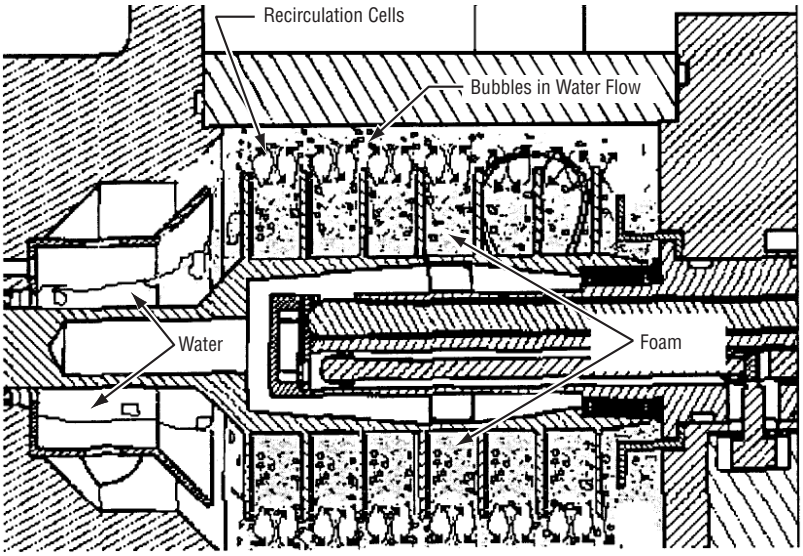

Figure 7. Recirculation within the MLS.

Additionally, some of the observed H_2O carryover (actually foam carryover) resulted from the air holes in the first disk shearing through H_2O, producing an unwanted source of agitation. Because of its location in the front of the MLS, the rotation of the H_2O ring is not fully established at the first disk.

A final design change corrected these problems by first adding edge rings to the ends of the disks, which virtually eliminated any recirculation. The small spacing between each disk is sufficient to allow air bubbles to rise to the center of the chamber and separated liquid to flow to the H_2O ring. Second, the air holes on the first and last disks were covered (all covered on the first disk, half on the last disk), allowing the air/H_2O mixture to flow without agitation to the edge of the disk, where sufficient centrifugal force exists to achieve phase separation. These changes represent, in effect, the third-generation MLS design, and can be seen in figure 8.

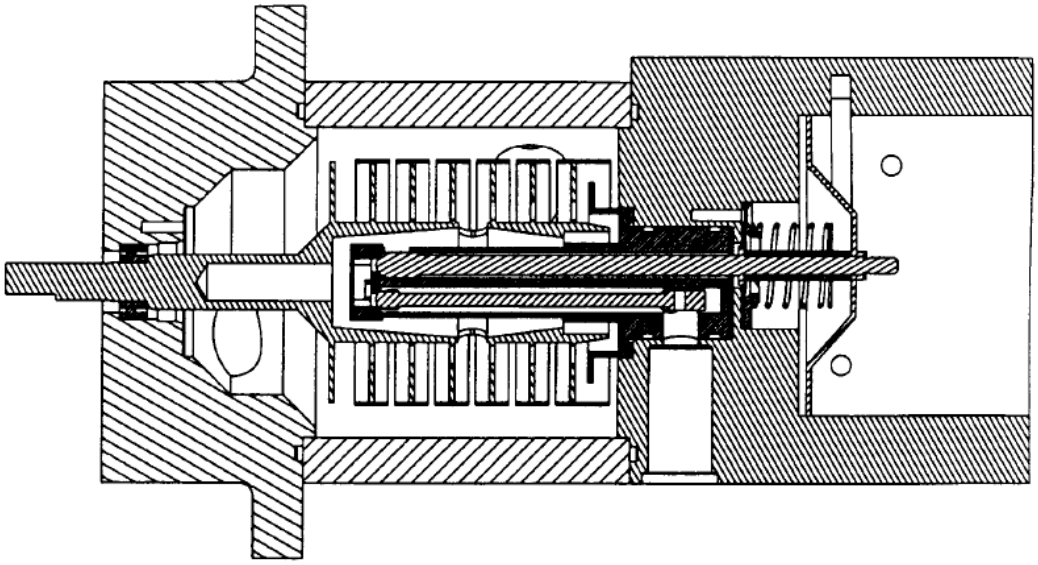

Figure 8. Third-generation MLS design cross section.

Initial testing with the third-generation MLS indicated that H_2O was entering the gas vent valve (H_2O carryover), suggesting that the control stem seal was again leaking as it had been earlier in the program. A new replacement seal corrected this problem. It was recognized that a flight design for the MLS would have to address the robustness of this seal.

With the newly incorporated design changes in place, a new motor operating speed of 1,600 rpm was established (lower than the 1,725 rpm that had originally been set for this MLS). The chosen speed, however, was based more on establishing the proper H_2O ring depth on the disks than it was on selecting the lowest speed possible.

Air carryover performance was measured for the third-generation MLS using a 1,600-rpm operating speed. The MLS was oriented horizontally, vertically with the inlet up, and vertically with the motor down. These different orientations were intended to verify that performance is insensitive to gravity. The inlet-down position, however, placed the motor beneath a leaking shaft seal (a feature that

would not be present in a flight design, as it would use a canned motor) and a leaking H_2O inlet connection. Despite efforts to prevent it, some of the leaking H_2O entered the motor, eventually causing it to fail.

After motor replacement, only the inlet-up orientation was subsequently used. The previous MLS program only used the inlet-down orientation during soap and H_2O testing; therefore, comparisons of performance in the vertical orientation should be judged accordingly.

Based on previous program results, there was evidence that aging of the soap and H_2O solution would in fact help performance. This was attributable to the soap having sufficient time to react with the dirty system H_2O. Once reacted, the soap would no longer be as prone to foaming. The same phenomenon was evident in this program as well, and so test procedures were modified early on to replenish a portion of the test rig soap and H_2O mixture during each day.

The final phase of performance testing was conducted using collected shower H_2O, using a soap mixture and soap/H_2O concentration as described in the previous section. Air carryover performance was again measured using a 1,600-rpm operating speed, and the MLS was tested while oriented horizontally and vertically (inlet up) at both extremes of expected backpressure. As was done during the soap and H_2O test phase, a portion of the test rig H_2O was typically replenished each day of testing.

The next phase of testing was the extended performance test. The objective was to assess how the MLS performed when operated over an extended period using shower H_2O. This test would begin to assess the robustness of the MLS design, and assess how the expected formation of biofilm within the MLS would affect its performance.

The MLS was operated while oriented horizontally and with maximum backpressure. The test was run with an inlet flow rate of 100 pphr, as this is expected to be the flow rate that the MLS will primarily experience in its intended application. The test ran for 135 days and accumulated 1,012 hr of operating time (≈10.5 hr/workday duty time). To ensure that biofilm would have a chance to develop, ≈50 percent of the rig H_2O was replenished weekly at the suggestion of the HS microbiologist. Assays were taken weekly of both the test rig H_2O and replenishment H_2O to guarantee and document that the test was conducted with biologically active H_2O.

The performance of the MLS was remapped after the extended performance test to determine if its performance had deteriorated over time. The tests were conducted using shower H_2O and followed the same procedure as originally used to map performance.

The H_2O carryover performance was assessed, and a near-constant H_2O carryover threshold motor speed of 1,050 rpm was established. The constant rpm indicated that H_2O carryover was unaffected by the extended duration performance test.

After conducting the extended performance test, it was not possible to achieve the maximum inlet flow rate (960 pphr) at maximum backpressure. Maximum achievable flow rate at maximum backpressure was ≈800 pphr when the MLS was oriented horizontally, and ≈740 pphr when oriented vertically (inlet up). This inability to achieve 960-pphr flow was attributed to a change in the test rig, specifically to increased pressure losses in the inlet and exit plumbing connected to the MLS.

Final observations concerning the MLS design and performance are the following:

• The use of constant backpressure and a constant-speed motor improved the performance of the MLS.

• Recirculation flow was occurring between disks and elevating air carryover percentages. The addition of edge rings to the disks virtually eliminates this condition.

• The inclusion of air-flow holes in the disks at either end of the MLS was agitating the air/H_2O mixture, causing foam to be generated within (in the presence of a soap and H_2O mixture) and resulting in H_2O carryover into the gas vent line. Eliminating all or some of these holes in the disks, respectively, eliminates this condition. The temporary nature in which these holes were sealed did not last, however. At the conclusion of the extended performance test, none of the air vent holes were covered on the first disk, and only two of six remained so on the last disk.

• The control piston was not originally limited in its movements within its housing, causing the control stem seal to be damaged.

• Leakage of H_2O from the control housing past the control stem seal and into the gas vent passageway causes H_2O carryover. It is sometimes difficult to trace and verify the source of this leakage. An improved method of providing this seal is required.

• The incorporation of O-ring seals in the gas vent and solenoid control valve improved the sealing of these valves.

• Optimal placement of the mechanical microswitches, intended to provide override control signals, could not be achieved.

• Although the test H_2O was partly replenished daily, it was observed that air carryover percentages would improve in just a few hours, and was directly attributable to how much foam the soap and H_2O mixture would produce.

• After the conclusion of the extended performance test, the maximum achievable flow rates when operating at maximum backpressure were decreased, possibly as a result of biofilm formation which increased H_2O line delta (Δ) pressure (P).

• The H_2O replenishment throughout the extended performance test maintained a biologically active H_2O environment. Biofilm formation within the MLS primarily occurred in the control housing. One of the low-pressure passageways appeared to be blocked.

The following conclusions are made regarding the performance of the MLS:

• The performance of the MLS met the separation design requirements. Air carryover percentages are typically <0.025 percent versus a requirement of 0.4 percent.

• The performance of the MLS designed during this program (the third-generation design) exceeds the performance of the MLS designed in the previous development program (the first-generation design).

• 1,600 rpm is an acceptable operating speed using a minimum control valve spring setting.

• A constant-speed motor improves MLS performance.

• Operating with constant backpressure improves MLS performance.

• Transient changes in inlet flow had no effect on performance.

• No performance degradation of the MLS was noted after an extended performance evaluation that lasted for 134 days and accumulated 1,000 operating hours.

• The test rig could not produce a 960-pphr inlet flow through the MLS at maximum backpressure after the extended performance test.

• The sensor piston and attached linkages transmit well enough to enable override control signaling.

• The use of microswitches to signal override conditions was judged to be impractical.

• Allowing sufficient time for any newly added soap and H_2O mixture to react with dirty system H_2O will improve the air carryover performance of the MLS.

The current MLS development program successfully demonstrated the ability to meet the *ISS* WP requirements when operating at 1,600 rpm for any H_2O condition with 0- to 14-percent air in the inlet stream. Performance exceeded that obtained in the previous MLS development program and was achieved while operating at a lower speed. The override switching function of the MLS was successful, although only partially tested, and some further development work is required to finalize its design. Constant backpressure was shown to improve MLS performance and was provided by the test rig during this program. Development of an actual constant backpressure valve to meet the requirements of the MLS and the *ISS* WP is additionally recommended.

MLS design recommendations are as follows:

• Sealing of the control stem to the flexible seal through which it passes needs to be improved.

• A mechanism to limit the amount of movement of the control piston should be incorporated into the design.

• The mechanical microswitches intended to signal override conditions should be replaced with electro-optical switches.

The following are system design and development recommendations:

• A constant backpressure valve that meets the requirements of the MLS and *ISS* WP should be designed, developed, and tested with the MLS to evaluate performance.

• The MLS should be retrofitted with recommended design improvements, tested, and evaluated.

• Continued extended performance testing in shower H_2O should be performed using a test setup that also incorporates more of the WWORU features; i.e., override control, process pump, and wastewater tank.

• Consideration should be given to the WWORU design to see if incoming H_2O can be placed directly in the wastewater tank before being processed by the MLS. This may enable the MLS to be sized to accept a constant inlet rate.

4.2 Process Pumps[3]

The process pump is an integral component in the WWORU. The WWORU is used for receiving, degassing, storage, and pressurization of the *ISS* wastewater. The process pump must be capable of surviving the harsh environment imposed by the wastewaters. This fluid, which is corrosive as well as nonlubricating, has proven to be a considerable challenge for this pump application. The process pump has numerous requirements imposed to ensure that it will provide its intended function. These requirements cover the categories of performance, life, cost, schedule, reliability, and safety, to name a few. While many pump technologies can satisfy some of the requirements, it is not obvious which technology is best suited to achieve optimal performance. The trade study addressed the problem of identifying the optimum pump technology for meeting the requirements of the *ISS* WP pump.

System development efforts have led to the conclusion that the process pump is a major risk to system performance. The off-the-shelf pumps evaluated initially provided unsatisfactory life (using the fluids, flow rates, and pressure head requirements defined by the WP system). Pumps tested have operated no longer than 1,500 hr, which is much less than the system operating requirement of 40,000 hr. Due to the failures and perceived high risk associated with the process pump, the current development program was implemented. This program evaluated various pump technologies, selected candidate technologies for the application, designed prototype pumps for selected technologies, and fabricated and then tested the endurance of the prototype designs.

The phase 1 effort on this program was initiated in November 1995 and has concluded with the completion of a phase 1 report. Several tasks were conducted throughout phase 1 of the development program. Initially, a trade study for different pump technologies was performed. From this trade study, four positive displacement pump candidate technologies were identified. Suppliers were selected to design an external gear pump, piston pump, and a diaphragm pump. The diaphragm pump is an off-the-shelf design. HS received customer approval to incorporate a fourth design, the rotary vane pump from Lucas Aerospace, into the contract which was based on evaluating only three test pumps. After reviewing their proposal and visiting their facility, HS highly recommended Lucas as a fourth pump supplier. It appeared that the Lucas rotary vane pump had a very good chance of meeting the pump requirements.

The process pump trade study was designed to be as objective as possible. In order to ensure that the optimum technologies were selected for development of the pump head, all available pump technologies were considered. No option was eliminated unless it failed to meet certain absolute criteria listed in table 1 or subsequently compared unfavorably with other options against the pump requirements.

Table 1. Absolute (go/no go) criteria.

Operates safely	Has gas-handling capabilities
Meets minimum life of 4,000 hr (1 yr)	Is a mature technology
Is compatible with *ISS* power supply	Has no visible external leakage
Meets head and flow requirement	Is capable of cyclic operation
Meets realistic weight, power, and volume limits	Handles inlet pressure, fluid temperature, and ambient temperature

Additionally, the pump requirements themselves were subject to examination. These requirements are summarized in table 2. If any single requirement was identified as an exclusive driver which influenced the study outcome by either challenging the state of the art, excluding a significant number of technologies, or by other means, that requirement was to be challenged to reduce its impact.

Table 2. Performance requirements—*ISS* WP process pump.

Flow rate	16.5±1.5 lbm/hr
Head	40–96 psid
Power	53 W
Inlet pressure	10.2–19.7 psia
Maximum operating pressure	164.7 psia
Life	87,600-hr installed life (10 yr) 40-percent duty cycle
Operating fluid	Mixture of shower, handwash, and mouthwash wastewater
Cycles	3,300 cycles (off-on-off)
Temperature, operating	6–113 °F fluid 63–105 °F ambient
Leakage	No visible leakage
Envelope	Minimized
Weight	Minimized
Material selection	Flight approved

The method of quality function deployment (QFD) was used to conduct the trade study and select the pump technologies used for the development. The recommended pump technologies include an external gear, a piston, diaphragm, and a rotary vane pump.

There were 35 request for proposals (RFP's) sent to various pump suppliers (11 gear, 12 piston, 6 rotary vane, 6 diaphragm). Of the 35 RFP's, only 11 proposals were received (4 gear, 4 piston, 2 rotary vane, 1 diaphragm).

Matrix diagrams were generated assigning relative weights to various decision factors for each of the four technologies. The 11 pump suppliers for each of the 4 pump technologies were ranked by HS design, materials and project engineering personnel. The suppliers with the highest ratings following this assessment were selected for phase 1 prototype design, and are Micropump, Inc. (gear pump), Phillips Engineering (piston pump), Prominent (diaphragm pump), and Lucas Aerospace (rotary vane pump).

The four pumps procured for phase 2 (procurement and testing) were obtained from Phillips Engineering (piston), ProMinent (diaphragm), Micropump (gear), and Lucas Aerospace (vane). Prototypes of each of the four selected technologies were fabricated and performance tested. All of the materials selected for the piston, gear, and vane pumps were approved prior to pump fabrication and operation. The diaphragm pump was an off-the-shelf design made of 316 Stainless Steel (SS), ceramics, Teflon®, and a composite Teflon®-faced fabric diaphragm.

The wastewater used for the life testing consisted of shower, handwash, distilled urine, and mouth wash H_2O. The actual makeup of the wastewater is defined in table 3. Igepon® soap 6503–45–4 and Crest toothpaste will be used for the testing. The Igepon® soap formulation is identified in table 4.

Table 3. Wastewater composition.

Wastewater	Space Station (lb/day)	Space Station (% Total)	Test Water (% Total)
Shower water (Igepon® 6503–45–4)	24.00	20.20	50.10
Oral hygiene (Crest regular flavor toothpaste)	3.20	2.70	2.70
Urine distillate (Oxone®/H_2SO_4)	13.24[a]	11.10	14.80
Urine flush	4.40	3.70	[b]
Handwash	24.00	20.20	[c]
Fuel cell	11.74	9.90	32.40[d]
Wet shave	3.52	3.00	[c]
Humidity condensate	24.00	20.20	[e]
Samples/checks	2.72	2.30	[e]
Wash cloth bath	8.00	6.70	[c]
Total	118.82	100.00	100.00

[a]Pretreat with 5 g of Oxone® and 2.3 g of H_2SO_4 into 6.25 cc of H_2O per liter of raw urine
[b]Mix 33.3-percent urine flush (DI water) into urine prior to distillation
[c]This water is included in the shower water
[d]DI water will be used to simulate this water
[e]This water is included in the fuel cell water.

Table 4. Igepon® soap test formulation.

Shower/Handwash Ingredients	Formulation 6503–45–4 (% by Weight)
Sodium-n-coconut acid-n-methyl taurate (SCMT) (24% active)	98.75
Lecipur 95–F (soybean Lecithin)	0.50
Luviquat FC–500 (polyquaternium 16)	0.75

Oxone® (a registered trademark of the DuPont Company) and sulfuric acid (H_2SO_4) were used to pretreat the distilled urine. The Oxone® and H_2SO_4 pretreat concentrations are 5 and 2.3 g/L of urine, respectively. DI H_2O was used to simulate the urinal flush H_2O. The percentage of pretreated urine to flush H_2O is 75 and 25 percent, respectively. Each wastewater batch was monitored and the data recorded for total organic carbon (TOC), thermocouple (TC), conductivity, and pH.

The operating conditions for the test were:

- 70 psid (across the pump)
- Flow rate: 15–16 pphr
- Operating cycle: 5.5 hr on, 0.5 hr off
- Operating time: 24 hr/day, 7 days/week.

Note: On April 25, 1997, the urine distillate in the wastewater was replaced with an ersatz for availability reasons. Table 5 shows the ersatz composition.

Table 5. Urine ersatz composition.

Compound	mg/L	Compound	mg/L
Acetic acid	0.99	Proplonic acid	2.53
Acetone	0.353	Urea	3.3
Ethanol	3.85	Chloride	1.1
Formic acid	4.4	Sodium	1.07
Methanol	1.9		

After 14 days minimum of life test operation, the test rig was flushed with clean H_2O and the single-point performance check was conducted on each pump. This check consisted of operating the pumps at the conditions listed in table 6, which was used to track any performance changes through the life test.

Table 6. Conditions for process pump performance check.

Pump Manufacturer	Speed	Outlet Pressure (psig)
ProMinent (diaphragm)	60% stroke @100 sec/min	70
Lucas (vane)	4,800 rpm	70
Micropump (gear)	4,200 rpm	70
Phillips (piston)	3,300 rpm	70

After accumulating 4,842 operating hours, and following the final performance map, the gear pump was disassembled and the cartridge components were inspected. The inspection revealed a fractured “driven” shaft at the notch, used for locking the shaft to prevent rotation. Also, the top wear plate (surface contacting the driven gear) showed some wear. This is the surface closest where the “driven” shaft failed. Note: This same surface in question initially had a small amount of wear prior to *ISS* wastewater testing. The remaining components (bottom wear plate, “drive” shaft, cavity plate) visually looked good.

After accumulating 4,370 operating hours, the piston pump was disassembled and the cartridge components were visually inspected, revealing a broken braze joint between the tube and the valve cover. Also, the upper journal bearing was allowed to rotate due to a failed set screw that keeps the bearing from rotating. The set screws are made from stainless steel (SS) with a nylon tip on the end. The nylon tip prevents the journal bearing from rotating.

The diaphragm pump life test was stopped on April 23, 1997, after 3,214 hr into the life test, as a result of wastewater leaking out of a weep hole at the bottom of the plastic housing (pump head end). A partial pump teardown and inspection was conducted which revealed significant damage to the plastic pressure housing and a tear in the diaphragm. The diaphragm pump was eliminated from consideration at the conclusion of this phase of life testing.

After accumulating 2,783 operating hours, the vane pump was disassembled and the cartridge components were inspected. The inspection revealed all eight vanes were severely worn on the sides. The vane tips indicate normal wear as indicated by LUCAS, as they were present during the disassembly of the pump. The two spring washers made from AMS5120 spring steel coated with Sermetal type W, used to preload the cartridge, showed severe corrosion. This material selection was a concern during the design review. All the other components (shaft, port plates, rotor, thrust plate, and transfer cylinder) visually looked good.

4.3 Water Processor Gas/Liquid Separator Development[4,5]

The WP for the *ISS* (fig. 2) requires the removal of free gas from the effluent of the catalytic oxidation reactor. An excess of oxygen (O_2) is injected into the reactor to ensure oxidation of organic compounds. To provide system flow stability and to prevent pump cavitation, removal of excess O_2, CO_2, and nitrogen (N_2) generated is desirable. The G/LS removes this free gas. The most recent WP G/LS design employs a passive membrane separator that utilizes hydrophilic and hydrophobic membranes. Recent integration testing at MSFC has indicated a shorter than expected operating life with the WP influent. To improve the G/LS operating life, evaluation of other technologies for gas/liquid separation for the *ISS* WP, will be investigated.

HS conducted a detailed evaluation of technologies for free gas removal in the reactor effluent. The goal of this task was to identify up to three candidate technologies for further evaluation at HS and MSFC. A trade study considered G/LS requirements and investigated phase separation technologies (both passive and active). The trade study compares requirements with abilities of the technologies and will identify best-suited technologies for the application.

HS obtained quotations for separator selected in the trade study. Upon receipt of supplier information, HS performed another trade study to determine which separator to procure. HS shall procure up to three devices (technologies). The hardware procured will be engineering development hardware. Due to cost and schedule constraints, only off-the-shelf or existing prototype hardware will be considered for procurement and test.

HS performed a functional test of the separators which includes proof and leak tests and performance evaluations. The performance evaluation will use a two-phase mixture of DI H_2O and air at flow

rates and pressures comparable to that of the WP. The purpose of the evaluation is to baseline the separator's performance. Upon completion of the tests, HS will package and ship the separators to MSFC for integration testing with an H_2O challenge, representative of the *ISS* WP challenge.

A trade study was performed to identify the most appropriate phase separation technologies for use as the G/LS in the *ISS* WP. Known technologies were evaluated against a developed list of weighted criteria to identify the recommended technologies.

This trade study was designed to be as objective as possible. All available gas separation technologies were initially considered. Options were only eliminated where they failed to meet certain absolute screening criteria.

The method of PV was used to conduct the trade study and select the top three phase separation technologies. This is a proven, structured, decision-making process that identifies and categorizes decision criteria and finally identifies the best selection(s) from the various candidate choices. The choices refer to the available phase separation technologies that were included in the trade study.

The decision process is described in the following paragraphs. The trade study was conducted by a group of HS engineers from differing functional areas. Group discussions were used throughout the study and viewpoints of in-house experts were sought. Decisions were made by consensus to ensure that sound judgment was applied throughout the study.

The first step in the QFD process was to identify requirements, obtained from the zero gravity G/LS assembly minispec developed for this program. The minispec defines not only requirements but design goals as well. Table 7 summarizes the requirements and goals separately.

These design requirements formed an initial screening of the possible phase separation technologies. Those judged unable to meet the design requirements were no longer considered in the trade study.

Table 7. G/LS performance requirements and design goals.

Requirements	Goals
Water with 0.08 lbm/day of free O_2 and 0.05 lbm/day of free CO_2 and $<10^2$ ppm of acetic acid	Minimize gas carryover
No external leakage	Minimize water carryover
Operating flow of 11 to 17 lbm/hr of H_2O	Minimize water vapor carryover
Fluid temperature of 41 to 191°F, nominally 150 °F	Minimize weight
Fluid pressure of 9.7 to 25 psia	Minimize envelope
Max design pressure of 52 psig (nonoperating)	Minimize power consumption
Gas handling ability in 1 and 0 g	Minimize water side pressure drop
Must not contaminate water	Gas pressure drop
	Transient performance
	Service life
	Proven technology
	Robust design
	Reliable design
	Short manufacturing lead time
	Minimize cost
	Minimize development cycle

The design goals derived from the minispec were considered in the decision criteria portion of the trade study.

The second step in the QFD process was to develop a set of decision criteria that would subsequently be used to evaluate each phase separation technology. Using the set of design requirements and design goals derived from the minispec as a starting point, a set of decision criteria was developed during a brainstorming session (presented in table 8).

Table 8. Decision criteria.

Capable of 0 and 1 g performance	Minimal air carryover
Handles ambient dew point	Handles on/off cycles
Handles ambient pressure	Minimal power consumption
Handles ambient temperature	High reliability
Compatible with fluid, dissolved chemicals, and particulates	Minimal water outlet-to-gas side pressure drop
	Handles transient performance
Does not contaminate water	Minimal water carryover
Handles fluid flow rate	Minimal water pressure drop
Handles fluid pressure	Handles water vapor transfer
Handles fluid temperature	Minimal development cycle time
No external leakage	Minimal manufacturing lead time
No leakage in no-flow condition	Development cost
Envelope	Life cycle costs
Weight	Service life
Robust	Technology risk

The brainstormed list contains many derived design goals that are not stated explicitly in the minispec. Examples of these derived design goals include cost and schedule drivers (development cost, development cycle time, etc.), technology risk, and robustness drivers. These derived goals are included because they help determine how well each technology will meet customer expectations.

Based on the results of the trade study, three technologies with the highest rankings are hydrophobic, hydrophobic sheets, and the MLS.

Hydrophobic-based separators score high due to their passive nature and because their membranes are much less susceptible to fouling/failure than a hydrophilic membrane. Scoring differences between the hydrophobic-based technologies are primarily due to their physical design; for example, hydrophobic spiral-based separators offer the most efficient packaging, but they are also the most difficult and costly to develop. Hollow fiber membrane-based separators offer the best hydrophobic-based solution because their packaging offers a good compromise between simplicity and packaging efficiency, and because the tubular membranes are best able to withstand the fluid pressure requirements.

The MLS, although a motor-powered design, scored well due to its apparent robustness and due to HS's experience with its design. The other active designs scored lower than the MLS because they would require more development effort and because they score lower in terms of performance or requirements.

Hydrophilic-based separators offer the disadvantage of requiring a membrane through which the inlet fluid must pass. This membrane can and will act as a filter to constituents within the H_2O, such as particulates, chemicals, or proteins. Past test experience has shown that this unwanted side effect can greatly limit the useful life of such a device.

Future vendor searches will be focused on these three technologies. Based on the vendor responses, the second phase trade study will factor in design specifics along with cost and availability to identify the top units for procurement. These units will be procured, tested, and delivered.

4.4 Water Processor Prefilter Assessment[6]

The first step in the *ISS* potable H_2O treatment system is to remove the particulate material from the wastewater prior to the removal of the dissolved inorganic and organic compounds. The TOC of the wastewater can range from 150 to 500 mg/L, depending upon the H_2O usage practices. Particulate size analysis reveals that for a given wastewater sample, the particle size (based on volume percentage) ranges from 0.04 to 2,000 μm with the mean size of ≈31 μm. These particles are primarily composed of particles that deform and change shape, and may be soap particles or other organic particles with soap attached to them.

Due to the high concentration of dissolved solids (soap) in the H_2O, precipitation of the suspension of dissolved solids combined with the particulate matter occurs in the solution and on the particulate filter surface.

The baseline filter is a depth or graded density pressure filter and is used to remove particles <0.5 μm in size (PALL model No. AB3Y005 7P, Profile II 0.5-μm polypropylene absolute depth filter 43 in. in length, 2.5 in. in outside diameter, 1-in. wall thickness, ideal operating pressure 1 psi, and maximum operating pressure 20 psig). Stage 10 testing at MSFC showed that the filter life was ≈25 days. Used test filters showed that a soapy cake was deposited onto the exterior of the filter and halfway inside the filter.

It is proposed to increase the particulate filter life to reduce the cost of expendables. Past restriction on the filter cutoff of 0.5-μm absolute has been recently abandoned and is presently the purpose of the particulate filter to maximize the life of the multifiltration beds (MFB's). The purpose of the particulate filter will now be to precipitate as much of the dissolved solids as possible that would otherwise be removed by the MFB's. Consequently, a particulate filter trade study was performed to evaluate and identify new or improved filtration technologies for possible use in the *ISS* portable H_2O treatment system.

A total of 29 potential filter manufacturers were solicited with respect to providing new-and-improved filtration technology for the *ISS* potable H_2O treatment system. Two major manufacturers, PALL Filtration Corporation (East Hills, NY) and the Memtec Group, a division of U.S. Filter/Filtration (Lansing, MI) were identified as having new and improved filtration technology that may be easily adapted to the present *ISS* particulate filter hardware. Both companies have developed advanced filtration technologies, described below, that may be beneficial to the *ISS* potable H_2O treatment system.

There are three basic cartridge filter types: edge, surface, and depth. The edge filter consists of a solid fabricated structure where the media consists of the edges of a stack of specially formed thin discs mounted on a central perforated core (shaft), and held under compression so as to form a continuous cylindrical outer surface. Each disc contains grooves cut into it such that very fine and carefully controlled gaps are formed between each adjacent disc. The gap openings are 5 μm in size and larger. Filtration occurs when the flow is inward through the narrow gaps between the discs while the particles are strained or filtered on the outer surface.

The depth cartridge or graded density filter holds to the meaning of depth filtration whereby the particles are trapped in the interstices of the internal filter structure. The density of the filter medium increases from the external surface to the center of the filter, causing the porosity to decrease and smaller particles to be removed deep in the filter. The two main types of depth cartridges are bonded and wound. Both filter types are simple, compact disposable units that have a high dirt-holding capacity able to remove solid particles from H_2O down to 0.22 μm. These filters have small surface areas but can be increased by cutting grooves on the outer surface, which increases the service life by delaying plugging.

Bonded cartridges are composed of fine, cellulose and polypropylene materials built into a thick-walled tube by a filtration technique wherein the fibers are formed wet. After drying, the tube is impregnated with resin and cured, forming a light, very porous rigid structure with good dirt-holding capacity. The cartridges do not require a central support structure and dirt-holding capacity is improved by changing the density of the medium.

Wound cartridges are spun fibers of wool, glass, and synthetic materials such as polypropylene. The fibers are usually brushed to raise the nap after each layer is wound on a hollow perforated core until the desired thickness is obtained. The nap forms the filtering medium by varying the closeness of the winding from the inside to the outside layer. The porosity of the medium is determined by control of the winding pitch, tension, fiber length, and other characteristics.

Surface filtration cartridges are made of thin sheet-form of cellulose paper or resin-treated paper. These filters are normally corrugated or pleated to increase useful filter life and filter surface area. A single surface cartridge can have up to 2.8 m^2 of surface area. The bulk of the filtration takes place on the surface but some depth filtration also takes place.

4.4.1 U.S. Filter/Filtration

U.S. Filter was given a sample of the wastewater to make a preliminary evaluation of the type of filter that would be most beneficial to the *ISS* potable H_2O treatment system. A gravimetric analysis of the wastewater was performed (table 9).

U.S. Filter observed that the wastewater contained many particles that easily deformed and changed shape (typical of soap particles) and that the dirt load to the filter was high. With this type of H_2O matrix, a depth filter was not recommended. Because the nature of the particles and the high dirt load, blinding can occur where the particles are trapped at the external surface of the filter. Consequently, the filtration capacity inside the depth filter is not utilized. U.S. Filter recommended using a surface filter with a high external surface. The POLY-FINE II series filter was recommended. These

Table 9. Summary of the U.S. filter gravimetric analysis.

Sample ID: "NASA Shower Water Sample" Membrane Disk Used: 0.2 polyester Volume Filtered: 10 mL Concentrations: 188.5 mg/L	
Particle Size Distribution	
μ Range	**Percent**
0.25–0.31	27.1
0.31–0.40	26.5
0.40–0.50	10.4
0.50–0.80	9.8
0.80–1.00	10.8
1.00–1.50	10.2
1.50–2.52	4.7
2.52–3.17	0.5

are high surface area, absolute rated, pleated filter cartridges. The filters are made of chemically inert materials listed by the Food and Drug Administration for food and beverage contact. The filter media is polypropylene and is temperature rated up to 40 psid at 150 ˚F. The filters come in μ ratings of 0.2, 0.25, 0.45, 0.8, 2, 3, 5, 10, and 30 µm. The filters come in single open ends, like the PALL filter presently used in stage testing at MSFC. These filters have an outside diameter of 2.6 in. (nominal) with available filter sizes of 10, 20, 30 and 40 in. in length. Custom lengths can be made upon order. For testing purposes, U.S. Filter recommends the following filters: (1) 20-in. PFT0.45–20US–M3 pleated polypropylene filter which has a 1.2-μm absolute rating with 222 silicone O-rings; (2) 20 in. PFT3.0–20US–M3 pleated polypropylene filter which has a 7-μm absolute rating with 222 silicone O-rings; and (3) 20-in. PFT10.0–20US–M3 pleated polypropylene filter which has a 15-μm absolute rating with 222 silicone O-rings.

The cost of these filter cartridges is between $100 and $125. There are several types of filter housings that can be used, depending on the filter size and application. For stage testing purposes, U.S. Filter recommends catalog No. 150158 #20 which holds single open-end 222 O-ring 20-in. filters. The cost of the cartridge housing is $117.

4.4.2 PALL Corporation

PALL Corporation was given a sample of wastewater and a used 0.5-μ PALL Profile II filter (P/N AB3Y0057P) from stage 10 testing for evaluation. The returned filter was examined for visual signs of contamination by cutting the filter across the cross section. The bulk of the contamination was observed to be confined to the outermost filter layer. The Profile II filters have an absolute-rated (for particulates) downstream section, and a continuously graded pore size upstream section, which serves as a prefilter and increases the service life. In this case, it appears that only the upstream prefilter section is being used, with very little evidence of contamination of the absolute-rated (particulate) downstream section. PALL says the results are consistent with the particle size analysis of the wastewater provided by Michigan Tech University. The results show that the volume percentage of particles that are <0.5 μ is <1 percent. The median of the particulate size distribution is 25 μ and roughly 90 percent of the particles are >2 μ.

Care must be taken in evaluating the particle size analyses. The particle size analysis provided by Coulter is for the clumped particles in the H_2O. The particle size analysis performed by U.S. Filter is a better description of the wastewater particle size analysis because the H_2O sample was sonicated for 0.5 hr to unclump the particles prior to analysis. The Coulter test experiment was conducted at a low velocity and thus enabled particles to clump together or the particles may have already had enough time to clump together before the experiment. The clumping of particles in this type of soapy wastewater is common. In addition, Coulter used an optical laser to evaluate the particles and this test can give unreliable results because small particles can hide behind larger ones and not provide an accurate particle count. The true particle size distribution may be the one provided by U.S. Filter. However, there is probably enough residence time in the wastewater storage tank to allow the particles to flocculate and clump together. Consequently, the particle size distribution observed by Coulter is the same one observed by the particulate filters.

PALL suggested testing their 4.5-μ Ultipleat Profile depth filter. This filter will perform very well, given that the particle size distribution data indicated that a large fraction of the clumped particles (>85 percent) was 5 μ or larger. PALL also suggested testing the 3-μ Profile II depth filter but it was felt that the results would be similar to the 4.5-μ Ultipleat filter. PALL suggested using the Ultipor GF Plus filter for polishing after the depth filters, something worth considering if a polishing filter is necessary. The cost of the filters and housing are probably very similar to those given by U.S. Filter, since U.S. Filter is a major competitor of PALL. The filter sizes are standard 2.5-in. OD with standard filter lengths of 10, 20, 30, and 40 in. Some are also available in 2.75-in. OD as well.

All filters recommended above (except for the Ultipor GF Plus filter) are available in 1-in. segments, which may be used for filterability testing. The filterability tests can be conducted at high flux rates (compared to the process) to quickly determine an optimal scheme for additional full-scale tests. These tests will have to be done on site due to the large volumes of H_2O needed to simulate the process throughput requirement (5,000 L) even at the 1-in. segment scale. The Ultipor GF Plus filters as the 0.45-μ rated membrane filters are available as 47-mm discs that can be used for filterability testing.

Based on the results of this trade study, several filters were procured for testing in the upcoming WP expendables evaluation test (EET) to be conducted in-house at MSFC in 1999. A list of the filters to be tested is provided in table 10.

Table 10. WP particulate filters.

Manufacturer	Filter	μ Rating (absolute)	Length (in.)	Filter Type
PALL	Profile II[a]	0.5	10	Depth
PALL	Ultipleat Profile	4.5	10	Depth
U.S. Filter	POLY–FINE II	0.5	10	Surface
U.S. Filter	POLY–FINE II	5.0	10	Surface
PALL	Ultipleat Profile	10.0	10	Depth
U.S. Filter	POLY–FINE II	12.0	10	Surface
PALL	Ultipleat Profile	40.0	10	Depth
U.S. Filter	POLY–FINE II	40.0	10	Surface

[a]Stage 10 filter.

4.5 Urine Pretreatment[7]

The urine pretreatment prefilter assembly (UPPA) is being developed for purposes of providing a simple, safe, and convenient method of handling the chemical pretreatments required for urine processing in a microgravity space environment. The Oxone® and acid tablets along with the filter and covering of UPPA have been defined and tested in previous test programs for MSFC. Reference figure 9 which shows the configuration of the UPPA.

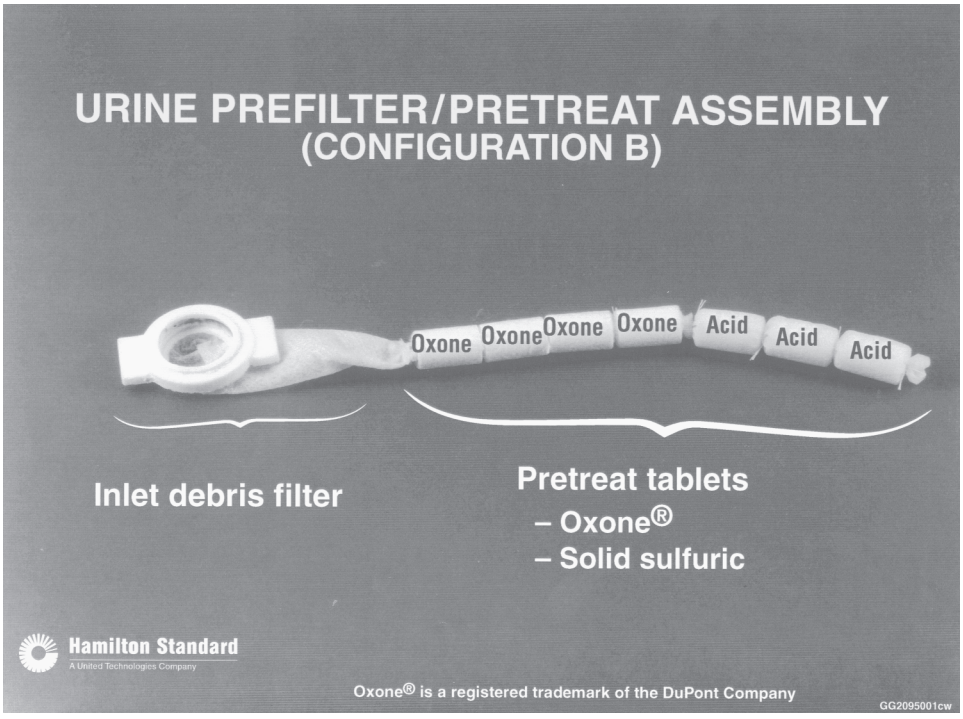

Figure 9. Urine prefilter/pretreat assembly.

There are several problems and considerations for the proper collection, storage, and processing of urine in a microgravity environment for long-duration, manned spacecraft missions, such as the Space Station. Urine processing for H_2O reclamation usually requires the addition of chemicals to fix the urea, provide microbial control, and minimize urine precipitate deposits. Also, since there is minimal use of flush H_2O, the additive chemicals are required to eliminate precipitate deposits in equipment and plumbing which can cause premature failure of hardware and systems. Since the original conception of the Space Station system layout, the urine pretreat chemical additive has been defined as an oxidizer of potassium monopersulfate compound (Oxone®) and a concentrated solution of H_2SO_4. The present requirements for chemical concentration ratios with urine are 5 g of Oxone® per liter of urine and 2.3 g of H_2SO_4 per liter of urine. These ratios are driven by the downstream urine processing system to fix the urea and eliminate urine precipitates. These pretreat chemicals have been considered to be introduced at various points in the urine collection and processing system. Considerations such as crew safety, ease of handling, envelope volume, interface, and maintenance all entered into the decisions. The original system approach was to introduce the Oxone® as a mixed solution of H_2O and Oxone®

powder upstream of the urine separator and inject a concentrated solution of H_2SO_4 directly into the urine outlet line downstream of the urine separator. Part of the decision to introduce only the Oxone® upstream of the separator was to minimize the potential hazard of H_2SO_4 injection in the proximity of urine collection from the body. Also, it was established that injection of Oxone® alone upstream of the separator was sufficient pretreat to keep the urine collection, separator, and associated hardware and plumbing clean.

The first phase of the urine pretreat injection system study was conducted by HS from September 1994 to June 1995, which successfully demonstrated the feasibility of introducing Oxone® only into the two-phase urine/air stream in a solid tablet form. The results of this investigation and testing were presented in the HS report No. SVHSER17066, rev. A.[8] The continuation of this investigation and testing through the second phase successfully demonstrated the feasibility of fabricating a solid H_2SO_4 tablet and defining the UPPA configuration for full urine pretreatment. The results of UPS–II study were presented in the HS report No. SVHSER17575, rev. A.[9]

4.5.1 Discussion

The combined effort for the third phase of the urine pretreatment injection system investigation and test program was conducted to define a safe and convenient method for storage and handling of the previously developed UPPA for the Space Station. The effort for this third phase specifically addressed packaging, storage, and handling of the UPPA's along with their effect on the prefilter housing design and the urinal flow/ΔP. The following tasks and studies are included in this report:

- Long-term storage tests of UPPA materials
- Recommendation of the optimum handling method and insertion/extraction procedures along with long-term storage provisions of the UPPA
- Design definition of handling and storage devices in "SVSK" drawing format
- Evaluation of prefilter filter housing for interface with the UPPA
- Evaluation of the flow/differential pressure effects on the urine fan/separator
- Investigation and recommendation for improved fabrication efficiency of the UPPA
- Recommendations for zero gravity sensitive issues.

4.5.2 Long-Term Storage Test of UPPA Materials

Various tests were conducted to define the extent and complexity of packing for long-term UPPA storage for the Space Station logistical and flight timeline. Long-term testing was conducted by two different approaches. One was to conduct accelerated materials compatibility testing using concentrated H_2SO_4. The other was actual long-term testing using various packaging concepts with enclosed Oxone® and acid tablets.

Accelerated materials testing consisted of exposing various UPPA assembly and packaging materials that were being used or considered being used for the UPPA program. The test was conducted by immersing samples of the materials in a beaker or petri dish of concentrated 98-percent H_2SO_4 solution for an unspecified period of time. The primary goal of this test was to get a quick visual worst-case indication of compatibility with concentrated H_2SO_4. If the solution remained clear, it was an indication that the immersed material was relatively compatible. If the material being tested changes or the solution becomes slightly tinted, a reaction is taking place and further investigation is necessary. Table 11 shows the results of this investigation.

Table 11. Materials compatibility with concentrated 98-percent H_2SO_4 solution.

Description	Material Type	H_2SO_4 Change	Material Change
Gore-Tex™ thread	Teflon™	None	No visual change
Gore-Tex™ membrane	Teflon™/nonwoven polyester	None	Polyester disintegrate
Membrane (hair net)	Nonwoven polypropylene	Slight tint	No visual change
SUPOR membrane	Polyether sulfone	Slight tint	Charred/disintegrated
PVDF membrane	PVDF	Medium tint	No color change
Combitherm XX115	Nylon/LDPE	Slight tint	Nylon-charred LDPE—no change
Vinyl gloves	Vinyl	Medium tint	Slight wrinkle wetted and turned clear
PALL PNW 50	Nonwoven polypropylene	None	No visual change
PALL HDC 2.5	Polypropylene	None	No visual change
VET glove	Polyethylene	None	Slight color change

Long-term testing consisted of packaging the UPPA chemistry (Oxone® + polyethylene glycol (PEG) and H_2SO_4 + $KHSO_4$) in tablet form using proposed packaging films and methods. One of the primary reasons for conducting the long-term test was to define the best vapor barrier for storage of the UPPA with acid tablets that still retain the highly hydroscopic properties of the H_2SO_4.

Preparation for the long-term storage test involved making Oxone® and acid tablets and packaging them in film with fabric coupons of Gore-Tex™, nonwoven polypropylene, and Teflon® thread. All samples included one piece of the following items sealed in each bag:

- 5-g Oxone®/PEG tablet (tablet wrapped in nonwoven polypropylene fabric and tied at both ends with Teflon® thread)

- 5-g H_2SO_4/$KHSO_4$ tablet (tablet wrapped in Gore-Tex™/nonwoven polypropylene fabric and tied at both ends with Teflon® thread)

- Dog bone tensile shape of Gore-Tex™

- Dog bone tensile shape of nonwoven polypropylene

- Length of Teflon® thread.

Test sample bags S/N 001–030 were made from packaging film Combitherm XX115 and heat sealed with the previously listed items in a dry N_2 gas backfill. Test sample bags S/N 031–060 were identical except they were vacuum sealed. Test sample bags S/N 101–106 were only "zip-lock" bags backfilled with dry N_2 gas. The "zip-lock" bags were to be used as a worst case packaging procedure, only to be used as a baseline for the recommended Combitherm XX115 packaging film. The test timeline was set up to take a sample from the Combitherm XX115 packaging groups every 4 wk and from the zip-lock bag every 12 wk. For each data point, the following information would be analyzed and recorded:

- Final sample bag weight
- Percent active Oxone® content
- Acidity equivalent/gram
- Tensile test on dog bone test pieces
- Visual observation.

The Combitherm XX115 packaging film, which is considered to be a relatively good vapor barrier in the food packaging industry, still showed some vapor penetration. After 20 wk, the N_2 backfilled showed an ≈4-percent weight increase. Furthermore, the samples showed a visual indication of free liquid inside the packaging film which is unacceptable. A visual review of the remaining samples up through S/N 030 also indicated that free liquid had collected for all of the N_2 backfilled bags. The data for the vacuum-filled bags show a reduced level of weight increase over the same 20-wk timeline with no visual evidence of free liquid in any of the samples up through S/N 060. Also all of the remaining bags show the vacuum sealing still intact. Based on the above observation, it is recommended that vacuum sealing should be used in the UPPA packaging. Also it is concluded that a single layer of Combitherm XX115 is not sufficient to provide for long-term storage requirements and, therefore, an aluminum foil should be considered for the final outside film.

The observed H_2O vapor transmission through the Combitherm XX115 packaging film based on 20 wk of long-term test for 25 samples of each type of sealing is as follows:

Average package H_2O increase (20 wk):

GN_2 sealing	9.22 percent (0.46 g)
Vacuum sealing	2.97 percent (0.15 g)

Average daily package H_2O increase:

GN_2 sealing	0.35 g=0.0025 g/day140 days
Vacuum sealing	0.15 g=0.0011 g/day140 days.

Based on the results of the long-term test, it is recommended to use the vacuum bag sealing method to seal the UPPA's in packaging film. An additional advantage for using the vacuum method over GN_2 backfill method is a significant packaging volume reduction.

4.5.3 UPPA Packaging and Handling Design

Design of special packaging and definition of insertion and removal procedures for the UPPA was a significant part of this program since the UPPA chemistry required special handling in a microgravity environment after possibly years of storage. The initial step was to establish the design requirements for the UPPA's for preflight, flight use, and postuse disposal. An internal minispec was generated which included requirements, design, goals, assumptions, and definitions regarding packaging, handling, storage, and disposal of the UPPA.

The minispec for the UPPA storage/handling/disposal container is presented below:

- Requirements

  – Provide safe storage of used and unused UPPA
  – Provide safe handling of used UPPA (removal of old and insertion of new)
  – Provide an H_2O vapor barrier for unused UPPA to limit tablet weight increase to 2 percent
  – Packaging shall be operable (opening, closing, storage, etc.) with gloved hand
  – Last removed package layer shall be transparent (view damage)
  – All materials that can contact UPPA (new or used) shall not cause a hazardous condition.

- Design Goals

  – Packaging should minimize stowage and disposal volume
  – Logistics should consider launch with or without a UPPA in the urinal hose
  – Visual indicator inside packaging would help with detecting damage to UPPA
  – Opening feature should not generate additional pieces
  – Desirable not to have to use tools to open containers packaging
  – Keep it simple
  – Logistics should consider returning used UPPA in original launch packaging and stowage location.

- Assumptions

  –Maintenance gloves are not provided with the UPPA but are available to the crew member as part of onboard waste management logistics
  –Most likely scenario is to launch without a UPPA installed in the urinal hose.

- Definitions

  –Safe: Double containment
  –Storage life: 2-yr minimum, 3-yr design goal from date of manufacture to end of useful life. Also, from date of installation into vehicle, life should be 1-yr minimum
  –Disposal life: 270 days from date of removal to date of ground disposal.

The challenge of providing a sufficient H_2O vapor barrier to protect the acid tablet which retained the hydroscopic property of H_2SO_4 was a primary design consideration for packaging. A search for a suitable packaging film considered many types of film. It was felt that the first (inside) package layer should be clear, such that any UPPA damage or apparent moisture intrusion would be evident and the package would not be opened for use. One initial choice was Kynar® because of its very low moisture vapor transmission rate. In fact, Kynar® was used to package the initial UPPA's supplied to support the stage 10 testing at MSFC. The result of using Kynar® for packaging was disastrous since there was some apparent reaction with the acid tablet, causing premature degradation and discoloration of the Gore-Tex™ wrap. At that time in the program, contact was made with the JSC food group in Houston with an inquiry as to what material was used to package the dehydrated food for long storage periods for Shuttle and *Mir* missions. One of the clear packaging films used was Combitherm XX115 supplied by Wolff Walsrode. The basic structure of this film is an outside layer of nylon and an inside sealable layer of polyethylene. Samples of this packaging film which is used in the food industry were obtained and used successfully to repackage the UPPA's for the stage 10 test program. Since the clear Combitherm XX115 was already used for space application, it was considered a prime candidate for UPPA use. Combitherm XX115 was used as the test media in the long-term storage test previously discussed, which indicated that one layer of clear packaging film was not a sufficient vapor barrier. The JSC food group also recommended an aluminum foil packaging film similar to the military meals-ready-to-eat, which provides a superior vapor barrier. Samples of the aluminum foil packaging film were received from Smurfit Flexible Packaging in Schaumburg, Illinois, and is identified as Flex No. 70464. The basic structure of this film is polyester film, 0.0005-in. aluminum foil, and 4-mil polypropylene layered together.

The UPPA is sealed in three layers of packaging. The Tertiary bag is the outside layer of Flex No. 70464 foil packaging used as the primary vapor barrier. The secondary bag of the clear Combitherm XX115 film is used as a backup packaging layer for the primary bag. The primary bag is also a clear Combitherm XX115 packaging film with two sealed pockets: one pocket contains the UPPA and the other contains a protective glove for use during removal and disposal of a used UPPA. Vacuum-sealing procedures are used for each of the three bags.

The previous discussion of packaging and handling of the UPPA's was based on seven 5-g tablets. This configuration had 20 g of Oxone® (four tablets), and 15 g of H_2SO_4 and $KHSO_4$ (three tablets), used to pretreat a total of 4 L of urine. This related to 14.5 micturations at an average volume of 275 mL per use. In addition to 4 L of urine was an automatic 80-mL flush with H_2O after each use.

Several adaptations or modifications of the UPPA configuration and packaging approach are possible, which would affect topics such as UPPA changeout frequency, flush H_2O use, trash volume, etc.

The first two urine pretreat injection system (UPS) studies assumed a UPPA changeout frequency of twice a day for a crew size of four, which was ≈14 micturations per UPPA. A study was conducted to determine the best configuration to increase the pretreat chemistry from 35–70 g but still not affect the air entertainment flow area in the urine collection hose. Various items were allowed to change; i.e., number of tablets, diameter of tablets, and inside diameter of hose. Refer to table 12 which presents the various parametric relationships of the variables. If the number of baseline size tablets was doubled to 14, the length of UPPA would be ≈20 in. long and is considered less convenient for handling

Table 12. UPPA study for the amount of chemical to provide a once-a-day changeout with a crew of four.

Baseline Configuration							
Tablet Weight (g)	**Tablet Length (in.)**	**Tablet Diameter (in.)**	**Tablet Density ($g/in.^3$)**	**Current Hose Diameter (in.)**	**Number of Tablets**	**Current Area "X" ($in.^2$)**	**Current Total Length of UPPA (in.)**
5	0.64	0.5	39.789	0.875	7	0.405	10.18

Study Spreadsheet							
Tablet Diameter (in.)	**Weight for Seven Tablets (g)**	**Weight for Nine Tablets (g)**	**Weight for Eleven Tablets (g)**	**Approximate Length for Seven Tablets (in.)**	**Length for Nine Tablets (in.)**	**Length for Eleven Tablets (in.)**	**Hose ID to Maintain "X" (in.)**
0.500	35	45	55	10.18	N/A	N/A	0.875
0.565	45	57	70	N/A	N/A	13.14	0.914
0.600	50	65	79	N/A	N/A	N/A	0.936
0.625	55	70	86	N/A	11.66	N/A	0.952
0.700	69	88	108	N/A	N/A	N/A	1.003
0.705	70	89	109	10.18	N/A	N/A	1.006
0.800	90	115	141	N/A	N/A	N/A	1.075

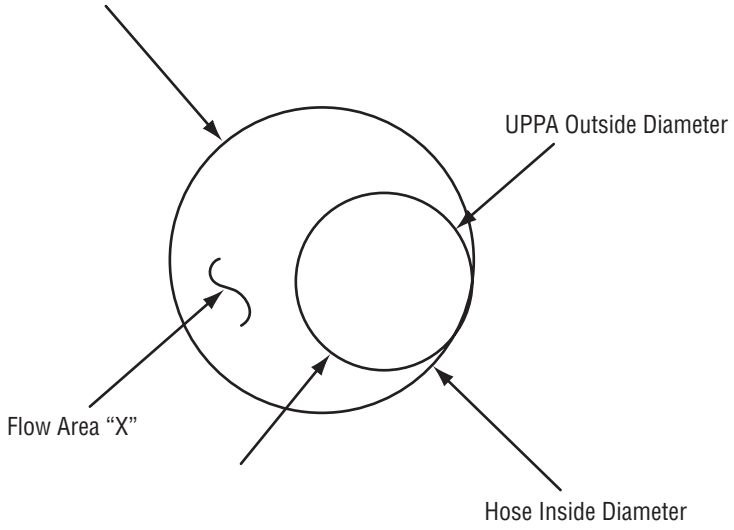

in microgravity. An option would be to increase the outer diameter of each tablet, for a total of nine tablets, and increase the hose internal diameter to ≈1 in. for minimum effect on air flow.

An issue for once-a-day changeout that would need some review is the dissolution rate for the UPPA with a total of 70 g of pretreat chemistry. The dissolution rate can be slowed down by several methods; the following would be considered:

• Changing to nine tablets as listed in table 12 would optimize the Oxone® tablet length to diameter ratio closer to one

• Increase the PEG content of the Oxone® tablet

• Smaller pore size of the tablet covering membranes

• Eliminate the automatic 80-mL H_20 flush or reduce the quantity of each flush. This would have a significant effect by deleting up to 1.16 L of H_20 for every 4 L of urine collected.

Changing out the UPPA once a day would have the advantage of a more convenient and natural daily use cycle for the crew members in regard to scheduled maintenance duties and body function routine. Deleting the automatic 80-mL H_20 flush after each reinsertion of the prefilter housing would directly reduce the quantity of H_20 required. A manual (momentary contact type) flush feature is still recommended that could be used for the UPPA changeout procedure or any time an H_20 flush is desired.

The volume of trash, which is always excessive, was based on the seven-tablet UPPA and the UPPA minispecification defined in this report. The resulting trash volume can be reduced by several methods; the following would be considered:

• Decrease UPPA changeout time from twice to once a day which would cut the quantity of trash packaging in half, assuming the same packaging method is used

• Package two primary/secondary bags with a UPPA in one tertiary (foil) bag

• Eliminate the secondary bag if there is no safety issue

• Consider the use of the empty waste collection assembly fecal bag stowage container (soft pouch) for excessive trash.

4.5.4 Flow/Differential Pressure Evaluation

A series of urine fan/separator flow versus pressure drop tests were conducted using the prototype urine inlet housing. The one-piece prototype housing was defined in previous UPS study programs to minimize the pressure drop associated with the smaller inlet diameter of the original hinged-type housing. The test consisted of operating the fan/separator with a 0.875-in. internal diameter flight-like urine collection hose and the prototype housing attached upstream of the separator. A pressure pickup point was located just downstream of the hose and prior to the fan/separator.

In test No. 1, the difference between dry filter (no pretreat) and dry full "UPPA" (inlet hose vertical) is a minimum ΔP of 0.4 in. of H_2O (1.8–1.4=0.4-in. H_2O). A maximum transient ΔP of 0.8 in. of H_2O occurs in an inlet hose which is held vertical, allowing the UPPA tablets to "flutter" slightly (2.2–1.4=0.8 in. H_20). Another larger transient condition occurs when liquid (H_2O at 37 mL/sec) is introduced into the system and the ΔP increases to 4 in. of H_20 and then falls off to 2 in. of H_2O 1 min after the H_2O flow rate is stopped.

Performance of the extended duration orbiter (EDO) urinal fan will change with the addition of the UPPA tablets for urine pretreat. The addition of these tablets in the line after the funnel and before the fan's inlet increases the system's resistance. Figure 10 shows baseline performance, indicated by point 1. The new design point performance is indicated by point 2. Point 2 falls on the system resistance line determined by the addition of the pretreat tablets in a dry condition while still maintaining a flow of 10 cfm. Point 3 shows operation with a wet pretreat assembly. As point 3's condition is temporary (only several seconds for each use), it is not selected as a design point. Therefore, the flow at point 3 will momentarily fall below 10 cfm, but only down to ≈9.4 cfm. Table 13 summarizes performance at these three operating points.

All performance quotations are based on no-swirl flow entering the fan, as the only test data we have is under this condition. Performance with swirl entering the inlet significantly reduces the ΔP achieved, so actual fan speed required to produce a ΔP of 12 in. of H_2O or more may be significantly higher than quoted here. Swirl flow is defined as the output flow of the separator, which due to the rotation of separator drum enters the fan inlet with an imparted swirl-type flow.

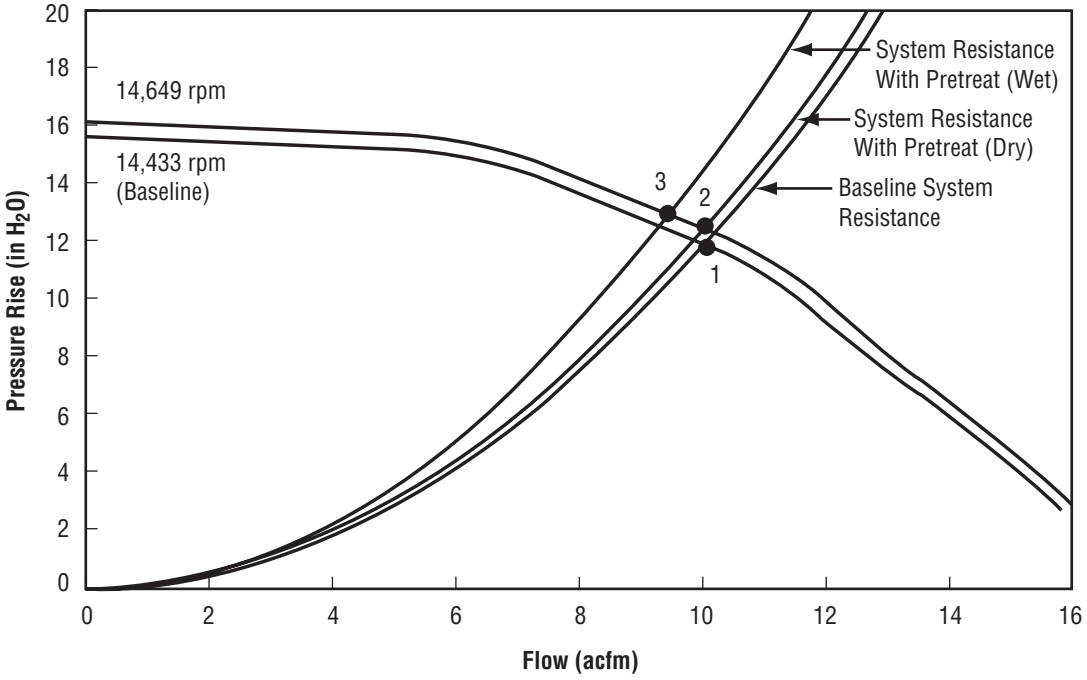

Figure 10. EDO urinal fan performance with urine pretreat (based on 0° fan inlet swirl).

Table 13. Operating point performance.

Point	Flow (cfm)	DP (in. H_2O)	Speed (rpm)	Power (W)
1	10.4	12.0	14,433	68
2	10.4	12.5	14,649	71
3	9.4	14.6	14,649	70

4.5.5 Investigation for Improved Fabrication Efficiency of the UPPA

The UPPA's that were made at HS to support the 150-day stage 10 test for MSFC were fabricated in a manual-intensive, limited production process in the advanced engineering laboratory. The pretreat chemistry for the tablets was mixed in small batches (200–300 g range). The mix was individually weighed out, 5 g at a time, loaded in a single-cavity die, and pressed manually in a hydraulic lab press. The membrane sleeves of nonwoven polypropylene and Gore-Tex™ membrane were cut by hand and seam sealed in a manual package sealer.

For higher production rates, some degree of limited automation would be incorporated. Also some of the fabrication, like tablet pressing, membrane fabrication, tablet assembly and tie-off, and final packaging, could be done outside to reduce costs.

One aspect that was completed in this program was the design and fabrication of a three-cavity die with nonmetallic liners and anvils for corrosion protection. The liners were first made from Teflon® tube which was unsuccessful since the Teflon® would cold flow and not survive the pressing loads. The liners were replaced by Vespel®. With this configuration, three tablets could successfully be pressed at one shot.

Several new membranes were received from PALL Corporation which were compatible with H_2SO_4. One membrane, which was hydrophobic and appeared to have similar proprietary to the Gore-Tex™ and nonwoven polypropylene double covering over the acid tablets, was tested for dissolution rate information. The dissolution rate for the PNW50 was expected to be slightly faster when tested against the original Gore-Tex™ membrane. The new PNW50 membrane is thinner and has larger pores which would allow the noted faster dissolution rate. It is feasible to obtain a tighter, nonwoven PNW hydrophobic membrane which should decrease the dissolution rate.

4.5.6 Recommendations

The following recommendations are made regarding any further activity with the UPPA or related areas:

- The *ISS* Safety Review Board concur with the approach presented in the UPS studies.

- The extra UPPA's (≈48) that were shipped to JSC to support the Lunar Mars Life Support Test program should be repackaged in the UPS III-defined package concept to verify 2–3 yr storage limits.

- Fly a design test objective DTO UPPA mockup to minimize handling/safety concerns.

- Revise UPPA baseline from twice-a-day changeout to once a day which will minimize crew effort and trash volume.

- Litmus strip should only be used as a cautionary indicator and not as a reject criteria indicator.

ISS urine pretreatment responsibility has been transferred to JSC and will be worked as a part of the *ISS* commode development. A representative from JSC attended the phase III urine pretreatment study briefing in June 1997 and a handover of responsibilities was accomplished at that time.

4.6 Portable Fan Assembly Development[10]

A trade study was performed by ION Corporation to determine the most cost effective and highest quality fan hardware for use as a portable blower for off-nominal crew activity (e.g., exercise, rack servicing, etc.). Off-the-shelf technology and current/past space program technology were considered in the initial evaluation of candidate fan technology for this application. Table 14 shows the requirements placed on the fans for the initial survey.

Table 15 lists the matrix of fans considered in the initial search of applicable vendors and fans from both commercial and aerospace inventories. Commercial manufacturers were selected from the Thomas Registry and contacted for applicable products.

Table 14. Portable fan requirements.

Hard Requirements	Soft Requirements
120-Vdc electrical interface Vane directional exit flow Inlet debris screen 40 mesh Materials acceptance and qualification (as per SSP30233) Rack mount interface	Operation maximum 6 hr/day 50–150 ft^3/min flow 60–80 ft/min exit velocity Dual speed operation (if applicable) Meet *ISS* program requirements as applicable (noise, vibration, op. env., human factors, etc.)

Table 15. Initial candidate fans.

Aerospace Fans	Commercial Fans
Space Station IMV/standoff fan Space Station avionics air fan Shuttle/lab avionics fan (HS) Shuttle/lab avionics fan (Allied Sig.) Space Shuttle IMU fan Spacehab ventilation fan Spacelab transfer tunnel fan/Skylab Shuttle cabin air fan	EBM Papst 4400 series EBM Papst 4300 series COMAIR Rotron Muffin XL SUNON fan EG&G Rotron 1984SF and 1936SF Vaneaxia EG&G Rotron Corsair, Lightning, Propimax 3&3B, Aximax Ametek 120-Vdc single stage blower

The major fan parameters used to evaluate each fan, where available, are listed in table 16. These quantities were used to limit the fan selection process. Cost was also considered but was, in some cases, competition-sensitive material and is excluded here.

The initial field was narrowed to three fans, each having properties that were too significant to delete. These fans, shown in table 17, were each tested at MSFC and evaluated individually for performance, reliability, power, etc. and the final fan selected was chosen by evaluating this data versus the overall program goals and requirements.

Table 16. Fan evaluation major parameters.

Fan Title	Electrical		Parameters			
	Watts	Voltage	Flow (cfm)	Volume	Noise	Mods[a]
Aerospace Fans						
Space Station IMV/standoff fan	55	120 Vac	140	10.4 in.×7 in.¥9.5 in. D	NC40	I[b]
Space Station avionics air fan	160	120 Vdc	40–120	23 in.×7.75 in.¥10.75 in.	NC40	I[b]
Shuttle/lab av. fan (HS)	180	115/200 Vac	150	5.467 in.×6 in. D	NC40	I[c]
Shuttle/lab av. fan (Allied Sig.)		115/200 Vac	150–350	6.34 in.×6.6 in. D	NC40	I[c]
Space Shuttle IMU fan	50	110 Vac	32	8 in.×3.5 in.×10.5 in.	NC40	I[c]
Spacelab ventilation fan	290	120 Vdc	175–275	6.2 in.×6.3 in.×4.3 in. D	NC40	I[b]
Spacelab transfer tunnel fan/Skylab	22	28 Vdc	80–150	7 in.×5 in. D	NC40	I[c]
Shuttle cabin air fan	495	115 Vac	295–342	35.6 in.×12.2 in.×27.1 in.	NC40	I[c]
Commercial Fans						
EBM PAPST 4400 series	5	24 Vdc	100	1 in.×4.7 in.×4.7 in.	TBD	II[d]
EBM PAPST 4300 series	5	24 Vdc	100	1 in.×4.7 in.×4.7 in.	TBD	II[d]
COMAIR Rotron Muffin XL	–	115/200 Vac	108–115	1.54 in.×4.7 in.×4.7 in.	TBD	II[d]
SUNON fan	–	12/24 Vdc	84–108	4.7 in.×4.7 in.×1.5 in.	TBD	II[d]
EG&G Rotron 1984SF Vaneaxial	14.88	48 Vdc	65	3.14 in.×3.14 in.×1.5 in.	NC50	II[d]
EG&G Rotron 1936SF Vaneaxial	10.4	26 Vdc	65	3.14 in.×3.14 in.×1.5 in.	NC50	II[d]
EG&G Rotron Corsair	15	28 Vdc	126	4.7 in.×4.7 in.×1.5 in.	NC50	II[d]
EG&G Rotron Lightning	7.8	26 Vdc	118	4.7 in.×4.7 in.×1.5 in.	NC60	II[d]
EG&G Rotron Propimax 3 & 3B	23.5	48 Vdc	100	3.75 in. D×1.73 in.	–	II[d]
EG&G Rotron Aximax 3	45.5	26 Vdc	101	3 in. D×2.31 in.	NC70	II[d]
AMETEK 120 Vdc blower	200	120 Vdc	200	7.4 in.×6 in.	TBD	II[d]

[a]Mods I and II: I—Noise suppression, electrical interface, integrate into portable assembly; II—same as I + materials verification, reliability
[b]Fan currently in development/production
[c]Fan out of production
[d]Fan is available through commercial vendor.

Table 17. Fan test article selection.

Fan Title	Electrical		Parameters			
	Power (W)	Vdc[a]	Performance (cfm)	Volume (in.)	Noise	Mods[b]
Aerospace Fans						
Spacelab transfer tunnel/Skylab	22	28	80–150	7 in.x5 in. D	NC40	I
Commercial Fans						
EG&G ROTRON MIL–901	19.68	28	218	6.375 in. Dx2 in.	TBD	II
AMETEK 120-Vdc blower	~220 peak	120	200	7.4 in.x6 in.	TBD	II

[a]All 28 Vdc fans require voltage conversion from 120 to 28 using the VICOR dc-dc converter
[b]Mods I and II: I—Noise, electrical, portable assembly; II—Same as I + materials verification, reliability.

The test system was similar for each of the fan system tests. Polyvinyl chloride (PVC) smooth wall duct was installed upstream and downstream of each fan. Pressure gauge taps were installed in each duct a specified distance from the fan inlets and outlets. A hot wire anemometer/flowmeter is used to determine the air velocity, volumetric flow rate, temperature, pressure differential, and relative humidity. Deflection pressure gauges were also used to determine pressure differential across the fan. Figures 11 and 12 show the two major test systems used to evaluate the three fans chosen for testing.

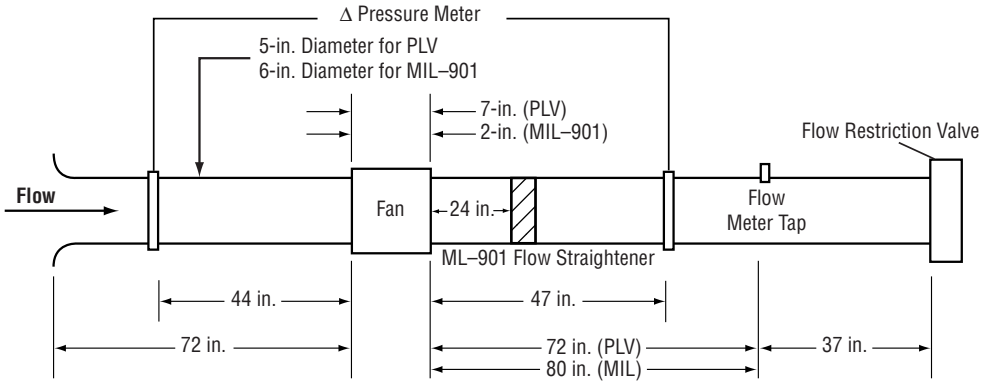

Figure 11. Test system schematic for axial fans.

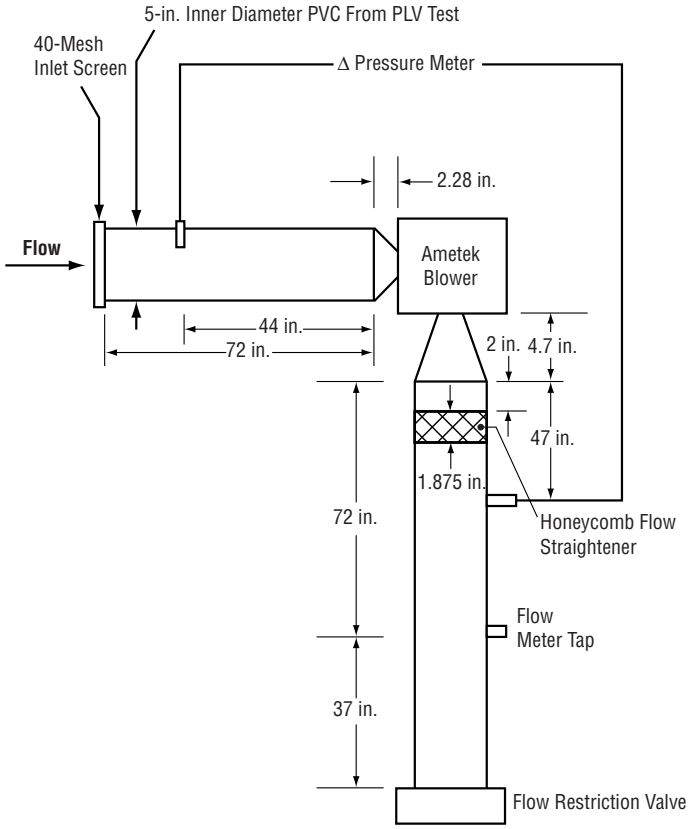

Figure 12. Test system schematic for Ametek blower.

The Skylab duct fan (derived from the Apollo capsule postlanding ventilation (PLV) fan) was applied to the Spacelab program as a transfer tunnel fan for Shuttle flights. As a result, there exist several flight-qualified fans available for use on other programs, and ultimately, for *ISS*. The quality, flight history, and design/performance range of the PLV fan makes it a very likely candidate for portable application. In fact, this duct fan was integrated into a portable housing developed for that purpose and used on Skylab. A schematic cutaway of this Skylab portable fan is shown in figure 13. Two configurations for the PLV fan were tested. The distinction between the two configurations was the power source. Configuration I used a straight 28-Vdc power supply wired to the fan through a three-position switch. Configuration II used a 120-Vdc power supply with the power attenuated to the fan by a 120- to 28-Vdc voltage converter. Configuration II was developed to verify the electronics required to run a 28-Vdc fan on the *ISS* 120-Vdc voltage bus.

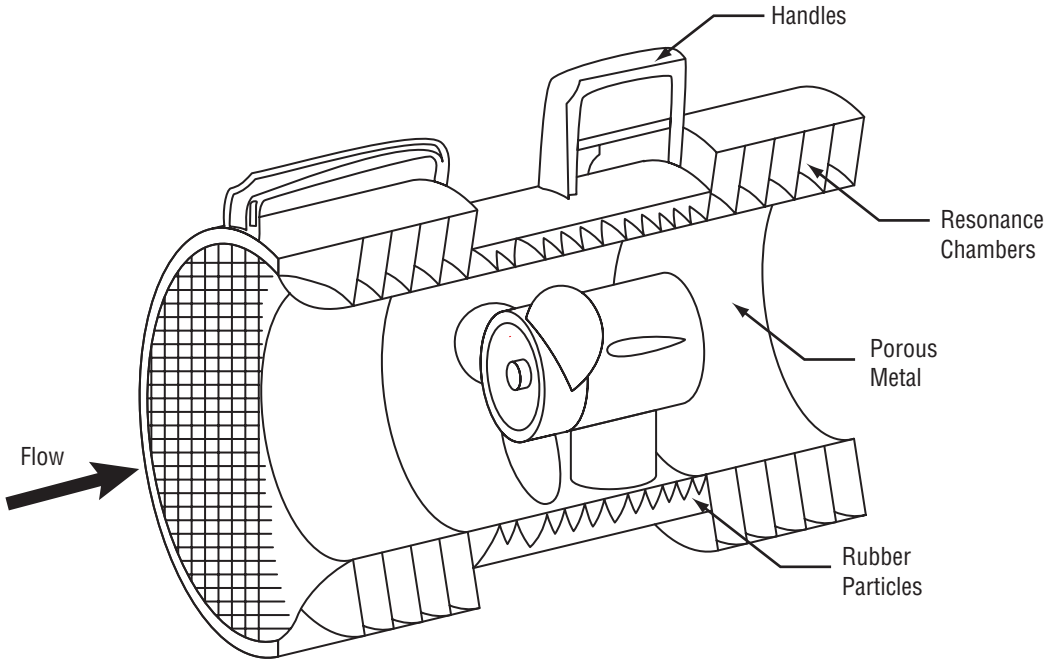

Figure 13. PLV portable fan assembly.

The second fan tested was an Ametek 120-Vdc brushless blower. This blower contains an electronically commutated dc motor that has a bridge rectifier to run ac at 120 V. As a result, this blower will operate with a dc voltage input as well as an ac voltage input at 120 V. The performance curves for the dc and ac configuration are somewhat different. The dc data does not peak as high and the slope of the plot of pressure versus flow is more pronounced. The blower has inlet and outlet ports of ≈1-in. outer diameter. A schematic of this fan is shown in figure 14.

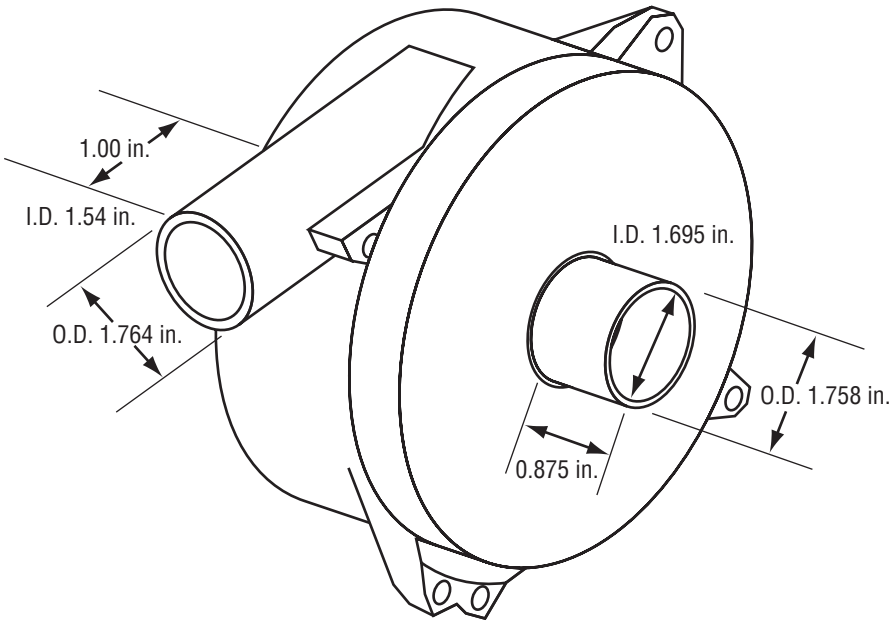

Figure 14. Ametek 120-Vdc blower schematic with dimension.

The last fan tested was a tubeaxial 28-Vdc MIL–901 fan from EG&G Rotron Custom Design Company. This fan had a 6-in. interface; therefore, a 6-in. duct was used to test this fan's performance. Figure 15 shows a picture of the MIL–901 fan tested. This fan was integrated into the duct system similar to the PLV fan. A collar was glued onto the outside of the duct and endplates were compressed onto the collar to seal the duct to the fan at a foam interface.

Figure 15. EG&G Rotron MIL–901 fan.

The PLV fan was operated in two configurations for over 200 hr each. The initial configuration utilized a direct 28-Vdc power supply and the second configuration used a 120- to 28-Vdc voltage converter with a 120-Vdc power supply (to emulate the Station power grid). This fan generated a pressure rise of 0.23 to 0.97 in. of H_2O. The maximum flow rate achieved was 205 cfm and the overall maximum power consumed was ≈22 W. The noise data indicate that the PLV will require only slight modifications to meet a reasonable noise requirement. No degradation in the fan performance was observed throughout the test.

The Ametek 120-Vdc blower operated directly from a 120-Vdc power supply, thus eliminating the power converter. Additionally, this blower was operated at two different performance setpoints for over 200 hr each. The varying setpoints were selected by manipulating an integrated, fully adjustable speed control potentiometer. A maximum and intermediate flow range was selected for the fan operation, generating (in high flow) a pressure rise of 0.12 to >15.5 in. of H_2O but only produced a maximum flow of ≈104 cfm. It should be noted that this blower will operate with either a 120-Vdc or Vac input. The blower consumed ≈200 W of power maximum. The noise generated by this fan (in high flow) was significant compared to the other test articles, resulting in more design modifications to meet a reasonable noise requirement. No degradation in the fan performance was observed throughout the test. No further evaluation is anticipated.

The MIL–901 fan was operated using a 120- to 28-Vdc voltage converter with a 120-Vdc voltage source. The fan was run for over 200 hr in this configuration, generating a pressure rise of 0.125 to 0.61 in. of H_2O. The maximum flow produced was ≈231 cfm. The fan consumed ≈25 W of power maximum. This fan exhibited the least noise of all the test articles and would therefore require the least design modifications to meet a reasonable noise requirement. No fan degradation was observed throughout the test.

As a result of the comparison of each set of fan performance data, further evaluation of the MIL–901 and PLV fans was undertaken. The Ametek blower was off-nominal when evaluated on an overall flow basis and power consumption and, therefore, was not considered for further testing. The PLV and MIL–901 fans were reintegrated into the test stand and run simultaneously to evaluate their endurance over an extended duration. The endurance testing setpoints for each fan were selected to bisect the operating pressure range of the fan as evenly as possible without falling within a transition region. For the MIL–901 fan, the full scale of operation was from 0.135 to 0.61 in. of H_2O; therefore, an operating setpoint was chosen at ≈0.3 in. of H_2O. The PLV fan varied from ≈0.25 to 0.96 in. of H_2O; therefore, a setpoint of ≈0.6 in. of H_2O was selected for this fan, which is clearly below the range of the PLV fan transition flow region. During the extended duration test, the PLV fan ran for 930 hr and the MIL–901 fan ran for 1,030 hr.

Fan performance data for the Rotron MIL–901 and PLV fans are provided in figures 16 and 17. Both figures show initial, post-200-hr test, and postendurance test data.

Each fan met a certain initial selection criteria prior to testing. Additionally, each fan tested was integrated into a test system designed to maximize comparable data and reduce any system-specific effects that would skew the data inordinately toward a specific fan. All fans fell within the soft and hard requirements initially placed on the fans. However, some of the parameters have not been specified

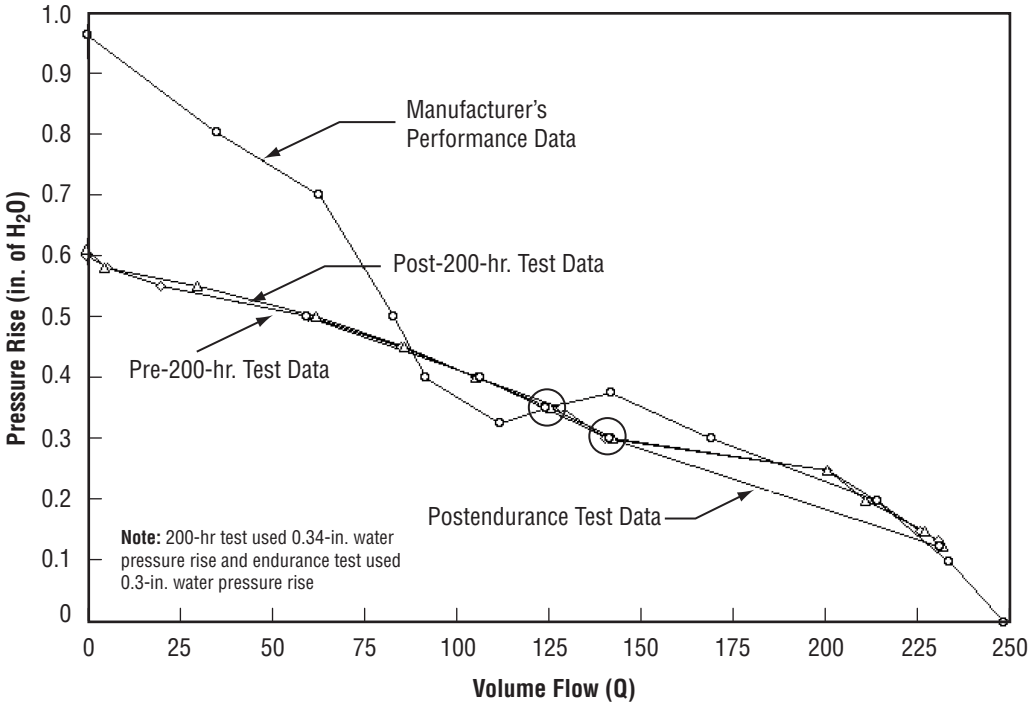

Figure 16. MIL–901 fan performance data comparing initial, post-200-hr test, and postendurance test data.

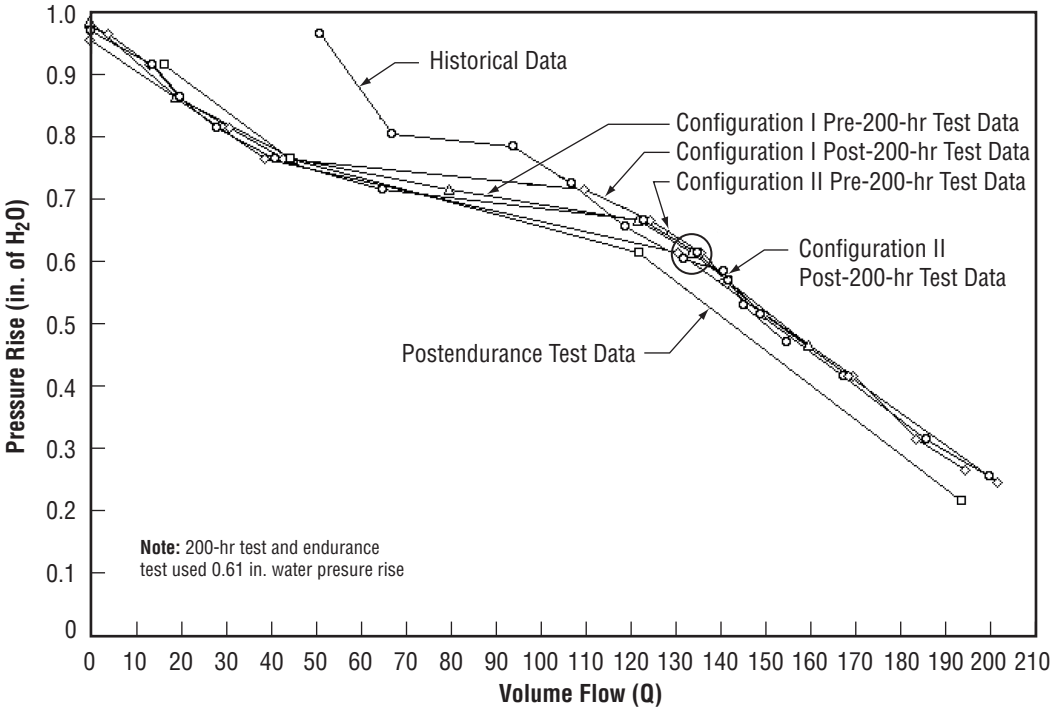

Figure 17. PLV fan performance data comparing initial, post-200-hr test, and postendurance test data.

for a portable fan application and one of the purposes of this test was to determine the envelope for some of these parameters. Principally, noise and power consumption levels were not maintained as hard requirements, although noise levels approaching NC40 or NC50 have been baselined for much of the Station equipment. Therefore, comparison of the fans in an equal basis, including the undefined parameters, led to an evaluation based solely upon "trade-off" analyses.

The endurance testing of the PLV fan indicated there may have been some degradation, since there was anomalous flow data at the endurance setpoint of 0.6 in. of H_2O. However, no other data indicate there was a degradation in performance or operation of this fan. The MIL–901 showed no performance reduction and the differences in the noise levels exhibited may be a simple function of normal break-in wear. Based upon these data, it was recommended to continue evaluation of the MIL–901 fan.

After selection of the MIL–901 Rotron fan, steps were taken by the ECLS Branch (ED62) to solicit support from various MSFC disciplines to develop and qualify a PFA for use on the *ISS*. Based on their inputs, manpower (civil service and contractor) and program cost numbers were developed. A concurrence sheet formally committing resources for the project was signed by all MSFC S&E directorate laboratories involved. In June 1997 the MSFC director of the Flight Projects Office approved completion of the qualification phase of this effort.

A PFA development unit was assembled utilizing existing hardware. The development unit included an inlet bellmouth, inlet screen, *ISS* intermodule ventilation (IMV) noise attenuation silencer and Boeing development "dummy" silencer, MIL–901 Rotron fan, honeycomb flow straightener, outlet louvers, and a development power supply module. Development tests run from July through November 1997 included acoustic noise, flow ΔP, and electromagnetic interference (EMI). The IMV silencer and dummy silencer were larger than anticipated for the PFA application but were utilized because they were similar to the design envisioned for the PFA with the internal acoustic foam "footballs" and, thus, should give a good indication of acoustic noise and flow ΔP characteristics.

Acoustic test data showed the IMV development muffler provided adequate noise attenuation at low fan speed to meet the NC40 requirement for all frequencies except 1,000 Hz. The requirement for intermittently operated equipment[11] used up to 8 hr/day was met at low speed and that for equipment used up to 3 hr/day was meet at the nominal speed. Flow ΔP characteristics are provided in figure 18. This performance data indicated that the PFA would meet the 50–150 cfm requirement. The power supply was only subjected to the conducted emissions (CE's) and conducted susceptibility (CS) tests based on SSP 30238 rev. C requirements. The purpose of this testing was to verify the compliance of the power supply to SSP 30237 rev. C requirements before integration with the remainder of the PFA. The power supply passed all CE and CS requirements. The PFA qualification unit will be subjected to a complete test of CE, CS, radiated emissions (RE's) and radiated susceptibility (RS).

A PFA preliminary requirements review (PRR) was held in February 1998 with the purpose of firming up PFA requirements and reviewing a preliminary design concept. Major documents available for review at the PRR included the PFA design and performance specification, PFA interface control document (ICD), hazards analysis, configuration management plan, requirements verification plan, program plan, and preliminary drawings. A total of 20 issues were written against the documents noted above.

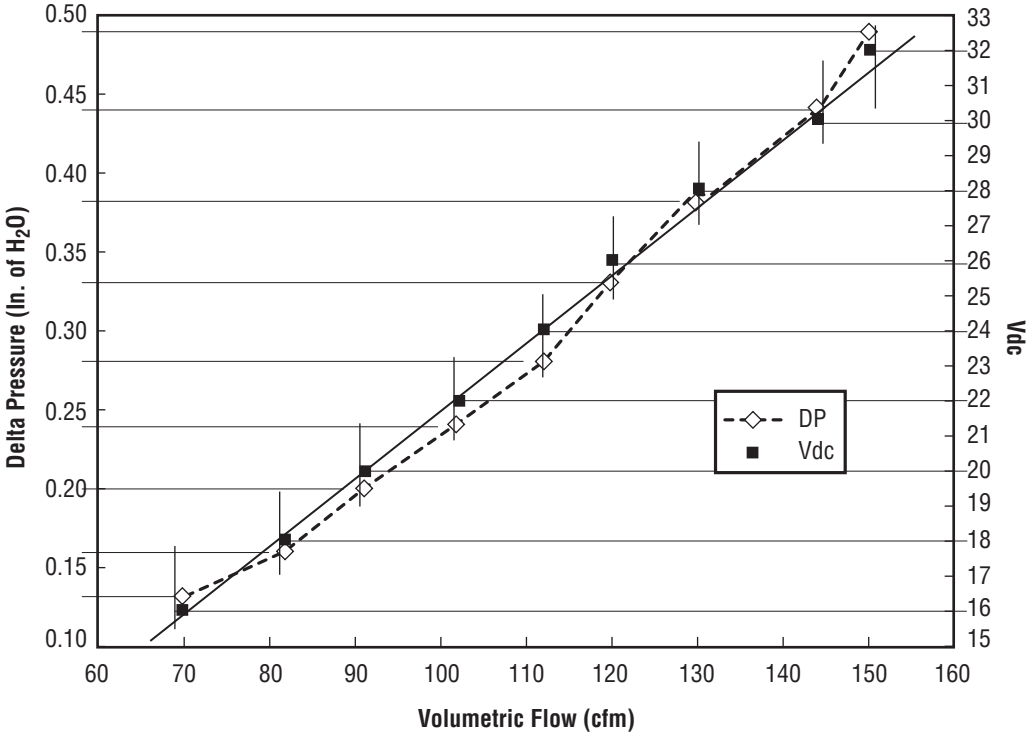

Figure 18. Portable fan development unit flow—ΔP characteristics.

Subsequent to the PRR, additional work was done on firming up a preliminary design and providing information to allow closure of the PRR issues. The PFA Design and Performance Specification and ICD were baselined after incorporation of PRR issues and placed under configuration control. The design and performance specification is contained in reference 12 and the ICD in reference 13. The preliminary design concept, as shown in figure 19, was finalized by the Structural Design Division and a mockup fabricated by the MSFC Model Shop. A mockup demonstration was conducted for the *ISS* Program Office in early May 1998. At the conclusion of the mockup demonstration, the *ISS* Program Office representative indicated that the design was unacceptable due to the overall envelope and the fact that the fan was not "portable."

Comments from the mockup demo resulted in a redesign effort with the focus to reduce the overall envelope of the PFA. Emphasis was placed on reduction in the size of the inlet and outlet silencers since they are the major contributor to the size of the assembly. A subcontract was let by ION Corporation to AcousticFab, Boeing's supplier of the silencers, to conduct analyses and develop smaller silencers. AcousticFab recommended silencers ≈4 in. in length with resulting noise attenuation characteristics that would allow operation of the fan for 2–3 hr at 18 Vdc and still meet noise requirements. During the course of the redesign, the inlet bellmouth, honeycomb flow straightener, and outlet louvers were deleted from the design.

The final design concept presented at the PFA critical design review (CDR) in November 1998 is shown in figure 20. This design includes: the fan, silencers, power supply module (dc-dc converter, on-standby switch, speed control knob), power cable connected to the *ISS* utility outlet panel, the handle,

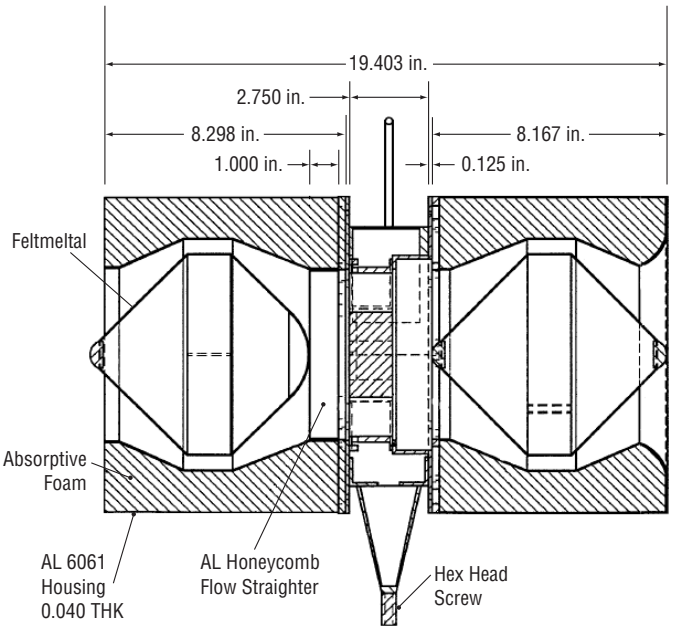

Figure 19. Preliminary PFA design concept.

and the rack seat track equipment anchor interface. Predicted PFA performance is provided in figure 21. Noise attenuation data, developed by analysis, is shown in figure 22. This figure shows predicted overall sound pressure levels for 18- and 28-Vdc operation with silencers and with no silencers (bare fan) with the noise requirement overlaid.

Upon satisfactory closure of design-related PFA CDR review item discrepancies (RID's), a qualification unit will be fabricated. Subsequently, a qualification test will be performed in-house at MSFC.

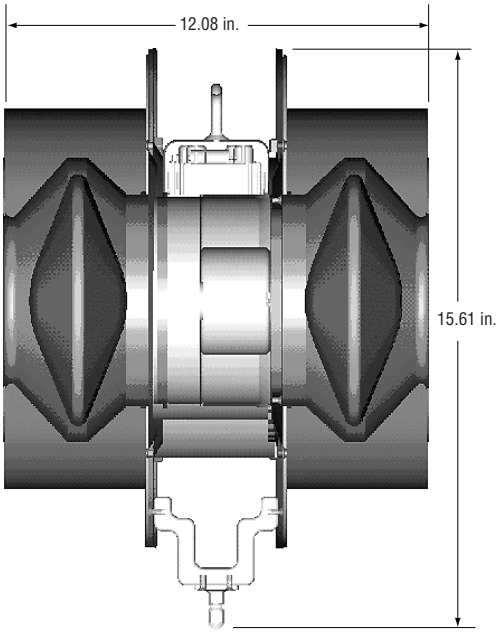

Figure 20. Final PFA design concept.

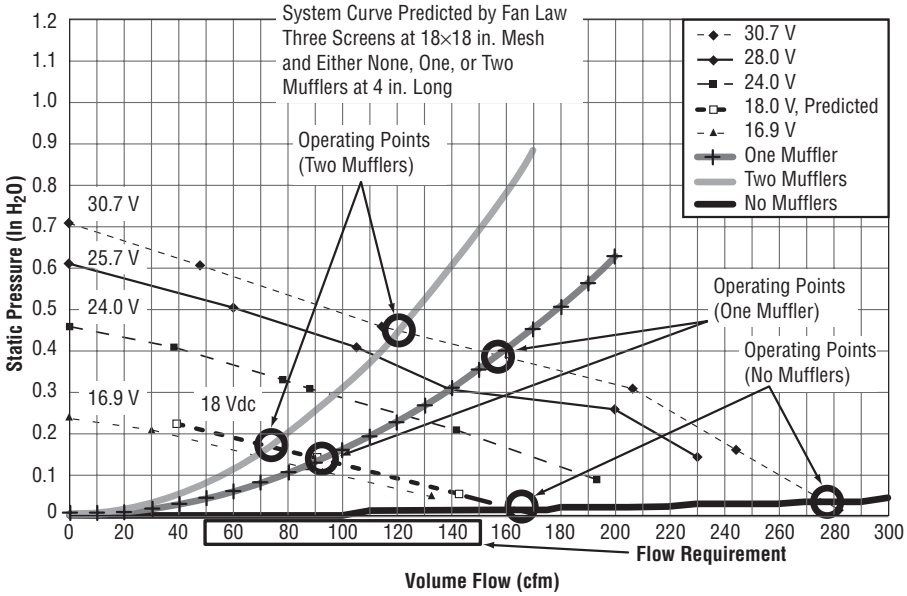

Figure 21. Predicted PFA performance.

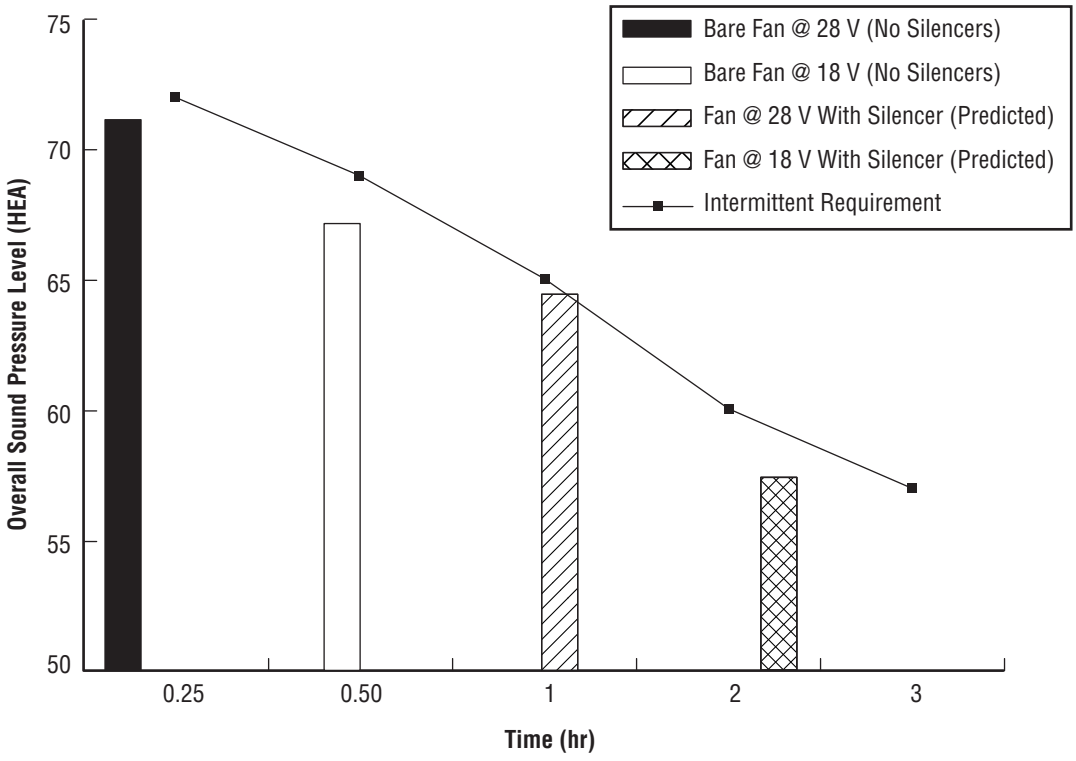

Figure 22. PFA final design sound pressure levels.

4.7 Flight-Like Condensing Heat Exchanger Refurbishment

The CHX used to outfit the ECLSS test bed in building 4755 are not flight-like and do not reflect the *ISS* design configuration. The CHX used in the stage 10 water recovery test (WRT) appeared to have leached an excessive amount of zinc stearate compound that may have caused premature fouling of the WP prefilters. In addition, the *ISS* Program Office has often expressed the need for a flight-like CHX to interface with the four-bed molecular sieve (4BMS). These two factors led MSFC to assess the availability of flight-like CHX units and solicit replacement units.

Discussions with HS, the supplier of the *ISS* CHX, indicated that two CHX cores damaged during development were available for refurbishment. HS was awarded a subcontract through ION Corporation to repair, refurbish, performance test, and deliver two flight-like CHX's. The two CHX units were to be provided by ION Corporation.

One CHX was delivered by HS in June 1998 and is currently being configured to be utilized as a part of the temperature and humidity control (THC) subsystem of the laboratory module for the ECLSS sustaining engineering test bed. A flight-like interface with the 4BMS will be fabricated and will allow for higher fidelity development testing with the 4BMS. The second CHX unit will be delivered in early 1999 and will be installed in the sustaining engineering node 3 and habitation module simulator. This CHX will interface with the node 3 WP providing condensate for processing by the WP.

4.8 Sabatier Carbon Dioxide Reduction Refurbishment[14]

Carbon dioxide reduction was included in the Space Station *Freedom* (SS*F*) baseline to completely close the O_2 loop and reduce the amount of H_2O that needed to be supplied. A comparative test program in 1989–1990 featured an HS Sabatier. The most recent testing of this technology by MSFC was conducted as part of the predevelopment operational systems test (POST) which occurred in early 1991. At the end of that testing, certain problems were noted and items were identified as needing refurbishment prior to any additional testing. HS has investigated the problems encountered during the POST and has identified several system improvements under independent research and development tasks. The purpose of this task was to refurbish and upgrade the existing POST Sabatier subsystem so that system level tests could be run at the ECLS test facility at MSFC.

4.8.1 Design and Configuration

This section describes the effort to refurbish the components of the Sabatier subsystem. Changes were made to the subsystem schematic and to the accompanying mechanical and electrical components. Each of the changes made and the supporting rationale is described here in further detail.

The schematic shown in figure 23 depicts the current subsystem configuration and should be used for reference regarding designation of items on the component list.

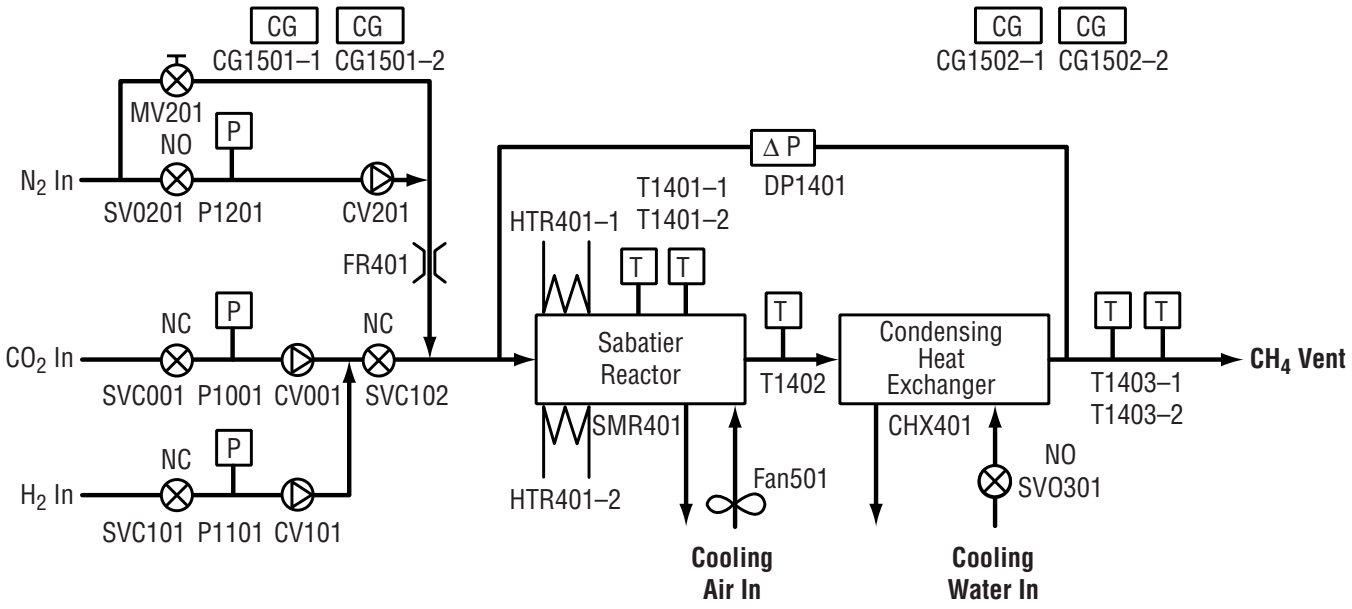

Figure 23. Sabatier reactor subsystem schematic.

The Sabatier reactor subsystem (SRS) consists of a catalytic reactor and an HX accompanied by the necessary valves and sensors for safe operation. The reactor converts CO_2 and H_2 to methane (CH_4) and H_2O according to the following equation:

$$CO_2 + 4\,H_2 \Leftrightarrow CH_4 + 2\,H_2O + \text{heat}\ .$$

The reactor includes heaters to initiate the reaction, and a forced-air cooling jacket to achieve maximum reactant conversion efficiency. The product CH_4 and H_2O are cooled in a CHX such that the liquid H_2O can be separated from the gaseous CH_4 in a phase separator. Valves control the inlet reactant and purge gases as well as cooling the H_2O. Pressure sensors are used on the inlet gases to detect loss of flow. Temperature sensors monitor the reactor and HX; the subsystem controller will shut down the system in the event of an overtemperature situation.

Several of the modifications to the subsystem operation resulted in a number of item changes in the schematic.

4.8.2 Subsystem Refurbishment

Most of the components of the original Tech-Demo Sabatier were nonfunctional upon receipt of the package. Valves and sensors originally designed to be manifold mounted were determined to be too expensive to replace with the same component. As a means of minimizing cost of the project, off-the-shelf items were procured and installed into the subsystem. The only items retained in the new system were the reactor with its associated heaters and thermocouples and the electrical interface box. The items in table 18 are the components of the refurbished subsystem. Table 18 indicates the item number per the schematic in Figure 23 and the vendor part number.

Table 18. Refurbished Sabatier component part numbers.

Item No.	Description	Vendor	Vendor Part Number
CG1501–1	Combustible gas sensor	General Monitors	S104–300–101–101
CG1501–2	Combustible gas sensor	General Monitors	S104–300–101–101
CG1502–1	Combustible gas sensor	General Monitors	S104–300–101–101
CG1502–2	Combustible gas sensor	General Monitors	S104–300–101–101
CHX401	Condensing heat exchanger	Exergy, Inc.	00517–1
CV001	Check valve	Swagelok	SS–4C–10
CV101	Check valve	Swagelok	SS–4C–10
CV201	Check valve	Swagelok	SS–4C–10
DP1401	Delta pressure sensor	Sensotec	060–0890–15A5D
FAN501	Reactor cooling fan	EG&G Rotron	036258
FR201	Orifice	Hoke	1315G4B
HTR401–1	Heater	Watlow	E6–HX–2A
HTR401–2	Heater	Watlow	E6–HX–2A
MV201	Manual valve	Swagelok	SS–1GS4
P1001	Pressure sensor	Omega	PX213–030–GV
P1101	Pressure sensor	Omega	PX213–030–GV
P1201	Pressure sensor	Omega	PX213–100–GV
SMR401	Sabatier reactor	Hamilton Standard	SVSK115480
SVC001	Normally closed solenoid valve	Automatic Switch Co.	EF8262G230,120/60, H2,25
SVC101	Normally closed solenoid valve	Automatic Switch Co.	EF8262G230,120/60, H2,25
SVC102	Normally closed solenoid valve	Automatic Switch Co.	EF8262G230,120/60, H2,25
SVO201	Normally open solenoid valve	Automatic Switch Co.	EF8262G152,120/60, N2,30
SVO301	Normally open solenoid valve	Automatic Switch Co.	EF8262G152,120/60, N2,30
T1401–1	Temperature sensor	RdF Corp	26563
T1401–2	Temperature sensor	RdF Corp	26563
T1402	Temperature sensor	Omega	PR–11–2–100–1/8–6–E
T1403–1	Temperature sensor	Omega	PR–11–Dual–2–100–1/8–6–E
T1403–2	Temperature sensor	Omega	PR–11–Dual–2–100–1/8–6–E

The combustible gas sensors were unreliable and therefore replaced. The original vendor part number was no longer available and was replaced by the part number listed in the table. There are four combustible gas sensors in the package: two over the valve area and two over the area where a phase separator could potentially be installed, as these are the most likely areas for leaks to develop. One of each pair is wired into the controller and displayed on the front panel. The other of each pair is hard-wired to cut power to the subsystem if combustible gas is present and the controller fails to recognize the condition.

The air-cooled HX was replaced with a liquid-cooled HX. Along with the heat exchanger (HX), the fan and air flow switches were removed from the package. Check valves were added to each of the gas inlet lines as a safety precaution to prevent back flow to the subsystems feeding the Sabatier. A spring force of 68.9 kPa (10 psi) was required to ensure that the check valves would close at zero flow condition. The original differential pressure sensor was no longer functional and was replaced. The replacement differential pressure sensor is designed to be used in a wet gas environment. Since the HX cooling fan was removed, a dedicated fan was installed for the reactor cooling function.

An orifice was installed in the N_2 line so as to restrict the N_2 gas usage in the event of a system automatic shutdown or power outage. Since the Sabatier subsystem will likely be run unattended, the orifice will prevent uncontrolled N_2 usage.

The reactor heaters, each 100-W rod heaters, remain unchanged. Both heaters are powered at the same time to heat up the reactor. However; in the event of a failure, a single heater element is sufficient to maintain proper operation.

A manual valve was included along with a separate line that bypasses the N_2 solenoid valve and check valve. In the event the N_2 valve or check valve fails closed, the manual valve can be opened to purge the system prior to maintenance.

Three pressure sensors were added to the gas inlet lines to check for the presence of reactant gases prior to startup and during operation. The pressure sensors are tied into the software shutdown logic. If the pressure drops too low, an indication of loss of reactants, the system will shut down.

The Sabatier methanation reactor is the same basic reactor with the modifications to the insulation and the new catalyst, as discussed in later sections of this report.

The solenoid valves were not functional and were replaced with off-the-shelf valves. This was deemed to be more cost effective than repairing the original valves or replacing the solenoids. The front end of the schematic has the same four inlet gas valves as before. An additional shutoff valve was added to the cooling H_2O supply.

There are five temperature sensors in the subsystem: two in the hot end of the reactor, one between the reactor and the CHX, and two at the exit of the HX. One of the reactor temperature sensors and one of the CHX exit temperature sensors are hardwired to shut down the subsystem in the event that the controller fails to detect an overtemperature condition. The other three sensors go to the controller for monitoring and control and are displayed on the front panel.

Because of the changes to the CHX and the fact that the manifold valves were no longer usable, the frame also had to be replaced. The new subsystem package was designed to accommodate the components with plenty of extra room so that a separator could be included inside the package in the future, if desired.

The reactor was removed from the subsystem package and repacked with improved catalyst. The proprietary catalyst was developed by HS and tested in 1997 under an Internal Research and Development (IR&D) program. This catalyst has higher activity than the previous catalyst and is also more resistant to caking. Acceptance test results are discussed in more detail later in this report. The reactor conversion efficiency of the lean component is 97 percent or better at all conditions tested.

HS has investigated the reactor insulation requirements previously under IR&D programs. The tests showed that the blue light reactor required an additional 6.3 mm (0.25 in.) of insulation in the heated end of the reactor to maintain the temperature above 150 °C (300 °F) through the 37-min standby cycle. This reactor insulation was modified slightly to improve the heat retention in the hot end of the reactor. During cyclic operation, the reactor temperature stays above 220 °C (425 °F) through the duration of the standby period. The catalyst can effectively restart the reaction as long as the temperature is above 150 °C (300 °F).

The air-cooled HX and associated fan and muffler were removed from the package. In place, a liquid-cooled HX was installed. The HX has an effectiveness rating of 98 percent from the manufacturer. The measured effectiveness achieved during acceptance testing was 95 percent. There is probably a certain amount of reheating of the gas stream that occurs, since the gas flow rate is so small and the fluid connections are all metal. The HX is a stainless steel (316L) tube-in-tube coil. The Sabatier subsystem package has cooling H_2O inlet and outlet interfaces on the front panel with a normally open solenoid valve to shut off the coolant flow during the OFF mode once the reactor outlet temperature is <65 °C (150 °F).

In addition to adding cyclic operation capability, controller modifications were necessary to accommodate the hardware changes detailed above. For example, removal of the HX cooling fan and the associated flow switch required modifications in the original control logic. The original software in the package, NSC–800, may not be supportable in the future. In light of the extent of required changes, it is prudent at this time to change the software platform to one that would have easier upkeep in the future. Allen-Bradley was chosen as the new platform since MSFC has experience with them in other applications. The controller is an SLC–5/03 with one analog input card and two digital output cards; only one of the digital output cards is used at this time. It also has a 1747–KE serial port module which has an RS–485 port and an RS–232 port for communications.

The controller uses ladder logic to control the SRS. It safely takes the system through the steps required to transition from one operating mode to another. The controller monitors the analog sensors and operates the valves, and heaters when required. The RS–232 port can be used to create an interface between the Allen-Bradley controller and a PC. The software packages LABVIEW and HighwayVIEW can be used together to communicate through this port.

The controller was programmed to allow both standalone and integrated cyclic operation. In standalone operation, the controller operates the system in PROCESS for 53 min and in STANDBY for 37 min. The standalone cyclic operation is initiated when the system is in PROCESS mode and the PROCESS SELECT button is pressed and held for 3 sec. Cyclic mode is also initiated if the system is in STANDBY mode and the STANDBY SELECT button is pressed and held for 3 sec.

4.8.3 Testing at Hamilton Standard

The following tests were performed on the SRS to show the performance capability of the major components under the expected range of operating conditions.

The assembled subsystem was proof tested at 30 psig, the maximum pressure allowed for the pressure transducers. The subsystem was pressurized and showed no detectable pressure decay over 24 hr.

The controller was tested per the SRS acceptance test plan, SVHSER19376. The controller operation was verified by transitioning the control through the various operating modes and checking for proper output to effectors. The following transitions were verified:

UNPOWERED ⇒ OFF
OFF ⇒ STANDBY
STANDBY ⇒ OFF
OFF ⇒ PROCESS
PROCESS ⇒ STANDBY
STANDBY ⇒ PROCESS
PROCESS ⇒ OFF.

Each of the mode transitions was initiated by pressing the corresponding button on the front of the user interface panel. Each of the transitions occurred as expected. During the testing, the code was modified to add a slight delay to the opening and closing of the mixed gas valve. This would ensure that the pressure sensors would properly detect gas pressure prior to proceeding to the next step. The acceptance test plan details each of the required steps in the transitions and explains the light-emitting diode (LED) indicators on the digital output module of the controller.

In addition to checking the mode transitions, all of the safety shutdowns were exercised. Where feasible, the out-of-tolerance condition was simulated. For example, for the loss of reactant hazard, the shutoff valve on the supply line was closed. In cases such as a high reactor temperature, an electronic signal was used to simulate the problem. Each of the safety shutdowns is detailed in the acceptance test plan, and is repeated in table 19. The controller properly responded to each situation and safely shut down the system. Also, during testing there were a few times when the supply gas bottles emptied during unattended operation. In each instance, the controller shut down the system in a safe manner.

Table 19. Controller shutdowns.

Process Mode				
Problem	**Sensor**	**Reading**	**Simulation**	**Error Message**
No H_2	P1101	<2 psig	Turn off H_2 supply	H_2 pressure: Low
No CO_2	P1001	<2 psig	Turn off CO_2 supply	CO_2 pressure: Low
Bed too cold	T1401	<300 °F	Reduce reactant flow	Bed temp: Low
Bed too hot	T1401–1	>1,200 °F	Unplug T/C	Bed temp: High
	T1401–2	>1,200 °F	Input 27 mV signal	Hardwired shutdown
Flow restriction	DP1401	>5 psid	Input 3 V signal	DP: High
No coolant flow	T1403–1	>150 °F	Shutoff coolant	HX temp: High
	T1403–2	>175 °F	Input mV signal	Hardwired shutdown
H_2 leak	CG1501–1	>25 % LEL	Apply calibration	CG #1: High
	CG1502–1		gas to sensors	
	CG1501–2	>25% LEL	Apply calibration	Hardwired shutdown
	CG1502–2		gas to sensors	
Purge Mode				
Problem	**Sensor**	**Reading**	**Simulation**	**Error Message**
No N_2 heat-up mode	P120	<2	Shut off N_2 supply	Purge pressure low
Heat-up too long	T1401	<300 °F for 5 min	No heater power or reactants	Heat-up time exceeded

The calculated HX effectiveness is listed in table 20. The HX effectiveness is calculated as the actual heat transfer divided by the theoretical maximum heat transfer. The theoretical maximum is the heat transfer that would occur if the hot gas stream were to exit the HX at the same temperature as the coolant inlet temperature. In other words, the maximum is achieved when there is no HX ΔT. The actual heat transfer includes both the latent heat of condensation and the sensible heat transfer. The calculated effectiveness, in most cases, is 95 percent.

Table 20. Heat exchanger effectiveness.

Test No.	CO_2 Flow (lb/hr)	H_2 Flow (lb/hr)	Treact In (°F)	Treact Out (°F)	T Cool In (°F)	T Cool Out (°F)	Q tot (Btu)	Q max (Btu)	Effectiveness (%)
1	0.346	0.106	155	53.4	46.3	48.1	935	981	95.3
2	0.43	0.106	167	53.7	46.5	48.8	1,237	1,294	95.6
2a	0.433	0.106	167	54.5	47.8	50.2	1,238	1,292	95.9
3	0.692	0.106	183	55.2	47.7	51.3	1,928	2,015	95.7
4	1.08	0.106	207	55.0	48.5	53.2	2,749	2,847	96.5
5	0.583	0.106	183	55.4	48.6	52.6	1,799	1,870	96.2
6	0.467	0.106	173	55.6	48.6	51.9	1,372	1,431	95.8
7	0.54	0.053	162	56.4	47.1	48.7	1,020	1,090	93.6
8	0.467	0.085	180	56.0	47.7	50.8	1,410	1,480	95.3
9	0.467	0.106	173	68.0	47.3	50.9	1,267	1,443	87.7

Figure 24 shows the test points selected with respect to the nominal *ISS* flow rates for H_2 and CO_2. The test conditions are reiterated in table 21, which gives the flow rates and molar ratios.

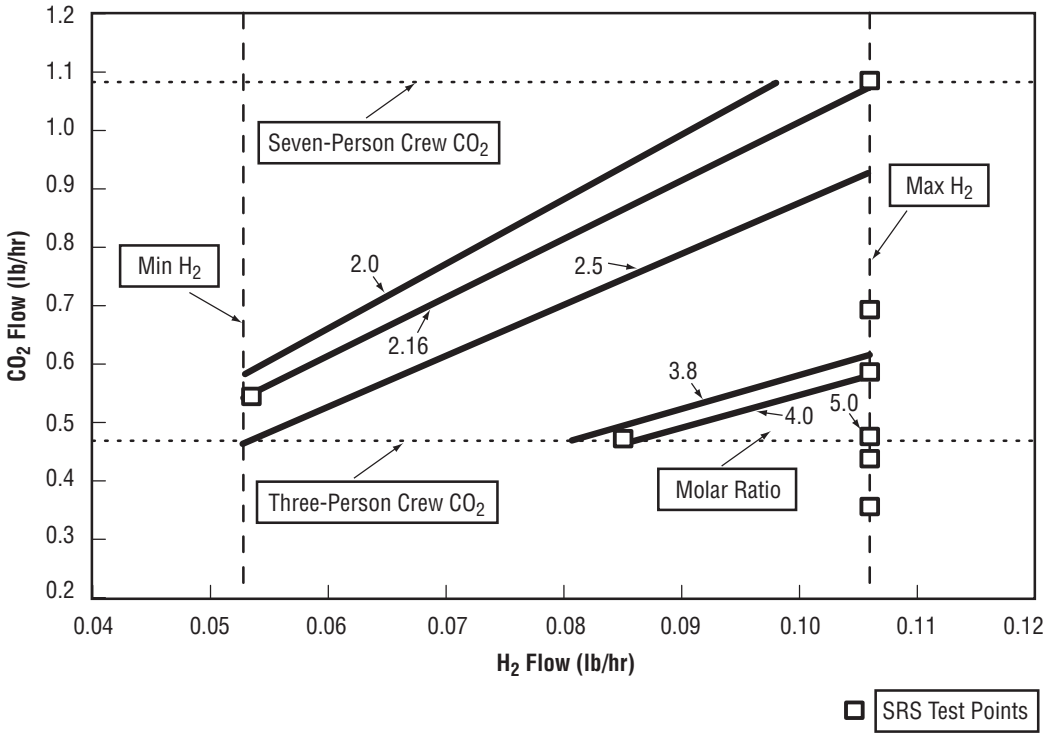

Figure 24. Sabatier operating regime.

The nominal operating regime shown above indicates the most likely operating scenario for a Sabatier subsystem on the *ISS*. The H_2 flow rate would vary between the maximum oxygen generation assembly (OGA) production rate of 48.1 g/hr (0.106 lb/hr) and the minimum flow rate of 24 g/hr (0.053 lb/hr), or 50 percent of the maximum. The CO_2 flow rate could vary between 212 g/hr (0.467 lb/hr), the nominal rate for a three-person crew, and 490 g/hr (1.08 lb/hr), the nominal rate for a seven-person crew.

A Sabatier subsystem designed for *ISS* would most likely operate at a fixed CO_2 flow rate and vary the H_2 flow according to the OGA operation. As an example, the CO_2 flow would be set at a constant rate of 210 g/hr (0.47lb/hr) (corresponding to a three-person crew) then the molar ratio of H_2/CO_2 would vary between 5 and 2.5 as the H_2 fluctuated between the maximum and minimum rate.

The acceptance test points for the SRS attempted to include this variety of operating conditions. The maximum and minimum flow rates of CO_2 and H_2 were included in the test matrix.

The CH_4 product from the reactor was analyzed by gas chromatography (GC) for the lean component. The results of gas analysis are given in table 22. The reaction efficiency is calculated based on the amount of the lean component detected in the product gas stream. The calculation determines the amount of the reactant that was used up, based on the amount remaining in the product stream. The accuracy of GC analysis is much better for smaller quantities of constituents. For these calculations, the lean component value, since it is the smallest quantity, is assumed to be the most accurate.

Further testing will be conducted at MSFC and will consist of three phases: checkout/standalone testing (using bottled CO_2 and H_2 supplies); integrated testing (connected with the 4BMS carbon dioxide removal assembly (CDRA) and the H_2O electrolysis O_2 generator); and integrated into the node 3 simulator testing. The facility must provide the necessary fluid, mechanical, data, control, and power interfaces. To monitor performance of the Sabatier, the mass flows of all fluids into and out of the unit must be monitored. Mass flow meters are needed on the gases (CO_2, H_2, N_2, and CH_4) into and out of the Sabatier. The product H_2O mass is monitored by using an electronic scale.

Table 21. Sabatier reactor subsystem test flow rates.

H_2 Flow g/hr (lb/hr)	CO_2 Flow g/hr (lb/hr)	Molar Ratio	Notes
48 (0.11)	160 (0.35)	6.7	Maximum H_2 flow
48 (0.11)	200 (0.43)	5.4	Max H_2
48 (0.11)	200 (0.43)	5.4	Max H_2
48 (0.11)	310 (0.69)	3.4	Max H_2
48 (0.11)	490 (1.1)	2.2	Max H_2
48 (0.11)	260 (0.58)	4.0	Max H_2
48 (0.11)	210 (0.47)	5.0	Max H_2
24 (0.053)	240 (0.54)	2.2	Minimum H_2 flow
24 (0.085)	210 (0.47)	4.0	Minimum CO_2 flow

Table 22. Sabatier product gas analysis.

Test Number	Molar Ratio	Lean Component	Percent Lean Component in Product	Reactor Efficiency (%)
1	6.7	CO_2	0	100
2	5.4	CO_2	0	100
2A	5.4	CO_2	0	100
3	3.4	H_2	5.3	98.2
4	2.2	H_2	2.1	98.9
5	4.0	Both	9.2 H_2 7.2 CO_2	97.2
6	5.0	CO_2	Sampling error	
7	2.2	H_2	0	100
8	4.0	Both	4.9 H_2 7.1 CO_2	98.5
9	5.0	CO_2	0	100

5. COMPUTER MODEL DEVELOPMENT

5.1 Volatile Removal Assembly[15]

The removal of trace organic contaminants in waste is necessary to meet discharge limits and to allow recycling. In spacecraft applications, such as the *ISS*, complete H_2O recycling is necessary and strict contaminant limits must be maintained in order to make the recovered wastewater streams potable for reuse onboard the *ISS*. Carbon adsorption and ion exchange can remove a majority of the pollutants in such streams. These techniques are incapable of removing a certain category of organic compounds that are weakly adsorbing, such as 2-propanol, 1-propanol, ethanol, and methanol. The alternative technique that will be applied to remove this category of weakly adsorbing organic compounds is a heterogeneous catalytic wet oxidation reactor system known as the volatile removal assembly (VRA), which was designed by NASA to perform this operation. The VRA technology is attractive because of its efficient gas-liquid contacting and lower temperatures and pressures than conventional wet oxidation.

The VRA reactor is a co-current packed column that uses a stoichiometric excess of gaseous oxygen (O_2) as the oxidant and a catalyst consisting of platinum metal on an alumina substrate. In Earth-based testing, the VRA is operated in an upflow mode, which makes the liquid phase the continuous phase. Due to the absence of buoyancy forces in zero gravity, the gas phase will be moved only under the influence of the H_2O's capillary, surface, and drag forces; therefore, the actual contacting time of the gas and liquid phases may be altered. In order to simulate the reactor prior to flight testing, a model must be derived that takes all of the important processes occurring within the model under consideration. The model must incorporate mass transfer, contacting patterns, reaction kinetics on the internal catalyst surface, and multicomponent catalyst adsorption competition in order to properly predict the reactor's performance.

The objective of this phase of the project (phase 2) was to develop a model that will adequately predict the performance of an upflow multiphase catalytic wet oxidation reactor. A similar model was developed during phase 1 of the project. The new models include the following additions: an accounting for byproduct formation and subsequent destruction, and an accounting for competitive multicomponent adsorption on the catalyst surface via the use of a system of Langmuir adsorption isotherms. To accomplish this task, two unsteady-state models were derived from the basic principles of material balances for two differential reactor sections (a cylindrical differential element of the fixed bed, and a spherical shell differential element of a catalyst particle). The two models that were developed are the two-phase pore diffusion model with reaction (PDMR2P) and the three-phase pore diffusion model with reaction (PDMR3P). The PDMR3P is a super set of the PDMR2P.

The kinetic data of adsorption and reaction for each parent contaminant was determined experimentally via the operation of a small-scale differential reactor containing the VRA catalyst. The remaining model parameters were estimated using correlations. The steady-state effluent concentration predictions are obtained by running the unsteady-state model for a sufficiently large amount of simulation.

5.2 Multifiltration Beds[16]

A schematic of an MFB is shown in figure 25. The MFB model was developed to enable engineers to predict the impact of changing process variables on the performance of the MFB. The model will also be used to simulate laboratory and pilot scale experiments. Process variables can be evaluated with the model. These variables include the time variable influent contaminant concentrations (including number and type of contaminants), empty bed contact time, sequence of the ion exchange resins and adsorbents (including number and type) within an MFB or multiple beds, and competitive interactions among ions and adsorbates.

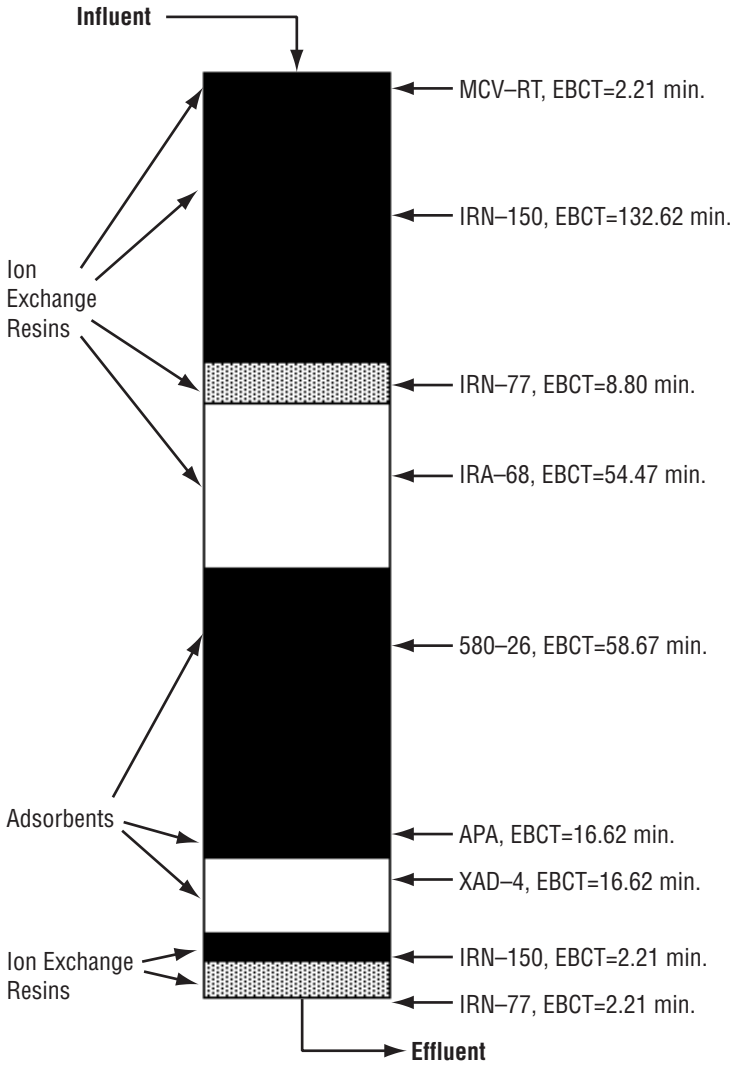

Figure 25. Multifiltration bed schematic.

The first phase of testing focused on verification of the model for a surrogate of the waste shower and handwash stream, termed "ersatz" H_2O. An ersatz H_2O was made up to mimic the TOC adsorption capacity of the actual waste shower and handwash H_2O as it exists after exiting the waste tank storage and prefilter (fig. 26). A TOC isotherm was performed to verify that the TOC adsorption capacity of the ersatz H_2O was similar to that of the actual waste shower and handwash H_2O. Once verified as a suitable surrogate in this manner, the ersatz was treated as an unknown mixture for modeling efforts. Waste shower and handwash H_2O is the most prevalent and most contaminated waste stream in the *ISS*, and contains the component sodium-N_2-methyl-N_2-"coconut oil acid" taurate (SCMT) which is "soap" used for hygiene purposes. Consequently, it was assumed that if the performance of the ion exchange and adsorption processes could be predicted accurately for this waste stream using the MFB model, then the model should be able to predict the performance of the MFB in treating other waste-water streams or their mixtures. A full-scale MFB experiment was performed using the ersatz shower and handwash waste stream. The combined ion exchange and adsorption model was verified by comparing the model predictions to empirical data.

The ion exchange model development includes multicomponent equilibrium as well as external and intraparticle mass transfer. Binary isotherms were conducted to determine separation factors for the ions of interest on each resin. Multicomponent isotherms were conducted and used to validate the multicomponent equilibrium description. Kinetic studies were performed to determine external and intraparticle mass transfer parameters and/or validate the application of literature correlations and validate the multicomponent fixed-bed model.

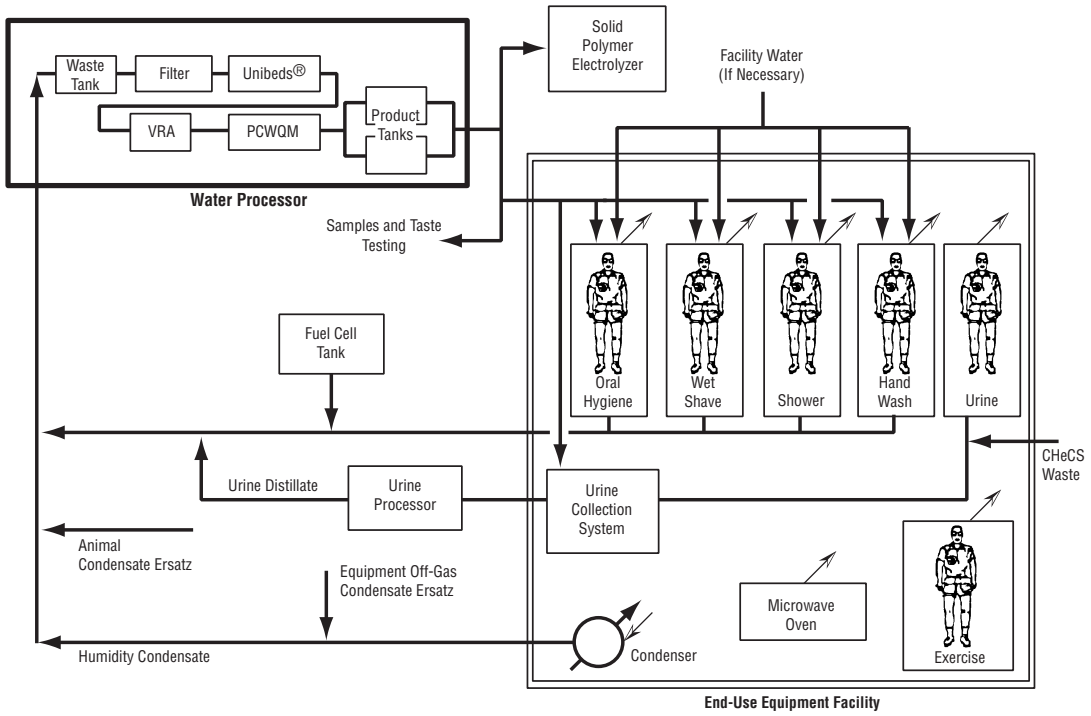

Figure 26. Water recovery system simplified functional schematic.

The adsorption model was developed to predict the removal of individual target compounds and TOC from mixtures of unknown composition. The fictive component analysis (FCA) was developed to describe the competitive interactions between individually known target compounds and the unknown background matrix making up the overall mixture TOC concentration. TOC and known individual target compound isotherms were performed on all the adsorbents and used to determine the fictive component (FC) concentrations. Column studies were performed on all the adsorbents and compared to model calculations to obtain intraparticle mass transfer correlations for the wide range of adsorbing contaminants expected in the *ISS* waste stream and to verify the fixed bed model.

The MFB model was designed for the Microsoft Windows™ environment with a graphical user interface (GUI) to maximize user friendliness. The Microsoft Windows™ interface was used because of its built-in file and hardware control features which frees the analyst from concerns over printer drivers and other machine issues and allows more attention to the computational algorithms. The GUI consists of a front-end shell written in Visual Basic® (Trademark Microsoft Corporation 1981–1995, all rights reserved) that calls Formula Translator (FORTRAN) computer program language subroutines in order to perform calculations.

5.2.1 Ion Exchange Modeling

Ion exchange resins are insoluble matrices containing fixed charged sites which exchange ions for aqueous phase ions. The main types of ion exchange resins are natural mineral ion exchangers, synthetic inorganic ion exchangers, and synthetic organic ion exchangers. The resins investigated in this work are synthetic organic ion exchange resins which include polymer chains crosslinked with divinylbenzene (DVB). Fixed functional groups contained within the matrix provide charged exchange sites as shown in figure 27. Ion exchange resins have been compared to a plate of spaghetti (polymer chain) cooled to the point of sticking (crosslinking) together.

The fixed exchange sites can be positively charged (anionic exchange resins), negatively charged (cation exchange resin), or amphoteric (capable of exchanging both cations and anions, depending on pH). Ion exchange resins are grouped by their functional exchange site characteristics. Ion exchange resins can be strong or weak: strong acid cation (SAC), weak acid cation (WAC), strong base anion (SBA), or weak base anion (WBA). This distinction is based on the functional pH ranges of the resins.

The total number of exchange sites per unit of resin is the total exchange capacity and is independent of the experimental conditions. The apparent capacity depends on experimental conditions, such as pH and solution concentrations, and is usually lower than the total capacity. The capacity of a resin also depends on the presaturant ion such as hydrogen (H_2) or sodium, since the density is different for each form of resin.

Total resin capacities and physical properties for each of the resins were experimentally determined. Fitted apparent capacities were also determined using the binary Langmuir equation. Both the total capacities and apparent capacities are comparable to the reported manufacturer's capacities.

Binary isotherms were performed on SAC (IRN–77), SBA (IRN–78), WBA (IRA–68), mixed-bed (IRN–150), and iodinated (microbial check valve (MCV)–RT) ion exchange resins. Separation

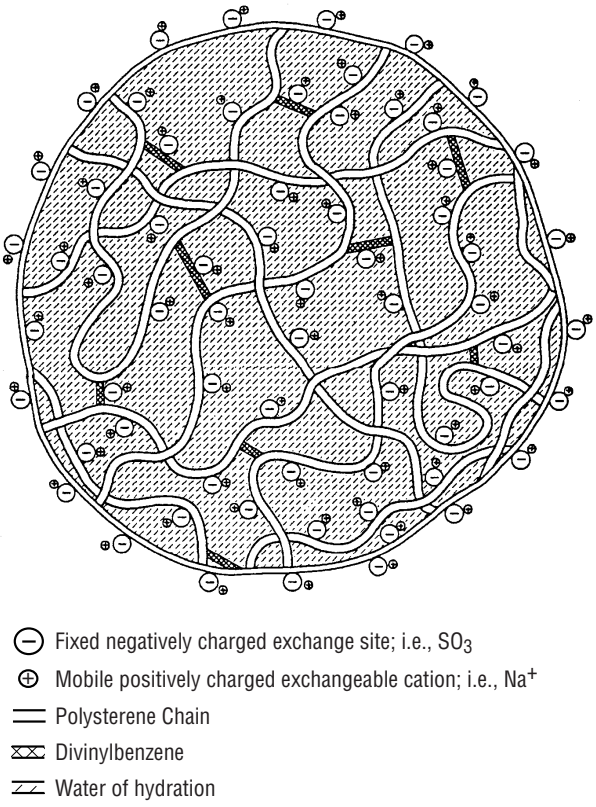

Figure 27. Schematic of hydrated strong acid cation resin.

factors/equilibrium exchange constants for IRN–77, IRN–78, and IRA–68 resins were determined from the binary isotherms. The separation factors for the IRN–77 and IRN–78 resins were able to describe equilibrium for the IRN–150 resin by coupling the H_2O formation reaction with the binary Langmuir equilibrium expression for each ion.

When the separation factors determined from binary isotherms were used, the multicomponent Langmuir equilibrium expression predicted six-component isotherm data for the IRN–77 and IRN–78 resins. The multicomponent predictions were within ≈10-percent error for liquid phase predictions and ≈50 percent for solid phase predictions.

A multicomponent isotherm with the IRA–68 resin was conducted to validate the Langmuir multicomponent equilibrium description for WBA resins. The preliminary model calculations showed promising results. However, more multicomponent equilibrium experiments are needed to verify the multicomponent Langmuir equilibrium expression for WBA resins.

The Langmuir multicomponent equilibrium expression was able to predict the ion exchange in the ersatz H_2O for IRN–77 resin, but overpredicted the amount of ion exchange for the IRN–78 resin. The separation factor determined for SCMT could be underpredicted, or fouling of the anionic resin by the negatively charged SCMT and organic contaminants may have caused the observed decrease in resin capacity.

The ersatz isotherms with IRN–77 did not indicate resin fouling. Fouling of SAC resins by organics, especially by polar and anionic organics, is not usually a problem because the functional groups of SAC resins are negatively charged. The ammonium ersatz isotherm data for IRN–77 resin showed an increased resin capacity for ammonium. A decrease in competition or an increase in capacity could account for this observation. It is possible that binding to soap (SCMT), present in the ersatz H_2O, could decrease the liquid phase concentration of ammonium, causing an apparent increase in solid phase concentration.

5.2.2 Adsorption Modeling

The fixed-bed adsorption model includes multicomponent equilibrium and both external and intraparticle mass transfer resistances. Single solute isotherm correlations were developed to predict single solute isotherm parameters for the components of interest. The single solute isotherm parameters were used in the multicomponent equilibrium description to predict the competitive adsorption interactions occurring during the adsorption process. Multicomponent isotherms were used to validate the multicomponent equilibrium description. Column studies were used to develop and validate external and intraparticle mass transfer parameter correlations for components of interest. The fixed-bed model was verified using the shower/handwash ersatz H_2O.

There were two overall objectives for the MFB adsorption model. The first objective was to predict the performance of the adsorption beds in series in the MFB's for removing TOC from the shower and handwash wastewater. The second objective was to predict the removal of target compounds in the MFB.

The fixed-bed model used in this study assumed both pore and surface diffusion were intraparticle transport mechanisms and that plug flow was the axial transport mechanism. It is named the pore and surface diffusion model (PSDM). Figure 28 illustrates the adsorption and diffusion mechanisms incorporated into the PSDM.

The assumptions and mechanisms that are built into the model are as follows:

- Plug-flow conditions exist in the bed (axial and radial dispersion are neglected).
- Hydraulic loading is constant.
- Single solute adsorption equilibrium is represented by the Freundlich isotherm equation.
- Ideal adsorbed solution theory incorporating the Freundlich isotherm equation describes the multicomponent adsorption equilibrium.
- Local adsorption equilibrium exists between the solute adsorbed onto the adsorbent particle and the solute in the intraparticle stagnant fluid. (The rate of sorption onto the adsorbent surface is much faster than the diffusion rate.)

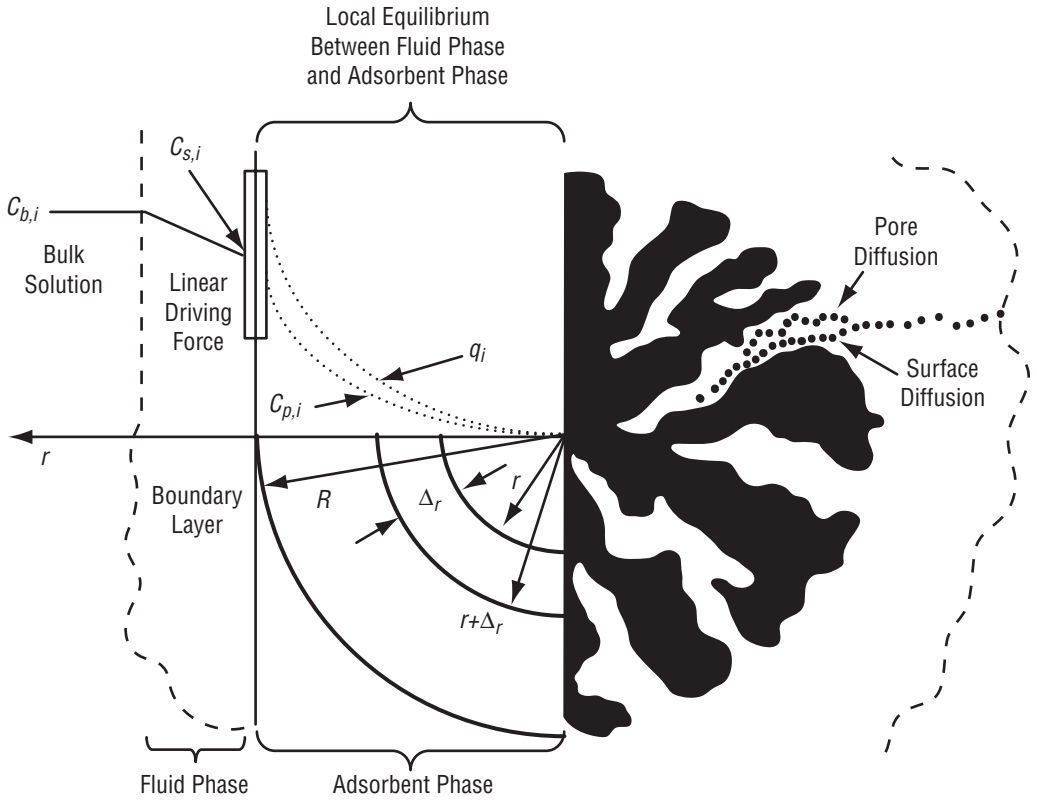

Figure 28. PSDM mechanisms.

• A linear driving force approximation describes the liquid-phase mass transfer flux at the exterior of the adsorbent.

• Intraparticle mass flux is described by surface diffusion and/or pore diffusion.

• There are no solute-solute interactions during the diffusion and/or pore diffusion.

A fixed-bed adsorption model employing the FCA was developed for use in modeling the adsorption processes within the Space Station MFB. This modeling approach was chosen because it can predict the TOC breakthrough as well as target compound breakthrough from the MFB in an unknown mixture. The modeling approach was verified using the shower/handwash ersatz H_2O.

The three adsorbents currently included in the MFB design were evaluated in this study. Those adsorbents were 580–26 granular activated carbon (GAC), APA GAC, and XAD–4 resin. The waste shower and handwash ersatz H_2O included SCMT, trichloroethylene (TCE), toluene, m-xylene, 1,2,4-trichlorobenzene (TCB), and naphthalene as its adsorbable components. These components represent a distribution of weak to strong adsorbing compounds. SCMT was included since it is reported to account for over 60 percent of the TOC in the actual waste shower and handwash H_2O. The ersatz H_2O also contained ions representative of the actual waste shower and handwash H_2O.

Single solute isotherm data were available for each of the adsorbates in the ersatz H_2O on each of the MFB adsorbents. The isotherm data were obtained over a concentration range of ≈10 μg/L to 10 mg/L and described using the Freundlich isotherm equation. The isotherms on the 580–26 and APA activated carbons were all linear on a log-log plot and the Freundlich equation fit the data well. The single solute isotherm on the XAD–4 resin exhibited some curvature on a log-log plot. For this reason, the XAD–4 resin Freundlich parameters were dependent on the concentration range fit.

The single solute isotherm data for each adsorbent were correlated using the Polanyi theory. Polanyi correlations were developed for each adsorbent using the molar volume of the compound as the correlating physical parameter, and the compound's aqueous solubility was used in determining the adsorption potential. The data were correlated so that Freundlich isotherm parameters for compounds other than TCE, toluene, m-xylene, 1,2,4-TCB, and naphthalene could be estimated. The error in the correlation could possibly be removed by refining the correlation for different compound classes. The use of different physical property correlating factors (other than molar volume) could also result in a better correlation.

A TOC isotherm was performed on the actual waste shower and handwash H_2O to determine its TOC adsorption capacity. The isotherm revealed, as expected, that the waste shower and handwash H_2O was a multicomponent mixture with a nonadsorbing TOC fraction. Unfortunately, this was the only isotherm data obtained for the actual waste shower and handwash H_2O.

Isotherms were performed on each of the adsorbents using the ersatz H_2O. The isotherms were analyzed for TOC and the individual constituents of the H_2O. The FCA was applied to this isotherm data to determine the TOC and tracer FC for each adsorbent. The FC's were determined from fitting the isotherm data in a manner which would facilitate beds in series modeling of the different adsorbents. The FCA was able to accurately fit the TOC isotherms for each of the adsorbents. This indicated that the TOC FC used in ideal adsorbed solution theory (IAST) calculations accurately simulated the TOC adsorption capacity of the ersatz H_2O.

The FCA was also able to fit the tracer isotherms well for each of the adsorbents. The tracer FC's were tested in IAST calculations to see if the equilibrium of the other ersatz H_2O constituents could be predicted based on the tracer fit. The results indicated that as the adsorbability of the compound increased, the accuracy of the model prediction to the data decreased. The model generally did a good job of predicting the equilibrium for TCE, toluene, and m-xylene. The equilibrium description consistently overpredicted the reduction in capacity for 1,2,4-TCB, naphthalene, and SCMT in the system. The reduction in capacity for naphthalene and 1,2,4-TCB was demonstrated by the adsorption of a weaker adsorbing tracer. The stronger adsorbing compounds were already represented by the FC's. Therefore, model overprediction is likely. The reduction in capacity for SCMT was overpredicted because SCMT made up such a large percentage of the overall TOC of the mixture. A component must make up a small amount of the TOC in the mixture because its adsorption potential is already accounted for by the FC. The fits and predictions were more accurate for the XAD–4 resin than for either of the activated carbons.

Column experiments were performed on each of the adsorbents using the ersatz H_2O. The breakthrough curves for each of the known ersatz H_2O constituents were fit on a single solute basis using the PSDM to determine the optimum fluid residence time in the packed bed and the surface to pore diffusion

flux ratio (SPDFR) for each compound. The fitting results were used to develop correlations for prediction of fluid residence time in the packed bed and SPDFR for other target compounds on each adsorbent. The results indicated that pore diffusion was the controlling mass transfer mechanism for both 580–26 and APA GAC's. Surface diffusion was ≈5 times more important than pore diffusion in describing the mass transfer for the XAD–4 resin. The mass transfer parameter correlations were used to predict the mass transfer parameters for the FCA.

The TOC FC's were used in the PSDM to predict the TOC breakthrough from each of the adsorption columns. The results indicated that the model slightly overpredicted the capacity of the columns for TOC adsorption. The model calculations involved using the six TOC FC's determined from fitting the TOC isotherms in fixed-bed calculations.

The tracers FC's were used in the PSDM with the known constituents of the ersatz H_2O to predict breakthrough of those compounds. The model calculations used the target compound and the five tracer FC's determined from fitting the tracer isotherms in fixed-bed calculations. The results were then compared to the experimental data to test the model. The model predictions were best for the weak to moderate adsorbing compounds. As the strength of the adsorbing compound increased, the accuracy of the PSDM prediction consistently decreased. This is due to the mass transfer parameters and tracer FC used in the system. The mass transfer parameters and tracer FC could be tuned to better predict the breakthrough of the stronger compounds.

One experiment was performed using a series of adsorbents and ion exchange resins set up in the same configuration as the actual MFB design. This experiment was also performed with the ersatz H_2O. The breakthrough of TOC and target compounds from the verification MFB was predicted with the fixed-bed model and compared to the breakthrough data. The model predicted the TOC breakthrough slightly before the experimental data, and did a good job predicting the SCMT breakthrough. The breakthrough prediction began slightly after the data but was steeper than the data, indicating that the mass transfer parameters used for the SCMT could use some fine tuning to get a better prediction. The model predicted TCE breakthrough occurred ≈15 percent earlier than the data. The error appears to be due to the mass transfer parameters. The predicted breakthrough of toluene is significantly later than the experimental data. However, it is difficult to determine if the error is due to mass transfer parameters of capacity since only part of the curve was observed during the experiment. The error in the MFB verification column predictions may have occurred since the SCMT was held up for some time period in the ion exchange resins but it was not held up in the experiments where the mass transfer parameter correlations were determined. This error could be corrected by tuning the mass transfer parameters for this situation. These results have shown that the FCA used in conjunction with the PSDM can predict breakthrough of both TOC and target compounds from the MFB. However, this verification was only on ersatz H_2O.

6. SUBSYSTEM AND INTEGRATED TESTING

6.1 Integrated Air Revitalization Test[17,18]

Testing of the *ISS* U.S. Laboratory baseline configuration of the Atmosphere Revitalization Subsystem (ARS) by MSFC has been conducted as part of the ECLSS design and development program. This testing addressed specific questions with respect to the control and performance of the baseline ARS subassemblies in the *ISS* U.S. Laboratory configuration. The test used pressurized O_2 injection, a mass spectrometric major constituent analyzer (MCA), a 4BMS CDRA, and a trace contaminant control subassembly (TCCS) to maintain the atmospheric composition in a sealed chamber within *ISS* specifications. Human metabolic processes for a crew of four are simulated according to projected *ISS* mission timelines.

The integrated atmosphere revitalization test (IART) builds upon previous integrated ECLSS testing conducted at MSFC between 1987 and 1992. The IART is designed to address ARS control and performance issues that are peculiar to the *ISS*. These issues resulted from the *ISS* ECLSS configuration development, design requirement changes since 1992, and the increased maturity of each ARS subassembly's design. IART test objectives, facility design, pretest analyses, test and control requirements, and test results are presented.

In order to determine whether the U.S. Segment ARS can adequately achieve *ISS* requirements, the phase 5 IART was conducted. Primary objectives for the test were the following:

1. Demonstrate integrated ARS operation under remote automatic control

2. Provide performance data on O_2 and CO_2 partial pressure ($ppCO_2$) control for a crew of four

3. Demonstrate automated O_2 partial pressure control using the MCA signal as control input to an O_2 injector

4. Demonstrate cyclic operation of the OGA and CDRA on a day/night orbital cycle to accommodate *ISS* power allocations

5. Demonstrate OGA performance using reclaimed H_2O from *ISS* WP testing

6. Determine the MCA H_2O vapor measurement accuracy through a remote sample delivery system.

These objectives addressed specific issues associated with the operation and control of the baseline U.S. Laboratory ARS configuration and its capability to achieve *ISS* program requirements.

It should be noted that they do not investigate trace chemical contaminant control. Based upon the complexity of such a test, TCCS performance is being conducted as a follow-up to the IART. Objectives for the contaminant injection test include investigating the effects of humidity, temperature, and the control assist provided by the CDRA and the THC subsystem.

6.1.1 Test Configuration

6.1.1.1 Test facility description. The phase 5 IART was conducted in the core module simulator (CMS). The CMS is a 175-m^3 (6,180-ft^3) sealed chamber that provides a closed working volume and connections to facility power, data, and consumable resources.

Facility support hardware is provided to simulate human metabolic production of H_2O vapor and CO_2, human metabolic consumption of O_2, and space vacuum. Facility THC are provided inside the CMS to maintain the temperature and humidity conditions within *ISS* specifications. Additional facility gas analysis capability is provided by a GC and an infrared (IR) CO_2 analyzer. These instruments are designed to not only provide a continuing verification for MCA results but also to study the CDRA process in detail.

The ARS hardware is mounted inside the CMS with control and data acquisition provided from remote workstations located in the control room. The MCA, gas chromatograph, and IR CO_2 analyzer are mounted externally to the CMS. Figure 29 shows the arrangement of the IART test hardware.

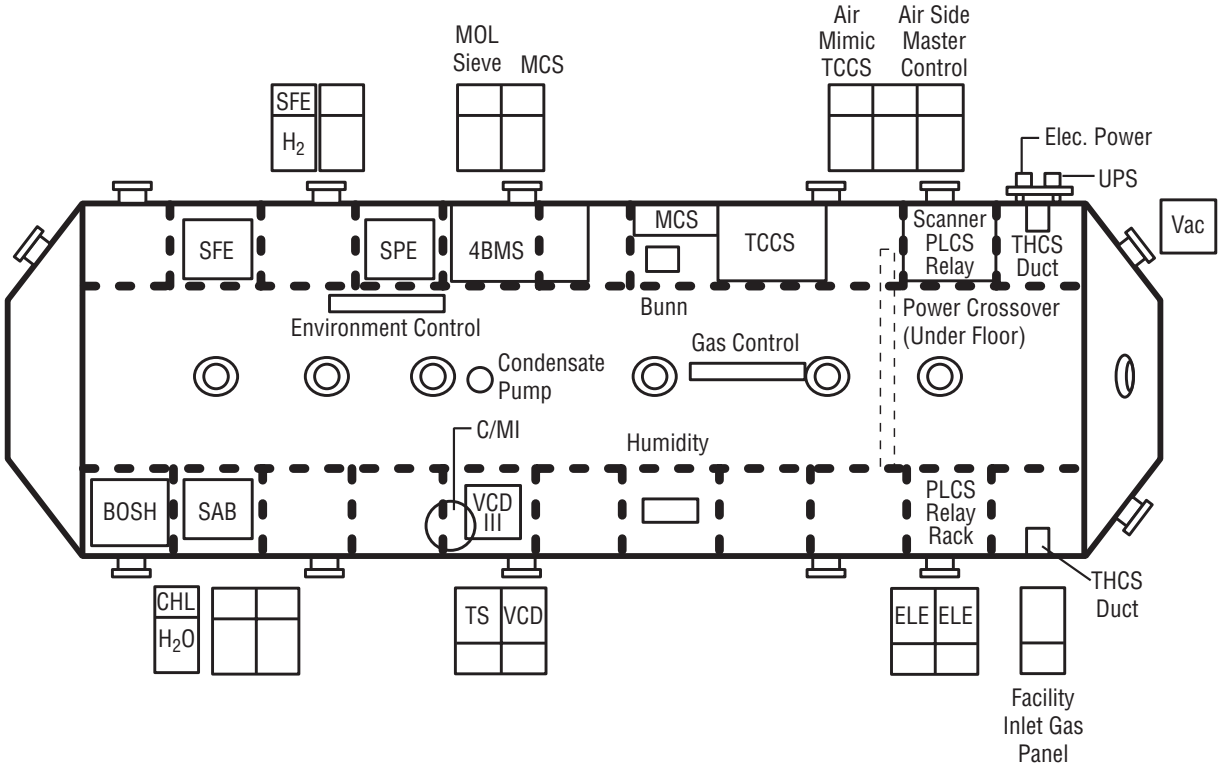

Figure 29. CMS hardware layout.

6.1.1.2 Atmosphere revitalization subsystem test configuration. During the test, facility-provided hardware removes O_2 and H_2O vapor from the CMS atmosphere. Temperature is also controlled by facility hardware. H_2O vapor and CO_2 are injected into the THC subsystem according to rates projected by *ISS* crew activity timelines. The CDRA inlet interfaces with the facility temperature and THC. Air processed by the CDRA exhausts into the THC upstream of the HX. The TCCS inlet interfaces directly with the CMS atmosphere and its exhaust combines with the CDRA exhaust before it is returned to the THC. Air samples are pumped to the externally mounted MCA and exhausted back into the CMS to minimize gas losses. The signal from the MCA is conditioned and sent to the OGA or O_2 injection control valve. Humidity condensate is collected and used in the metabolic simulator. Additional chamber air samples are collected and analyzed using grab sampling and an inline GC and a CO_2 analyzer.

6.1.2 Test Operations Summary

Integrated testing began on March 12, 1996, and continued until April 18. During this time, a cumulative total of 30 days of operation with two periods of uninterrupted operation was obtained. The first uninterrupted period lasted 7 days (March 22 through 29) while the second period continued for a 12-day duration (March 30 through April 12). An additional 4 days of testing was conducted on the MCA to investigate its response to transient humidity changes in the chamber. All testing was completed on April 18.

6.1.2.1 Subassembly performance. Overall, the ARS operated smoothly with no major subassembly anomalies. The MCA experienced a single shutdown on March 21 due to a high electrical current to its ion pump. This shutdown was traced to a failed delay circuit that was not flight-like and, therefore, not necessary for conducting the test. The circuit was bypassed and the MCA operated with no problems for the remainder of the test.

The CDRA experienced two anomalies. The first occurred on March 21 and caused the unit to shut down. The cause for the shutdown was traced to an airflow selector valve that was not in the proper position. The CDRA was restarted and the problem did not repeat during the remainder of the test. It is thought that a facility power surge or voltage decay may have caused an inadequate current to the valve resulting in its improper positioning. The second anomaly occurred on April 3 when one of the sorbent bed heaters did not receive electrical power for ≈3 hr. This problem corrected itself and no explanation could be found. The CDRA sorbent beds are to be refurbished following the test. Attention will be given to possible electrical shorts and other potential causes for this problem.

6.1.2.2 Facility performance. Facility anomalies accounted for the majority of problems encountered during the test. Most facility-related anomalies were minor and were corrected quickly. The first anomaly occurred on March 16 when the facility electrical power failed. This caused the entire test facility to shut down temporarily. About 1.5 hr of processing time was lost before the test was restarted.

Facility-provided gas monitors were responsible for several interruptions in the metabolic simulation program. During calibration of the GC, communication errors with the host computer caused the metabolic simulation program to shut down. These shutdowns had no impact to the test other than a brief interruption of the metabolic simulation. The program was quickly restarted in each case. On one occasion, however, this problem caused the H_2O injection tank to completely empty. As a result, the test

chamber had to be opened on March 30 to prime the injection pump. This caused an interruption in the consecutive uninterrupted test days; however, it could be argued that entering the chamber was no greater impact to the test than a pressure relief event, since the O_2 and $ppCO_2$ control was not affected.

The test chamber was also opened on March 13 and March 16 to make other repairs to the H_2O injection system. On March 13, the H_2O injection system pump failed. It was found that a metering valve was set too tightly and became blocked with debris. The valve was opened wider and control parameters were reset. After the facility power failure on March 16, H_2O injection system setpoints for the injection tank scale had to be reset. The test chamber was entered to reset the scale setpoints and connect it to an uninterruptable power supply to prevent a recurrence. In both instances, O_2 and $ppCO_2$ control was not affected.

The final test facility anomaly occurred on April 8 when the daily rate of O_2 injection into the chamber began to decline from its normal 3 to 4 kg/day (7 to 9 lbm/day) to 0.7 kg/day (1.5 lbm/day). At the same time, the N_2 injection rate increased. Analysis of the test data indicated that total pressure control had lost its assist from the O_2 injection system. A possible cause for this was O_2 removal subassembly failure. The gas removal rate for the O_2 removal subassembly did not change; however, an analysis of the gas composition from the subassembly showed a composition of 73.6 percent N_2 and 25.1 percent O_2. The normal outlet gas composition for this device is 99 percent O_2 and 1 percent N_2; therefore, it was confirmed that the unit had failed. Since the O_2 removal unit failure occurred near the end of the test and it did not effect the operations of the MCA, the test was not shut down to repair it.

6.1.2.3 Overall test assessment. The IART had the fewest problems of any integrated test conducted. With very few exceptions, the test facility operated flawlessly, allowing a very accurate assessment of the ARS's ability to assist in controlling total pressure, O_2 partial pressure, and $ppCO_2$, using *ISS*-specified operating conditions.

6.1.3 Discussion of Results

6.1.3.1 Carbon dioxide partial pressure control. The CDRA-provided $ppCO_2$ control throughout the test in the range of 333 Pa (2.5 mm Hg) to 467 Pa (3.5 mm Hg). This control range is well below the *ISS* 24-hr allowable of 706.6 Pa (5.3 mm Hg). Figure 30 shows a typical $ppCO_2$ profile based upon the MCA CO_2 response. This response was shown to compare favorably with facility-provided instrumentation during the course of the test. Similar responses were obtained for O_2 and H_2O vapor during the test.

The $ppCO_2$ remained within this range during the entire test except for a period of time on April 3, coinciding with the sorbent bed heater malfunction. During this time, the partial pressure rose to ≈507 Pa (3.8 mm Hg). Once the heater began functioning normally again, the $ppCO_2$ was reduced to <467 Pa (3.5 mm Hg).

During the test, the CDRA performance was monitored for potential H_2O breakthrough of the desiccant beds. This was a concern because of the lower regeneration temperature and shorter one-half cycle time used for the test. No evidence of H_2O breakthrough was observed during the test. The sorbent bed heater malfunction did give the appearance of H_2O breakthrough. However; once the heater began

to operate properly again, the CDRA's CO_2 removal performance returned to normal. It may be necessary for a much longer test to be conducted to determine how long the CDRA may operate in the low-temperature, power-saving mode before H_2O breakthrough occurs.

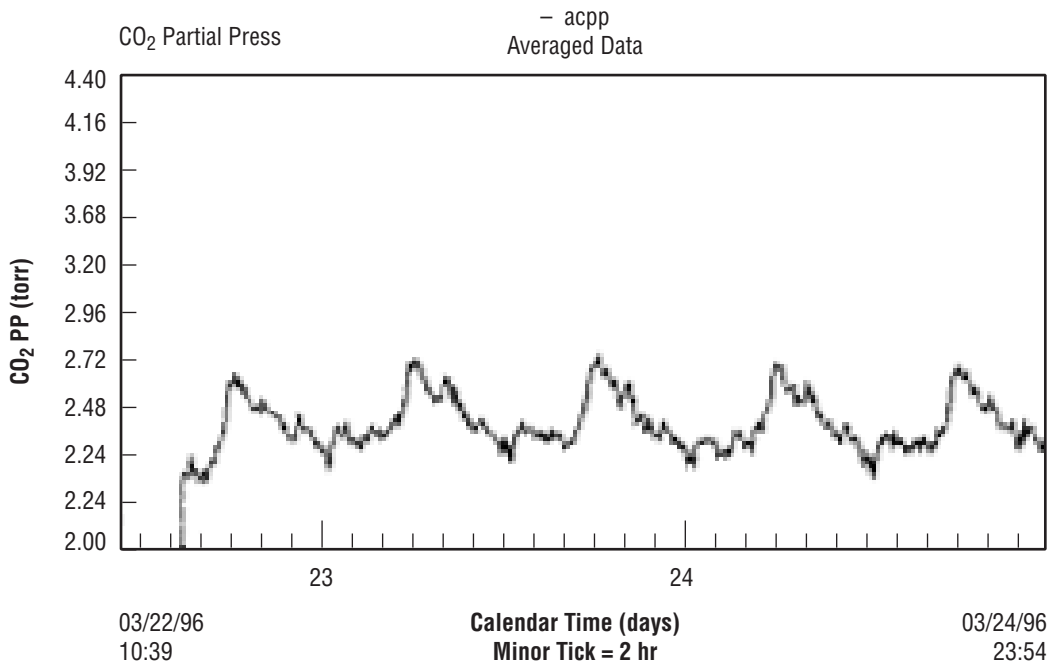

Figure 30. Carbon dioxide partial pressure profile (MCA).

6.1.3.2 Oxygen partial pressure control. Oxygen partial pressure was maintained between ≈20.5 kPa (2.98 psia) and 20.8 kPa (3.02 psia). A typical O_2 partial pressure profile is shown in figure 31. As with CO_2, the O_2 partial pressure fluctuated according to the metabolic simulation; however, the effects were not as strongly pronounced as for CO_2. Oxygen partial pressure was maintained within *ISS* specification for the entire test, thus demonstrating that the MCA O_2 partial pressure signal can be used for control.

6.1.3.3 Temperature and total pressure. Test chamber total pressure was maintained >0.40 kPa (3 mm Hg) above ambient pressure and did not exceed 1.6 kPa (12 mm Hg) above ambient pressure except on March 30, after the metabolic simulation program had malfunctioned. The excess pressure was vented. After this event, the total pressure was maintained within the specified range of 0.40 kPa (3 mm Hg) to 0.93 kPa (7 mm Hg) above ambient pressure. The test chamber temperature was maintained between 21 °C (70 °F) and 22 °C (72 °F) during the entire test. Figures 32 and 33 show typical profiles for total *P* and *T*.

6.1.3.4 Humidity control. The dewpoint inside the test chamber was maintained at ≈10 °C (50 °F). The MCA response to H_2O vapor was found to be steady and no measurable sensitivity to the sample line length was observed. Figure 34 shows a typical MCA H_2O vapor response.

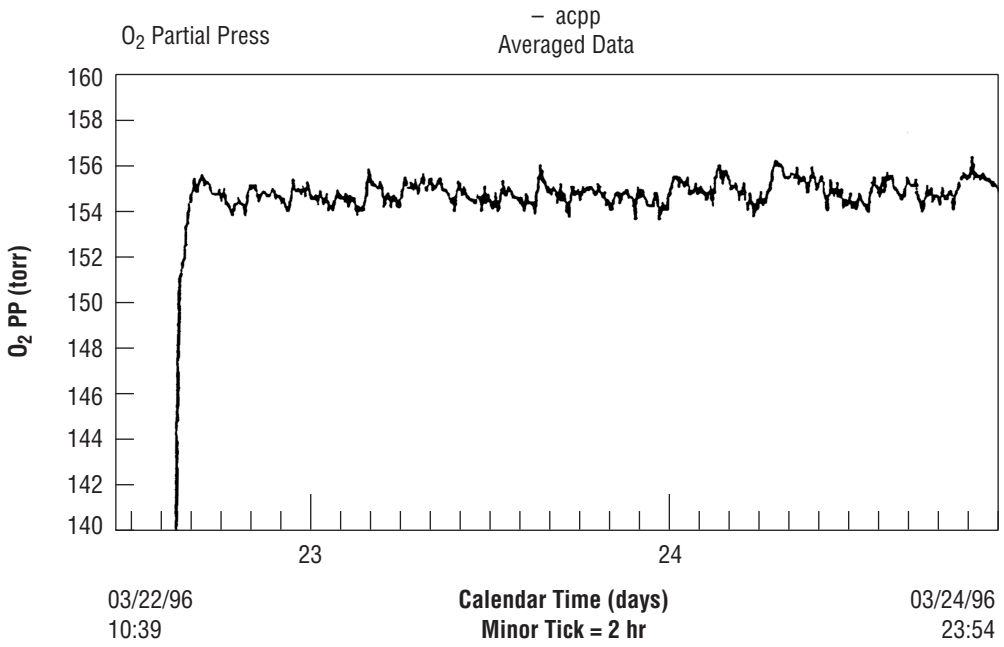

Figure 31. Oxygen partial pressure profile (MCA).

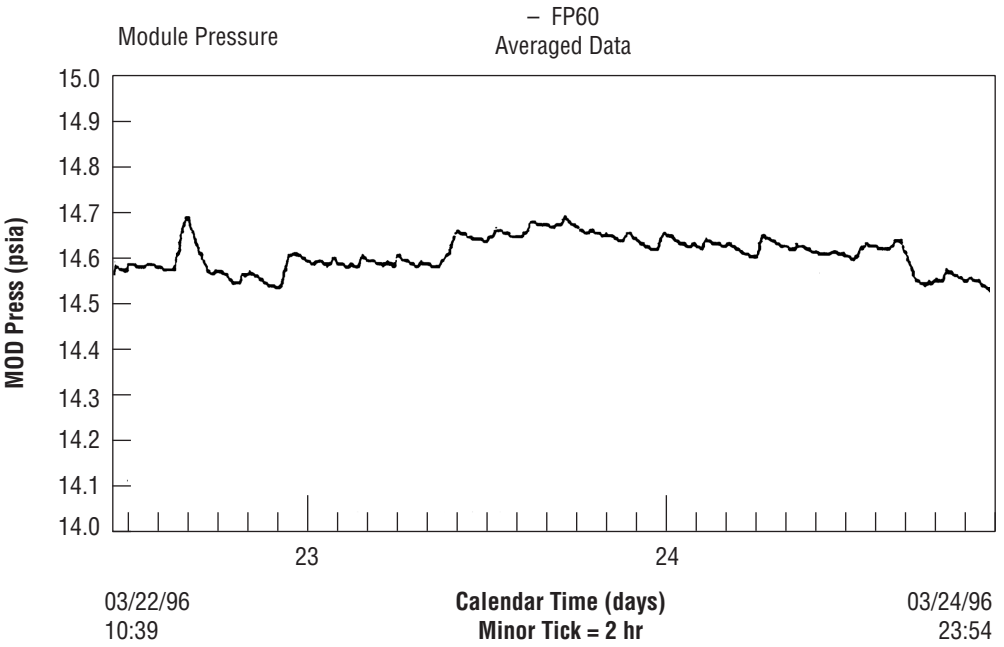

Figure 32. Typical test chamber total pressure profile.

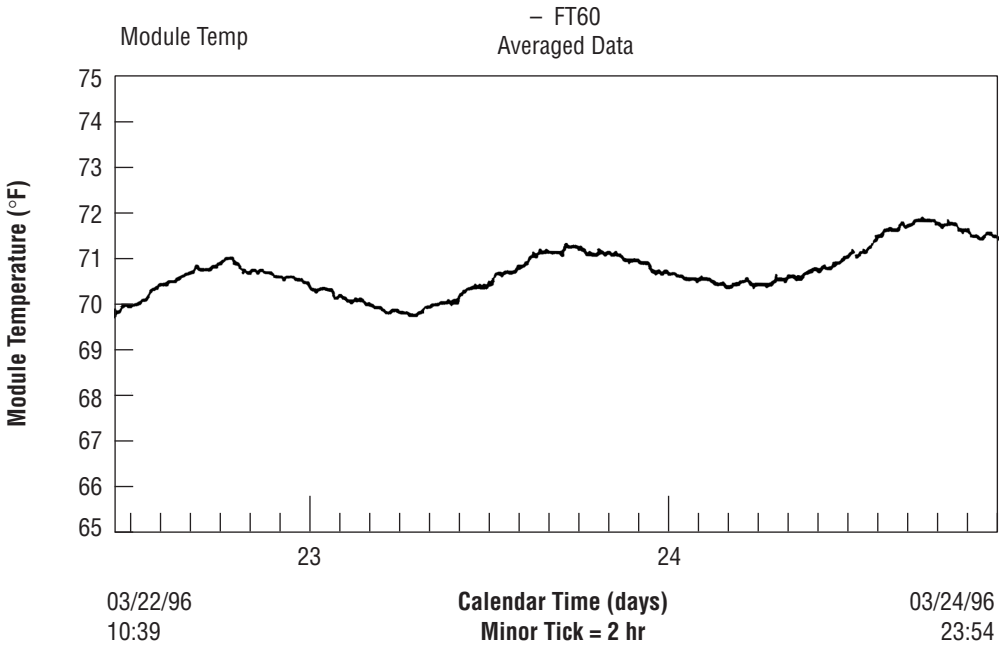

Figure 33. Typical test chamber temperature profile.

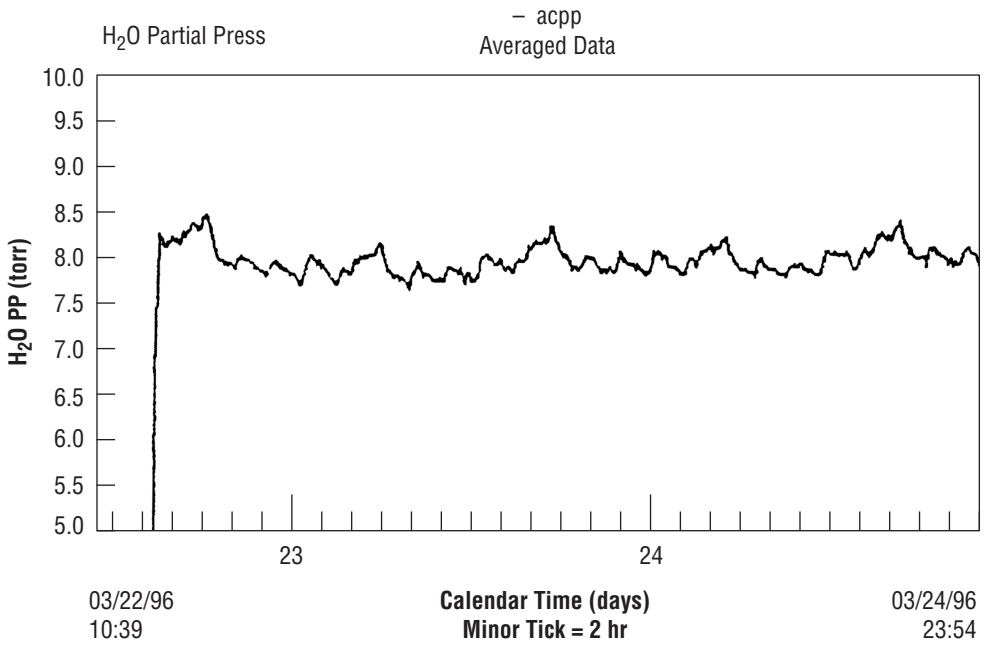

Figure 34. Typical MCA water vapor response.

6.1.4 Conclusions

Conclusions drawn from the individual subassembly checkout and the integrated ARS testing are as follows:

1. The CDRA can achieve CO_2 control specifications while cycling the desorption heaters in a day/night power cycle.

2. The CDRA power-saving mode with a heater temperature setpoint of 121 °C provides substantial power savings while meeting CO_2 removal specifications for injection rates tested.

3. Oxygen partial pressure can be successfully controlled using the signal from the MCA as input to an O_2 supply source.

4. The signal output provided by the MCA is very stable and is suitable for use in atmospheric composition control onboard the *ISS*.

5. The MCA H_2O vapor measurement is not sensitive to sample line length and is capable of accurately tracking humidity upsets in the *ISS* cabin.

6.2 Contaminant Injection Test[19]

Trace contaminant control onboard the *ISS* will be accomplished not only by the TCCS but also by other ECLSS subassemblies. These additional removal routes include absorption by humidity condensate in the THC CHE and adsorption by the CDRA. The trace contaminant injection test, which was performed at MSFC in November and December 1997, investigated the system-level removal of some common spacecraft trace contaminants by these *ISS* systems and subsystem. It is a follow-on to the IART conducted in 1996 (sec. 6.1 of this report).

In the closed environment of a spacecraft, such as the *ISS*, trace contaminant buildup is a major concern. Contaminants are generated by equipment offgassing, human metabolic processes, and the metabolic processes of animals. The contaminants, if not removed, will build up in the cabin atmosphere leading to an increased health risk to the crew. The TCCS was designed to remove trace contaminants from the *ISS* cabin air. Other equipment, such as the CDRA and the THC subsystem, is designed specifically to remove CO_2 and H_2O, respectively, from the atmosphere. It is suspected, however, that the CDRA and THC will also contribute to the removal of trace chemical contaminants found in the cabin atmosphere. The trace contaminant injection test (TCIT) was designed to evaluate the CDRA and THC with respect to its ability to remove trace contaminants. The test is a follow-on to the IART conducted in 1996.

There are numerous contaminants which may be found within the *ISS* cabin. The TCIT would be far too complex if all the possible contaminants were tested. That being the case, eight contaminants were chosen to represent the most common types expected. They are the following:

• Methane—A common metabolic byproduct, and a very difficult molecule to oxidize

• Ammonia—Another common metabolic byproduct, and an extremely H_2O-soluble chemical

• Carbon monoxide—A minor metabolic byproduct, a biological poison, and a common byproduct of incomplete combustion processes

• Carbon dioxide—The most abundant metabolic byproduct, and the target of CDRA operation

• Dichloromethane—A common solvent used in fabrication and the electronics industry, a typical offgas contaminant, and a relatively polar chemical

• m-Xylene—A common solvent used in fabrication and the electronics industry, a typical offgas contaminant and a very stable aromatic chemical

• Acetone—A common solvent used in fabrication and the electronics industry, a typical offgas contaminant and a relatively nonpolar chemical

• Methanol—A common solvent used in fabrication and the electronics industry, a typical offgas contaminant, and a highly H_2O-soluble chemical.

The contaminants were injected into a test chamber at rates expected to provide equilibrium concentrations near the spacecraft maximum allowable concentration (SMAC) as determined by pretest analysis. The injection rates are summarized in table 23.

Table 23. Contaminant injection rates.

Contaminant	Rate	Contaminant	Rate
Acetone	23.63 μL/min	Carbon monoxide	0.61 mL/min
Dichloromethane	1.92 μL/min	Methane	8.59 mL/min
Methanol	9.39 μL/min	Ammonia	49.2 mL/min
m-Xylene	32.46 μL/min		

H_2O, N_2, CO_2, and O_2 were injected by a metabolic simulator. N_2, O_2, and CO_2 were maintained in the test chamber, at typical atmospheric levels, and H_2O at 50-percent relative humidity. The trace contaminant concentrations were then monitored at various points within the test chamber via a sample delivery system.

6.2.1 Test Configuration

6.2.1.1 Test facility overview. The CMS served as the test chamber for the TCIT. The CMS is a large, cylindrical SS vessel outfitted with facility test equipment. A door at one end of the CMS can be sealed, giving a nearly air-tight volume.

The TCCS, CDRA, and THC were integrated inside the CMS while the MCA was located outside. Instrumentation and equipment for gas analysis, gas sample collection, contaminant injection, and facility control are also a part of the CMS. Figure 35 provides an overview of the hardware architecture for the TCIT. The following discussion summarizes the major test equipment used during the TCIT.

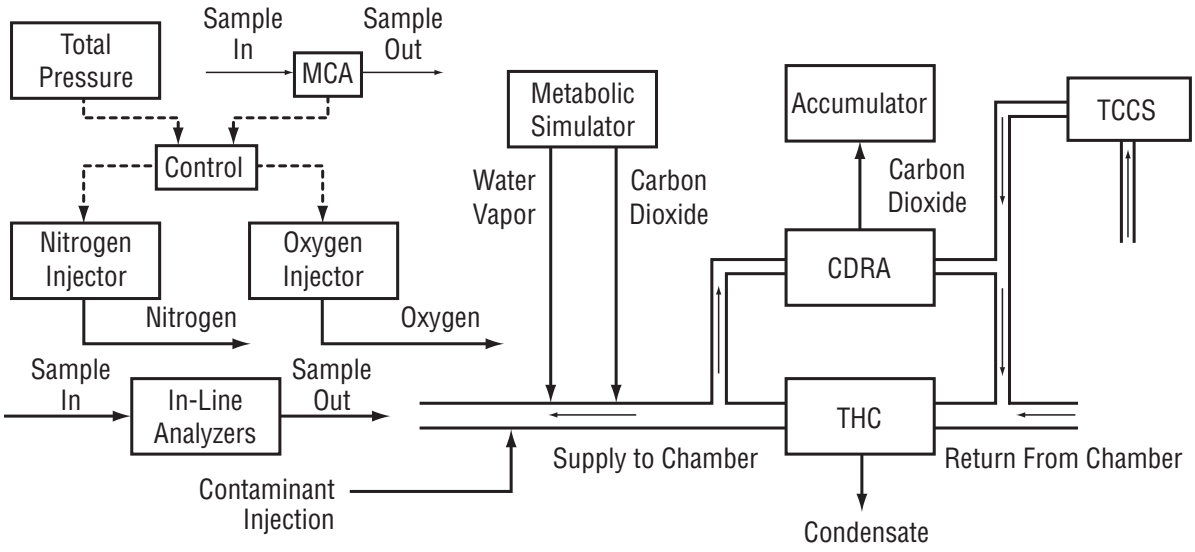

Figure 35. TCIT configuration.

6.2.1.2 TCCS overview. The TCCS, shown schematically in figure 36, utilizes phosphoric acid impregnated granular activated C_2, a high-temperature oxidation catalyst (0.5-percent palladium on 3.175-mm alumina pellets), and granular lithium hydroxide (LiOH) sorbent beds for contaminant removal. The primary oxidation byproducts are CO_2 and H_2O.

Trace contaminant-laden air enters the TCCS from the cabin atmosphere and through the activated C_2 bed at 15.29 m^3/hr (9 scfm). A portion of this air stream, 4.59 m^3/hr (2.7 scfm), is diverted to the catalytic oxidizer and the LiOH bed. Contaminants are oxidized at 400 °C (750 °F) within the catalyst bed and acidic byproducts are removed in the LiOH bed.

6.2.1.3 CDRA overview. The CDRA, shown schematically in figure 37, removes excess CO_2 from the cabin atmosphere. Air enters the CDRA at 50.97 m^3/hr (30 scfm) through a molecular sieve/silica gel desiccant bed. This bed removes all moisture from the air stream before it enters the CO_2 sorbent bed. The CO_2 sorbent bed consists of zeolite 5A molecular sieves, which removes CO_2 from the dry air stream. After being stripped of CO_2, the air stream passes through a moisture-laden desiccant bed which was loaded in a previous CDRA cycle. The dry air is saturated with moisture, and the now wet CO_2-free air, passes back into the *ISS* cabin via the THC duct network, which circulates at 737 m^3/hr (434 scfm). This all takes place while a second sorbent bed is being heated and exposed to a vacuum removing previously loaded CO_2. The CO_2 released is either stored in a pressurized vessel for recycling, or dumped to space vacuum. The system then flips cycle, and the process is repeated on the opposite pairs of sorbent and desiccant beds. Cooling H_2O to the CDRA circulates at 119.1 kg/hr (262 lb/hr) at a temperature of 15.1 °C (59.2 °F).

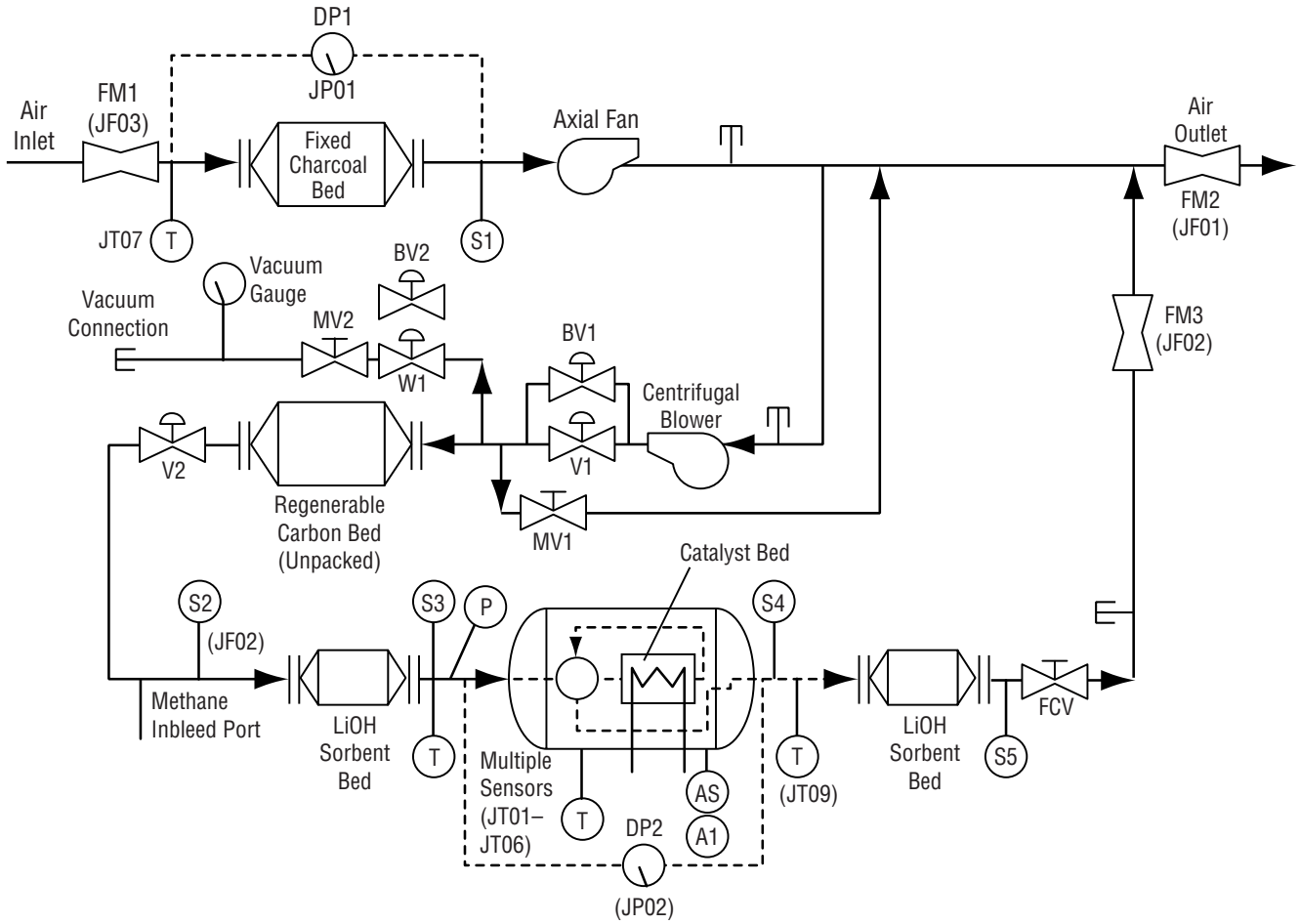

DP=Differential Pressure Sensor	MV=Manual Isolation Valve	S=Sample Port
V=Valve	T=Temperature Sensor	FCV=Flow Control Valve
VV=Vacuum Valve	A=Current Meter	FM=Flow Meter
BV=Bleed Valve	AS=High-Temperature Shutoff	F=Facility (ex.FT01)
J=Subassembly (ex. JT01)	( )=Life Test Port Designation	

Figure 36. Trace contaminant control subassembly.

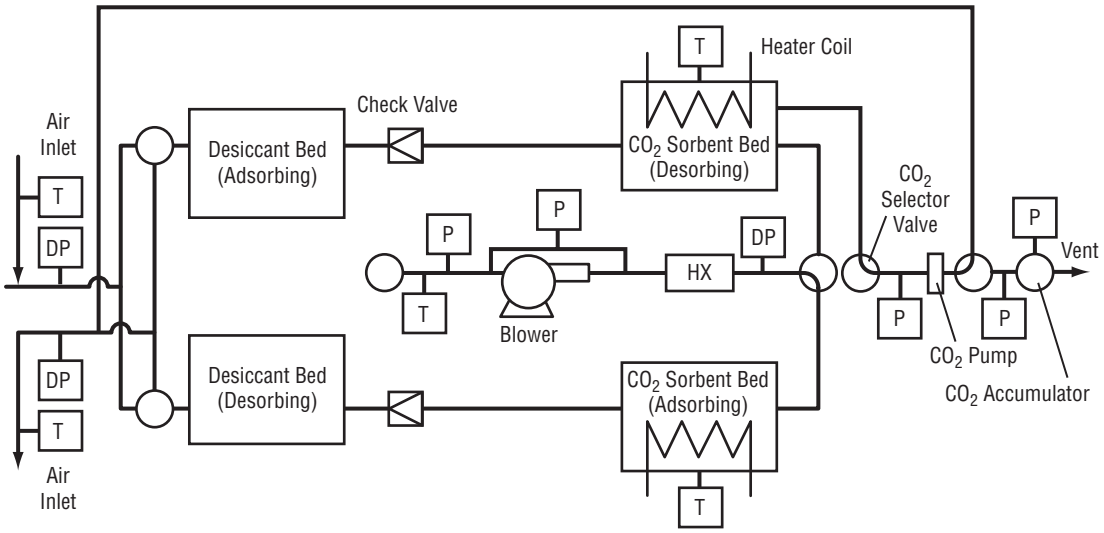

Figure 37. Carbon dioxide removal assembly.

6.2.1.4 Temperature and humidity control overview. The THC controls the *ISS* cabin temperature and humidity through the use of a CHX. During the test, cabin relative humidity was maintained at 50 percent. This provided enough moisture to maintain a steady condensate stream from the CHX without overloading the system. Temperature was maintained at ≈25 °C (77 °F).

6.2.1.5 Contaminant injection system. A system was developed for injecting contaminants into the TCIT test chamber. There were two basic systems connected to a common manifold: the solvent injector and the gas injector units. Air circulates from the test chamber, through the manifold, and back to the chamber at 25.48 m^3/hr (15 scfm). The manifold is held at 65 °C (149 °F) to ensure rapid vaporization of injected contaminants.

The solvent injector assembly includes four programmable syringe pumps, syringes, solenoid switching valves, and contaminant reservoirs, as shown in figure 38. When a syringe injects to its limit, the unit automatically cycles into the withdraw mode. When this happens, the solenoid valve switches from syringe pump-test bed plumbing to syringe pump-contaminant reservoir plumbing. This allows the pump to pull fresh chemicals from the reservoir and refill the syringe. The solenoid valve then switches again, and the freshly loaded syringe injects into the test bed. This process is repeated for the test duration. Liquid contaminant injection rates are listed in table 23.

The gas injector assembly shown in figure 38 is simpler than the solvent injector. Replaceable bags are filled with the contaminant gases. A programmable peristaltic pump is used to meter the gases from the bags into the test bed at the appropriate rate. When the bags are nearly empty, they are switched out by test personnel, utilizing quick-disconnect fittings. Gas contaminant injection rates are listed in table 23.

Within the CMS are two 10-port manifold valves, used to select the point from which a sample is to be collected within the CMS/test chamber. One 10-port valve was used for the distribution of GC

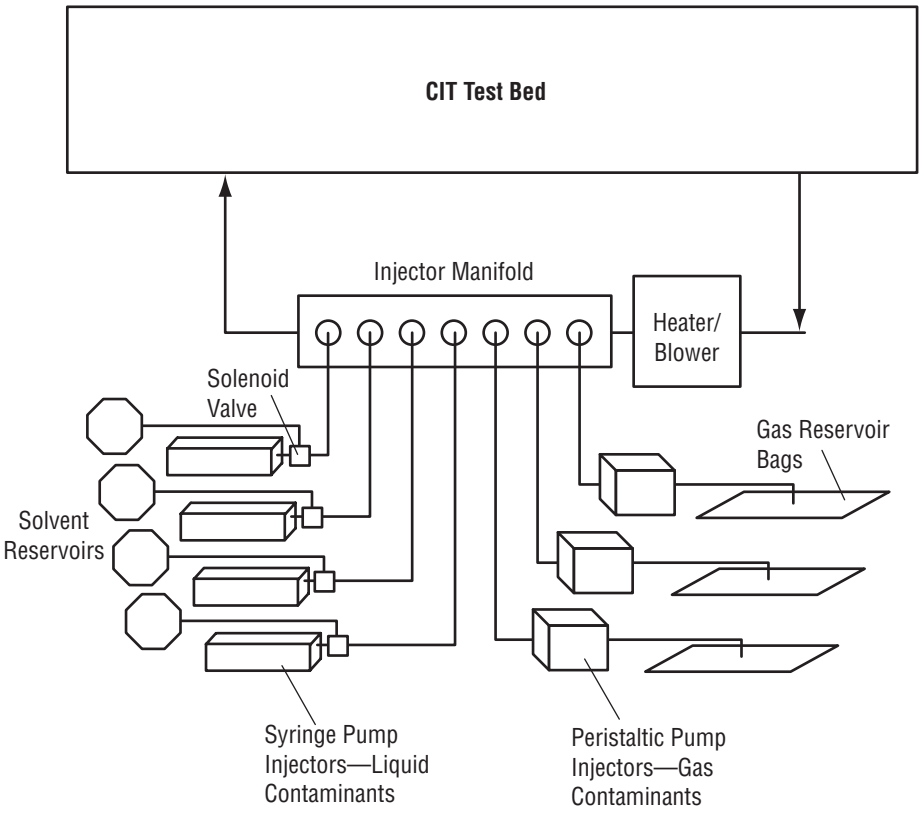

Figure 38. Contaminant injector assembly.

samples, and the other for distribution of ammonia analyzer samples. Sample collection points were the following:

- TCCS outlet (duct)
- TCCS oxidizer outlet
- CDRA outlet
- Rear chamber
- Mid chamber
- Front chamber
- CHX outlet.

The MCA has an individual sample distribution manifold which is built into the unit. This allows the MCA to draw samples from the following points:

- CHX outlet
- Front chamber
- Mid chamber
- Rear chamber
- TCCS outlet (duct)
- CDRA outlet.

Additional samples were collected manually from the CDRA accumulator tank to check for trace contaminants in the product CO_2. The samples were collected into Teflon® sample bags and prepared for analysis. These samples were analyzed by GC and with a dedicated ammonia analyzer.

6.2.1.6 Analytical methods. Several techniques were utilized in analyzing TCIT samples, including in-line analysis of trace contaminants by GC, in-line analysis of major constituents in the air by the MCA, and ammonia analysis with a dedicated analyzer. Humidity condensate samples collected from the CHX were partially analyzed on site and sent to an independent, certified laboratory for methanol, volatile, and alkalinity analyses.

Solvents in the air were analyzed with a Hewlett Packard (HP) 5890 Series II GC equipped with an HP 624/75 m/ 0.534 mm Megabore capillary column, and a flame ionization detector (FID). The method parameters utilized were the following:

- Injector temperature: 250 °C (482 °F)
- Detector temperature: 225 °C (437 °F)
- Oven temperature: 30 °C (86 °F)
- Hold time: 6 min
- Rate 1: 10 °C/min
- Final temperature 1: 145 °C (293 °F)
- Final time: 0 min
- Rate 2: 20 °C/min
- Final temperature 2: 225 °C (437 °F)
- Final time 2: 0 min
- Inlet A pressure: 137.9 kPa (20 psi)
- Inlet B pressure: 137.9 kPa (20 psi)
- Carrier gas: Helium at 15 mL/min
- Detector: FID.

Samples were collected on Tenax/Carbotrap mixed resin tubes for 5–15 min at a flow rate of 30 mL/min. Samples were desorbed for 10 min at 400 °C (752 °F) and a helium carrier flow rate of ≈15 mL/min. Desorption was accomplished with a thermal desorption (ballistic heating) injector assembly. This unit desorbed the sample directly onto the analytical column without the use of cryogenic trapping. Detection limits and SMAC concentrations are summarized in table 24.

Table 24. Liquid contaminant detection limits.

Contaminant	Detection Limit (ppm_v)	180-Day SMAC (ppm_v)
Methanol	5	7
Acetone	5	22
Dichloromethane	2	3
m-Xylene	5	50

Note: Contaminants were measured in an air matrix. Reliable results have been obtained below the detection limit, but due to limited funding, the method could not be fully developed to give certified limits below those reported above.

Gas contaminants, other than ammonia, were analyzed with the same HP 5890 Series II GC used for solvent analysis, but with a second column and analytical program. The column for this procedure was a SS, 60/80 mesh Supelco Carboxen 1000 column of 4.6 m × 0.32 cm (15 ft × 0.125 in.). Detection was accomplished by a thermal conductivity detector (TCD). The method parameters utilized were the following:

- Injector temperature: 150 °C (302 °F)
- Detector temperature: 200 °C (392 °F)
- Oven temperature: 35 °C (95 °F)
- Hold time: 7 min
- Rate 1: 20 °C (68 °F) per minute
- Final temperature 1: 170 °C (338 °F)
- Final time: 0 min
- Valve open: 50 sec
- Valve closed: 9 min
- Inlet A pressure: 137.9 kPa (20 psi)
- Inlet B pressure: 137.9 kPa (20 psi)
- Carrier gas: Helium at 30 mL/min
- Detector: TCD
- TCD sensitivity: High.

Sample injection was accomplished with a gas-controlled injector valve. The sample was injected directly onto the column. Detection limits for CH_4 and carbon monoxide (CO) are shown in table 25.

Table 25. Gaseous contaminant detection limits.

Contaminant	Detection Limit (ppm_v)	180-Day SMAC (ppm_v)
Methane	5	5,300
Carbon monoxide	5	50

Note: Contaminants were measured in an air matrix.

Ammonia was analyzed by a Pioneer in-line diffusion detector with a draw pump. Samples were drawn from the test bed, through the detector, and back into the test bed. The analyzer has a detection limit of 1.5 ppm_v, well below the ammonia 180-day SMAC of 10 ppm_v. As with the gaseous contaminants, ammonia was measured in an air matrix.

Humidity condensate samples were collected at the THC CHX to check for H_2O-soluble contaminants. Conductivity, pH, and TOC were analyzed on site. Samples for specific contaminants were analyzed at a certified laboratory. The methods utilized are summarized in table 26.

All samples were handled in compliance with the *Analytical Control Test Plan and Microbiological Methods for the Water Recovery Test*. This is a quality control (QC) document which covers such items as sample collection protocol, chain of custody procedures, and storage/shipping requirements.

Table 26. Humidity condensate analysis methods.

Contaminant	Detection Limit	Method
Methanol	6.0 mg/L	EPA 8015
Acetone	6.9 µg/L	EPA 624
Dichloromethane	0.36 µg/L	EPA 624
m-Xylene	0.19 µg/L	EPA 624
Ammonia	0.03 mg/L	EPA 350.3
Alkalinity	1.53 mg/L	EPA 310.1

Note: EPA methods—see additional sources.

6.2.2 Test Operations Summary

6.2.2.1 Initial contaminant loading. To accelerate reaching a steady-state contaminant concentration in the test chamber, an initial contaminant loading was performed. In this procedure, a known quantity of contaminants was rapidly injected into the test chamber. None of the contaminant removal equipment were operating during the initial loading. The chamber was then allowed to come to steady state before beginning continuous contaminant injection.

Rapid gas injection was accomplished during the initial loading by pumping a known quantity of gas directly into the recirculation duct using a high-capacity, analytical-grade pump. The pump is a bellows-type assembly with Teflon®-wetted parts.

A known quantity of gas was injected into an evacuated Teflon® sample collection bag. Quantification was accomplished through the use of calibrated mass flow controllers. Pure contaminant gasses were loaded into the bag using quick-disconnect fittings, and were then pumped into the test chamber.

Rapid solvent injection was accomplished during the initial loading by manually injecting a known quantity of pure solvent directly into the recirculation duct using an analytical syringe.

6.2.2.2 Contaminant injection. Contaminant injection was accomplished through an automated system of syringe pumps, peristaltic pumps, liquid contaminant reservoirs, and Teflon® holding bags (described above).

There was no need for solvent reservoir refill since ample volumes of solvent were available at test initiation. Gas contaminant holding bags were checked daily for adequate contaminant supply levels. These bags were replaced as necessary with full holding bags.

Contaminant injection equipment was checked at least three times daily for anomalous conditions. The primary problems observed were bubbles forming in the solvent injection train. These bubbles were easily removed, and involved little downtime.

6.2.2.3 Sample collection. Sample collection began as the initial task of each test day. Typically, two sets of samples were collected during weekdays and one set on weekends. Samples were collected at the lower concentration point first, followed by higher concentration points. On weekdays, when mechanical or technical problems arose, fewer than two full sets of samples were collected.

6.2.3 Discussion of Results

During the entire TCIT, each compound was injected into the test chamber at or near their respective target rates presented earlier in table 23. As the contaminants were injected, the TCCS, CHX, and CDRA removed them, producing the average chamber concentrations summarized in table 27.

Table 27. TCIT injection rates and concentrations.

Compound	Injection Rate (mg/hr)	Chamber Concentration (mg/m^3)
Acetone	1,118.5	39.0
Carbon monoxide	48.4	9.1
Dichloromethane	156.8	5.4
Methanol	445.9	26.6
m-Xylene	2,916.0	87.7
Methane	374.7	68.9
Ammonia	2,455.4	8.9

Analysis of atmospheric samples collected at the inlet and outlet of the TCCS, CHX, and CDRA, in addition to the analysis of humidity condensate, allowed for a determination of the relative percentage of the contaminant load controlled by each device. Atmospheric leakage, which was determined to be 0.038 m^3/hr (0.022 scfm), also contributed to contaminant removal from the test chamber.

Based upon the observed contaminant removal by the TCCS, CHX, CDRA, and atmospheric leakage, the overall percentage of trace contaminant removal contributed by each route can be calculated. These percentages are summarized in table 28.

Table 28. Contaminant removal by device.

Compound	Overall Contaminant Removal (%)			
	CDRA	TCCS	CHX	LEAK
Acetone	42.1	56.2	1.6	0.1
Carbon monoxide	0	99.2	0	0.8
Dichloromethane	52.9	47.0	0.02	0.1
Methanol	62.4	25.0	12.4	0.2
m-Xylene	54.2	45.7	0.003	0.1
Methane	0	99.1	0	0.9
Ammonia	22.1	22.8	55.0	0.06

As shown in table 28, the CDRA and the CHX provide a substantial assist to the TCCS for removing trace contaminants from a spacecraft cabin atmosphere. The role of atmospheric leakage is very small by comparison. Overall, the TCCS provides control for the entire CH_4 and CO load because of its catalytic oxidation capability. The CDRA and TCCS provide comparable control for most other compounds; however, some H_2O-soluble compounds are better controlled by the CDRA. The CHX provides a very significant contribution, mainly for ammonia and low molecular weight, polar compounds.

6.2.4 Conclusions

Based upon the results obtained during the TCIT, the following conclusions can be made:

• The TCCS receives significant assistance from the CDRA and CHX for removing trace contaminants from the cabin atmosphere.

• The primary compounds removed by the CHX are ammonia and H_2O-soluble compounds.

• Contaminant removal via humidity condensate absorption follows an enhanced Henry's Law relationship for ammonia and polar organic compounds.

• The TCCS is the primary removal means for CH_4 and CO.

• Contaminant removal by the CDRA is cyclic and can decrease over time as the sorbent beds become increasingly loaded.

6.3 Flight Unit Trace Contaminant Control Subassembly Test[20]

As part of the *ISS* TCCS development, a performance test was conducted to provide reference data for flight verification analyses. This test, which used the U.S. Habitation Module (U.S. Hab) TCCS as the test article, was designed to add to the existing database on TCCS performance. Included in this database are results obtained during *ISS* development testing; testing of functionally similar TCCS prototype units; and bench-scale testing of activated charcoal, oxidation catalyst, and granular LiOH. The present database has served as the basis for the development and validation of a computerized TCCS process simulation model. This model serves as the primary means for verifying the *ISS* TCCS performance. In order to mitigate the risk associated with this verification approach, the U.S. Hab TCCS performance test provides an additional set of data which serve to anchor both the process model and previously obtained development test data to flight hardware performance. The following discussion provides relevant background followed by a summary of the test hardware, objectives, requirements, and facilities. Facility and test article performance during the test is summarized, test results are presented, and the TCCS's performance relative to past test experience is discussed. Performance predictions made with the TCCS process model are compared with the U.S. Hab TCCS test results to demonstrate its validation.

The *ISS* TCCS includes an activated charcoal bed, a high-temperature catalytic oxidizer (HTCO), granular LiOH bed, blower, flow meter, and an electrical interface assembly. Figure 39 shows a simplified process flow schematic of the TCCS and figure 40 shows a view of the flight hardware configuration.

Trace chemical contaminants are removed from the *ISS* cabin atmosphere by circulating air through the charcoal bed to remove high molecular weight contaminants and ammonia. More volatile, low molecular weight contaminants such as CH_4, H_2, and CO are removed by the HTCO.

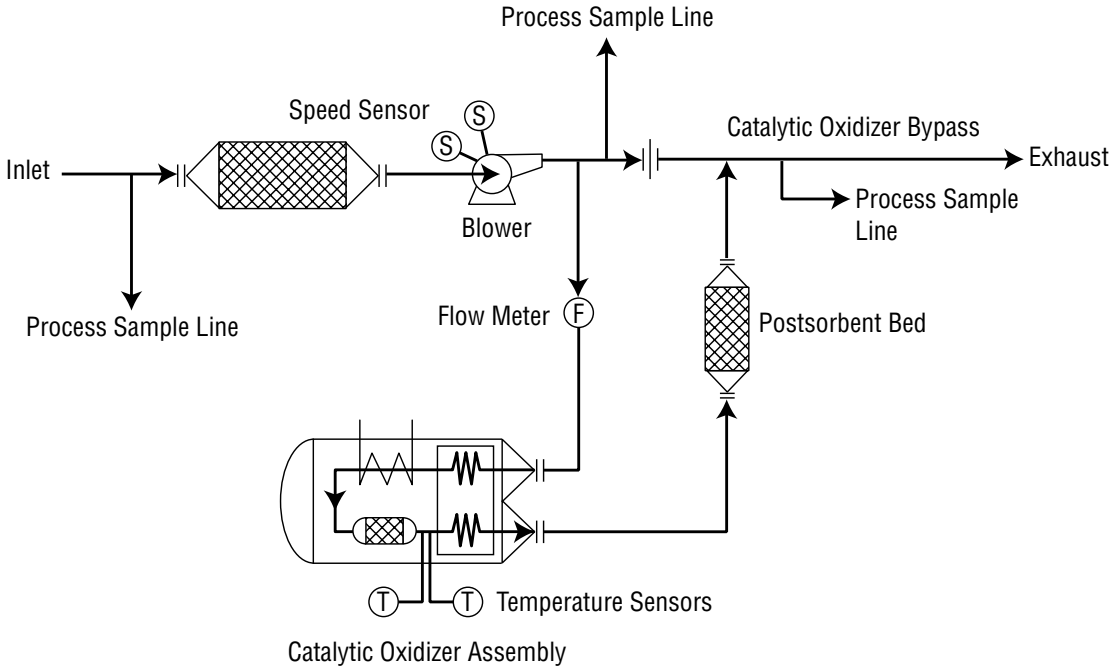

Figure 39. TCCS process flow diagram.

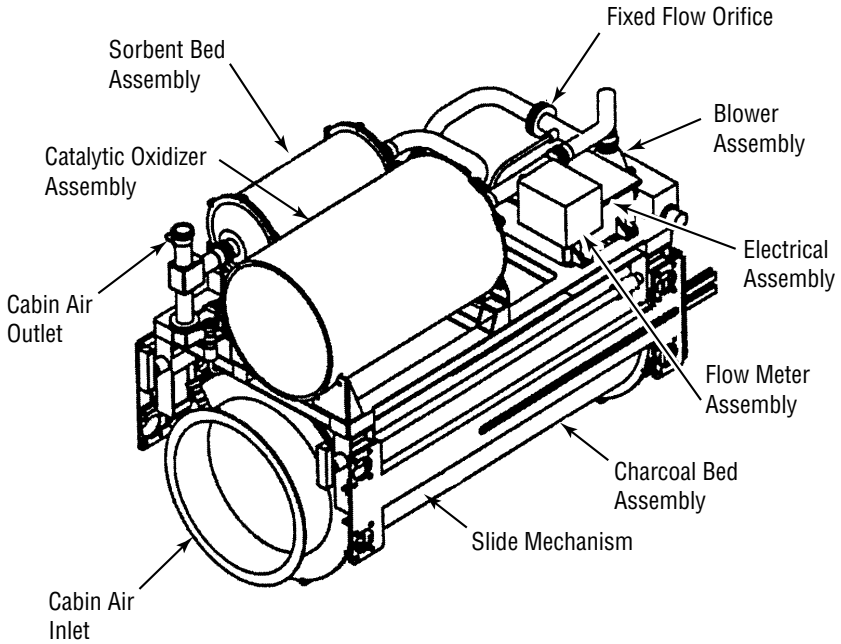

Figure 40. *ISS* TCCS flight configuration.

The HTCO includes three primary parts: a recuperative HX, an electric heater, and a catalyst bed. It is designed to provide a high, single-pass CH_4 oxidation efficiency. The HX assembly preheats the air as it enters the HTCO. Further heating is provided by the heater element. Final air heating occurs in the catalyst bed via radiation, conduction, and liberation of the heat of reaction from the oxidized contaminants.

The LiOH bed, located downstream of the HTCO, removes any acidic oxidation products that may be produced in the event that halocarbons break through the charcoal bed.

The blower and flow meter maintain a steady flow rate through the system that is sufficient to maintain individual trace contaminant concentrations below their respective SMAC. The total flow is passed through the charcoal bed while only a portion flows through the HTCO and LiOH bed. The split flow combines downstream of the LiOH bed before exhausting from the TCCS. Three sample ports are provided at the charcoal bed inlet, charcoal bed outlet, and the LiOH bed outlet.

The *ISS* program chose to verify TCCS performance via analysis using the TCCS Computer Program (TCCS–CP) version 8.1 developed by Lockheed Missiles and Space Company, Inc. This approach, while less expensive, deviates from the traditional approach of verification by testing. Therefore, it contains an element of risk even though the process model has been validated against integrated TCCS development testing data.

To address the perceived risk of this approach, the TCCS performance confirmation test (TPCT) was defined. The TPCT was designed to provide the necessary data that would further validate the TCCS–CP, supplement the existing TCCS test database, and tie the process model's validation and previous development test results to flight hardware performance.

Although the TPCT is not a formal part of the TCCS design verification process, the data collected during its conduct serve the important function of minimizing the perceived risk associated with hardware verification by analysis.

The TPCT was designed to confirm the ability of the *ISS* U.S. Hab TCCS flight unit to control a specified contamination load at representative cabin environmental conditions. Specific objectives of the TPCT are:

1. To challenge the TCCS with a trace contaminant load representative of the *ISS* to confirm performance.

2. To obtain contaminant concentration versus time data for use in process model validation.

3. To compare the performance of the TCCS flight unit with performance observed during development tests.

In order to properly confirm the U.S. Hab TCCS performance, the trace contaminant load and test volume atmospheric conditions must be defined. These parameters are central to the test design. The test volume atmosphere was required to be maintained between 18 °C (65 °F) and 27 °C (80 °F).

Relative humidity was required to be 50±5 percent. To prevent inward leakage of laboratory atmosphere into the test volume, it was required that the test volume pressure be maintained at a minimum of 3 mm Hg over the prevailing barometric pressure.

To achieve the primary test objectives, a trace contaminant load based upon *ISS* design specifications was defined. This load is based upon the combined equipment offgassing from 75,000 kg of spacecraft hardware and the metabolic production of 5.25 crewmembers. The metabolic loading is based upon four people plus a 1.25 human metabolic equivalent for laboratory animals. Equipment and metabolic rates used to determine the test injection rates are listed in table 29. The injection rates derived from table 29 equipment and metabolic rates were then adjusted to accommodate up to 0.23 kg/day (0.5 lb/day) outward atmospheric leakage, assuming that the TCCS provides 100-percent removal efficiency. The final test injection rates are listed in table 30.

Table 29. *ISS* equipment offgassing and metabolic rates.

Compound	Equipment Rate (mg/kg-day)	Metabolic Rate (mg/man-day)
Ethanol	7.85×10^{-3}	4
Methanol	1.27×10^{-3}	1.5
2-Propanol	3.99×10^{-3}	0
n-Butanol	4.71×10^{-3}	1.33
Toluene	1.98×10^{-3}	0
Xylene	3.67×10^{-3}	0
Chlorobenzene	1.54×10^{-3}	0
Dichloromethane	2.15×10^{-3}	0
1,1,2-Trichloro-1,2,2-trifluoroethane	1.89×10^{-2}	0
Trichlorofluoromethane	1.41×10^{-3}	0
Methane	6.39×10^{-4}	160
Acetone	3.62×10^{-3}	0.2
2-Butanone	6.01×10^{-3}	0
4-Methyl-2-pentanone	1.41×10^{-3}	0
Cyclohexanone	6.62×10^{-4}	0
Carbon monoxide	2.03×10^{-3}	23
Ammonia	8.46×10^{-5}	321

Table 30. Performance test contaminant injection rates.

Compound	SMAC (mg/m^3)	Injection Rate (mg/hr)
Ethanol[a]	2,000	25.4
Methanol	9	4.3
2-Propanol	150	12.5
n-Butanol	40	15.0
Toluene	60	6.2
Xylene	220	11.5
Chlorobenzene	46	4.8
Dichloromethane[a]	10	6.7
1,1,2-Trichloro-1,2,2-trifluoroethane[a]	400	59.1
Trichlorofluoromethane	560	4.4
Methane[a]	3,800	37.0
Acetone[a]	50	11.4
2-Butanone	30	18.8
4-Methyl-2-pentanone	140	4.4
Cyclohexanone	60	2.1
Carbon monoxide[a]	10	11.4
Ammonia[a]	7	70.5

[a]Primary test compounds comprising 63 percent of the *ISS* specification load.

Seven of the compounds included in the test load were considered to be of most interest. They are ethanol; dichloromethane; 1,1,2-trichloro-1,2,2-trifluoroethane (Freon 113); CH_4; acetone; CO; and ammonia. These seven compounds represent 63 percent of the total *ISS* design specification trace contaminant load. They also include the primary TCCS design drivers: dichloromethane, ammonia, CH_4, and CO. Of the additional compounds listed in table 29, methanol is of most interest because of its potential for rapid activated charcoal bed breakthrough. The total test load represents 87.5 percent of the total *ISS* design specification load. This loading was also deemed manageable for the in-line gas sample analysis system to be used during the TPCT.

According to *ISS* performance specifications, the TCCS must maintain each individual contaminant's concentration below 90 percent of its respective SMAC. Table 30 also includes a listing of SMAC's for the test compounds.

6.3.1 Test Configuration

The following summary provides a brief description of the TPCT facility, the integration of the test article with the facility and its control, and the analytical methods employed during the test. Detailed information on the test facility, test conduct, and test article restoration planning is provided in reference 21.

6.3.1.1 Facility description. The Trace Contaminant Control Test facility located in the Boeing-Huntsville Life Sciences Technology Center (LSTC) was used for conducting the TPCT. This facility was previously used to test a flight-qualifiable Russian *Mir* TCCS (sec. 6.4).

The test facility includes: a rack to control system atmospheric temperature, humidity, and chemical contaminant injection; a 9 m^3 SS mixing chamber; an in-line GC/mass spectrometer (MS) with a preconcentrator; and an in-line Fourier transform infrared (FTIR) spectrometer. These major components are interconnected by 5.1 cm (2-in.) electropolished SS tubing to create a closed air loop. The components were configured as shown in figure 41. The flight unit TCCS is mounted in its own transportation fixture, and connected to the closed air loop via approved adapters.

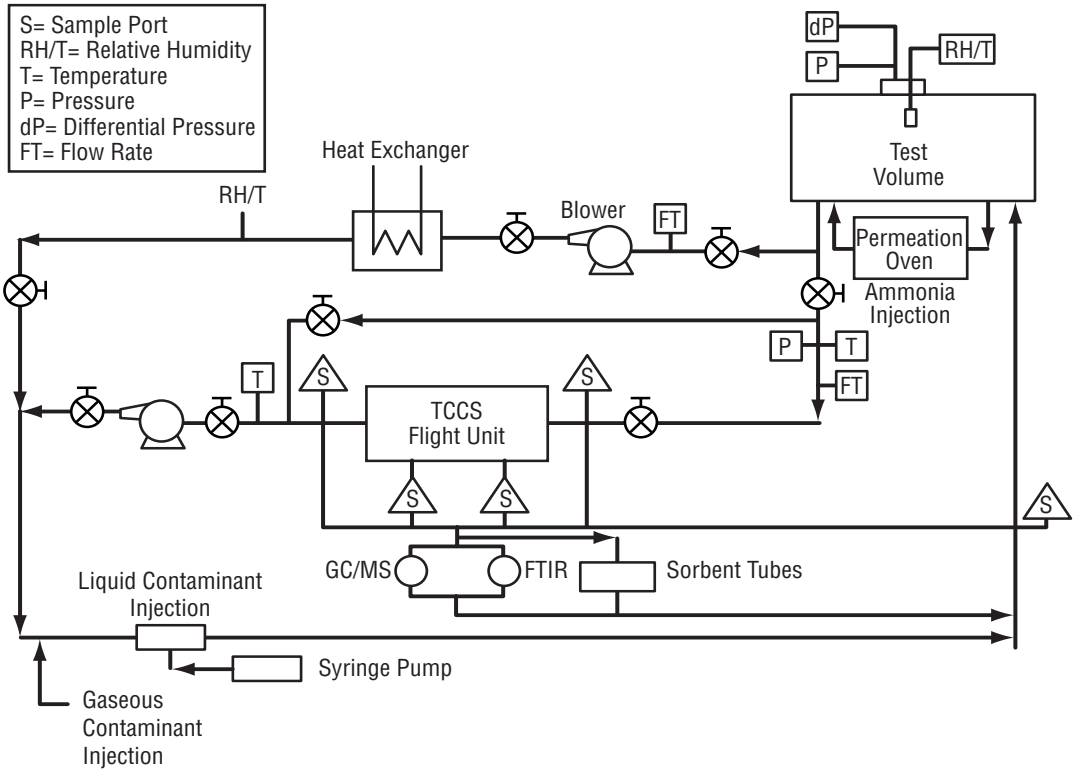

Figure 41. Simplified test facility layout.

The TCCS receives air from the system after it has been conditioned for temperature, humidity, and contaminant load. After processing by the TCCS, the air is directed back to the mixing volume. The entire system is a closed loop.

The test system is monitored for air flow, temperature, pressure, relative humidity, and contaminant load. Four sample ports are used to monitor the chemical composition of the test atmosphere. These ports are located at the TCCS inlet, downstream of the activated charcoal bed, downstream of the LiOH bed, and at the TCCS exhaust.

6.3.1.2 Contaminant injection. Both gaseous and liquid phase chemical contaminants were injected into the test chamber atmosphere during TCCS performance testing. The following discussion provides a summary of each of the three methods employed during the test.

Methane and CO gases were supplied from separate pressurized bottles containing the following certified percentages of each contaminant:

- 0.01 percent CH_4/balance N_2
- Carbon monoxide/balance air.

Methane and CO injection was controlled by individual mass flow controllers with upstream pressure regulation.

Liquid contaminants were injected as a single mixture. A syringe pump was programmed to pump the liquid mixture from a 10-mL glass vial to an injection port located on a heated bypass tube. The contaminants immediately evaporated upon injection and air flowing through the bypass tube swept them into the mixing chamber. The air from the mixing tank was then directed to the TCCS. The liquid contaminant vials were replaced daily, from Monday through Friday, to provide fresh stock solution during the data-gathering phase of the test.

Ammonia was injected continuously by a KIN–TEK model 585–C precision gas standard generator. This unit dispensed a stable flow of pure ammonia directly into the mixing chamber. The permeation tube was refilled periodically to maintain a constant ammonia injection rate for the duration of the data collection period.

6.3.1.3 Analytical methods. Atmospheric sampling and analysis methods used during the test are the following:

- Automated sample collection followed by analysis, using in-line GC/MS and FTIR instruments

- In-line sample collection using gas detector tubes

- Sample collection into evacuated cylinders followed by off-line analysis by GC/MS and GC instruments.

The in-line GC/MS system included an HP5890 series II GC and an HP 4972 MS system. The GC/MS was preceded by an Entech model 7000 preconcentrator. The automated GC/MS system collected and analyzed one sample per hour.

The FTIR system was a MIDAC Model I2001 containing a 20-m constant volume gas cell that utilized a 0.5-cm mercury-cadmium-telluride detector. The FTIR scan time per sample was ≈3 min. The FTIR, like the GC/MS system, was completely automated.

Additional in-line analysis for ammonia and CO was conducted as needed, using detector tubes manufactured by Drager. This technique was used to verify concentration order of magnitude only.

Grab samples were collected periodically using evacuated cylinders to check in-line analysis results. These samples were analyzed off line using several techniques, including GC/MS, GC combined

with an FID for CH_4 analysis, and GC combined with either a TCD or a helium ionization detector for CO analysis.

6.3.1.4 Instrumentation and control. The command and data handling (C&DH) subsystem processes commands and monitors TCCS process parameters onboard the *ISS* via a level 3 multiplexer/demultiplexer (MDM). This hardware is in high demand by other agencies and, therefore, was not available for the TPCT. This was not a problem because the purpose of the test was to measure contaminant removal performance, not integrated system command and control. Therefore, the control system used during flight hardware acceptance testing was used.

To simulate the function of the level 3 MDM, a VAX system configuration was used. In this configuration, a Sorensen power supply provided 120 Vdc to the TCCS. Interface control and TCCS mechanical and electrical operational parameters were monitored with an application generator (AG) VAX command and control system. The AG VAX system provided an interactive TCCS animated display to interface with the test article. Key parameters such as HTCO temperature and flow rate, blower speed, and electrical power were monitored via the AG VAX animated display. These parameters were logged into a Data Acquisition System (DAS) database to facilitate posttest data reduction and analysis.

6.3.2 Pretest Performance Analysis

A pretest TCCS performance analysis was conducted using the TCCS–CP version 8.1 process model. This analysis served to bound the expected TCCS performance and provide a preliminary performance baseline to which the actual performance observed during the test could be compared. A brief summary of the pretest analysis approach and results is provided in the following discussion.

6.3.2.1 Pretest analysis approach. The pretest analysis employed two data analysis techniques. The first, called variables search, was used to determine the most significant process and simulation variables. Those variables that most directly affect activated charcoal loading were investigated using this technique. Based upon the variables search analysis, the most significant variables were found to be contaminant liquid molar volume, TCCS flow rate, and relative humidity.

A final set of performance simulations was then conducted using design of experiments/robust design (DOE/RD) techniques. The set of simulations conducted using the DOE/RD approach allowed for a pretest prediction of the 95-percent confidence interval range for each contaminant's concentration, based upon the allowable variations in the test chamber atmosphere and TCCS process operations.

6.3.2.2 Predicted pretest performance. Based upon the series of pretest process simulations, it was predicted that methanol, dichloromethane, and ethanol would be the contaminants that would most likely saturate the charcoal bed. Methanol breakthrough was predicted as early as 9 hr and as late as 26 hr into the test. Dichloromethane breakthrough was predicted as early as 56 hr and as late as 394 hr after test startup. Breakthrough of ethanol may be observed as early as 411 hr and as late as 927 hr after test startup. Predicted nominal concentrations and the range associated with the pretest analysis 95-percent confidence interval are summarized in table 31.

Table 31. Pretest performance prediction summary.

Compound	Predicted Range (mg/m^3)	Nominal Level (mg/m^3)
Ethanol	1.4–2.1	1.7
Methanol	0.78–1.17	0.94
2-Propanol	0.68–1.01	0.81
n-Butanol	0.82–1.22	0.98
Toluene	0.34–0.50	0.41
Xylene	0.62–0.93	0.75
Chlorobenzene	0.26–0.39	0.32
Dichloromethane	0.37–0.55	0.44
1,1,2-Trichloro-1,2,2-trifluoroethane	3.2–4.8	3.9
Trichlorofluoromethane	0.24–0.36	0.29
Methane	7.1–10.5	8.4
Acetone	0.62–0.92	0.74
2-Butanone	1.0–1.5	1.2
4-Methyl-2-pentanone	0.24–0.36	0.29
Cyclohexanone	0.11–0.17	0.14
Carbon monoxide	2.1–3.1	2.5
Ammonia	3.8–5.7	4.6

6.3.3 Pretest Checkout Summary

6.3.3.1 Test volume leakage. The system volume is ≈9 m^3 including the mixing chamber and associated support system plumbing. The allowable system leakage was established at 0.23 kg/day (<0.5 lb/day). After the TCCS was installed in the system, the complete integrated system leakage as measured by pressure decay was found to be ≈13.6 g/day (0.03 lb/day).

6.3.3.2 Contaminant stability. Understanding the background contamination level and the interaction of the test contaminants with the internal surfaces of the test facility were considered to be highly important in conducting a test of this nature. Pretest efforts to develop this understanding and its relationship to test bias are provided in the following summary.

Before starting the test, a general chemical contaminant background check of the test rig was conducted. This investigation lasted several days and included, but extended beyond, the contaminants introduced during the test period. The primary instruments were the in-line GC/MS and FTIR used during testing. There were no extraneous contaminants found using the ion identification and search capability with a library of over 300,000 compounds. By including the test contaminant detection limits as a quantitative value, the total background was found to be 1.5 mg/m^3. If those contaminants which were found to be less than their respective detection limits are not included, then the background was ≈0.22 mg/m^3. The maximum allowable background contamination was 3.5 mg/m^3.

Before installing the TCCS in the test stand, a test of contaminant adsorption by the internal surfaces of the test rig was conducted. This was accomplished by injecting known quantities of the test contaminants into the test chamber and monitoring their concentration over time.

The liquid phase contaminants were injected as a composite mixture with a syringe pump in order to emulate the injection process to be used during the TPCT. Predetermined quantities of CH_4 and CO were injected continuously from pressurized gas bottles. A discrete amount of ammonia was continuously injected as a gas via the permeation tube. The expected concentrations are based on the contaminant mass injected and known system volume and pressure. Average steady-state concentrations were measured as well as mean standard deviations and associated 95-percent uncertainties using *t*-factors. System biases were determined by subtracting the observed concentrations from their respective target values.

A wide range of system biases was observed, from −36 percent of target for toluene to 48 percent for trichlorofluoromethane. Negative bias in the range of 30–37 percent of the target amount was observed for n-butanol, 4-methyl-2-pentanone, toluene, chlorobenzene, o-xylene, and cyclohexanone. Subsequent analyses using an off-line method did not show the same bias, so this was not attributed to system adsorption but was determined to be an artifact of the in-line trapping mechanism. As such, there was no observed system adsorption.

The above system biases were ultimately used in the final data reduction when establishing the relationship between projected tank concentration and observed steady-state concentration.

Prior to the start of contaminant injection, the TCCS was installed on line and was purged with TOC grade air. This was done to establish nominal functionality of the test article and set valve positions for flow rate through the unit.

6.3.4 Test Operations Summary

The TPCT began on January 19, 1998. The TCCS operated continuously until the test was completed on February 14, 1998. The overall test duration was 624 hr and all of the primary test objectives were satisfied. A summary of the TCCS and facility operations during the TPCT are provided in the following discussion. A brief assessment of the overall TPCT operations is also provided.

6.3.4.1 TCCS operations. Throughout the test, the TCCS operated flawlessly. Inlet air flow and HTCO temperature were maintained at steady levels. The HTCO flow rate adapted to the total system pressure to provide almost a constant command voltage to the flow meter by adjusting the blower speed.

6.3.4.2 Facility operations. The facility provided a closed loop which provided air to the TCCS within the required conditions, summarized in table 32. The average test conditions were the following:

- Air temperature: 22.5 °C (72.5 °F)
- Relative humidity: 50.4 percent
- System pressure: 760 mm Hg.

Test operations anomalies were very few and minor. During two test days, it was found that the liquid contaminant injection system was leaking. It was repaired and normal injections resumed. Also, one ammonia permeation tube dried up prematurely; however, it was replaced with minimal impact to the test operation. Adjustments were required to the CO injection after it was found to be injecting

at a lower than expected rate. The CO concentration in the test chamber was found to be within the expected range after adjusting the flow.

Despite these anomalies, the contaminant injection system provided a total contaminant load, as summarized in table 33. The average hourly injection of contaminants for the 624-hr test was actually very close to the specified rates listed in table 30.

Table 32. Required versus observed test conditions.

Parameter	Requirement	Observed Test Condition
Temperature	18.3–26.7 °C (65–80 °F)	21.6–23 °C (71–73 °F)
Pressure	750–786 mm Hg	751–780 mm Hg
Relative humidity	25–70 Percent	49–53 Percent

Table 33. Contaminant loading summary.

Compound	Total Mass Injected (mg)	Average Injection Rate (mg/hr)
Ethanol	15,444.5	24.8
Methanol	2,615.7	4.2
2-Propanol	7,602.9	12.2
n-Butanol	9,133.2	14.6
Toluene	3,775.3	6.0
Xylene	7,004.9	11.2
Chlorobenzene	2,931.8	4.7
Dichloromethane	4,073.7	6.5
1,1,2-Trichloro-1,2,2-trifluoroethane	35,938.4	57.6
Trichlorofluoromethane	2,692.8	4.3
Methane	23,082.3	37.0
Acetone	6,928.4	11.1
2-Butanone	11,425.4	18.3
4-Methyl-2-pentanone	2,687.7	4.3
Cyclohexanone	1,279.1	2.0
Carbon monoxide	5,858.8	9.4
Ammonia	41,525.9	66.5

6.3.4.3 Overall test assessment. During the TPCT, the TCCS performed electrically and mechanically without incident. All TCCS components performed within requirements; however, the CH_4 single pass removal efficiency was lower than expected. It was measured at 55 percent rather than the expected >90 percent.

6.3.5 Discussion of Results

During the test, the TCCS trace contaminant removal performance was, in general, as expected and was found to be consistent with past TCCS test results. The following discussion summarizes the observed performance for trace contaminant removal. Specific attention is given to the key TCCS design drivers and those contaminants that broke through the charcoal bed.

6.3.5.1 Contaminants of interest. Key contaminants of interest for the test included methanol, dichloromethane, ammonia, CO, and CH_4. Methanol was also of interest because of its potential for charcoal bed breakthrough early in the test. Dichloromethane was also of interest because of its potential for charcoal bed breakthrough in addition to its role as a TCCS design driver. Also of interest was the increase in CH_4 concentration that can result from catalyst poisoning as dichloromethane breaks through the charcoal bed. Ammonia and CO were considered key solely because they are TCCS design drivers.

6.3.5.2 Process performance. During the test, methanol was the first contaminant to break through the charcoal bed. This breakthrough is shown in figure 42. Late in the test, dichloromethane began to break through the charcoal bed as shown in figure 43. Dichloromethane breakthrough was still in progress at the test's conclusion. The test duration was not sufficient to observe any additional contaminant breakthrough of the charcoal bed; therefore, all the other contaminants were maintained at steady concentrations as shown in table 34. This performance was consistent with a 100-percent single-pass removal efficiency.

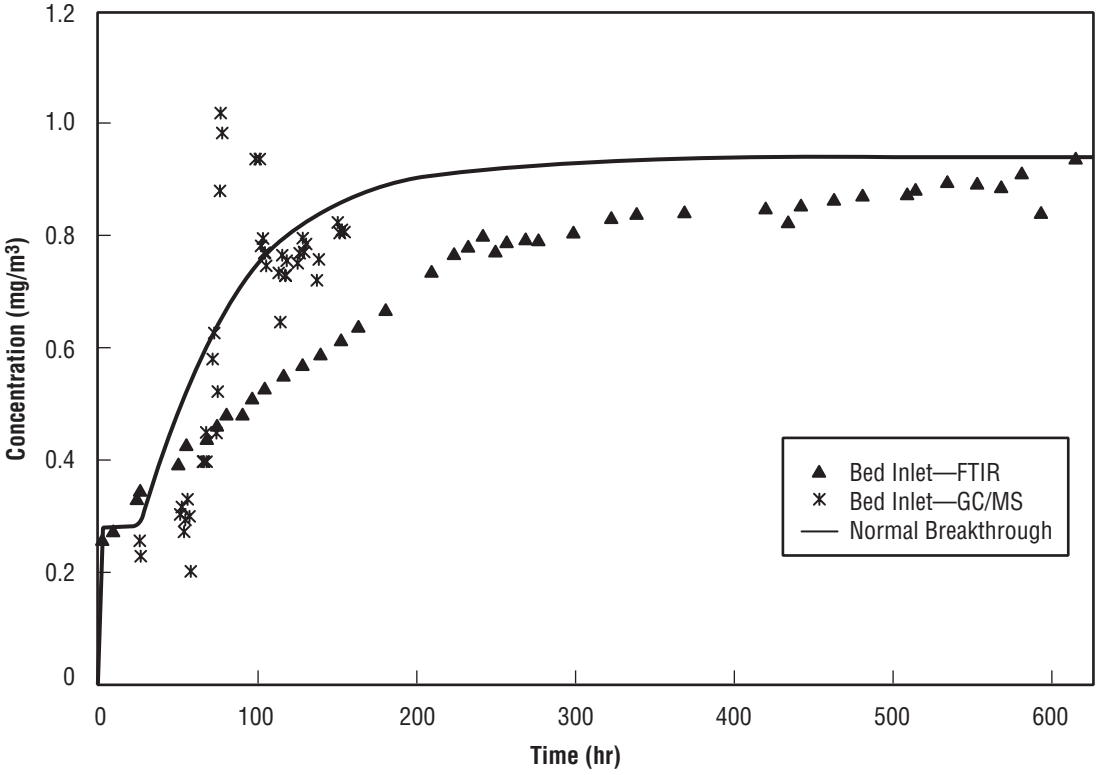

Figure 42. Methanol concentration trend.

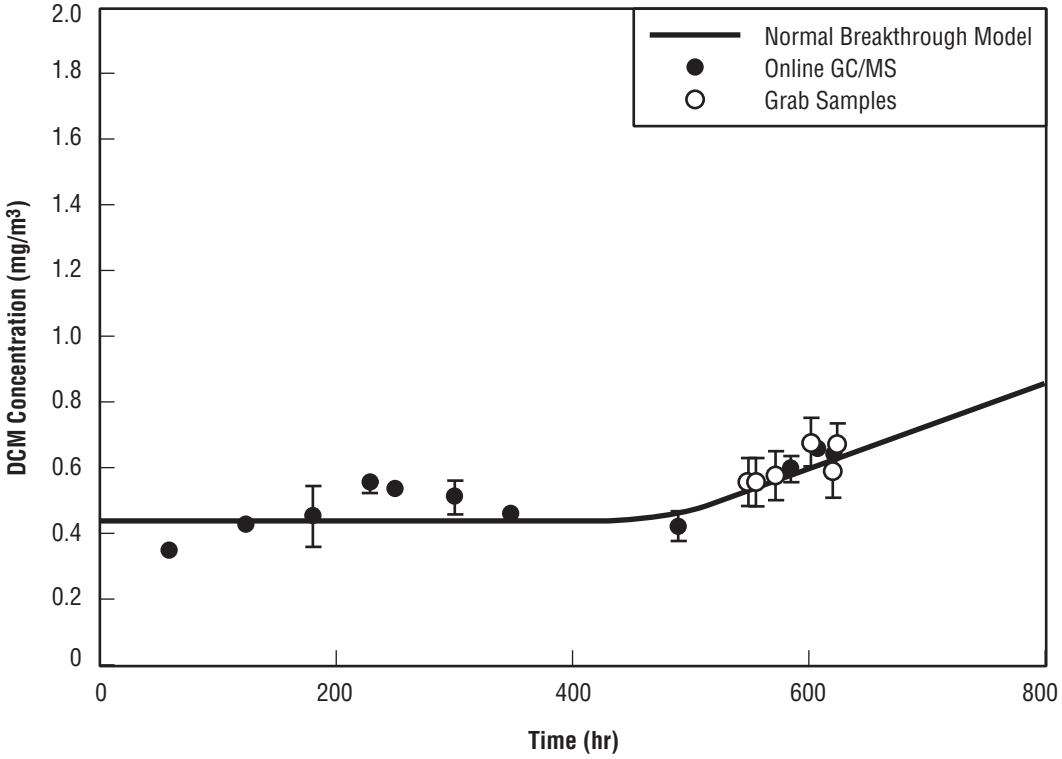

Figure 43. Dichloromethane concentration trend.

Table 34. Observed liquid contaminant concentrations.

Compound	Concentration (μg/m3)	
	Observed	Predicted
Ethanol	2,250 ±200	1,580 +175/–140
Trichorotrifluoroethane	3,530 ±710	3,670 +410/–330
Trichlorofluoromethane	300 ±50	270 +30/–25
Propanone	700 ±40	710 +80/–65
Propanol	870 ±90	780 +90/–70
Butanone	1,100 ±90	1,170 +130/–110
Butanol	910 ±70	930 +110/–80
Xylene	610 ±50	715 +80/–65
4-Methyl-2-pentanone	225 ±20	270 +30/–25
Toluene	320 ±30	390 +40/–35
Chlorobenzene	250 ±20	300 +35/–30
Cyclohexanone	110 ±10	130 +15/–10

Figure 44 shows the TCCS's performance for ammonia removal. Ammonia was controlled to between 4 and 5 mg/m^3. This result demonstrated 100-percent removal by the phosphoric acid-treated charcoal bed during the entire test. No ammonia breakthrough was observed.

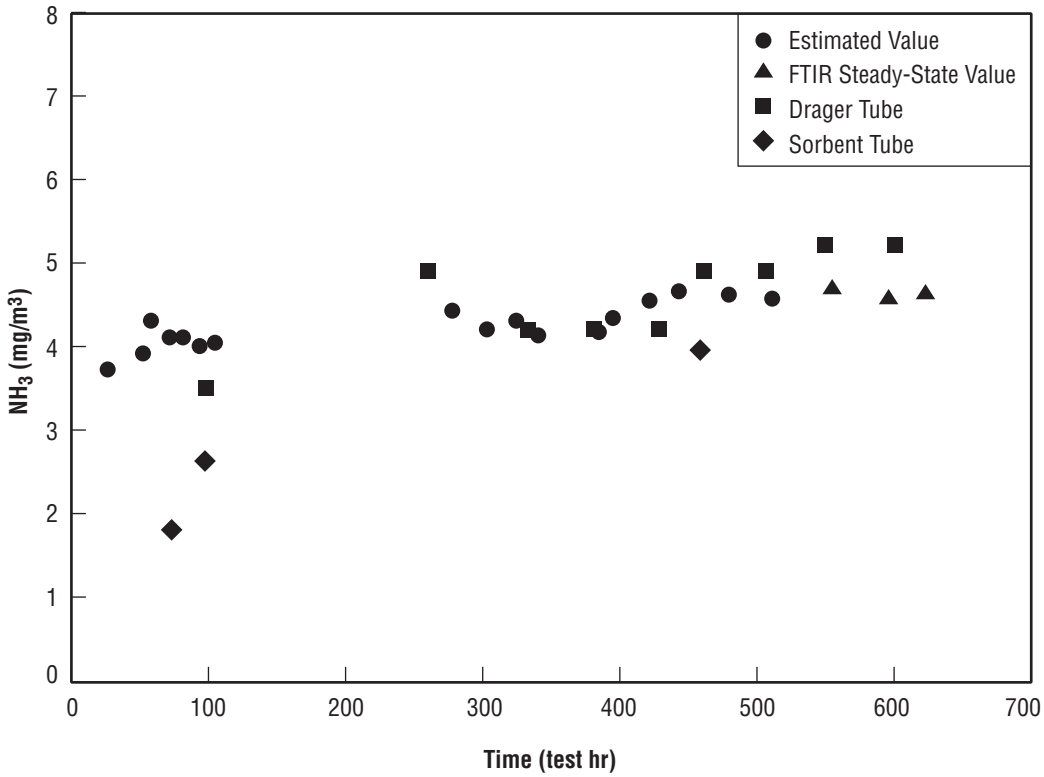

Figure 44. Ammonia concentration.

Methane was controlled to ≈13 mg/m^3 for the duration of test. Both samples collected at the TCCS inlet and just downstream of the charcoal bed (port 2) agreed well. This agreement demonstrated that CH_4 is not removed by the activated charcoal. The CH_4 concentration at the overall TCCS outlet (port 4) was consistently near 11 mg/m^3 while the concentration downstream of the HTCO (port 3) was consistently near 6 mg/m^3. A mass balance for CH_4, based upon these results, indicated a 55-percent CH_4 oxidation efficiency for the duration of the test. As shown in figure 45, the concentration began to increase at approximately the time that dichloromethane breakthrough of the charcoal bed was observed.

The oxidation efficiency for CO was 100 percent for the duration of the test. As shown in figure 46, the concentration was controlled to ≈1.2 mg/m^3 during the first 250 hr of testing and then to ≈2.5 mg/m^3 for the remainder of the test. The low concentration early in the test was caused by a lower than required injection rate. This test facility anomaly was corrected and the injection was increased to within specification for the remainder of the test.

The only observed process-related anomaly involved CH_4. During the entire test, the oxidation efficiency provided by the HTCO was ≈55 percent. Two hypotheses have been proposed for this performance. The first is that the catalyst settled and allowed a portion of the air to bypass it. Because the HTCO design is kinetically limited with respect to the CH_4 oxidation reaction, a small amount of air bypassing the catalyst could effectively reduce the reactor's residence time and, thus, lead to decreased efficiency.

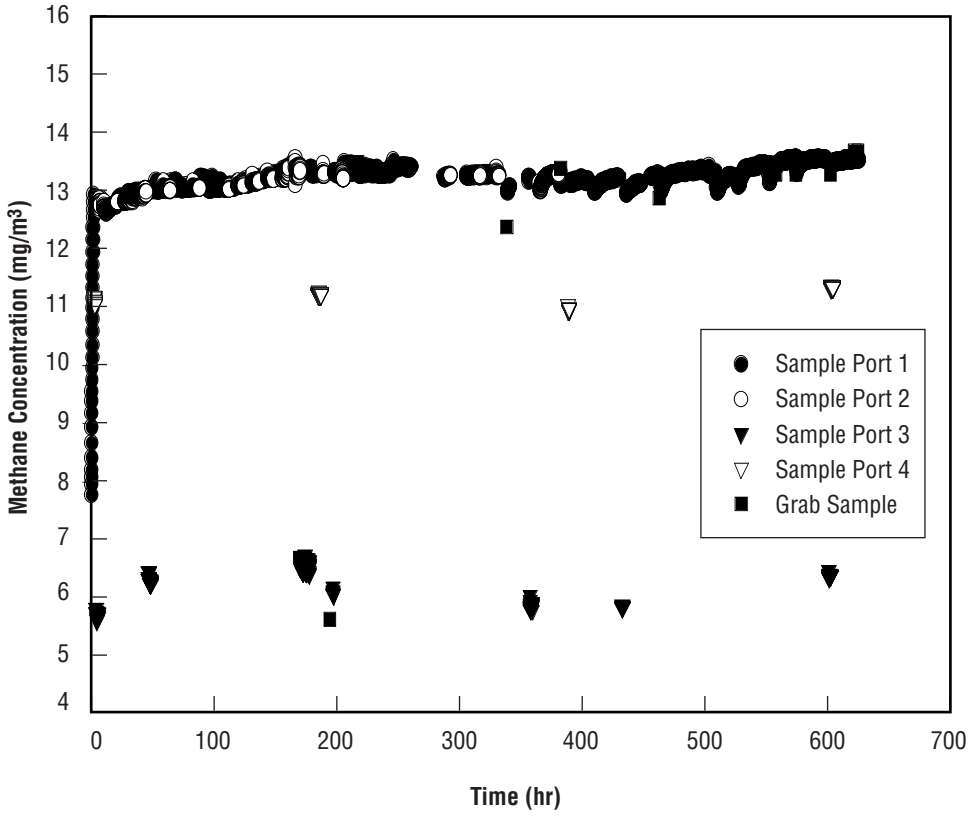

Figure 45. Methane concentration.

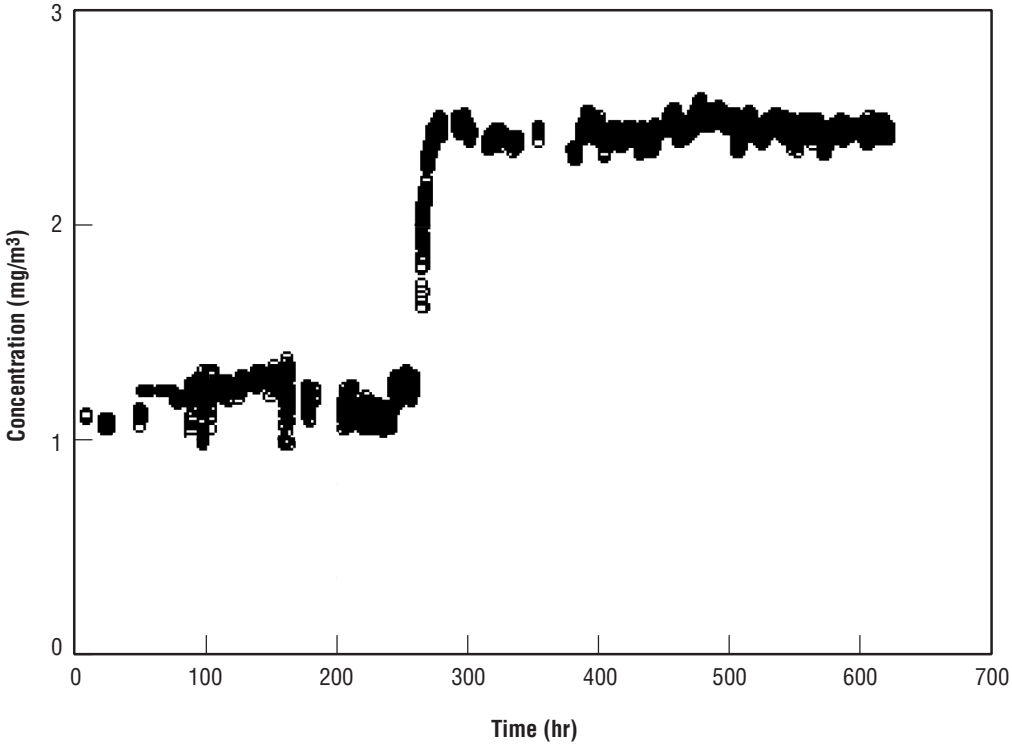

Figure 46. Carbon monoxide concentration.

The second possibility is also related to the kinetic limitation. It involves masking of the catalyst surface. Inspection of TCCS drawings indicated that Dow Corning DC111 silicone grease had been used in the seven duct couplings located between the charcoal bed outlet and the HTCO inlet. Offgassing of organosilicone compounds from this grease could have resulted in the formation of silica upon their oxidation. Silica has an extremely high melting point and, once produced, would immediately condense on the catalyst surface. Such a process would effectively mask or decrease the overall catalyst surface area leading to degraded CH_4 oxidation efficiency.

It should be noted that CO oxidation remained at 100-percent efficiency throughout the test. Since this reaction is diffusion limited rather than kinetically limited, it is quite possible for either a flow bypass or catalyst surface area reduction to have little measurable effect on the CO oxidation reaction.

Final determination of the root cause for the degraded CH_4 oxidation performance will be investigated before the TCCS is deployed on orbit. Despite this condition, the TCCS still has sufficient design margin to maintain the CH_4 concentration well below SMAC.

6.3.5.3 Comparison to model predictions. As stated earlier, one of the test objectives was to obtain data for process model validation. Central to this validation is the direct comparison of observed and predicted contaminant concentrations. A comparison of the observed and predicted concentrations for the liquid contaminants is provided in table 35.

As noted earlier, there were no breakthrough trends observed during the test, which was consistent with 100-percent single-pass removal predicted by the TCCS process model for each of these compounds. As such, a single test chamber average concentration describes the TCCS performance

Table 35. Russian normal contaminant load, maximum allowable concentration.

Trace Contaminant	Maximum Allowable Concentration (mg/m^3)	Amount of Trace Contaminants Loaded (Not Less Than) (mg/day)	Comments
Isopropyl-benzene	0.5	50	
Toluene	2.0	66	
Cyclohexane	3.0	200	
Ethylacetate	4.0	250	
Benzene	2.0	0.45	
Butanol	0.8	80	
Acetone	1.0	27	
Ethanol	10.0	250	Total of 300 mg/day added
Ethylene glycol	(100.0)	(50)	Not added—Ethanol added instead
Methanol	1.0	3.0	
Formaldehyde	0.3	10	
Acetaldehyde	1.0	24	
Nitrogen dioxide	0.3	13.5	
Ammonia	1.0	20	
Carbon monoxide	5.0	390	
Methane	0.5 vol %	30	
Hydrogen	0.5 vol %	1,200 (L/day)[a]	

[a]The hydrogen loading was adjusted for the volume of the test system (≈9 m^3) not to exceed the MAC.

for removing these compounds. All observed contaminant concentrations were found to be statistically consistent with the predicted concentration confidence intervals, except for ethanol. The analytical instrument used to provide this result is biased high. The alternate analytical instrument gave an observation which was biased low (below projected concentration). As such, it was assumed that the high ethanol concentration has no physical significance in terms of ethanol removal during the test period.

Both CO and ammonia concentrations were reliably predicted by the process model. Both were consistent with 100-percent removal efficiency by the HTCO and charcoal bed, respectively.

Predicting methanol and dichloromethane concentration as they break through the charcoal bed was considered to be the most significant challenge to process model validation. As shown in figures 42 and 43, both methanol and dichloromethane breakthrough trends were reliably predicted. At the same time, the CH_4 concentration trend during the time of dichloromethane breakthrough, shown in figure 45, was also found to be consistent with process model predictions.

These results are similar to those documented in reference 22. In that case and in the case of the TPCT, the process model predicted contaminant concentrations within an acceptable statistical range. Based upon the comparison of predicted and observed concentrations for the TPCT combined with their similarity to previous validation study results, the process model is considered to provide highly reliable predictions of TCCS performance.

6.3.6 Conclusions

Based upon the results of the TPCT, the following conclusions can be made:

- The TCCS design provides trace contaminant control for the load specified by the *ISS* program.

- Flight hardware performance is similar to that observed during previous development testing.

- The TCCS design is robust and provides sufficient margin to accommodate lower than expected HTCO CH_4 oxidation performance without approaching the SMAC.

- The process model is a reliable tool for predicting TCCS performance over time.

The *ISS* U.S. Hab Module TCCS was challenged with a representative trace contaminant load for 624 hr. During this time, methanol and dichloromethane broke through the activated charcoal bed. The approximate time of breakthrough for each contaminant was consistent with pretest process model predictions. In parallel with dichloromethane breakthrough, the CH_4 concentration began to rise as a result of catalyst poisoning, indicating a gradual poisoning of the CH_4 oxidation reaction by dichloromethane's oxidation products. This effect is consistent with previous observations during TCCS development and bench-scale testing.

Overall, the TCCS operated flawlessly. There were no mechanical or control anomalies noted for the flight hardware. Each trace chemical contaminant was controlled to less than its respective

SMAC and performance was consistent with earlier TCCS development testing. One exception was a lower than expected CH_4 oxidation efficiency provided by the HTCO during the entire test. Hypotheses have been prepared to explain this observation. Final determination of the root cause is to be made during posttest evaluation of the hardware. In spite of this performance deficiency, CH_4 never approached its SMAC.

6.4 Russian Trace Contaminant Control Test[23,24]

A filter assembly which is incorporated into the Russian trace contaminate control assembly (TCCA) was tested for removal of airborne trace chemical contaminants in a closed-loop 9 m^3 system. This test was conducted in the Boeing Huntsville LSTC.

The TCCA used on board the *Mir Space Station* has been in operation since April 1987. The TCCA, shown in figure 47, is composed of six primary components: a fan, a nonregenerable activated carbon canister (prefilters), two regenerative activated carbon canisters (fine filters), an ambient temperature catalyst canister, and a valve assembly. The TCCA processes 15–25 m^3/hr of cabin air, nominally 20 m^3/hr.

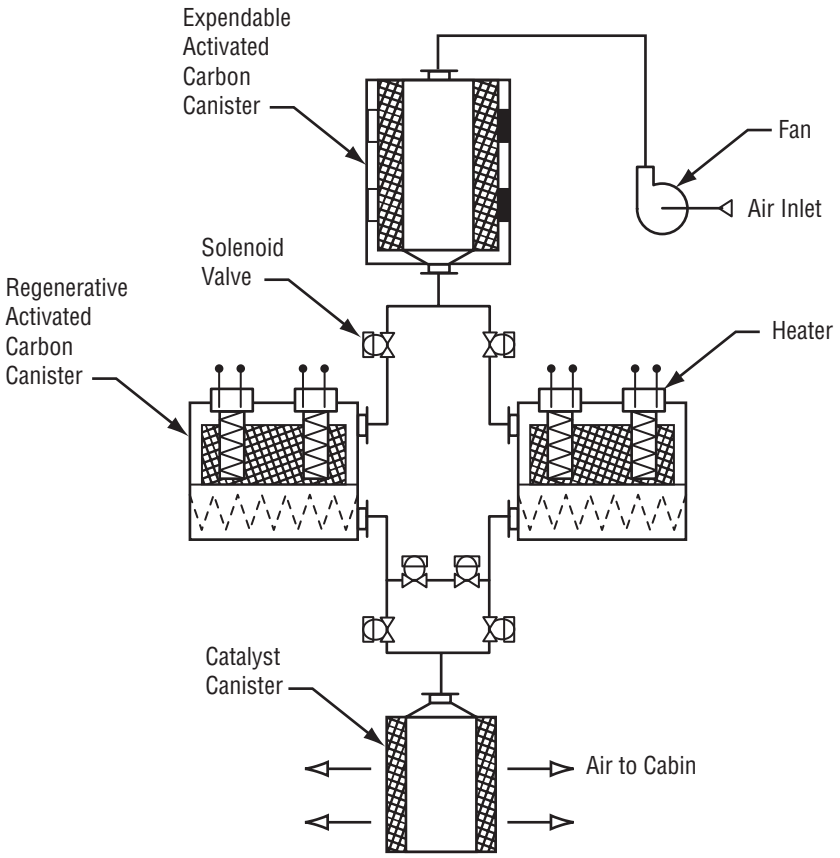

Figure 47. *Mir* trace contaminant control assembly.

The nonregenerable charcoal prefilter weighs 6 kg, is 22.5-cm long, and 20 cm in diameter. Air flows radially through ≈1.3 kg of activated charcoal and is designed to remove organic contaminants with molecular weight greater than ≈80. It serves to protect the regenerable filters from fouling with contaminants that are difficult to desorb from the charcoal.

The total TCCA air flow from prefilter is then split equally between the two regenerable filters. These axial-flow filters are designed to remove contaminants of lower molecular weight (<80). These filters each weigh ≈16 kg each, have a length of 29.5 cm, and a diameter of 25 cm. Each filter contains ≈1.4 kg of activated charcoal. Each of these canisters also contains four heater elements and three resistive temperature devises (RTD's) for thermal-vacuum regeneration every 20 operational days.

Downstream of the regenerable filters, the air streams recombine and flow through a radial flow ambient temperature catalyst filter, designed to oxidize CO and H_2. It has a length of 23.5 cm and a diameter of 12 cm. The catalyst filter's overall weight is 2.5 kg of which 0.5 kg is accounted for by the catalyst.

The Russian TCCA was designed to remove trace chemical contaminants from the *Mir Space Station* atmosphere at the rates specified in table 35. At these rates, the maximum allowable concentrations, also listed in table 35, were not to be exceeded.

6.4.1 Test Configuration

In 1996 Boeing conducted a system level test with a filter assembly which is currently used on the *Mir Space Station*. This assembly includes the following components:

- A prefilter element containing activated charcoal for removal of high molecular weight organics (<80).

- Two regenerable fine-filter canisters containing activated charcoal for lower molecular weight organic removal, heater elements, and RTD's.

- An ambient temperature catalytic filter element for primarily removing CO and H_2.

These filter components were incorporated into a nominal 9-m^3, closed-air loop ground test facility which emulated the *Mir* filter assembly operation. The filters were configured as shown in figure 48. The filters were then tested with a multicontaminant load from January 29 to April 25, 1996, under contract to MSFC. The goal of the test was to verify that the filter assembly would remove airborne chemical contaminants at specified daily loading rates and maintain concentrations to below Russian MAC's.

The Russian MAC and contaminant injection rates used for this test are given in table 35. All contaminants were injected continuously to create a multicontaminant system air loading which would simulate an on-orbit cabin air environment. Ethylene glycol was not injected for this test due to technical difficulties in obtaining gas-phase concentration of 100 mg/m^3 of ethylene glycol at ambient temperatures. The amount of ethanol injected daily was increased by the amount expected for ethylene glycol.

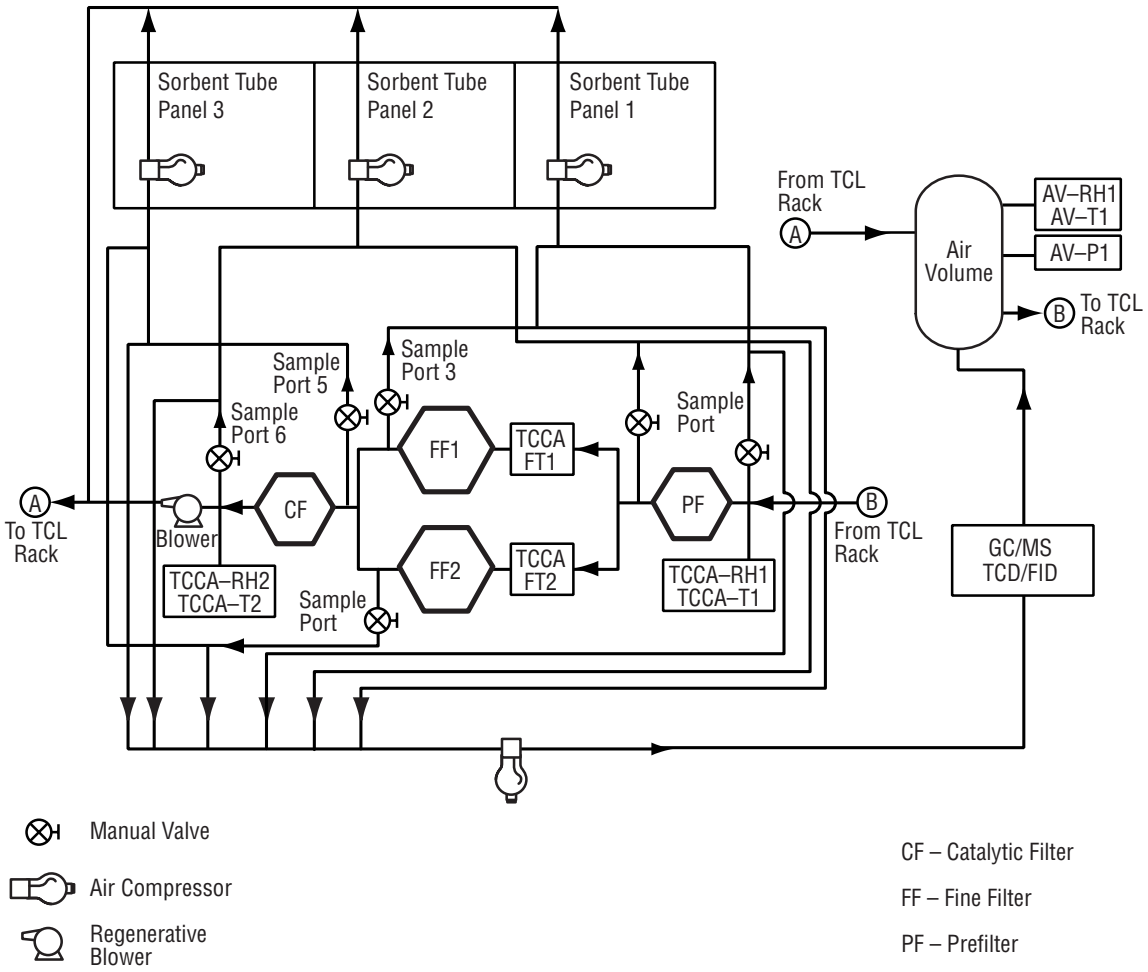

Figure 48. TCCA and sampling port schematic.

All contaminants, except H_2, were injected continuously for the duration of each test phase. Hydrogen removal was tested separately in the final phase of testing. Its presence and removal are considered to represent an off-nominal operational situation, such as leakage from the O_2 generator assembly. Methane was injected as part of the normal continuous contaminant load.

During this test, air flow rate was controlled to 21–22 m^3/hr (12.4–12.9 scfm), system air temperature to 21–24 ˚C (70–75 ˚F), system air relative humidity to 38–42 percent, and system air pressure to 750–850 mm of Mercury (mmHg) (14.5–16.51 psia). At these operating conditions, all Russian operating requirements were met.

6.4.1.1 Facility description. The trace contaminant control test facility incorporated a rack which housed the TCCA rack; a rack to control system air temperature, humidity, and to inject trace contaminants (TCL rack); a 9 m^3 SS tank; and an in-line GC/MS. These major components were interconnected by 2-in. SS tubing to create a closed-air loop. The components were configured as shown in figure 49. The TCCA rack receives air from the thermal control and contamination control loop (TCL) rack, which has been conditioned for temperature, humidity, and contaminant load. In the TCCA rack, the air is directed back to the TCL rack in a closed loop.

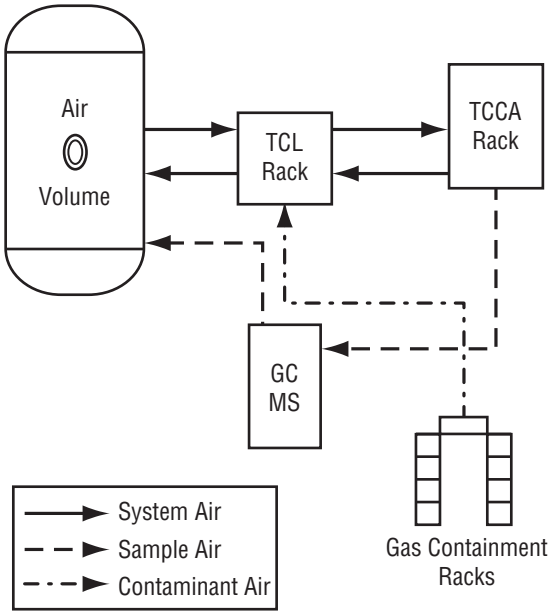

Figure 49. Test facility layout.

The TCCA system was air monitored for flow, temperature, humidity, and contaminant load. This monitoring point is in the TCCA rack just prior to the prefilter inlet. The chemical makeup of the test atmosphere is monitored at sample port 1, which is collected with instrumentation. As shown in figure 48, the TCCA rack contains six sample ports, used to sample around individual filter elements.

6.4.1.2 Contaminant injection. The gaseous contaminant injection assembly provided pressure regulation and mass flow control of the gas-phase contaminants used for contaminant loading during filter performance testing. During nominal performance testing, gas-phase contaminants were injected into the air volume tank. As a follow-on to nominal testing, H_2 was injected to a 0.5-volume percentage as an off-nominal condition. The gases were supplied from pressurized bottles containing a certified percentage of the contaminant in air as listed below:

- 0.295%±0.004 ammonia/balance air
- 4.0%±0.80 CO/balance air
- 0.515%±0.010 CH_4/balance air
- 0.145%±0.003 N_2 dioxide/balance air
- 0.199%±0.004 acetaldehyde/balance N_2.

The gases were injected continuously at varying rates into the system air at the TCL rack to achieve the required daily system mass loading specified in table 35.

Liquid contaminants were injected as two different mixtures at the TCL rack. The first was an aqueous mixture containing formaldehyde, methanol, ethanol, 1-butanol, and acetone. The second was an organic mixture containing isopropyl benzene, toluene, cyclohexane, ethylacetate, and benzene. Syringe pumps were programmed to inject the liquid mixtures into heated bypass tubes where the system air swept the evaporated contaminants to the air mixing volume. The air from the mixing volume

was then directed to the TCCA rack for filtration. Liquid contaminants were injected once every 4 hr, and the concentration pulses monitored hourly by automated in-line GC/MS.

6.4.1.3 Analytical methods. Sampling methods used during the test are the following:

- Automated in-line sample acquisition
- Sorbent tube collection
- Sample collection into pressurized cylinders.

In-line detection was performed with GC/MS for most organic trace contaminants, flame ionization detection, and TCD for H_2 analysis. Sorbent tubes were used primarily to analyze off line for butanol, methanol, formaldehyde, and ammonia. Carbon monoxide samples were collected in pressurized cylinders for off-line analysis by GC/TCD. All other contaminants were primarily analyzed by GC/MS automatically on an hourly basis.

6.4.2 Test Operations Summary

Fine filters regeneration was conducted during the system test similar to the regeneration schedule used on *Mir Space Station*, where one of the fine filters is regenerated every 20 days while the full TCCA air flow is directed to the fine filter not undergoing regeneration. During regeneration, the filter is continually exposed to space vacuum. After the filter is exposed to space vacuum for 60 min, power is applied to internal filter heater elements to raise the filter temperature to 180–200 ˚C for 1.5 hr. The filters continue to be exposed to space vacuum for an additional 2 hr. Vacuum is then disconnected and the filter is allowed to cool down to <45 ˚C. A bleed valve then opens, allowing the filter to be repressurized to cabin air pressure, and the filter is brought back on line.

During this test, both fine filters were regenerated simultaneously prior to the start of the testing and then at the end of the first performance test period. The initial regeneration was to establish a test baseline prior to the start of test. The second regeneration was to baseline the fine filters for testing of the assembly after accelerated aging of the prefilter, as discussed below.

Nominal performance testing was conducted in two phases. The first phase was a 20-day performance test period where the system air contaminants were injected at the rates in table 35 and the filter elements were new. These data provided a new filter assembly performance baseline.

Prior to the start of the second 20-day performance period, the age of the prefilter was accelerated to ≈80 percent of its expected 3-yr design life. This was accomplished by loading the prefilter over a 15-day period with isopropylbenzene, toluene, cyclohexane, and benzene with the amounts indicated in table 36. During this period, air flow did not go through the fine filters or catalytic filter. These contaminants were chosen since the prefilter preferentially adsorbs them over the other chosen test contaminants. The filter was then allowed to equilibrate by circulating system air over the next 5 days without contaminant injections.

The second performance period was conducted identically to the first after reinstalling the fine filter and the catalytic filter.

Table 36. Summary of trace contaminant loading during test.

Contaminant	20-Day Phase 1 (gm)	20-Day Preload[a] (gm)	20-Day Phase 2 (gm)	20-Day Target (gm)
Acetaldehyde[b]	0.57	–	0.47	0.48
Ammonia[b]	0.47	–	0.42	0.40
Acetone	0.55	–	0.54	0.54
Benzene	0.03	0.040	0.009	0.009
Butanol	1.61	–	1.59	1.60
Isopropyl-benzene	1.02	43.3	0.998	1.00
Toluene	1.35	57.3	1.32	1.32
Cyclohexane	4.00	137.3	3.91	4.00
Ethanol	6.03	–	5.89	6.00
Methanol	0.075	–	0.057	0.060
Ethylacetate	4.99	–	4.91	5.00
Formaldehyde	0.20	–	0.20	0.20
Carbon monoxide	8.35	–	7.91	7.80
Methane	0.64	–	31.0	0.60

[a] The preload phase was designed to accelerate the age of the prefilter to an ≈80 percent of its 3-yr design life with selected components.

[b] The gas-phase contaminants were injected in a steady rate manner but with varying levels.

6.4.3 Discussion of Results

Table 36 summarizes the masses of contaminants which were loaded during the two performance and interim preload phases of testing. The four gas-phase contaminants listed were injected at a steady rate, and the liquid-phase contaminants by pulse injection every 4 hr. Nitrogen dioxide (NO_2) was also injected, 639.7 mg during phase 1 and 73.4 mg during phase 2. Due to some difficulty with the analytical method, results for removing NO_2 from the system air are not discussed in this paper. However, it is important to note that NO_2 was a part of the multicontaminant background. Methane injection is shown in table 36. No significant adsorption of CH_4 was detected during either test phase which could not largely be accounted for through test rig leakage. Some temporary adsorption (1 percent) was detected early in phase 1 while filters were largely unloaded, as shown in figure 50. Methane was displaced, however, by other contaminants which had greater thermodynamic potential for adsorption.

In all of the test phases, contaminant concentrations did not exceed the Russian MAC's in table 35. Table 37 summarizes the removal performance results for the gas phase contaminants acetaldehyde, ammonia, and CO. Acetaldehyde was injected at two different rates during the 20-day, phase 1 test period. The 0.02 mg/min rate was a nominal 24-hr/day continuous rate. During this rate of injection in phase 1, acetaldehyde concentration in the tank was 0.06–0.08 mg/m^3, which is 10 times less than MAC. An acetaldehyde injection rate 8 times greater than that specified in table 35 (0.13 mg/min) was employed for 3 days, resulting in a small increase in system concentration. However, the acetaldehyde tank concentration remained at one-half the MAC. During the 20-day, phase 2 test period only the 0.02 mg/min acetaldehyde continuous injection rate was used. Some breakthrough was observed (0.05 to 0.14 mg/m^3); however, the concentration remained well below the acetaldehyde maximum allowable concentration of 1 mg/m^3.

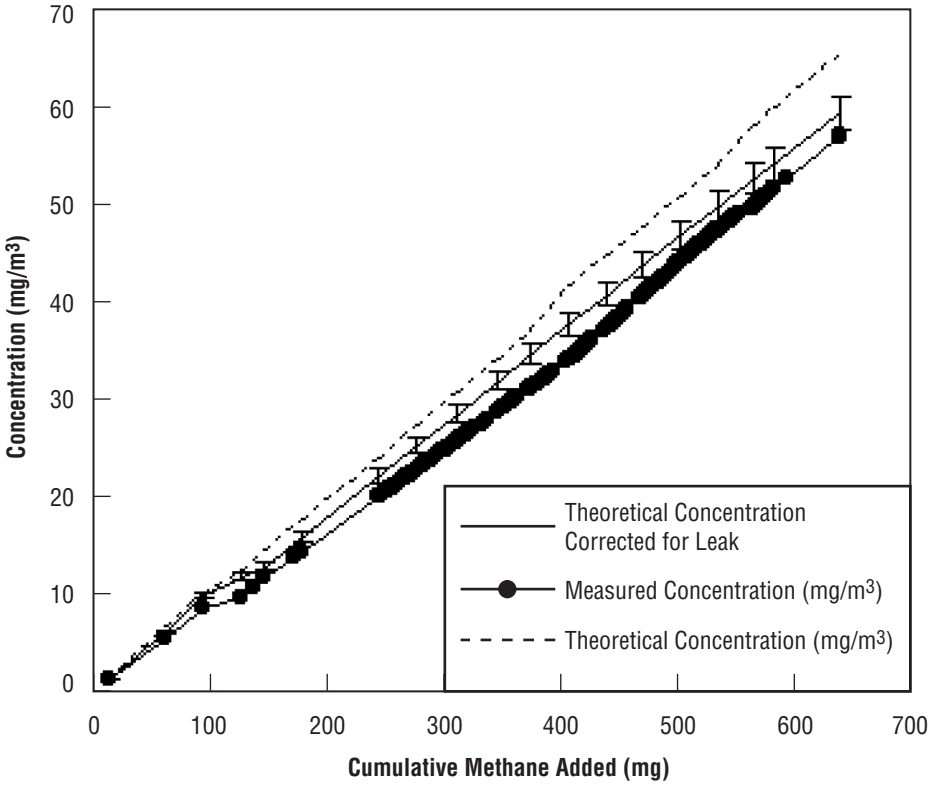

Figure 50. Methane concentration during phase 1.

Table 37. Gas phase contaminant removal performance.

	Russian MAC (mg/m^3)	Phase	Injection Rate[a] (mg/m in.)	System Concentration[b] (mg/m^3)	Error	Detection Limit (mg/m^3)
Acetaldehyde	1	1	0.02	0.06–0.08	±0.01	0.028
Acetaldehyde	1	1	0.13	0.36–0.42	±0.03	0.028
Acetaldehyde	1	2	0.02	0.05–0.14	±0.01	0.006
Ammonia	1	1/2	0.02–0.08	0.12	±0.04	0.01–0.03
Carbon monoxide	5	1/2	1.14–1.55	2.4	±0.8	1.0

[a]Gas phase contaminant injection rate
[b]Sample collection by sorbent tube (analysis by GC/MS).

Ammonia was injected at various rates (0.02–0.08 mg/min) during both phases 1 and 2. There was little sensitivity of system concentration to injection rate; therefore, the analytical results were treated as a single group. Based on samples taken before and after each filter element, ammonia removal efficiency was generally shown to be 100 percent, maintaining a system concentration of ammonia at ≈0.12 mg/m^3.

The results for removing CO from air were also treated as a single group. Some variation in injection rate was used, as indicated in table 37. Carbon monoxide concentration in the system air was maintained at ≈2.4 mg/m^3 by oxidation in the catalytic filter.

Liquid-phase contaminant removal results are summarized in table 38. These contaminants were pulse-injected every 4 hr. Table 38 shows the mass of each pulse and the system concentration after each pulse which would be expected without any removal by filtration. In the cases of isopropylbenzene, butanol, ethylacetate, and cyclohexane, the system concentration of these contaminants, without any removal by filtration after a single pulse, would exceed MAC's. The results in table 38 are from continuous sorbent tube collection, with sample collection periods ranging from 40 min to 4 hr. These samples were collected at sample port 1 (see fig. 35) which represented tank (system) concentrations.

Table 38. Liquid contaminant removal performance.

	Injection Mass[a] (mg)	Injection Conc.[b] (mg/m^3)	Russian MAC (mg/m^3)	40 Min[c] (Phase 1)	1 Hr[d] (Phase 2)	2 Hr[d] (Phase 2)	3 Hr[d] (Phase 2)	4 Hr[d] (Phase 2)
Isopropyl-benzene	8.49	0.91	0.5	0.31	0.29	0.18	0.13	0.09
Toluene	11.2	1.2	2	0.41	0.36	0.22	0.16	0.12
Benzene	0.08	0.008	2	<0.024	<0.02	<0.01	<0.007	<0.005
1-Butanol	13.48	1.45	0.8	0.52	0.48	0.29	0.20	0.14
Ethanol	49.88	5.35	10	1.96	2.49	1.81	1.53	1.24
Methanol	0.5	0.05	1	0.20	0.11	0.04	<0.018	0.014
Ethylacetate	41.8	4.48	4	1.66	1.58	0.99	0.74	0.54
Acetone	4.58	0.49	1	0.21	0.18	0.14	0.10	0.09
Formaldehyde	1.69	0.18	0.3	0.06	–	0.03	–	0.010
Cyclohexane[e]	33.3	3.57	3	2.100	1.92	1.22	0.87	0.700

[a]Milligrams of liquid contaminant injected every 4 hr
[b]Calculated concentrations expected in the system (@ STP) after injection, with no removal by filtration
[c]Contaminant concentrations on day 20 of phase 1; sample collection for 40 min following injection
[d]Contaminant concentrations for day 20 of phase 2:
1-hr continuous sorbent tube collection after injection
2-hr continuous sorbent tube collection after injection
3-hr continuous sorbent tube collection after injection
4-hr continuous sorbent tube collection after injection
[e]Sample analysis by on-line GC/MS, values are integrated average concentrations over the respective sample periods of 1, 2, 3, and 4 hr.

During phase 1, samples were collected for the 40-min period immediately following the injection. These results provided a good indication of contaminant removal. As shown in table 38, all 40-min sample results were less than MAC's. However, a 40-min sample collection time did not provide complete monitoring of the system concentration between injections. Therefore, during phase 2, system air samples were continuously collected for 1, 2, 3, and 4 hr following injection. The 4-hr sample normalizes the system air concentration following the injection over a 4-hr period. This effectively provides a system level steady-state concentration for each contaminant. In summary, none of the 4-hr liquid phase contaminant concentrations exceeded the Russian MAC's.

The system air concentrations were monitored by GC/MS during each 4-hr injection cycle over the 20 days of each test phase. There were four in-line GC/MS samples taken after each injection. The fourth sample of each cycle represented the system air concentration just prior to the next injection, and therefore, the residual mass in the system. This residual mass indicated <100-percent removal efficiency in the operation of the filter assembly. Figure 51 shows the residual mass for the test phases 1 and 2 for some of the liquid-phase contaminants.

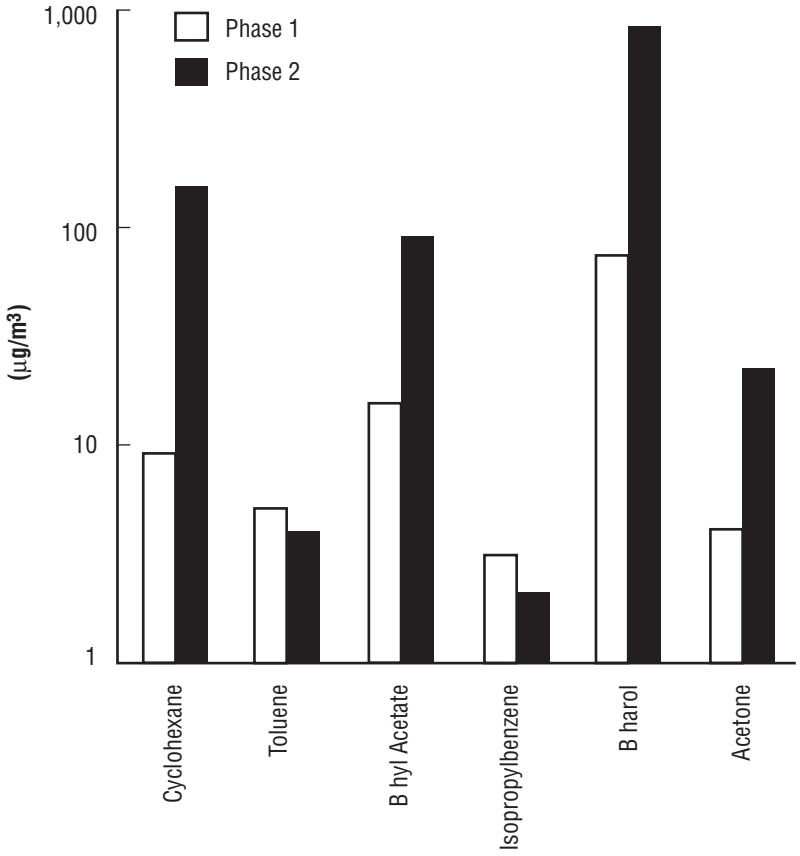

Figure 51. Residual concentrations 4 hr after liquid injection by test phase.

An increase in residual concentrations of certain of the liquid phase contaminants was observed between test phases 1 and 2. These results are also shown in figure 51. Four of the contaminants showed significant increase in residual system air concentration between phases 1 and 2: ethanol, cyclohexane, ethyl acetate, and acetone. These contaminants were displaced from the prefilter after the preloading phase, basically reducing the system capacity for these contaminants during phase 2. However, these concentrations are still well below MAC's.

Hydrogen removal is performed by the catalytic filter. Hydrogen was tested separately at the end of the two 20-day performance periods. After the last contaminant pulse injection, H_2 was injected into the air tank, raising the system air H_2 concentration to 0.5 percent by volume. Hydrogen removal represents an on-orbit contingency situation in the event of a leak in the O_2 regeneration assembly. This test was designed to demonstrate the H_2 removal efficiency of the catalytic filter. As shown in figure 52, H_2 concentration decayed from 450 mg/m^3 to ≈130 mg/m^3 in 70 min. Ultimately, H_2 concentration decayed to detection limit (50 mg/m^3) within 48 hr.

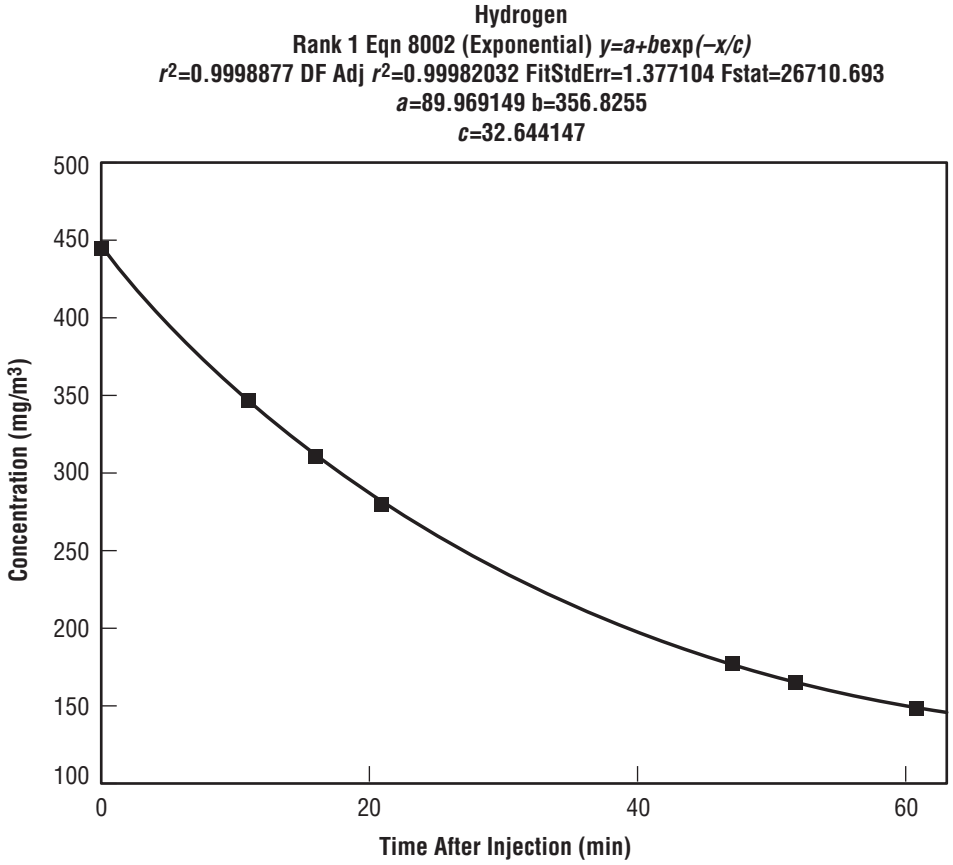

Figure 52. Hydrogen concentration decay.

6.4.4 Conclusions

Based on table 35 loading rates, the following conclusions can be made:

• The Russian TCCA can maintain contaminant concentrations below Russian MAC's when the filters are new.

• The Russian TCCA can maintain contaminant concentrations below Russian MAC's after aging the prefilter with ≈80 percent of a 3-yr loading of isopropylbenzene, toluene, cyclohexane, and benzene.

• The assumption that the prefilter has a useful life of 3 yr is valid, based on the loading rates in table 35, for the high molecular weight organic compounds. No significant increase in test chamber concentration was observed, based on the aged prefilter.

• The thermal vacuum regeneration of the fine filters enabled the filter system to maintain contaminant concentrations to within the limits of table 35.

6.5 Metal Monolith Trace Contaminant Control Subassembly Catalyst Development[25]

A retrofit to the primary design of the TCCS's catalytic oxidizer was proposed by Precision Combustion, Inc. (PCI) of New Haven, Connecticut. The proposed retrofit utilizes an advanced technology, lightweight metal monolith catalytic converter based upon PCI's Microlith® technology. MSFC has funded PCI's fundamental research and performance characterization of the metal monolith for TCCS applications via Small Business Innovated Research Program contracts. Based upon the results from this work, preliminary engineering analysis conducted by MSFC has indicated that significant improvements to the TCCS's process economics may be realized by integrating the metal monolith into the TCCS HTCO. Also, a prototype metal monolith-based reactor has been designed and built to demonstrate its integration with a flight-like TCCS catalytic oxidizer assembly.

In order to fully understand the benefits which may be realized by retrofitting the TCCS with a metal monolith assembly, it is necessary to operate the prototype reactor under representative process conditions. To achieve this requires integrating the prototype reactor with a highly efficient recuperative HX that is similar in function and design to that used by the *ISS* TCCS and operating the integrated assembly under a range of process conditions. The metal monolith performance demonstration project was developed to do that. It investigated specific performance characteristics which could not be readily addressed by the preliminary engineering analysis or the development work conducted by PCI. These performance characteristics include the actual average power requirement, the ease of physical integration, startup transient duration, and process control. The performance demonstration project has allowed the metal monolith's energy requirements and the duration of expected thermal transients to be quantified and compared to those of the *ISS* TCCS. Also, the feasibility of physically integrating a metal monolith assembly with the existing TCCS design has been demonstrated. These data are key to developing a final metal monolith catalytic converter retrofit design.

The metal monolith catalytic converter developed by PCI is based upon innovative reactor design techniques. These techniques include the use of a series of high cell density, short channel length metal monoliths combined with a specialized catalyst coating process. The series of metal monoliths provide a significant reduction in boundary layer buildup that occurs in conventional monolithic substrates. A comparison of the boundary layer buildup of the metal monolith with that of a conventional monolith is illustrated in figures 53 and 54. By using a series of short channel length metal monoliths, a significant decrease in thermal mass can be obtained that results in a lightweight reactor design that has shorter startup transients. Because the metal monolith minimizes boundary layer buildup, it is characterized by a significantly improved mass transfer rate. The specialized catalyst coating technique provides a durable, high-surface area catalyst that is highly resistant to activity loss resulting from sintering. The coating also resists spalling.

The metal monolith catalytic reactor is intended to replace the existing heater assembly and catalyst bed of the TCCS HTCO assembly. Its low thermal mass allows for more rapid heating of the catalyst substrate and, therefore, allows for more flexible operation of the TCCS during both normal and contingency situations. As summarized earlier, the objectives of this project are designed to provided data to quantify the potential benefits.

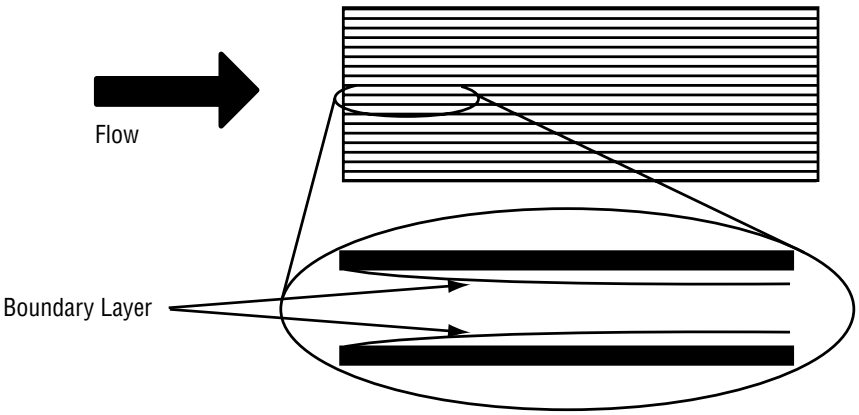

Figure 53. Boundary layer buildup in a conventional monolithic converter.

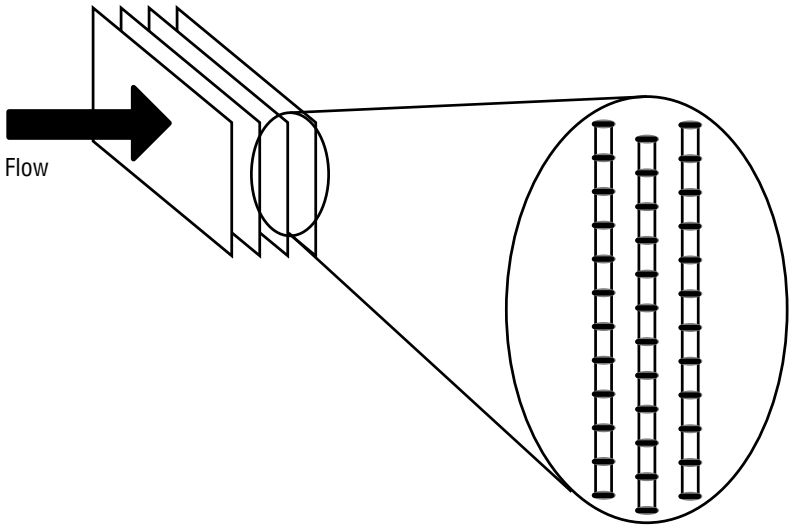

Figure 54. Boundary layer minimization by PCI's metal monolith technology.

6.5.1 Test Configuration

The TCCS hardware used in this project is functionally similar to the flight hardware. The test unit, shown schematically in figure 55, contains an activated charcoal bed containing ≈18.1 kg (40 lb) of Barnebey-Sutcliffe type 3032 activated charcoal, an axial blower, centrifugal blower, regenerable activated charcoal bed, LiOH presorbent bed, HTCO assembly, postsorbent bed containing ≈1.4 kg (3 lb) of Cyprus Foote Mineral Co. LiOH, and associated instrumentation.

For the purpose of this test project, the regenerable activated charcoal bed remained empty while the LiOH presorbent bed remained packed to serve as a static mixer for injected test gases. The HTCO was modified to accommodate the metal monolith catalytic converter test article. The TCCS hardware was located inside the CMS housed in the north high bay in MSFC's building 4755.

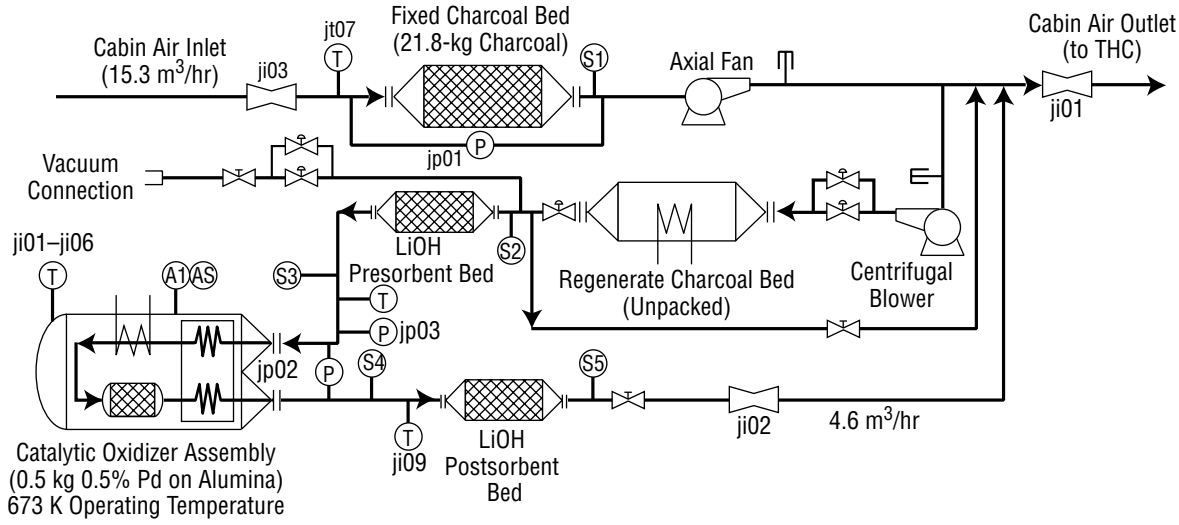

Figure 55. TCCS process and instrumentation diagram.

Process air enters the TCCS directly from the chamber or facility high bay atmosphere. The TCCS exhaust enters the chamber or high bay atmosphere directly. No interface with the facility THC system was required for this project. A facility-supplied manual valve located at the TCCS process air intake reduced the nominal inlet flow rate from 59.5 m^3/hr (35 scfm) to 15.29 m^3/hr (9 scfm). The flow to the HTCO assembly was set to the normal 4.59 m^3/hr (2.7 scfm) via the use of a manually actuated needle valve.

The metal monolith catalytic converter test article which was integrated into the existing HTCO assembly is shown isometrically in figure 56. The metal monolith includes a catalyst/heater element assembly, support structure, interface adapter, and an endplate adapter containing instrumentation feedthroughs. The unit is design to facilitate a straightforward retrofit into the existing TCCS with minimal modifications to the existing HTCO catalyst container. As can be seen by examining figure 57, which shows an exploded isometric view of the flight TCCS HTCO, there are geometrical similarities to the existing system that will enable the Microlith®-based metal monolith assembly to be integrated with the existing catalyst canister. Its similarity with the heater assembly shown in figure 57 is especially noteworthy.

For this test, the TCCS was configured to stand alone; i.e., both the inlet air and outlet air interfaces were direct with the chamber atmosphere. All testing was conducted with the CMS door open since there was no need to condition the entire chamber atmosphere. Methane injection was accomplished by metering a 3-percent-by-volume, CH_4-in-air mixture into the TCCS process flow stream just upstream of the presorbent bed. The presorbent bed served as a static mixer to ensure a uniform CH_4 concentration was maintained at the HTCO inlet. Both CH_4 and CO_2 were monitored at the HTCO inlet and outlet. Samples were collected and pumped to analytical instruments located outside the CMS. Carbon dioxide analysis was accomplished by using two Horiba analyzers and CH_4 analysis was accomplished by using an HP GC. Details on these instruments are provided later. The TCCS was outfitted with a Sorensen variable voltage power supply, an HP data scanner, and the necessary sensors and instrumentation for ensuring that the proper test conditions were being maintained. A simplified schematic of the TCCS test stand is provided in figure 58.

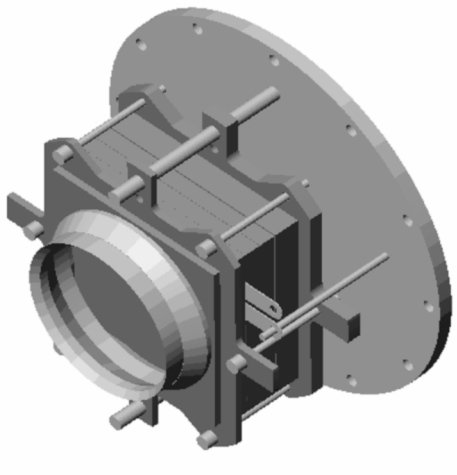

Figure 56. Prototype Microlith®- based metal monolith assembly.

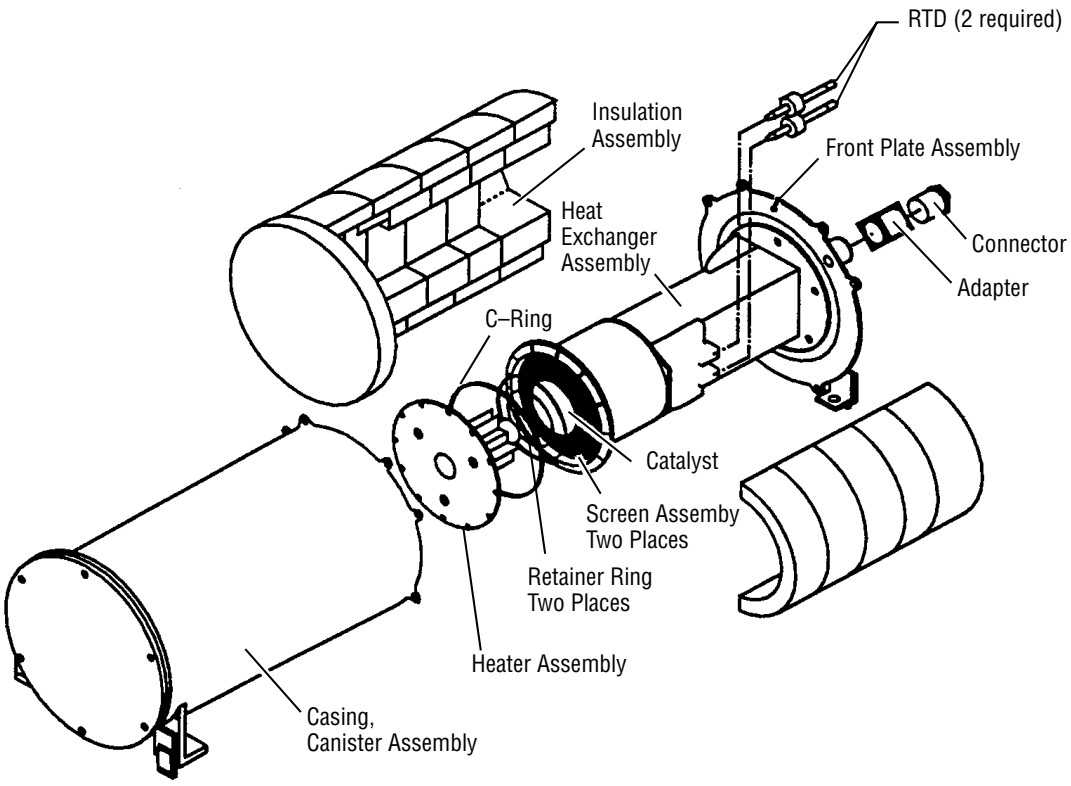

Figure 57. *ISS* TCCS HTCO exploded view.

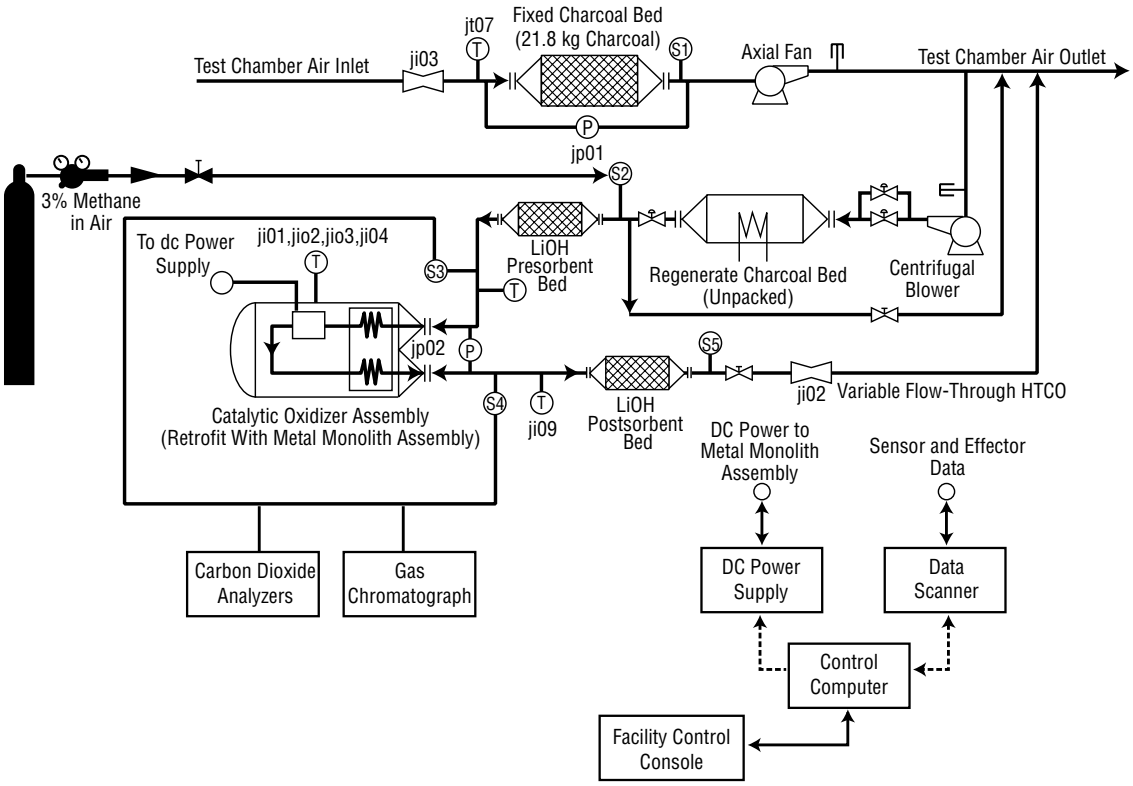

Figure 58. Metal monolith performance demonstration test stand schematic.

6.5.2 Test Operations

Integration of the metal monolith assembly with an existing flight-like TCCS HTCO HX assembly was conducted May 12–14, 1998. Representatives from the metal monolith assembly's developer, PCI, participated in the integration process. The first subtask was to determine whether the metal monolith assembly would seal properly at its interface with the HX. Precise measurements were made of both the HX and metal monolith assemblies. It was found that the metal monolith assembly dimensions were appropriate for providing an adequate seal.

The metal monolith assembly included two type K TC's: one was in contact with the last metal monolith element and the second was in the air gap between the catalyst stack outlet and the endplate. A third TC was added. This TC extended into the HX's hot side inlet heater, approximately the same location as that for the RTD's used in the flight TCCS design to control heater operations. The metal monolith assembly was integrated into the HTCO. Two layers of Manville Q-Fiber felt insulation were secured around the HTCO flange and endplate to complete the integration.

After successfully integrating the metal monolith assembly with the HX assembly, the HTCO was installed into the TCCS test stand and checkout tests were conducted over the next 2 days. Metal monolith power control was based upon temperature signals from the TC in contact with the last metal

monolith element. The temperature signal from the TC in the air gap served as the backup control sensor. Some minor problems with the communications bus were found and resolved. Formal test runs, however, could not begin until the week of May 25 because final calibration and checkout of the in-line CO_2 analyzers and GC were not yet completed.

Once the gas analyzers were ready, the thermal transient test runs began on May 27 and were completed on May 29. A single run was conducted each day to allow each run to start cold. This allowed for an accurate measurement of the thermal transient duration. No CH_4 was injected during these tests because the focus was on measuring the thermal transient. Process air flow to the HTCO was set at 4.59 m^3/hr (2.7 scfm) for all runs. No process anomalies were experienced during this test series.

Following thermal transient testing, three power-save operating mode tests were conducted beginning on May 30 and ending on June 2. As with the thermal transient testing, a single run was conducted each day beginning from a cold start. The first diurnal run began the power cycling after the HTCO reached its temperature control band of 400 °C ± 5.6 °C (750 °F ± 10 °F). The second run started the power cycling in the daylight mode at the same time that power was applied to the metal monolith assembly. This run was designed to provide data on how much the startup transient would expand if the power-save mode was used during all TCCS operating modes. The third run was similar to the second with the exception that startup transient timing started at the beginning of the night mode. The process air flow was 4.59 m^3/hr for all runs.

No process anomalies occurred during the power-save mode tests. However, one facility-related anomaly occurred during the final test run on June 2. The TCCS outlet was inadvertently blocked, causing the flow rate to drop below its low-limit alarm and then the TCCS to shut down. Since the run had to start from a cold condition, this run was restarted and completed successfully the following day.

Between June 9 and 19, the steady-state operations test runs were conducted. The first series, conducted from June 9–11, basically repeated the thermal transient test. Again, the process air flow was set at 4.59 m^3/hr. In each run, the HTCO was allowed to reach its temperature control band and cycle for about 1 hr. At that time, the 3-percent-by-volume, CH_4-in-air mixture was injected at a rate of 237 standard cm^3/min (sccm). This injection rate provided ≈65.4 mg/m^3 (100 ppm) concentration at the HTCO inlet.

The CO_2 concentration was monitored at both the HTCO inlet and outlet before CH_4 injection began to provide a baseline. Two separate Horiba CO_2 analyzers were used: one dedicated to monitoring the inlet and one to the outlet. These instruments monitored the process air continuously and sent results to the DAS.

After CH_4 injection began, the CO_2 analyzers were temporarily taken off line and a process sample was pumped to the GC for direct CH_4 analysis. By monitoring both CH_4 and CO_2, two means for determining oxidation efficiency were provided. The CH_4 analysis provided a direct inlet and outlet concentration for the calculation. Because CH_4 is converted to CO_2 on a 1:1 molar basis, the rise in CO_2 at the HTCO outlet provided a check for the CH_4 analysis results.

The second set of steady-state operations runs was conducted between June 12 and 16. All conditions and procedures were the same as for the first set except for the flow rate, which was set

at 1.7 m^3/hr (1.0 scfm). The CH_4 injection rate was again 237 sccm which provided a concentration of ≈170.6 mg/m^3 (260.7 ppm) at the HTCO inlet. This set of runs experienced a TCCS shutdown on June 12 which was caused by an overtemperature alarm. The controller overtemperature limit had been set at 415 °C (780 °F) to avoid damage to the metal monolith assembly. This limit is extremely conservative given the metal monolith assembly's ability to operate above 538 °C (1,000 °F). The limit was exceeded because at the lower flow rate, the HTCO's thermal inertia resulted in a larger control band overshoot. The limit was changed to 421 °C (790 °F) and the test series continued without incident.

After completing three runs at 1.7 m^3/hr, the process air flow was changed to 6.8 m^3/hr (4 scfm). Methane was again injected after reaching the temperature control band. The 237 sccm CH_4-in-air injection rate provided an average concentration of 44.5 mg/m^3 (68 ppm) at the HTCO inlet.

The three high-flow rate runs were completed with no process anomalies. Once, a data acquisition anomaly occurred on June 10 during which the payload and components remove automated test system (PACRATS) was found to be off-line. The DAS was restarted and the test run completed. Since two additional runs with a complete data set were obtained for this condition, an additional run to make up for the lost data was not conducted.

Methane oxidation reaction light-off tests were conducted on June 22–24. This test series was conducted at the normal TCCS HTCO flow condition of 4.6 m^3/hr (2.7 scfm). The procedure for these test runs was somewhat the reverse of that used during the steady-state performance runs. Process air flow was set and the CH_4 injection at 237 sccm was started before applying power to the metal monolith assembly. Inlet CH_4 concentration was verified via GC analysis. Carbon dioxide was monitored continuously at both the HTCO inlet and outlet during the entire run. Once the CH_4 concentration was verified, power was applied to the metal monolith assembly. After achieving the temperature control band, gas samples were collected at the HTCO inlet and outlet and analyzed with the GC. There were no process or facility anomalies during this set of runs.

At the conclusion of the process performance tests, the HTCO was removed from the TCCS test stand. The metal monolith assembly was removed, inspected, and mated with a special vibration test fixture on August 4. The metal monolith assembly was found to be in excellent condition. The vibration test fixture was specially designed to allow the metal monolith assembly to be securely attached to the vibration test stands located in MSFC's building 4619. On August 5, the vibration test fixture and metal monolith assembly were transported to the vibration test laboratory. A 3.1-g root mean square (rms) random vibration load was applied in each axis for 1 min. No process anomalies were noted.

At the conclusion of vibration testing, the metal monolith assembly was reintegrated with the HTCO heat exchanger assembly and reinstalled into the TCCS test stand. The metal monolith assembly was operated successfully for more than 24 hr before a communications bus problem caused the TCCS to shut down. This problem was resolved during the next week and the metal monolith was restarted on August 14. The primary test objective of a postvibration test run of 48 hr was successfully met on August 16. In order to further demonstrate long-term operations, the metal monolith assembly was operated continuously until September 14. Methane oxidation performance was checked on August 26 and found to be within the range observed during previous testing. During this testing phase, the metal monolith assembly operated continuously for just over 30 days.

The HTCO was removed from the TCCS test stand for inspection and disassembled on October 20. The insulation was removed from the endplate and the 12 hexagonal bolts loosened. One of the bolts seized and had to be cut to remove it. The metal monolith assembly was removed, inspected, and photographed.

6.5.3 Discussion of Results

The metal monolith assembly was operated successfully in a power-save mode. In this operating mode, power is applied to the HTCO during the worst-case orbital daylight period, and is switched off during the orbital night. Process air flow is continuous. The worst-case orbital day/night cycle results in a 53-min day and a 37-min night. Figure 59 shows a representative temperature profile for the metal monolith-based HTCO during typical power-saving mode operations. This particular run shows the effects of starting a power-saving mode after first achieving the standard temperature control band. The effects of starting the HTCO in a power-save mode are illustrated in figure 60. As can be seen, the startup transient duration is effectively doubled. An additional 37 min is added to the startup transient if power is applied at the beginning of the orbital nighttime period.

When operated in a power-saving mode, the catalyst temperature fluctuates between 400 °C (750 °F) and 233 °C (451 °F). Analysis of CH_4 reaction light-off data obtained during this project show that oxidation efficiency would range between 87 and 18 percent for these temperatures. Over the entire 90-min cycle, the temperature averages 315.8 °C (600.5 °F) and provides an average CH_4 oxidation efficiency of 52.5 percent. This average temperature is also sufficient to oxidize most other common spacecraft cabin air contaminants such as formaldehyde, benzene, acetone, and dichloromethane.[20]

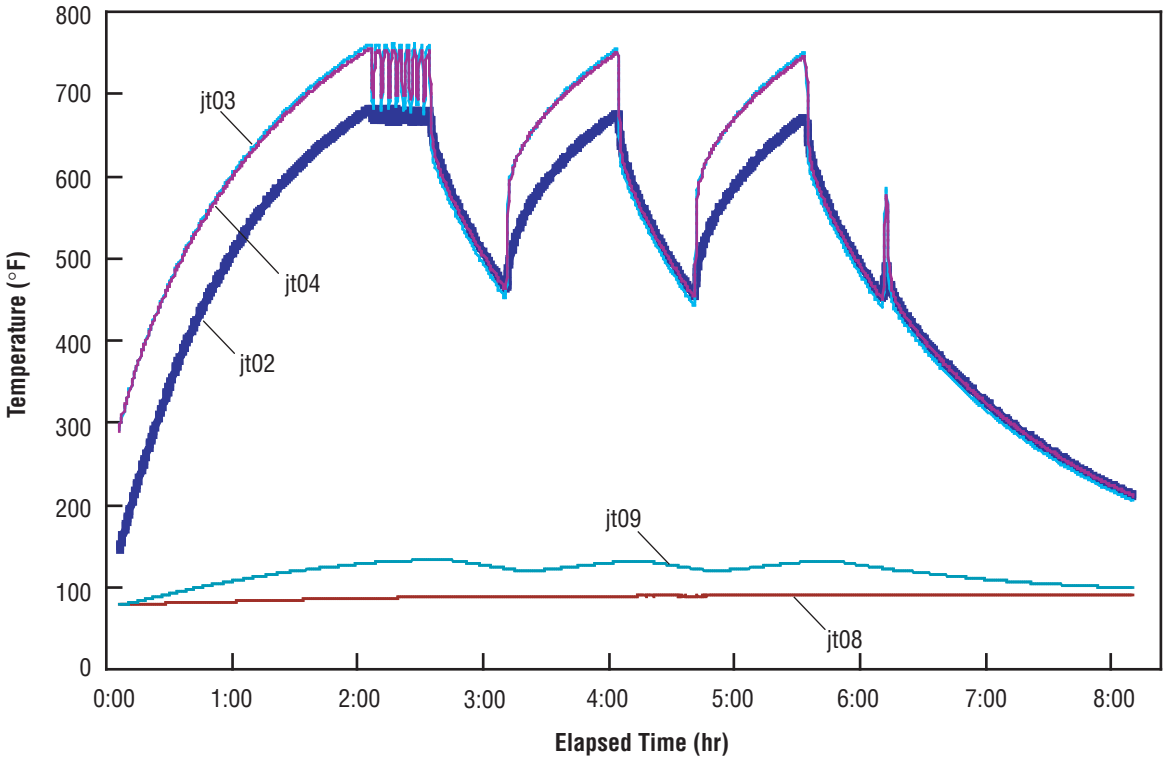

Figure 59. Typical metal monolith power-saving mode temperature profile.

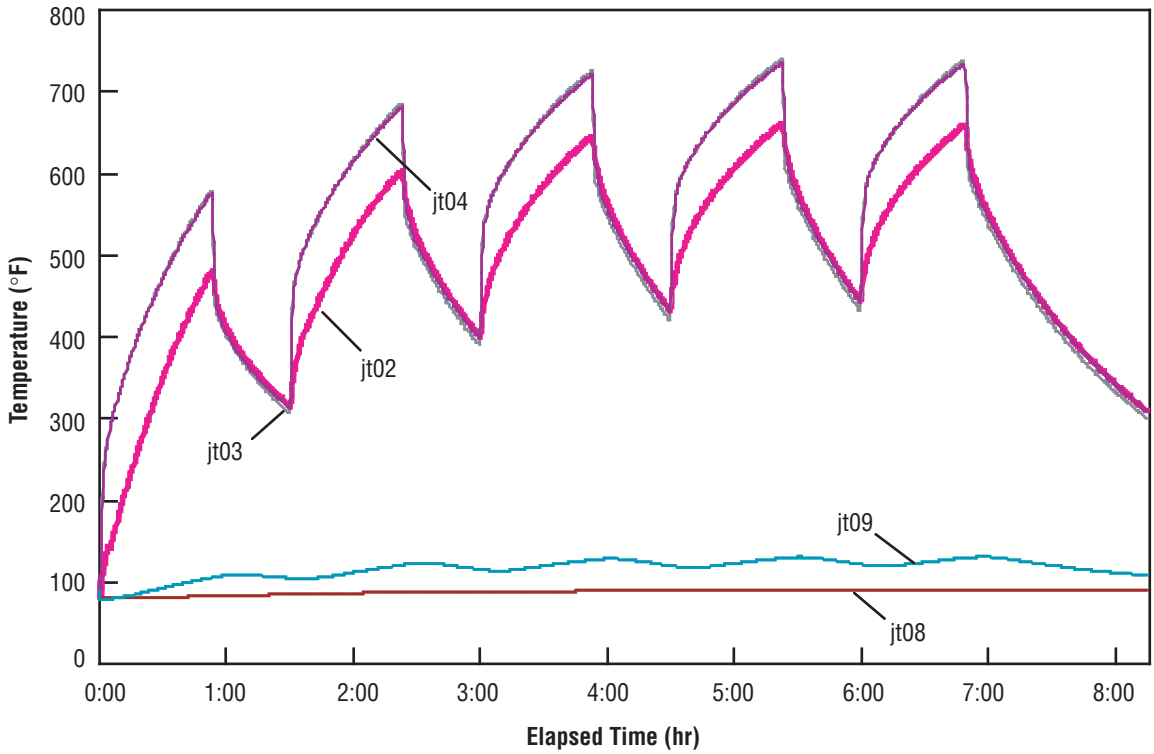

Figure 60. Effect of initiating power-save mode simultaneously with TCCS startup.

Given that O_2 is in excess during all stages of the reaction, it is not anticipated that any partial oxidation products would result during the observed temperature swing.

The metal monolith assembly's temperature was controlled by regulating its 28-Vdc power supply. Power was switched on when the control temperature reached 393 °C (740 °F) and switched off when it reached 404 °C (760 °F). The duty cycle was measured directly using a stop watch and also analytically from reduced data. Results from both measurement approaches agreed very well. Duty cycles for 1.7, 4.6, and 6.8 m^3/hr were determined to be 0.64, 0.73, and 0.84 m^3/hr, respectively. An additional measurement was made at 5.3 m^3/hr (3.1 scfm) during endurance testing. The duty cycle was found to be 0.78 m^3/hr at this additional flow rate.

The effect of flow rate on pressure drop, as shown in figure 61, is not linear and is best represented by a semilogarithmic plot. Pressures used to construct this plot have units of pascals. The correlation coefficient for the semilogarithmic plot is 0.999.

Analysis of process sample data shows that CH_4 oxidation efficiency ranged from 94.8 percent at the low-flow condition to 75.2 percent at the high-flow condition. At the normal HTCO flow rate, 4.6 m^3/hr, the CH_4 oxidation efficiency was found to average 87.3 percent.

The time that elapses between metal monolith startup and CH_4 oxidation reaction light-off was determined by analyzing CO_2 concentration at the HTCO inlet and outlet during a typical startup

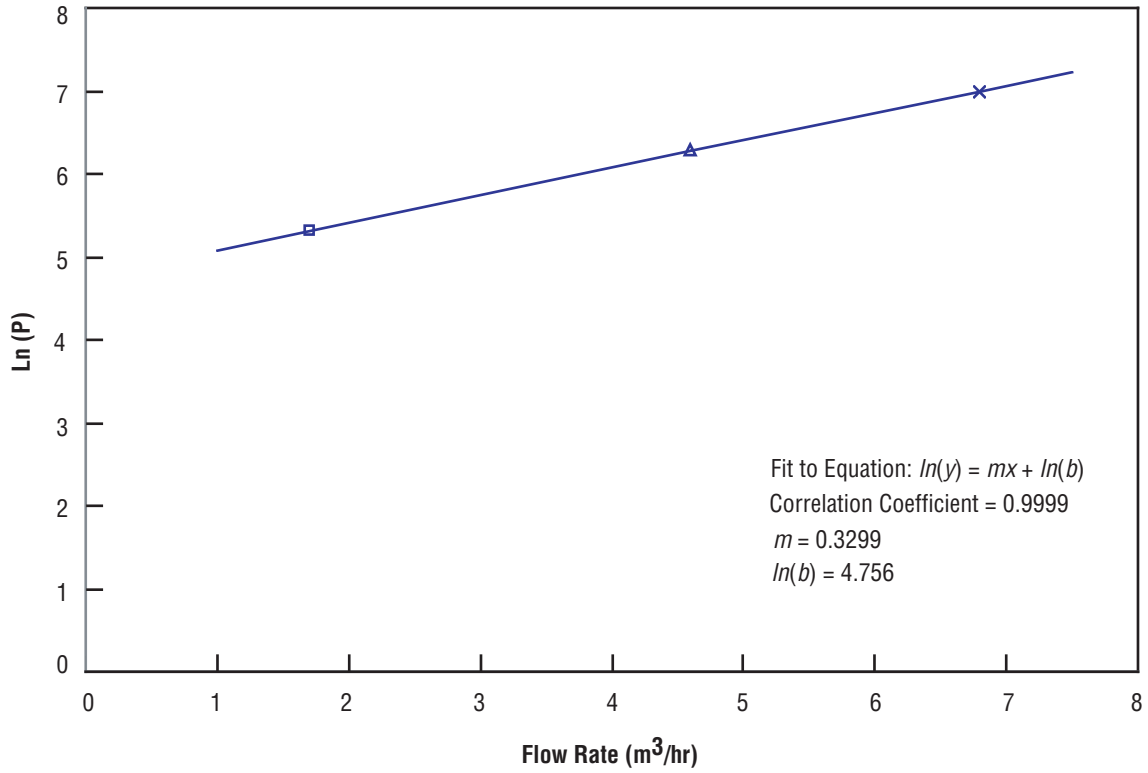

Figure 61. Effect of process air flow rate on HTCO pressure drop.

transient. Light-off is defined as the point at which outlet CO_2 concentration begins to increase. Figure 62 shows a representative CO_2 concentration profile. Three separate runs were conducted to investigate reaction light-off. Light-off was observed at an average metal monolith temperature of 224.3 °C (435.7 °F), reached ≈0.423 hr (25.4 min) into the startup transient. Fifty-percent CH_4 oxidation efficiency was observed at an average 337.6 °C (639.7 °F) ≈1.246 hr (74.76 min) into the startup transient.

The metal monolith assembly was removed from the HTCO before it was subjected to vibration testing. Visual inspection upon its removal showed it to be in excellent condition. In order to subject the assembly to vibration testing, a special fixture was designed and fabricated. This fixture was an aluminum "donut" which allowed the metal monolith assembly to be mounted on the vibration test stands, as shown in figure 63.

Once secured to the vibration test fixture, the metal monolith assembly was subjected to a 3.1-g rms random vibration load for 1 min in each axis. This load is specified for the TCCS launch and landing environment.[24]

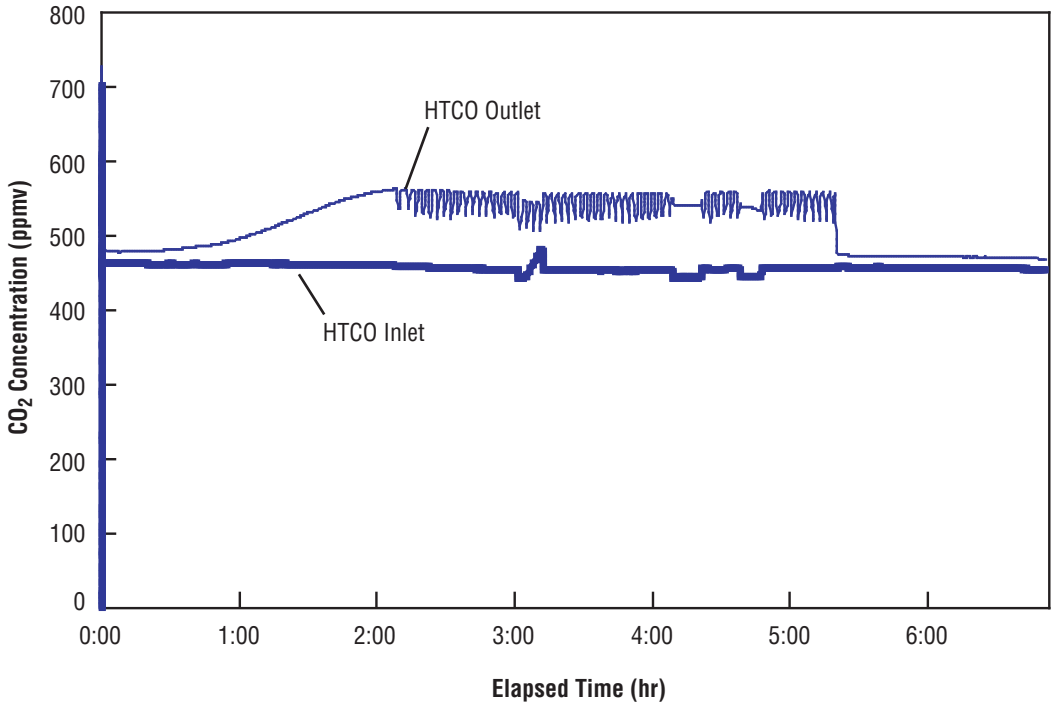

Figure 62. Carbon dioxide profile indicating methane reaction light-off.

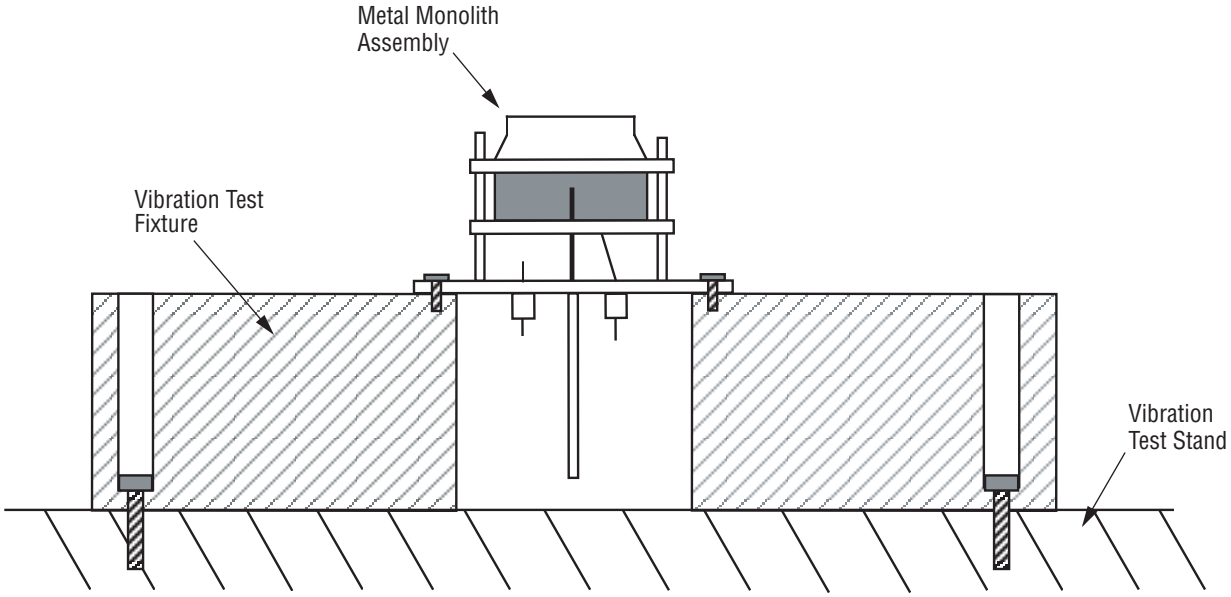

Figure 63. Cross-sectional view of the metal monolith assembly mounted on the vibration test fixture.

Observation of the testing indicated no problems. The metal monolith assembly was not damaged and it functioned as it had before vibration testing. Based upon the vibration test observations and the subsequent baseline performance run, it can be concluded that the metal monolith assembly can withstand launch vibration loads and then function properly.

After completing 30 days of continuous operation, the TCCS was shut down and the HTCO removed from the test stand. Disassembly of the HTCO showed the metal monolith assembly to be in excellent condition. No changes in resistance or excessive wear were observed. The metal surfaces of the metal monolith assembly had become duller in appearance when compared to the beginning of the test.

6.5.4 Conclusions

Applying the metal monolith catalytic converter technology to spacecraft air QC problems may realize benefits in the areas of logistics, crew time utilization, process startup, and process operations. Basic research and technology development conducted by PCI has demonstrated that the metal monolith technology possesses significantly enhanced mass transfer properties. The observed tenfold enhancement in mass transfer provides for a more robust catalytic oxidizer design with a larger performance margin with respect to poisoning. Because of this added margin, a metal monolith-based catalytic oxidizer can recover from a poisoning event more rapidly. While it takes the pellet-based catalyst HTCO design more than 100 hr to recover from a poisoning event, the metal monolith can recover from the same magnitude event in 100 min—98-percent faster.

The demonstrated design robustness may also lead to significant benefits in TCCS process economics. The metal monolith technology has been demonstrated to perform properly in a harsh automotive exhaust environment after an accelerated 5-yr life (50,000 mi or 10,000 mi/yr). In comparison, the present TCCS oxidizer design has been validated for a 2-yr service life. Its service life has been set conservatively at 1 yr by the *ISS* program. By extending the HTCO's service life to 5 yr, an annual logistics savings of 19.4 lb can be realized and ≈0.29 hr of crew time saved annually.

The metal monolith's robust design may also allow the charcoal bed to become more saturated than previously allowed. An analysis of in-flight trace contaminant loads observed during the Spacelab program shows that the only cabin contaminants which could be a threat to the metal monolith reactor, with respect to irreversible poisoning, are organosilicone compounds. When oxidized, these compounds form silica, which immediately condenses on the catalyst surface. A catalyst masked by silica cannot be restored by thermal treatment and must be replaced. Expected loads of organosilicone compounds, however, would take nearly 30 yr to saturate the charcoal bed and reach the catalyst. Since the present experience base for expendable charcoal bed service life is limited to that of the Russian *Mir Space Station*, a service life no longer than 3 yr is considered reasonable. By changing the charcoal bed every 3 yr, annual logistics and crew time savings may be as high as 296 lb and 2.5 hr, respectively.

Even though more halocarbons will be allowed to enter the metal monolith-based HTCO, it is not anticipated that the LiOH postsorbent bed would have to be replaced more frequently. In fact, analysis of the total halocarbon load expected for the *ISS* indicates that the replacement will be needed

at ≈2-yr intervals. Therefore, it can be expected that the minimum logistics and crew time savings that may be realized by deploying a metal monolith catalytic oxidizer on board the *ISS* are 315 lb and 2.5 hr, respectively.

Other benefits which may be realized pertain to electrical power savings and operational flexibility. Demonstration testing showed that the TCCS startup transient can be reduced from 9.5 to 2.1 hr. This represents a reduction of 77 percent and a savings of 1,100 Whr during every process startup. Also, the ability to operate the metal monolith assembly in a power-saving mode may lead to additional continuous power savings. The power-saving mode effectively reduces the heater duty cycle from 72 to 41 percent, yielding an average continuous power savings of 1,116 Whr. It must be noted that the pellet-based HTCO design may also achieve this power savings; however, its operation in a power-saving mode has not be demonstrated by testing.

6.6 Four-Bed Molecular Sieve Independent Subsystem Testing[26]

4BMS testing includes the performance enhancement test (PET) which is being conducted to determine the enhancement potential of performance to meet reduced $ppCO_2$ exposure levels. In addition, certain tests are planned to address 4BMS "flight issues."

A preliminary PET was conducted in August 1996 to provide initial data to verify that 4BMS operational changes could be made such that the Life Sciences requirement of 2.2 mmHg $ppCO_2$ was met. A high-fidelity 4BMS was utilized for this testing. Testing was conducted in the CMS which is a part of the MSFC ECLSS test facility located in building 4755. 4BMS parameters of air process flow rate, cycle time, and sorbent bed heater set-point temperature were varied to determine removal capability for the various operational configurations. Six operational configurations were evaluated in a period of 15 consecutive days.

Preliminary results from the PET are shown in table 39, along with other recent test results for comparison from the MSFC integrated AR test and the CO_2 removal rate and electrical power consumption evaluation test conducted by Allied Signal. PET results are from July 14–August 11, 1996. Review of the test data (table 39) indicates that process air flow rate has the greatest influence on CO_2 removal capability. CO_2 removal rate divided by inlet $ppCO_2$ is plotted against flow rate to illustrate this relationship (fig. 64).

The 4BMS test setup has been upgraded with flight system sorbent beds, a commercial blower with higher flow rate capability, and facility upgrades to increase control over the process air dewpoint and temperature. Phase II PET testing was completed in July 1998 and the data are being analyzed.

4BMS "flight issues" include: testing with 4BMS process air pulled from the cabin rather than downstream of the THC CHX, testing to determine desiccant bed breakthrough in the power-save mode, characterization of the cyclic humidity spike, and testing at a 10-person level. There is concern that liquid H_2O droplets possibility carried over from the CHX will poison the desiccant beds with resulting degradation in CO_2 removal performance. An alternative is to pull 4BMS process air from the cabin or from inside the AR rack. When the 4BMS is operated in the power-save mode with a sorbent bed heater setpoint of 127 °C, the H_2O breakthrough in the desiccant beds will eventually occur. No testing has

Table 39. PET, IART, and development 4BMS results.

Test Day	Power Mode 1=Cont 2=D/N	One-Half Cycle Time (Min)	CO_2 Removal MEQ	Flow Rate CFM	Heater Set Point (°F)	CO_2 Inlet (pp mmHg)	CO_2 Removal (lb/hr)	CO_2 Removal Rate lb/hr per mmHg (Based on Inlet)	Water Loss (lb/day)	Power Avg. (W)	Blower Power Avg. (W)	Heater Power Avg. (W)
MSFC Data												
2/9/96	1	160	5.968	17.97	400	3.77	0.547	0.15	N/A	724	54	642
2/22/96	2	160	3.979	16.83	400	2.72	0.365	0.13	N/A	586	52	506
3/1/96	2	144	3.979	20.04	260	2.59	0.365	0.14	N/A	399	60	307
3/14/96	2	144	3.977	18.71	260	2.69	0.365	0.14	N/A	500	58	403
3/27/96	2	144	3.979	18.40	260	2.57	0.365	0.14	N/A	482	59	387
4/11/96	2	144	3.976	17.59	260	2.62	0.364	0.14	N/A	489	57	396
7/14/96	2	144	4.199	18.80	260	2.99	0.385	0.13	N/A	493	58	399
7/28/96	2	144	3.979	21.41	400	2.12	0.365	0.17	0.000	641	86	515
7/30/96	2	160	3.979	20.79	400	2.15	0.365	0.17	0.000	633	86	515
8/4/96	2	144	3.431	24.17	400	1.54	0.315	0.20	0.176	652	110	504
8/6/96	1	144	3.432	23.83	400	1.55	0.315	0.20	0.086	821	109	674
8/8/96	1	144	5.972	24.93	400	2.73	0.547	0.20	0.046	828	109	684
8/11/96	2	144	5.971	24.84	400	2.80	0.547	0.20	0.127	680	109	531
Allied-Signal Data												
11/30/95	1	160	8.105	20.22	400	6.00	0.743	0.12	N/A	N/A	N/A	521
12/7/95	2	160	6.327	20.44	400	3.88	0.580	0.15	N/A	658	148	449
12/9/95	2	160	5.204	20.22	400	3.04	0.477	0.16	N/A	658	148	448
12/11/95	2	160	3.109	20.00	400	1.90	0.285	0.15	N/A	658	148	446
12/13/95	2	144	6.469	22.67	250	3.72	0.593	0.16	N/A	556	163	343
12/16/95	2	144	5.476	22.89	250	2.96	0.502	0.17	N/A	566	163	318
12/18/95	2	144	3.349	22.22	250	1.90	0.307	0.16	N/A	566	163	312
1/25/96	1	160	6.360	20.00	400	3.88	0.583	0.15	N/A	817	148	607
1/30/96	2	160	6.589	21.11	400	3.80	0.604	0.16	N/A	743	148	535
1/31/96	1	160	6.480	20.89	400	3.80	0.594	0.16	N/A	658	148	444

Power Mode: For continuous power mode (Cont), no interruptions are made to the 5A sorbent bed heater power during the test. For day/night (D/N) cycling, the heater power is cycled off during a simulated orbital "night." These tests used an orbital cycle of 90 min and night duration of 37 min.
One-Half Cycle Time: Duration of half the total 4BMS cycle.

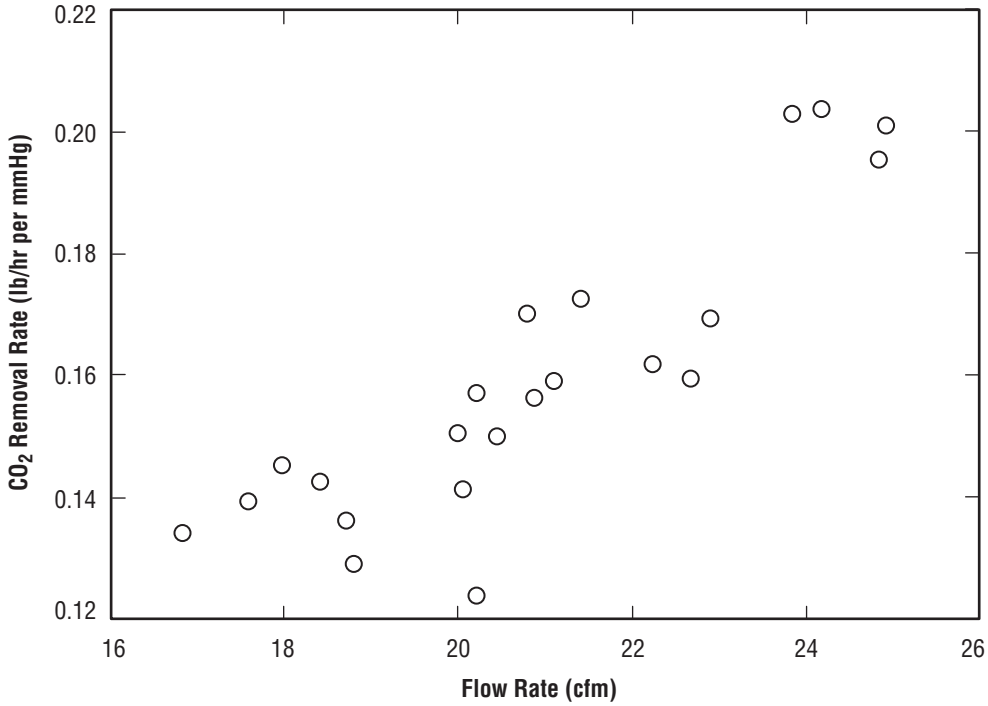

Figure 64. Carbon dioxide removal versus flow rate.

been conducted to determine when the desiccant beds break through and need to be regenerated. Testing will characterize the humidity spike caused by desorption of the desiccant beds. All flight issue testing (except for the characterization of the cyclical humidity spike) has been completed and the data are being compiled.

6.7 Stage 10 Water Recovery Test[27]

A test has been completed at MSFC to evaluate the water recovery and management (WRM) system and waste management (WM) urinal design for the United States on-orbit segment of the *ISS*. Potable and urine reclamation processors were integrated with wastewater generation equipment and successfully operated for a total of 128 days in recipient mode configuration to evaluate the accumulation of contaminants in the H_2O system and to assess the performance of various modifications to the WRM and WM hardware.

The integrated WRT program has been conducted in open-loop "donor" mode in which human test subjects generated wastewaters from nonrecycled H_2O and closed-loop "recipient" mode in which reclaimed H_2O was returned to test subjects for reuse and subjective assessment. Donor and recipient mode tests with dual-loop (potable and hygiene) H_2O recovery system configurations were completed in 1990 and 1991 and have been reported elsewhere. Donor and recipient mode testing of a single-loop system representative of the SS*F*and modified to utilize the baseline WP technology was completed in early 1992. Additional single-loop testing completed in late 1992 evaluated the impact of eliminating the WP presterilizer on Unibed® life and overall WP performance. After the redesign of SS*F* to the *ISS*, Boeing's predevelopment operational system test (POST) for the WRM system was deleted and replaced

with WRT stage 9, which was operated with an automated system level control scheme in a simulated recipient mode.

WRT stage 10 was conducted to evaluate H_2O quality and hardware performance in extended recipient mode operation while evaluating hardware modifications and investigating issues originating in stage 9. The stage 10 test is the subject of this section.

6.7.1 Test Configuration

Details of the WRT system design and test requirements are reported elsewhere and are only summarized here. An overall schematic showing the WRT bed as it was configured for stage 10 is provided in figure 65. The WP, urine processor (UP), and process control water quality monitor (PCWQM) assemblies were located adjacent to the EEF. Equipment dedicated to the generation, collection, and distribution of various wastewaters were located in and around the EEF and were interfaced to appropriate portions of the H_2O recovery system. The oxygen generation assembly (OGA) was located in the CMS, adjacent to the EEF.

The WRM included hardware for the recovery of potable H_2O from wastewaters generated in end-use equipment within the EEF and from urine.

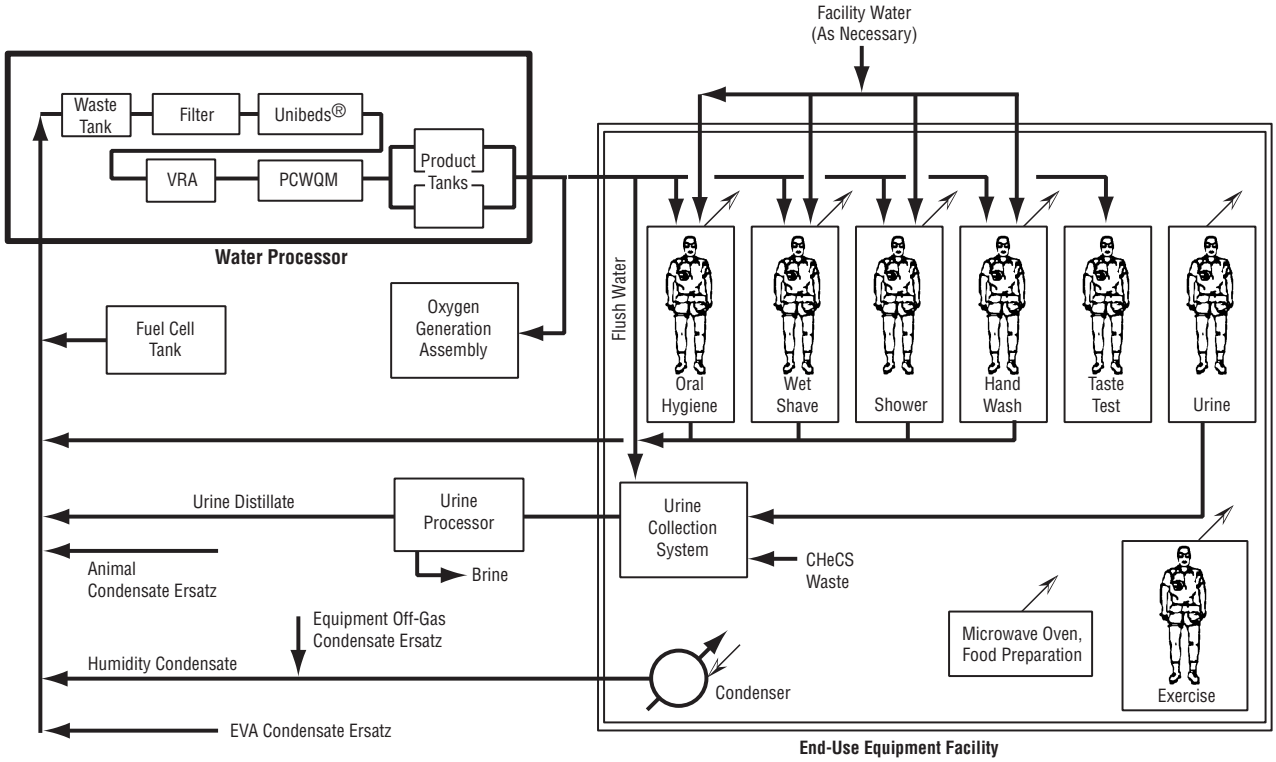

Figure 65. WRT system, stage 10.

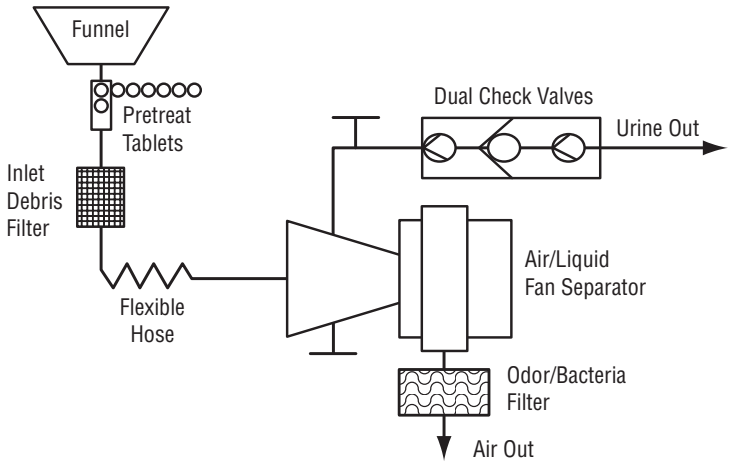

Figure 66. Schematic of urine collection system.

The urine collection system (fig. 66) was used to collect urine, reclaimed flush H_2O, and crew health care system (CheCS) wastewater. The design ratio of urine to flush H_2O in pretreated urine is 3 parts urine to 1 part flush H_2O by volume. This design ratio was achieved by manually adding 80 mL of flush H_2O to the urine collection system (UCS) following each donation. The UCS fan/separator turned on when the urinal cover was moved from the top of the funnel. When the separator reached the correct operating speed (3,500 rpm), a light would indicate that the UCS was ready to accept donations. At the inlet to the UCS, Oxone® and H_2SO_4 were added to the urine stream using solid tablets developed at HS. These tablets were designed to add 5 g Oxone® and 2.3 g H_2SO_4 per liter of urine or CHeCS waste. These tablets replaced the previous design concept of liquid injection of the pretreatment chemicals. The fan drew air through the UCS hose at 10 ft^3/min. The separator function was to separate the air from the liquid. Once the liquid and air were separated, the liquid was delivered to the UP wastewater storage tank. The air flowed into an odor/bacteria filter before being exhausted to the EEF environment.

The UP utilized vapor compression distillation (VCD) technology (see fig. 67) to process CHeCS waste and urine/flush H_2O collected by the UCS. Wastewater is circulated through the distillation unit by a four-section peristaltic fluids pump. The feed section of the pump discharges wastewater to the inner surface of the evaporator drum at a higher rate than the distillation rate. Vapor is generated along the heated surface of the evaporator drum and passed through a demister to prevent H_2O droplets from entering the compressor. The vapor is then compressed and condensed, thus generating heat for the distillation process. The condenser/evaporator drum is rotated by a brushless dc motor via a magnetic, fluid-sealed, direct-drive coupling. The evaporation/compression/condensation process takes place between 90–110 °F by operating the subsystem at 0.5–0.8 psia. Noncondensable gases are purged from the condenser every 10 min using the purge pump, which employs the same design as the fluids pump. Any H_2O condensed in the purge stream is separated by a static membrane G/LS and sent to the product H_2O line, while the noncondensable gases are vented to the atmosphere. The distillate collected in the condenser is pumped out of the distillation unit. Distillate with a conductivity above the setpoint of 150 μmhos/cm is returned to the recycle loop for reprocessing. Distillate with a conductivity <150 μmhos/cm is delivered to the WP waste tank as it is generated. Excess wastewater feed is returned through a 22-L recycle filter tank by the second and third sections of the fluids pump. Two pump

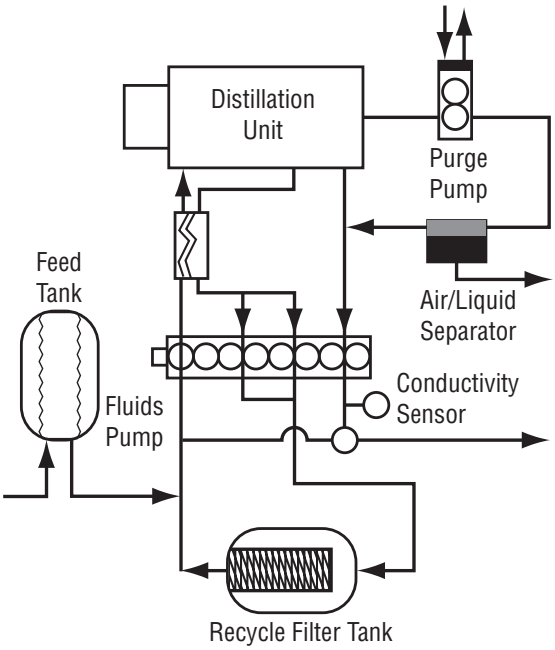

Figure 67. Schematic of VCD urine processor.

sections of the fluids pump are used to insure that the flow rate out is always greater than the rate in, which avoids flooding the evaporator drum. Prior to stage 10, the VCD–V recycle tank was modified from a pair of 25-μ filters to a 10-μ filter. However, after observing a significant accumulation of solids in the recycle tank during the brine tank replacement, a 30-μ filter and the previous 25-μ filter design were also used. This issue is discussed further in the section on UP performance.

The schematic for the WP is shown in figure 68. The WP operated at the flight design flow rate of 15 lb/hr. The WP employed particulate filtration, adsorption, ion exchange, catalytic oxidation, and phase separation to produce potable quality H_2O. Wastewater initially passed through a 0.5-μ depth filter to protect the Unibeds® from particulate loading. When the pressure drop across the filter reached 15 psid, the filter was considered loaded and was replaced. The MFB train followed, which consisted of two Unibeds® in series which removed ionic and organic contaminants present in the H_2O. Each Unibed® was identical and contained a series of media (table 40) designed for removal of particular groups of contaminants expected in the wastewater streams. Conductivity sensors located at the inlet and outlet of each Unibed® were used to monitor the performance of the bed and determine when bed saturation had occurred.

The Unibed® train effluent was treated by the VRA. The VRA was designed to remove low molecular weight, polar organics that are not efficiently removed by the Unibeds®. The process H_2O was saturated with O_2, heated to 265 °F, and passed through a catalytic oxidation reactor to oxidize the organics to CO_2 and/or to ionic compounds. The reactor was modified following stage 9 by HS to provide improved oxidation of acetone, which was commonly detected in the stage 9 product H_2O. The reactor modifications included the development of a more active catalyst and increasing the reactor's length-to-diameter ratio. Free gas in the reactor effluent is removed via a phase separator

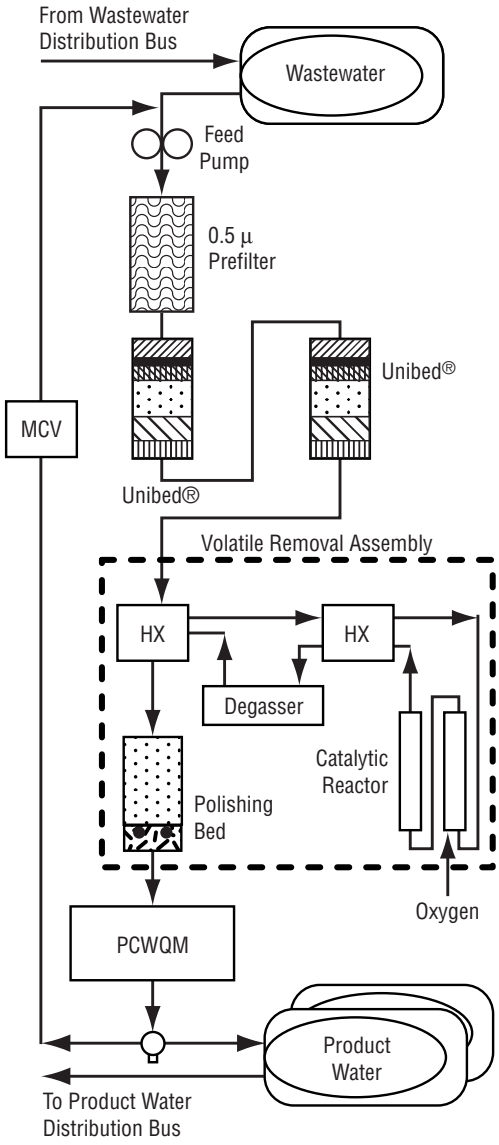

Figure 68. Schematic of the water processor.

Table 40. Stage 10 Unibed® media (in direction of flow).

Media	Volume (cc)	Description
MCV–RT	200	Iodinated anion exchange resin
IRN–150	9,750	Equal mix of strongly basic anion and strongly acidic cation exchange resin
IRN–77	695	Strongly acidic cation exchange resin
IRA–68	4,275	Weakly basic anion exchange resin
580–26	4,630	GAC produced from coconut shell
APA	1,325	GAC produced from bituminous coal
XAD–4	1,325	Polymeric adsorbent
IRN–150	200	Equal mix of strongly basic anion and strongly acidic cation exchange resin
IRN–77	200	Strongly acidic cation exchange resin

operated at 130–135 °F and 3–5 psig. The phase separator was also modified prior to stage 10 by HS and relocated to a location between the two VRAHX's, rather than downstream of both HX's (the stage 9 configuration). The stage 10 configuration allows for improved gas removal since the process will be at a higher temperature. Following the phase separator, the process H_2O is passed through an ion exchange bed for removal of ionic byproducts from the reactor and addition of a residual level of iodine (I_2) (1–4 mg/L) as a biocide.

Effluent from the VRA was analyzed by the PCWQM. The PCWQM provides on-line H_2O quality monitoring for TOC, I_2, pH, and conductivity. The I_2 and conductivity sensors are located in the WP process line. TOC and pH are measured in the PCWQM sample loop. In the sample loop, a 1 mL/min stream from the process line is initially passed by the pH sensor. The stream is then acidified by a solid phase resin to drive all inorganic carbon to CO_2, which is subsequently removed by a gas/liquid membrane. At the same time, the stream is saturated with O_2 to be used for the oxidation of organics in the ultraviolet lamp to CO_2. Finally, the stream passes by a second gas/liquid membrane integrated with an IR detector cell. Carbon dioxide in the H_2O reaches equilibrium with the CO_2 in the IR cell where it is measured and reported as TOC.

If the product H_2O failed to meet the H_2O quality specifications as measured by the PCWQM, it was recycled to the inlet of the WP for reprocessing. If the product H_2O was within specification, it was stored in one of two product H_2O tanks, each independently interfaced via a common distribution manifold to the various EEF equipment items requiring potable H_2O.

The OGA utilized solid polymer electrolyzer (SPE) technology to produce O_2 and H_2 from WP product H_2O. WP product H_2O was fed to the SPE at ≈7.2 lb/day. Electrolysis occurred in the cell stack, which includes 18 electrolytic cells with a solid polymer electrolyte material located between a perforated anode and cathode sheet. The product O_2 and H_2 streams are each passed through their respective static phase separators to ensure all liquid is removed from the product stream. The product gases were vented to the atmosphere in stage 10 and thus not consumed by the test subjects. The operation of the SPE during stage 10 was part of an ongoing SPE life test program. A more complete description of this test can be found elsewhere.

6.7.2 Test Operations

An average of 17.4 test subjects per day participated in EEF activities to generate wastewater for WRM processing. The EEF included a shower, handwash basin, microwave oven, exercise equipment, UCS, and CHX. High purity air was continuously fed to the EEF to maintain atmospheric CO_2 concentrations <1.2 percent and to ensure a positive pressure in the EEF. Housekeeping wipes were used in the EEF at rates similar to those anticipated on the *ISS*. The specifications for these wipes are provided in table 41. An ersatz solution was added to the humidity condensate collected in the EEF to make it more representative of the humidity condensate expected on the *ISS*. Animal condensate consisted of an ersatz solution based on experiment data. CHeCS waste was added to the UCS weekly to simulate *ISS* conditions. The formulation for the various ersatz solutions is reported elsewhere. All wastewater processed were independently prefiltered (105 μm) and input into the system as described previously. The cleansing agent used in the shower and handwash is listed in table 42.

Table 41. Housekeeping wipes specifications.

Wipe Description	Usage Rate/Day	Wipe Material[a]	Use Solution (gm/wipe)	Constituency of Use Solution[b]
Utensil detergent	12	Dupont 8801	9.2	50% alkyldimethylbenzyl-ammonium chloride 50% alkyl distribution (40% C12, 50% C14, 10% C16)
Utensil sanitary	12	Dupont 8027	9.2	2.5% Ninox L 5.7% Steol cs–330 6.75% Stepanol WAC 0.473% Kathon CG–ICP II 0.169% magnesium chloride 0.0625% citric acid 84.015% deionized water
General use detergent	24	Dupont 8801	9	99.8% deionized water 0.1% Rewoteric AMB–14 0.1% Kathon CG–ICP II
General use disinfectant	24	Dupont 8027	9	99.52% deionized water 0.48 % Barquat 4250–Z

[a]Dupont 8801 is 55% wood pulp and 45% polyester; Dupont 8027 is 100% polyester
[b]Utensil detergent use solution is diluted to 1.514 gm/gal of deionized water. Utensil sanitary use solution is diluted to 800 gm/gal of deionized water.

Table 42. Cleansing agent formulation.

Type	Shower
Designation	6503–45–4
Ingredients (% by weight):	
sodium-n-coconut acid-n-methyl taurate (SCMT) (Igepon TC–42, 24% active)	98.65
Formaldehyde (Formalin, 37% active)	0.10
Lecipur 95–F (soybean lecithin)	0.50
Luviquat FC–500 (polyquaternium 16)	0.75

Iodinated facility H_2O was produced as described previously. Facility H_2O was delivered to the EEF during the first day of recipient mode testing for shower, handwash, wet shave, and urinal flush. Following this activity, facility H_2O was used exclusively for the generation of wastewater during donor mode operation (after test day 128).

Primary laboratory support was provided by the Boeing Defense and Space Group's Environmental Laboratory and the MSFC Environmental and Development Test Branch Chemistry Laboratory in accordance with an independent program level quality assurance (QA) and QC plan.

All analytical and QC data generated during stage 10 is archived on the Functional Environmental Database System (FEDS) which resided on the MSFC Information Network System (MINS2), at the time this test was conducted.

Stage 10 operated for a total of 146 days, including 128 days in recipient mode operation. Significant test results and lessons learned relative to the physical, chemical, and microbiological performance of the WP and the UP during stage 10 are summarized below.

During stage 10 the WRM system processed ≈17,690 lb of wastewater (pretreated urine/flush H_2O, ersatz CHeCS waste, ersatz animal condensate, humidity condensate/equipment off-gas ersatz, ersatz fuel cell H_2O, and waste handwash, wet shave, shower, and oral hygiene H_2O) with 17,470 lb of potable H_2O produced and 294 lb lost as urine brine. The WRM system percent H_2O recovery was ≈98.3 percent, based on the mass of H_2O lost as brine.

6.7.3 Discussion of Results

Analysis of the WRM system in recipient mode will focus on issues related to H_2O quality and the mass balance of H_2O in the system. Recipient mode lasted for the first 128 days of the test, during which time 15,350 lb of H_2O was produced by the WP and 128 product H_2O tanks were filled for use by the test subjects. Analysis of the WP product H_2O over the course of the test indicates no degradation in H_2O quality. Figures 69 and 70 provide product H_2O TOC and conductivity data over the course of recipient mode operation. On test day 7, a software anomaly allowed process H_2O to be delivered to the product H_2O tank at the beginning of the WP process cycle (when organic leachates are being flushed out of the VRA ion exchange bed). This anomaly caused this specific product H_2O tank to have elevated TOC levels on test days 7 and 9 (1.6 and 0.58 mg/L, respectively). Since the source of the elevated TOC was known and determined not be a hazard to the test subjects, this H_2O was used for continued recipient mode operation. The installation of new Unibeds® on test days 49 and 83 reduced the product H_2O TOC by providing limited adsorption of the low molecular weight, polar organics normally removed by the reactor. As these organics saturate and pass through the Unibed®, the TOC in the product H_2O gradually increases until a new Unibed® is installed. No trends in product H_2O conductivity were observed during stage 10.

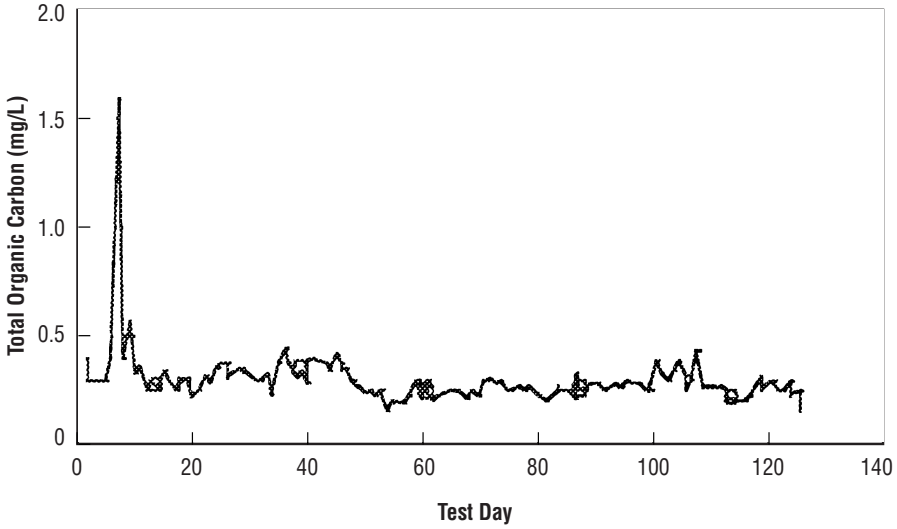

Figure 69. Recipient mode—product water total organic carbon.

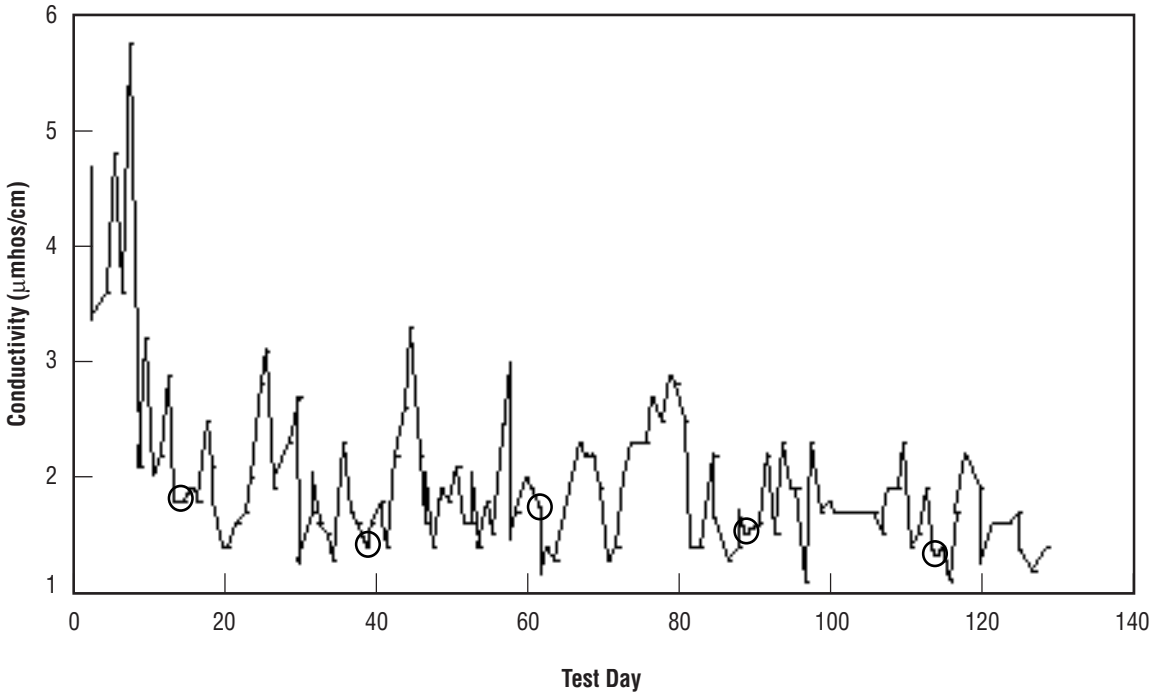

Figure 70. Recipient mode—product water conductivity.

Sample analyses for specific contaminants were also conducted using the methods detailed in table 43. No increasing trends for any contaminant were detected, thus indicating the long-term operation in a closed H_2O recovery loop will not lead to an accumulation of any specific contaminants in the H_2O recovery loop.

The WRM subsystem coordination logic worked as expected. No anomalies occurred related to the coordination of the WP, UP, and OGA operation. During stage 9, the completion of the PCWQM recirculation and calibration modes frequently interfered with the initiation of the WP processing mode. Prior to stage 10, the timing for the PCWQM modes was modified so that these modes would be conducted when the WP was normally in standby mode. This modification to the subsystem control logic, successfully minimized interference between the PCWQM and the WP processing mode.

Table 43. Detection methods for product water analysis.

Parameter	Detection Method
Alcohols	Heated headspace/GC with flame ionization detection
Volatile fatty acids	Ion chromatography with conductivity detection
Glycols	Liquid chromatography with pulsed amperometric detection
Aldehydes	Precolumn derivatization/liquid chromatography with diode array detection
Volatiles	Purge and trap GC/mass spectroscopy
Semivolatiles	Liquid/liquid extraction with GC/mass spectroscopy
SCMT	Liquid chromatography with diode array detection
Proteins	Colormetric procedure
Urea	Liquid chromatography with UV detection
Cations and anions	Ion chromatography with conductivity detection
Metals	Inductively coupled argon plasma

Difficulties with the PCWQM data interpretation function during stage 9 were resolved in stage 10. The most significant control issue was addressing the product H_2O TOC spike observed when processing is initiated each day. This spike occurs because leachates (primarily methanol and trimethyl amine) from the VRA ion exchange bed accumulate during standby mode and are flushed out when processing is initiated. Following stage 9, the recommendation was to replace the IRN–78 resin with a resin that would not generate the leachates. However, further research showed no such resin is available that will operate in this system and provide similar performance. Thus the remaining option was to program the PCWQM data interpretation function to accurately address the TOC spike. This issue was resolved by developing a data derivative function that would determine when the TOC spike had peaked. Once the peak value had passed and the absolute value was <500 ppb, process H_2O was routed into the WP fill tank. No anomalies were observed with this approach.

Two significant issues occurred during stage 10 recipient mode related to H_2O management. First, the system's mass balance was not maintained, resulting in a low system mass and the frequent addition of fuel cell H_2O early in the test. Second, hygiene activities were delayed on numerous occasions because product H_2O was not available for use. The following discussion addresses why these anomalies occurred and their impact on the WRM design.

Based on the *ISS* mass balance requirement and results from stage 9, the stage 10 mass balance was established to anticipate an average daily fuel cell input of 1.9 lb. However, a reduction in wastewater generation impacted this value. Tables 44 and 45 summarize the appropriate mass balance data for the test. Humidity condensate and pretreated urine generation did not meet the required 21.4 and 17.65 lb/day, respectively. The average urine distillate generation was 12.9 lb/day through test day 42, after which the pretreated urine collected by the UCS was supplemented to reach the nominal urine distillate production. The average humidity condensate input was an average of 5.9 lb/day below the *ISS* requirement. Also, the stage 10 mass balance did not consider latent hygiene losses, which were estimated to be up to 2 lb/day during stage 10. Because the masses of inputs were not meeting those expected while the mass removed was meeting the expected values, the overall mass of H_2O in the system was decreasing more rapidly than anticipated. The result was the frequent addition of fuel cell H_2O to maintain the system's H_2O mass between 232.5 and 242.5 lb. Figure 71 shows the input of fuel cell H_2O on a daily basis. Through test day 64, the average fuel cell addition was 11.8 lb/day, which is roughly equivalent to the deficiencies in the urine distillate and humidity condensate generation. Since the primary objective of stage 10 was to evaluate the accumulation of contaminants in the WRM H_2O over an extended duration, efforts were made to minimize the addition of fuel cell H_2O and the subsequent dilution of the wastewater. This objective was accomplished by reducing the mass of H_2O removed from the system as simulated drinking H_2O.

Simulated drinking H_2O was removed from the WP product H_2O tank several times each day. The mass of H_2O removed was initially related to the *ISS* requirements for drinking H_2O, food preparation H_2O, animal drinking H_2O, wet trash, and payloads. The mass of H_2O removed also accounted for the H_2O removed from the system for samples and deficiencies in the urine distillate generation. During the test, the simulated drinking H_2O was modified to also compensate for the deficiency of humidity condensate. Furthermore, H_2O removed from the system to simulate payload usage was eliminated after test day 63 to provide further buffer against a reduction in the system's H_2O mass. Following these modifications, fuel cell H_2O addition was reduced to two occasions over the last 64 days of recipient mode operation and the system mass was maintained above the minimum setpoint.

Table 44. Average waste stream quantities during WRT stage 10 recipient mode.

Waste Stream	Average From Stage 10 (lb/day)	*ISS* Nominal Range (lb/day)[a]	*ISS* Acceptable Range (lb/day)[a]
Shower	19.4	24	16–24
General hygiene	41.8	42.7	32–46.7
Handwash	35.1	36	32–40
Wet shave	3.6	3.5	0–3.5
Oral hygiene	3.2	3.2	0–3.2
Pretreated urine/flush water	17.25	17.65	6.9–22.4
CHeCS waste	1.34	1.44	0–1.44
Humidity condensate	15.5	21.4	16.04–57.56
Equipment off-gas ersatz mixture	1.5	2.2	–
Animal condensate	7.4	7.92	N/A
Fuel cell water	6.3	3.72	N/A

[a]All nominal values and acceptable ranges for the waste streams were taken from reference 10 and are based on a four-person crew.

Table 45. Average product water consumption during WRT stage 10 recipient mode.

Product Water Outputs	Average From Stage 10 (lb/day)	*ISS* Nominal Range (lb/day)[a]	*ISS* Acceptable Range (lb/day)[a]
Drinking water and samples	–	46.08	27.56–48.76
Drinking water	16[b]	14.24	2–15.6
Food prep water	–	6.68	3.6–8
Animal drinking water	–	7.34	N/A
Wet trash	–	3.2	0–3.2
CHeCS sample	1.5	1.54	N/A
Payloads	[c]	4.8	0–4.8
O_2 generation	6.8	8.28	N/A
Samples	1	N/A	N/A

[a]All nominal values and acceptable ranges for the waste streams were taken from reference 10 and are based on a four-person crew

[b]Drinking water value includes drinking water, feed prep water, animal drinking water, and wet trash inputs

[c]No pulls were taken for payloads on test days 5, 63–101, and 103–146. On days when water was pulled for payloads, the average value was 4.74.

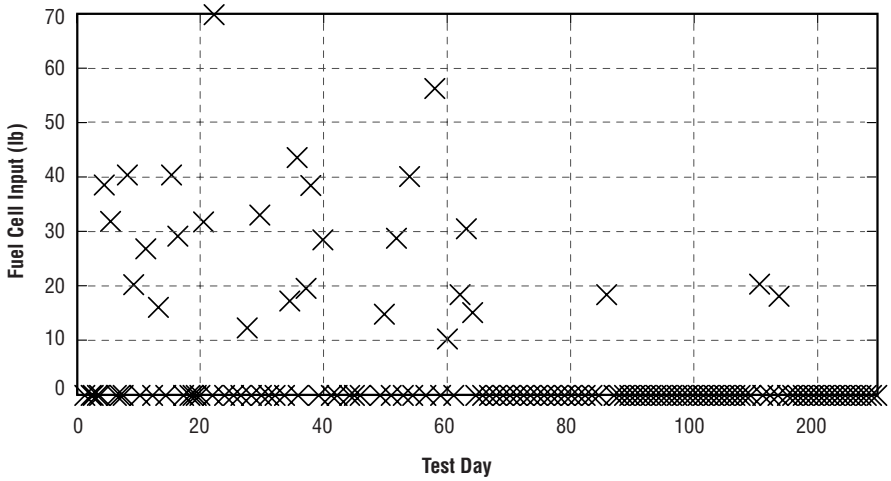

Figure 71. Stage 10 daily fuel cell input.

Product H_2O was not available for use by the test subjects on a minimum of 10 occasions during stage 10. On three test days, this anomaly occurred because delays in WP operation prevented the fill tank from being filled before the deliver tank was emptied by the day's nominal H_2O usage. These delays in WP operation were caused by the need to resolve anomalous WP pump performance (caused by gas in the pump inlet) and for prefilter replacement. On the remaining test days, the lack of available product H_2O occurred because of a low mass of H_2O in the system (<220 lb). On these test days the low system mass meant that either the deliver or fill tanks were at lower than nominal levels. If the deliver tank was low, H_2O usage would empty this tank more quickly than normal and before the fill tank was ready to transition. If the fill tank was low, the WP would require more time to fill the tank, again allowing the deliver tank to be emptied before the fill tank was ready to transition.

The UCS collected and pretreated 2,190 lb of urine, flush H_2O, and CHeCS waste during stage 10. The UCS provided the required pressure to deliver the liquid to the UP feed tank. The separator operated nominally for the majority of its operation. Several test subjects observed an intermittent loss in separator speed during a donation. However, at no time did this decrease in separator speed prevent delivery of the pretreated urine or proper operation of the UCS upon subsequent use. Also, after raising the urinal cover to donate, test subjects observed that the separator was unable to reach its normal operating speed on three occasions. This anomaly occurred because pretreated urine leaked through the seal between the separator's rotating drum and the stationary housing. The drag between the liquid and the drum prevented the separator from reaching its operating speed. Once the separator was drained of the liquid (<10 mL of fluid), UCS operation returned to normal.

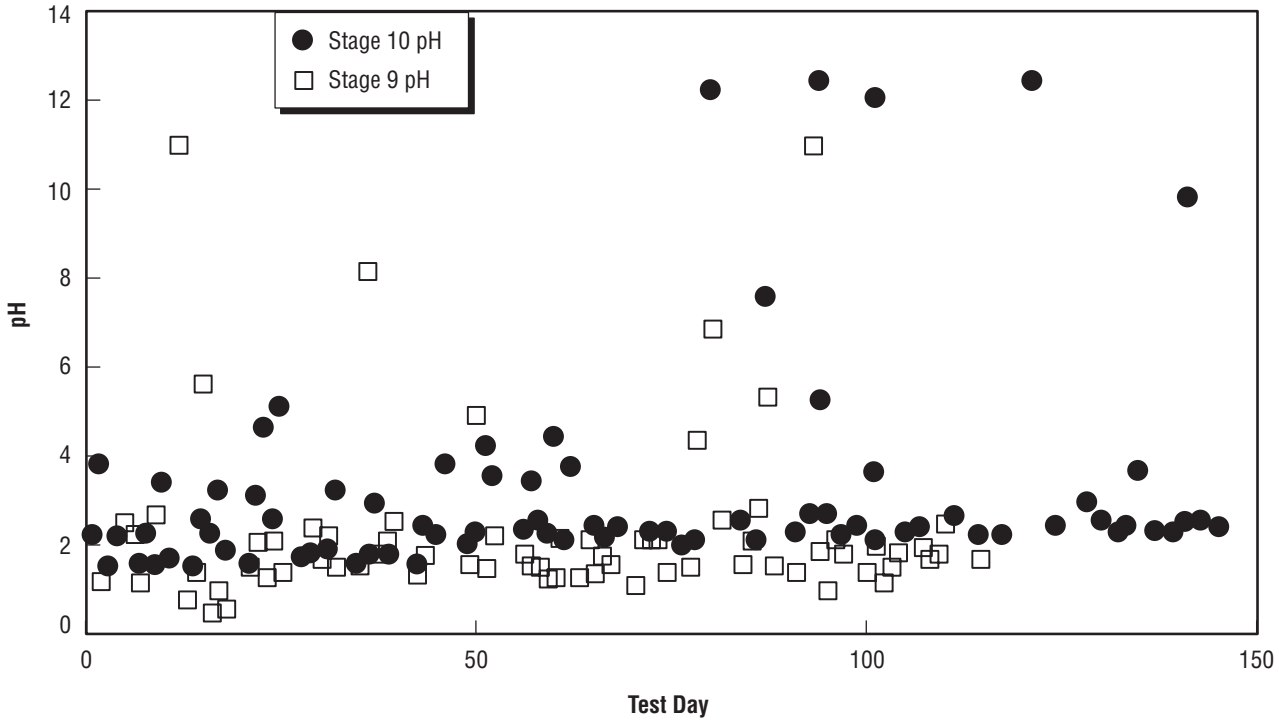

Figure 72. Pretreated urine pH for stages 9 and 10.

During stage 10 testing, 182 pretreatment filters were used at an average of 12.6 donations per filter (2,299 donations). The H_2O quality results on the pretreated urine indicate that the solid tablets provided similar pretreatment to the liquid injection approach. Furthermore, a posttest disassembly of the UCS showed no accumulation of chemical or biological matter in the UCS plumbing. Figure 72 illustrates the pH of pretreated urine obtained during stages 9 and 10. The spikes observed in the data occurred when CHeCS waste was added to the urinal. Over the course of the test, CHeCS waste was added with varying levels of pretreatment, depending on how much usage the solid pretreatment tablets had seen prior to CHeCS addition. Since CHeCS waste has a very basic pH, its addition to the pretreated urine tank tended to initially drive the tank pH basic. However, the test data show that as the level of CHeCS pretreatment increases (i.e., less usage on the solid tablets), the quicker the pH of the pretreated urine tank will return to <3. In spite of the variance in pH caused by the CHeCS waste, the elevated pH levels did not lead to any microbial or chemical accumulation in the UCS (based on the physical disassembly of the UCS following the test) and did not prevent the pretreated urine tank from maintaining a pH of <3 in subsequent operation.

A total of 2,585 lb of pretreated urine/flush H_2O and 192 lb of CHeCS wastewater was processed by the UP during 565 hr of operation with 2,403 lb of distillate delivered to the WP waste tank. The UP recovered ≈88 percent of the pretreated urine/flush H_2O/CHeCS waste. The average production rate of the UP was 4.25 lb/hr.

During stage 9, the VCD experienced numerous high-temperature alarms when the VCD transitioned to normal mode. This anomaly occurred when gas not removed by the UCS would accumulate in the top of the UP waste bellows tank and be fed to the distillation unit when normal mode was initiated. This volume of gas would frequently exceed what the VCD could remove in its initial 10-min purge. Once processing was initiated, the compressor would overheat because it would be fed the excess gas rather than the steam needed to cool the compressor's gears and lobes. A purge-control algorithm was therefore written and implemented prior to stage 10 to continue pulling a vacuum on the distillation unit until the pressure was <45 mm Hg, indicating sufficient gas removal. This algorithm effectively prevented the high-temperature alarms from occurring in stage 10.

High precipitant levels were observed in the brine recycle tank during the replacement of several brine tanks. Several filter types were used in the test to determine if the precipitant formation was a result of the filter size or design. The filter types include the flight-like 10-μ pleated filter, a 30-μ pleated filter, and a pair of 25-μ, spiral-wound filters (stage 9 design). The first three brine tanks that were replaced on test days 35, 61, and 84 contained a relatively large mass of solid precipitation in the tank, including a cake on the exterior of the 10-μ filter. The concentration of solids for these two filters exceeded 25 percent because the algorithm used for this calculation did not account for pretreated urine added to the waste tank during UP processing. The higher concentration of solids in the brine would have contributed to the increased precipitation observed when the filters were replaced. The 1-μ filter was replaced on test day 84 with a 30-μ pleated filter. However, the results were similar when the filter was replaced on test day 108. On test day 108, the pair of 25-μ filters was installed. This filter pair was replaced on test day 131, at which time the level of precipitation observed in the brine tank was similar to that seen in stage 9 testing. Subsequent use of the 10-μ filter resulted in the formation of solid precipitation observed earlier in stage 10. Further analysis will continue to determine the reason for the solids precipitation.

The VCD's Vespel® compressor gear was replaced on test day 37 after Vespel® particles were observed in the product distillate. The original gears had a backlash of 0.011–0.021 in., while the new gear set had a backlash of 0.004–0.005 in. The Vespel® gear had ≈8,000 hr of operation, including 700 hr of operation at MSFC in WRT stages 9 and 10.

The urine distillate quality was typical of that observed in previous testing except for conductivity. The average conductivity reported in stage 9 was 60 μmhos/cm, while in stage 10 the conductivity increased to 70 μmhos/cm. Furthermore, conductivity alarms occurred throughout the test when the product distillate conductivity exceeded the setpoint of 150 μmhos/cm. The anomaly occurred most frequently at the initiation of processing and as the brine solids concentration reached its maximum level. Test results indicate that the higher conductivity levels were caused by several ionic compounds that are also present in the pretreated urine feed, as opposed to a single contaminant introduced after the condensate process. These data indicate that the VCD is experiencing carryover of the pretreated urine or a leak of pretreated urine into the urine distillate. The most probable source of the carryover would occur when the evaporator drum starts and/or stops spinning and the pretreated urine along the wall falls onto the demister. As the evaporator drum is evacuated, portions of this pretreated urine may then pass through the demister and compressor to the distillate. A redesign of the demister may eliminate this anomaly, while further analysis will also be conducted on this issue.

The PCWQM provided on-line monitoring of the WP product H_2O TOC, conductivity, I_2, and pH. Performance analysis of the respective sensors was accomplished by comparing analytical data of samples pulled from the VRA effluent with the PCWQM data and by comparing analytical data of product tank samples (port 120) with PCWQM data generated over the time period that a specific tank was filled. The analysis of the TOC sensor was incomplete at the time this paper was published and will therefore be presented in the stage 10 final report.

As was observed in stage 9, a comparison between the PCWQM pH sensor and laboratory data shows significant variance. The pH reported by the PCWQM was consistently lower than the laboratory pH. Analysis of sensor data indicates that the PCWQM pH sensor was properly calibrated during the test. Additional analysis of the stage 10 test data and the pH sensor performance will be conducted with the results reported in the stage 10 final report. The PCWQM conductivity sensor provided consistent agreement with the laboratory data. This result is consistent with observations made during stage 9 and further verifies the adequacy of this sensor. A preliminary analysis of the PCWQM I_2 sensor indicates good agreement with the laboratory data. The average difference between the two data points was <0.4 mg/L over the first month of testing. The PCWQM I_2 value is consistently higher than the laboratory data, a trend also observed in stage 9 and indicating the possibility of I_2 degradation between sample time and sample analysis. Though a complete analysis will be presented in the stage 10 final report, the preliminary data indicates that the I_2 sensor performance was acceptable.

The PCWQM TOC and I_2 sensor experienced anomalies during stage 10 that required each sensor to be taken off line for a period of time to complete repairs. An LED in the I_2 sensor failed on test day 41 and was replaced on test day 65. This failure is not considered to be a design issue, as the LED passed class S requirements for electronic semiconductors. The TOC sensor experienced three membrane failures during stage 10. Two membranes failed on test day 8 because the membrane housing was not tightened sufficiently, allowing process H_2O to leak past the seal. To facilitate a timely repair,

a commercial O-ring was used for the repair of one of the membranes. On test day 85, this membrane again failed because the commercial O-ring was deficient. After the O-ring was replaced, no further anomalies occurred with the TOC sensor.

The WP operated for ≈1,130 hr in processing mode, 260 hr in reject mode, and 2,120 hr in standby mode and produced 17,470 lb of product H_2O.

In order to assess the effects of recipient mode operation on the performance of the WP, component expendable rates and effluent H_2O quality were compared from stage 10 to previous single-loop integrated tests. Table 46 shows the throughput of the WP expendables throughout stage 10 and compares expendable rates with stages 7–9.

The Unibed® throughput for two of the three beds loaded was similar to that observed during stage 9. The second Unibed® loaded during stage 10 was removed from the WP on test day 83 because of a high *ΔP* observed across the Unibed®. Subsequent analysis indicated that the inlet screen had been coated with a substance containing primarily zinc, SCMT, and large organic acids (C12 through C18). Zinc is a cation and will readily form a precipitant with anionic compounds such as a surfactant (SCMT) or a large organic acid. This precipitant had deposited on the Unibed's® inlet spacer and had reduced the flow path to the point that the *ΔP* across the bed was too high for the process pump. Further investigation identified two significant sources of zinc in the humidity condensate. The first source is the equipment off-gassing ersatz, to which zinc was added to reflect the anticipated level of zinc imparted to the humidity condensate from the *ISS* CHX coating. These data were obtained prior to stage 9, based on development work performed at HS. Prior to stage 10, a new CHX was installed in the EEF that employed the *ISS* coating, thus providing additional zinc to the humidity condensate. The presence of this coating was not known to test personnel until the investigation following the Unibed® anomaly.

The filter throughput significantly decreased in stage 10 from previous tests (table 46). The decrease in filter life is theorized to have also resulted from the precipitants that caused the Unibed® *ΔP* anomaly. Analysis of the filter material again detected high levels of SCMT, zinc, and the large organic acids. After the zinc was identified as the probable source of the anomaly, it was removed from the equipment off-gassing ersatz. Following this modification, the WP prefilter life increased from an average of 8 days to an average of 17 days, which is similar to the prefilter life in stage 9. It should also

Table 46. Expendable throughputs for test stages 7–10.

Expendable	Average Throughput (lb)			
	Stage 10	Stage 9	Stage 8	Stage 7
Filter	1,310	2,513	6,647[a]	4,798[b]
Unibed®	5,716[c]	5,539	N/A	N/A
VRA polishing bed	17,947.9[d]	9,156[b]	6,716[b]	4,605[b]

[a]Only one filter was loaded during stage 8
[b]Expendable was never loaded throughout the test
[c]Includes only Unibeds® 1 and 3
[d]Includes water processed in Interim WP test
N/A—not applicable, different size Unibed®.

be noted that the prefilter life decrease from stages 7 and 8 to stage 9 was likely due to the presence of zinc in the ersatz (not used in stages 7 and 8), which was worsened in stage 10 because of the additional zinc introduced by the CHX coating. Information obtained during stage 10 indicates that the current *ISS* CHX design will have a zinc concentration of 0.65 mg/L, rather than the ersatz concentration of 15 mg/L. Accordingly, the zinc should have a minimal impact on the *ISS*. However, other ionic contaminants may also form a similar precipitant that would also impact prefilter and Unibed® life. Furthermore, physical observations made during stage 10 on the percent of filter material loaded indicate that the prefilter is not being fully loaded. A redesign of the prefilter may be required to more fully utilize the available weight and volume while also addressing the impact of precipitant formation.

The VRA polishing bed was expended during post stage 10 testing (discussed later in this TM). The bed processed 17,470 lb during stage 10 and an additional 610 lb during poststage 10 testing prior to breakthrough. The bed breakthrough was marked by a high concentration of bicarbonate and organic acids. It should be noted that an undefined volume of gas was introduced to this bed following the removal of the *ISS* phase separator on test day 38, though the impact of gas on the life of the polishing cannot be defined. The concentration of residual I_2 imparted by the bed continually decreased over the course of the test to the point that it was near the lower limit (1 mg/L) of the H_2O quality specification. This decrease in the concentration of residual I_2 imparted by the bed's MCV resin has not been observed in previous WRT testing. Since this bed was manufactured in 1990, further analysis will be conducted to determine if the bed's MCV resin experiences degraded performance after remaining in storage for an extended duration.

Another significant hardware anomaly that occurred during stage 10 was the WP GLS, which failed on test day 38 when a high ΔP (60 psid) was observed across it. This component was procured for use in the test because it was baselined for use in the flight design. The component was replaced with the GLS used in stage 9. The stage 9 GLS was unable to remove all free gas from the product H_2O for ≈6 days, after which it performed without incident for the remainder of the test. An analysis of the failed GLS at HS indicated that the hydrophilic membrane had chemically reacted with a contaminant and become impenetrable to the flow of H_2O. Further analysis detected the presence of phthalate esters on the hydrophilic membrane, though no obvious source for this contaminant has been identified. A similar failure of this GLS design occurred in the early human testing initiative phase IIA test at JSC. Though the analysis of the phase IIA membrane indicated a similar failure mechanism, laboratory analysis detected the presence of fluorocarbons and hydrocarbons instead of phthalate esters. These data suggest that the hydrophilic membrane is sensitive to an array of organic compounds. Since only trace levels of these organics should have been introduced to the GLS, the GLS may require a redesign to enable it to perform in this environment.

Table 47 summarizes the H_2O quality data at various points in the WP and compares the data to that generated during stage 9. The technologies employed by the WP for contaminant removal performed as anticipated in stage 10. Conductivity levels were reduced by over 99 percent in the Unibed® train, indicating the bed's ion exchange resin effectively removed the ionic contaminants present in the wastewater. Approximately 96 percent of the wastewater TOC was removed in the Unibed® train. The TOC removed in the Unibeds® would consist primarily of the surfactant SCMT and the organic acids.

Table 47. Water quality.

Wastewater[a] Parameter	Units	Potable Spec.	Stage 9/10 Detection Limit	Stage 10		Stage 9	
				Times Detected/ Sampled	Detected Average[b]	Times Detected/ Sampled	Detected Average[b]
Conductivity	µmho/cm	N/A	–	112/112	380	18/18	409
pH	S.U.	6–8.5	0–14	89/89	6.9	18/18	7.03
Total organic carbon	mg/L	0.5	1	89/89	203	18/18	212
1-Propanol	mg/L	N/A	0.03	6/6	1.7	18/18	3.1
2-Propanol	mg/L	N/A	0.04	6/6	3.5	18/18	8
Acetone	mg/L	N/A	0.05	6/6	0.95	18/18	2.30
Ethanol	mg/L	N/A	0.04	6/6	5.5	15/18	7.49
Ethylene glycol	mg/L	N/A	0.25	0/6	–	4/18	1.20
Methanol	mg/L	N/A	0.05	6/6	2.07	18/18	3.13
Urea	mg/L	N/A	0.5	–	–	6/16	4.67
Total inorganic carbon	mg/L	N/A	1	89/89	11.8	18/18	12.5
Total bacteria count	CFU/100 mL	100	–	–	–	–	–
AEM plate count/2 day	CFU/100 mL	–	1	–	–	15/15	8.90E+08
R2A plate count/7 day	CFU/100 mL	–	1	–	–	15/15	1.06E+09
VRA Influent (Port 126)							
Conductivity	µmho/cm	N/A	–	85/85	1.69	68/77	1.99
pH	S.U.	6–8.5	0–14	52/52	7.26	77/77	7.11
Total organic carbon	mg/L	0.5	1	49/50	8.41	60/66	13.3
1-Propanol	mg/L	N/A	0.03	27/36	1.31	57/65	3.03
2-Propanol	mg/L	N/A	0.04	33/36	3.31	56/65	5.78
Acetone	mg/L	N/A	0.05	25/36	0.58	39/65	1.23
Ethanol	mg/L	N/A	0.04	35/36	5.52	62/65	10.51
Ethylene glycol	mg/L	N/A	0.25	29/35	1.9	28/47	1.12
Methanol	mg/L	N/A	0.05	35/36	1.22	64/65	1.15
Urea	mg/L	N/A	0.5	13/19	3.62	57/61	3.67
Total inorganic carbon	mg/L	N/A	1	2/50	1	0/68	–
Residual iodine	mg/L	15	0.1	0/20	–	0/17	–
VRA Effluent (Port 127)							
Conductivity	µmho/cm	N/A	–	86/86	2.04	80/80	2.12
pH	S.U.	6–8.5	0–14	22/22	6.95	81/81	6.66
Total organic carbon	mg/L	0.5	0.2	52/52	0.28	69/77	1.6
1-Propanol	mg/L	N/A	0.03	–	–	32/37	0.19
2-Propanol	mg/L	N/A	0.04	–	–	4/37	0.14
Acetone	mg/L	N/A	0.05	–	–	28/37	0.37
Ethanol	mg/L	N/A	0.04	–	–	5/37	1.25
Methanol	mg/L	N/A	0.05	–	–	25/37	5.1
Urea	mg/L	N/A	0.5	–	–	0/18	–
Residual iodine	mg/L	15	0.1	–	–	6/6	3.63
Product Tank (Port 120)							
Conductivity	µmho/cm	N/A	–	128/128	1.95	51/51	2.25
pH	S.U.	6–8.5	0–14	125/125	6.80	51/51	6.27
Total organic carbon	mg/L	0.5	0.2	128/128	0.30	42/42	0.48
1-Propanol	mg/L	N/A	0.03	0/20	–	33/42	0.17
2-Propanol	mg/L	N/A	0.04	4/20	0.14	3/42	0.06
Acetone	mg/L	N/A	0.05	4/20	0.12	28/42	0.23
Ethanol	mg/L	N/A	0.04	2/20	0.16	0/42	–
Ethylene glycol	mg/L	N/A	0.25	0/20	–	0/42	–
Methanol	mg/L	N/A	0.05	4/20	0.21	28/42	0.27
Urea	mg/L	N/A	0.5	0/20	–	0/42	–
Residual iodine	mg/L	15	0.1	128/128	2.34	51/51	3.3
Total bacteria count	CFU/100 mL	100	–	–	–	–	–
AEM plate count/2 day	CFU/100 mL	–	1	25/113	1	8/42	1.1
R2A plate count/7 day	CFU/100 mL	–	1	26/113	1.4	16/41	1.4

[a]Averages are based on the samples in which detectable concentrations were measured and do not account for samples in which detectable concentrations were not found

[b]Stage 10 data based on prefilter effluent (port 134), stage 9 data based on waste water tank (port 124).

Product H_2O TOC and organic characterization data confirm that the reactor redesign was effective at the removal of organics in the reactor influent. The rise in TOC over the course of a process cycle (seen in stage 9) was not observed in stage 10. As shown in table 47, only trace levels of acetone, 2-propanol, ethanol, and methanol were detected in the product H_2O. The TOC levels observed in stage 10 were the lowest reported in any of the WRT stages.

Conductivity levels were consistently low in the product H_2O, indicating the absence of any significant level of ionic contaminants. As with previous testing, the pH of the product H_2O fell below the potable specification on several occasions due to the absence of ionic contaminants needed to buffer the H_2O's pH. Residual I_2 levels were maintained within the potable specification of 1–4 mg/L during the test, though there was a gradual decrease in the I_2 level during the test as the MCV resin in the ion exchange bed was depleted. This decrease in the biocide concentration was not accompanied by any increase in the microbial population or change in the product H_2O microbial species.

The data obtained in the microbial analysis of the system show that the WP's ability to control the microbial population was unaffected by recipient mode operation. Analysis of the product H_2O shows that there was no increase in the population of any microbial species over the course of the test. During the test, 78 percent of both the Heterotrophs on microbial growth media (R2A) media and aerotolerant eurtropic mesophilic on Chocolate Agar media plate counts were <1 colony forming unit (CFU)/100 mL. The highest plate count reported during the test was 12 CFU/100 mL, well below the potable specification of 100 CFU/100 mL. As in previous WRT tests, all bacteria cultured in product H_2O samples were identified. The bacteria most frequently identified in the product H_2O were *Staphylococcus* and *Bacillus*, which is typical of previous WRT data. None of the bacteria isolated from the product H_2O samples are considered to be a health hazard. Additional media was used in an attempt to culture bacteria that do not grow well on Chocolate Agar or R2A media. These bacteria included *Salmonella* and toxigenic *E. Coli*. None of these pathogens were isolated from product H_2O samples during the test.

Biofilm coupons were used during the test to assess the extent of biofilm accumulation in the WRT plumbing. This effort, along with the ongoing biofilm life test at MSFC, addresses the issue related to the accumulation of biofilm in *ISS* plumbing and the potential for blocking H_2O flow and/or corrosion of the tubing. Two sets of coupons were installed prior to the initiation of testing, one located in the product H_2O distribution bus immediately upstream of the shower and the other between the WP particulate filter and the first Unibed®. Each set contained five sections of tubing, each 2 in. in length and connected by quick disconnects. The wastewater coupons were 0.25 in. 316 L SS and the product H_2O coupons were 0.5 in., 316 L SS. Each month one section of tubing was removed from each set and analyzed for biofilm formation. Analysis of the coupons showed insignificant biofilm activity in the product H_2O coupons. The wastewater coupons exhibited limited biofilm formation as anticipated in a test of this length. The organisms isolated in the wastewater biofilm coupons were typical of those observed in this portion of the WP. Further analysis will be presented in the stage 10 final report regarding the depth of the biofilm formation and any biofilm activity on the SS tubing.

At the conclusion of the integrated testing, the WP underwent a viral challenge to verify its ability to meet the *ISS* specification of <1 plaque forming unit (PFU) per 100 mL. The WP had been challenged with viruses in the wastewater during stage 9, with the resulting data showing no viral

contamination downstream of the MFB's. In stage 10, the viruses were injected between the MFB's and the VRA to ascertain the ability of the VRA for viral removal. The viral solution was seeded with four bacterial viruses (bacteriophages) so that the VRA influent was at a concentration between 1×10^6 and 1×10^8 PFU/100 mL. Bacterial viruses were used to avoid any safety concerns associated with human viruses and were selected to represent specific human viruses that would be considered dangerous and likely to be found in H_2O. The challenge was run for 5 days while samples were taken in the reactor influent and effluent for subsequent analysis. Of the four viruses assayed, two were not detected in any samples following the reactor, one was recovered at low levels in one out of ten samples, and the other was recovered at low levels in three out of ten samples. The viral removal capability of the reactor was estimated to be a minimum of 12 log units. In contrast, conventional H_2O treatment systems achieve a reduction of ≈6 log units of viruses. These results indicate that the VRA is very effective at inactivating a large viral population. Combined with the results from stage 9, these findings indicate that the WP has an excellent capacity for reducing the disease hazards posed by viruses in the H_2O being processed for potable use onboard the *ISS*.

Following the completion of stage 10, the H_2O recovery system was modified to reflect operation anticipated in the *ISS* early hab configuration, illustrated in figure 73. In this evaluation, the VCD operated as it had in stage 10. However, the interim water processor (IWP) processed only urine distillate and humidity condensate. Also, the IWP's Unibed® was replaced with a small bed of IRN–150 for the removal of ionic contaminants from the wastewater. A summary of the five processing runs and the resultant data is provided in table 48.

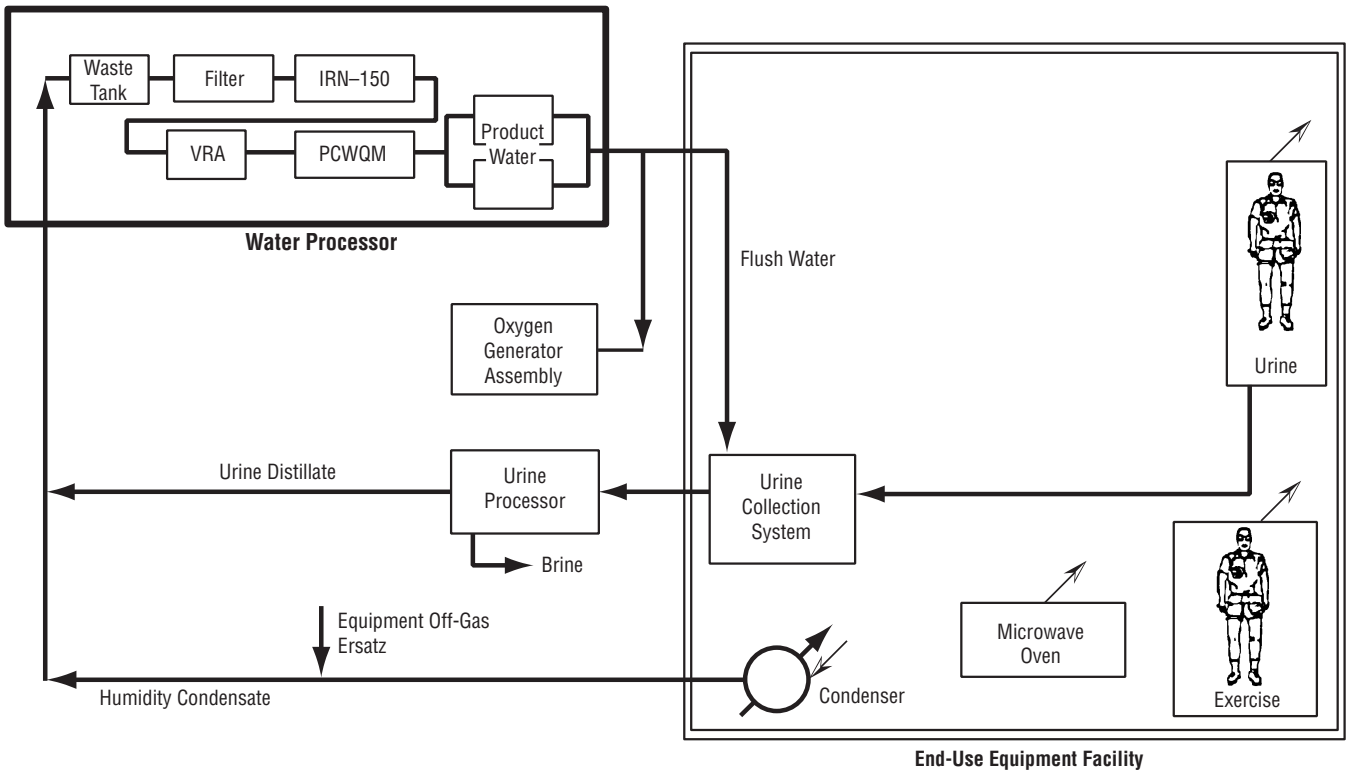

Figure 73. WRT system, early hab configuration.

Table 48. Interim water processor evaluation—data summary.

Test Day	Humidity Condensate (lb)	Urine Distillate (lb)	Time (hr)	Reactor Influent TOC (mg/L)	Reactor Influent Conductivity (μS)	Product Water TOC[a] (mg/L)	Product Water Conductivity (μS)
1	38.4	34.1	4.1	28	1.2	219	2.3
2	29.2	33.5	3.9	34	1.3	490	1.6
3	46.1	35.0	5.0	38	1.3	414	2.0
4	63.8	50.9	7.2	47	3.0	376	4.8
5	49.2	34.9	5.1	43	3.3	272	3.2

[a]Product water TOC calculated from average PCWQM TOC during process mode.

Approximately 400 lb of wastewater was processed during the IWP evaluation. The IRN–150 resin provided acceptable removal of ionic contaminants, based on an effluent conductivity ranging from 1.2–3.3 μmhos/cm. The TOC level in the reactor influent was ≈4 times higher than in stage 10, since no media for the removal of organics was employed before the VRA. However, the VRA successfully oxidized and removed the organic constituents to TOC levels ranging from 219–490 μg/L in the product H_2O. No anomalies occurred during this test to indicate that the IWP would not be able to meet the requirements of potable H_2O provision during the *ISS* early hab configuration.

In early 1997 the *Mir Space Station* experienced several coolant leaks that allowed ethylene glycol to escape into the atmosphere, condense in the humidity condensate (at a concentration reported initially to be 160 mg/L), and subsequently enter the potable WP. The elevated levels of ethylene glycol exceeded the removal capability of the processor and contaminated the potable drinking H_2O supply. Based on this experience, NASA management requested an evaluation of the WP to determine its ability to remove a similar level of ethylene glycol. To complete this evaluation, the appropriate wastewaters were generated in the EEF and fed to the WP. Additionally, a spike of ethylene glycol was added to simulate its concentration in the wastewater if a coolant leak occurred on the *ISS* similar to that observed on the *Mir*. A summary of the significant test data is provided in table 49. The concentration of ethylene glycol was increased on test day 4 to reflect its concentration in the wastewater in the early habitation

Table 49. Summary of test data in ethylene glycol evaluation.

Test Day	Waste-Water Input[a] (lb)	Ethylene Glycol Concentration[b] (mg/L)	Process Time (hr)	Reactor Influent TOC (mg/L)	Reactor Influent Conductivity (μS)	Product Water TOC (mg/L)	Product Water Conductivity (μS)
1	116.6	209	8.1	23	1.7	0.29[c]	1.1
2	98.7	211	6.6	11	1.7	0.18[c]	1.0
3	97.5	208	6.7	186	3.8	1.6	6.9
4	98.4	620	6.5	142	3.3	10.1[d]	11.3

[a]Included 1-day requirements for shower, handwash, oral hygiene, wet shave, urine distillate, and ersatz solutions for humidity condensate and animal condensate
[b]Represents concentration in humidity condensate
[c]TOC values calculated from average PCWQM TOC
[d]TOC values measured from archived sample.

configuration (where wastewater includes only humidity condensate and urine distillate) in the event of an ethylene glycol leak. All amounts of ethylene glycol added were higher than those initially reported on the *Mir* to provide a more difficult challenge for the WP. However, data reported subsequent to the completion of this test indicated that the ethylene glycol concentration in the *Mir* humidity condensate reached ≈350 mg/L, thus only the last day of this test provided a scenario more challenging than that observed on the *Mir*.

The concentration of ethylene glycol in the Unibed® effluent decreased during the 4-day test. On the first day the reported concentration was 40.3 mg/L, which is similar to the expected concentration in the wastewater. However, the ethylene glycol concentration dropped to 0.45 mg/L on the second day and <0.25 mg/L on the last 2 days. Conversely, the concentration of ethanol increased from 1.9 and 3.4 mg/L on the first 2 days to 9.6 and 12.1 mg/L on the last 2 days. These data indicate that the ethylene glycol is reacting in the Unibed®, partially to ethanol while other byproducts are unknown at this time. The removal of ethylene glycol in the Unibed® was also observed in the stage 9 test, though at lower wastewater concentrations than employed in this evaluation. Though the ethylene glycol was not present in the reactor influent on the last 2 days of the evaluation, product H_2O analysis indicated that the reactor performance did degrade during the last 2 days of this test. PCWQM analysis of the product H_2O indicated elevated TOC and conductivity levels. Furthermore, laboratory analysis of the product H_2O indicated the presence of high levels of acetone (4 mg/L), methanol (0.4 mg/L), 2-propanol (0.3 mg/L), ethanol (0.3 mg/L), isobutyric acid (3.8 mg/L), and formic acid (0.75 mg/L). The presence of these contaminants indicates two conditions. First, the presence of ionic contaminants indicates that the VRA ion exchange bed was saturated after 18,100 lb of throughput during stage 10, the IWP evaluation, and the ethylene glycol evaluation. The saturation of the ion exchange bed during the ethylene glycol evaluation was simply coincidental and has no bearing on assessing the WP's ability to effectively remove elevated levels of ethylene glycol.

Of greater significance, the presence of acetone and alcohols indicates that the reactor was not able to fully oxidize the contaminants in the reactor influent. As stated previously, the reactor employed during stage 9 was unable to achieve the complete oxidation of 2-propanol, resulting in elevated levels of acetone in the product H_2O. During stage 10, the modified reactor successfully removed all organics in the reactor influent. The presence of acetone during the ethylene glycol evaluation indicates that the high concentration of organics in this test prevented the reactor from completely oxidizing all organic contaminants in the influent, primarily acetone. Though ethylene glycol was not present in the reactor influent on the last 2 days, it likely caused the high concentration of organics that resulted in elevated organic levels in the product H_2O.

The data generated in the ethylene glycol evaluation are inconclusive. The removal of ethylene glycol in the Unibed® by a means yet unknown leads to uncertainty in assessing the WP's ability to effectively remove this contaminant from the WP wastewater. Though the level of organics in the product H_2O was above nominal and the TOC requirement was not met, it should be noted that, under *ISS* conditions, the product H_2O would be reprocessed as the PCWQM reported TOC levels above the potable requirements. In conclusion, this test indicates that the removal of significant levels of ethylene glycol would require, in a worst-case scenario, reprocessing to meet the potable requirements.

6.7.4 Conclusions

The stage 10 test provided valid test data for verifying the operation of the *ISS* WRM in an integrated, recipient mode operation. This test demonstrated that the WRM has the capability to remove contaminants introduced to the system by the various wastewaters and prevent the accumulation of contaminants in the system. Though the amount of fuel cell H_2O added during the first half of recipient mode operation exceeded the expected level, trace contaminants not effectively removed by the WP would be kept in the system by using WP product H_2O as the fuel cell H_2O ersatz, rather than diluting the system mass by using facility H_2O as the fuel cell H_2O ersatz. Furthermore, when fuel cell H_2O was minimized during the last half of the test, product H_2O quality maintained a level well within the potable specification.

The WRM H_2O management during recipient mode operation indicated a potential issue related to product H_2O availability. Though off-nominal conditions in the WRM system mass led to lack of product H_2O availability, the occurrence of this scenario in stage 10 requires additional analysis to ensure that it does not occur on the *ISS*.

Significant test data were acquired during stage 10 on the operation of the UCS and performance of the solid pretreatment tablets. The UCS was able to successfully collect, pretreat, and deliver waste urine, flush H_2O, and CHeCS waste to the UP. Operational issues with the solid tablets were resolved during the test, while performance data indicate that the tablets can provide adequate urine pretreatment without involving the safety and long-term storage issues associated with liquid pretreatment.

The UP recovered ≈88 percent of the wastefeed while providing the WP with urine distillate that met its H_2O quality specification. The VCD's Vespel® gear failed during the test after ≈8,000 hr of operation, which is acceptable for this component. High levels of precipitant observed in the brine tank during replacement of the brine tank filter will be investigated by analysis and additional testing.

The WP provided the highest product H_2O quality observed in integrated WRT testing at MSFC. Modifications to the VRA design, especially the reactor, resolved anomalous performance observed in stage 9 related to the oxidation of acetone. TOC, conductivity, and microbial levels were well below the potable H_2O requirements. Significant anomalies during the test included the abbreviated life of the second Unibed® and the prefilter due to precipitant formation and the failure of the G/LS. Though the concentration of zinc in this test is significantly higher than the expected *ISS* concentration, other cations may also cause precipitation of this nature. Design modifications will therefore be considered to enable the WP to better handle this potential issue. Modifications to the G/LS design will be considered to determine the approach best suited for the VRA application.

The viral challenge of the VRA further validated the ability of the WP to remove viral contaminants. Test data showed that the VRA has the potential to remove ≈12 log unit of viral contaminants. Since stage 9 test data also indicated that the Unibed® has an excellent capacity for viruses, the overall capability of the WP for removing viral contaminants appears to be excellent.

Two separate tests were conducted following the conclusion of stage 10 to address *ISS* program issues. The performance of the WP, modified to reflect the early hab configuration, was excellent. Over

400 lb of urine distillate and humidity condensate were processed to product H_2O that met the potable specification. This test verified that the UP and IWP design can provide potable H_2O to the crew from pretreated urine and humidity condensate. The performance of the WP when processing high concentrations of ethylene glycol was inconclusive. Though the test data show that ethylene glycol was not present in the product H_2O, its high concentration in the wastewater likely impacted the reactor performance and the product H_2O quality. Though further analysis and testing would be required to conclusively complete this evaluation, the data generated do show that potable H_2O can be produced in this scenario, though reprocessing may be required to meet the potable requirements.

The OGA produced 994 lb of O_2 from 1,120 lb of WP product H_2O during stage 10. No hardware anomalies were experienced during the test, though a steady increase in the SPE cell voltage will be further assessed in the OGA life test. The focus of this investigation will be to isolate the cause for the cell voltage and make whatever design modifications are necessary to alleviate the rise and thereby lengthen the life of the cell stack.

Overall, this test demonstrated that the WRM hardware can provide potable H_2O for crew use under the appropriate operational scenarios. Issues identified during stage 10 will be investigated and resolved as necessary to ensure the safe and successful operation of the WRM on the *ISS*.

7. LIFE TESTING

Testing conducted to determine life characteristics include both subsystem and component level testing. Subsystems tested include the 4BMS, TCCS, solid polymer electrolysis, O_2 generator, and VCD UP. Component-level life testing includes the MCA, H_2O degradation study, WRM biofilm test, and the THC system CHX microbial growth test.

7.1 Four-Bed Molecular Sieve[28]

The 4BMS life test startup was achieved in January 1993 with the test continuing until November 1995 when sorbent bed heaters failed. The 4BMS life test resumed in January 1997 after delivery and replacement of the sorbent bed heaters. A flight-like blower was procured and installed in the subsystem in September 1997.

A significant finding of this test was that some of the adsorbent material was migrating past the containment screens and coating the internal surface with dust. The flight containment design was updated to include a finer mesh screen and batting material, in addition to a bead of silicon sealant, to provide a continuous seal that prevented the material from leaving the sorbent bed.

This test determines the life characteristics of the desiccant and CO_2 material. There has been no noticeable degradation in performance of the bed material after 28,128 hr of testing. The flight-like 4BMS blower has operated 4,224 hr without anomaly. The blower was removed from the system for routine inspection on September 15, 1998. No visible dust collection on the blower housing was observed.

7.2 Trace Contaminant Control Subassembly[28]

The TCCS life test began in November 1992 and concluded in January 1995. The purpose was to test the TCCS high-temperature catalyst for its thermal stability. No degradation in catalyst performance was noted after 18,288 hr of testing.

The life test showed that the TCCS high-temperature catalyst life was longer than previously estimated. While the *ISS* logistics plan calls for the catalyst replacement every 180 days, this life test showed that under nonpoisoning conditions, the catalyst will remain effective in excess of 2 yr.

A TCCS catalyst poisoning test investigated catalyst poisoning using a subscale bench test. The *ISS* catalyst was exposed to various poisoning agents at different concentrations. Test results indicated that catalyst material was poisoned by dichloromethane, freon-113, and halon-1301 but was easily regenerated with pure air at operating conditions of the catalyst. Hydrogen sulfide irreversibly poisons the catalyst but is readily adsorbed by SS at operating conditions. This testing, in addition to the MSFC life testing, shows that the operational life of the TCCS catalyst can be extended to the life of the *ISS*.

7.3 Solid Polymer Electrolyzer[28]

The SPE O_2 generator testing at MSFC included a 30-day performance test conducted in 1995, limited daily testing February–May 1996, and is on-going. This test identifies cell degradation or other long-term effects.

7.3.1 Test Summary[29]

The production summary (table 50) includes all testing conducted since the refurbished SPE OGA testing began at MSFC in August 1995. The operating hours commenced at zero and are currently at 9,408 (just over 1 yr). The total O_2 produced is 2,834 lb mass (lbm), and the total H_2 produced is 354 lbm.

The type of feedwater consumed is important data, and is tabulated in table 50.

Table 50. SPE OGA feedwater.

Feedwater	Amount (lbm)
Stage 9 potable wate	583
Stage 10 potable water	1,119
Stage 10 interim WP (reduced quality)	234
Deionized water (between stages 9 and 10)	332
Deionized water (after stage 10)	920
Total potable (iodinated) feedwater	1,936
Total deionized feedwater	1,252
Total feedwater	3,188

One of the concerns of the testing is the cell stack potential increase that has occurred during the life test. This increase has not yet been explained or characterized. It is desirable to operate the SPE OGA continuously (without shutdowns) to provide more information on the phenomena, but this has not yet been possible because of scheduling and modifications required for other testing and many shutdowns not caused by the SPE OGA. The longest period of continuous operation thus far has been 30 days, with the next longest period 14 days. Figure 74 illustrates the potential over the total MSFC testing, in operating hours. In general, a drop or jump in potential indicates a shutdown.

Anomalies due to occurrences outside the SPE OGA will not be discussed in this TM. In this reporting period, there has been a relay failure in a commercial power supply, and a leak in the flight-like H_2 phase separator. The investigation on the H_2 separator leak has not been completed, but the following information is provided.

Evaluation of past data has revealed that the leak began in May 1997, and increased in severity until a shutdown occurred on March 2, 1998. The SPE OGA combustible gas sensor at the O_2 outlet, which detected the failure, is set at 25 percent of the lower explosive limit for H_2 in O_2. Both the redundant sensor in the O_2 outlet and the test facility sensor detected the increase.

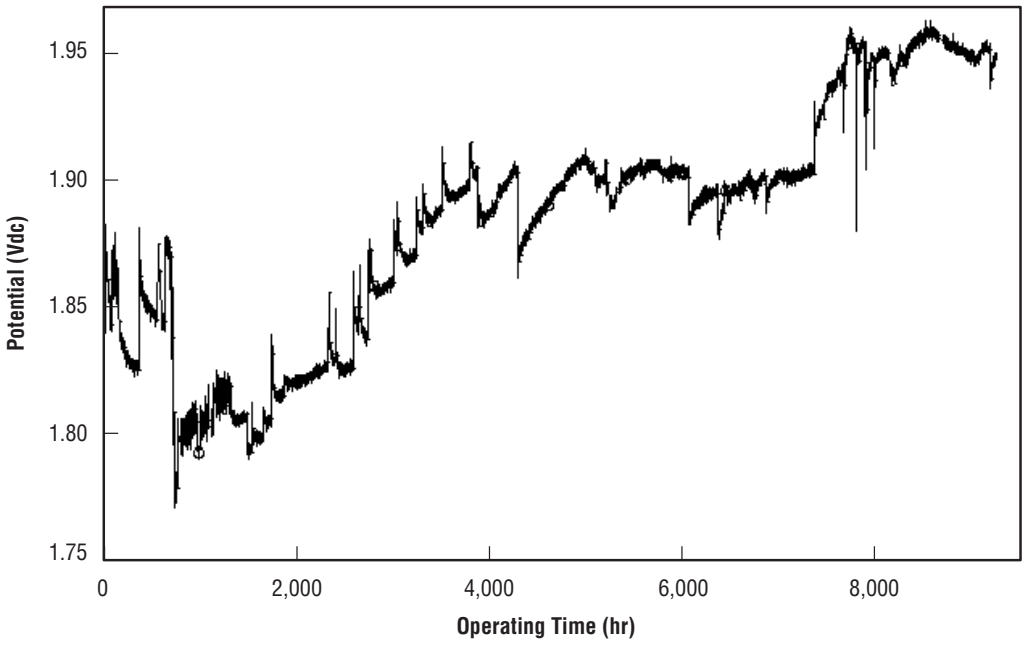

Figure 74. SPE OGA potential versus time.

The H_2 phase separator was sent to HS, the provider of the SPE OGA, for evaluation and refurbishment. The leak location was determined to be on the inlet (two-phase) side of the membrane. A particle, which was not found, appears to have been wedged between the screen and the membrane. Compounding the effect of the particle on the membrane, the tear in the membrane is adjacent to a screen on the opposite side of the membrane.

The H_2 phase separator was refurbished to the original design and cleanliness standards, and was reinstalled in late August 1998. Life testing was resumed. Alternative separator development may be conducted separately from the SPE OGA life test.

Testing has been extended, since the actual operating time will be <1 yr and the cell stack operation and life has not yet been characterized. The SPE OGA is also planned to provide H_2 for Sabatier CO_2 reduction testing.

7.4 Major Constituent Analyzer Sample Pumps and Filament Assembly[30]

The MCA is the system designed to monitor the atmosphere of the *ISS* for H_2, O_2, CH_4, N_2, CO_2, and H_2O. The analyzer receives samples from the cabin atmosphere via the sample distribution system (SDS) and uses MS to determine relative concentrations of each specie.

Due to the major differences between predevelopment-level MCA hardware and the flight design, and the cost associated with obtaining an entire MCA system, the decision was made to build test beds containing the components of the system most likely to fail and whose failure would make a significant impact to the operation of the system. The two components chosen for extended duration testing were the sample pump and the filament assembly.

The sample pump test stand contains eight pumps, a power supply, timer, and a vacuum pump along with appropriate gauges to measure and control the system. Ideally, there would be a separate power supply for each pump, but due to the cost associated with that piece of hardware, it was decided to use a single power supply and individual potentiometers to control the power for each pump. Due to the series configuration of the pumps, the setting of one will affect the others, but since the pumps are all in the same range, a little extra attention should keep this factor from becoming too significant.

There was uncertainty concerning the sample pumps during previous design reviews, and improvements to the design have been made to address some of these concerns. The life testing program at MSFC should provide valuable data to factor into the understanding of this system's operation and maintainability.

On July 16, 1996, the MCA sample pump life test assembly was checked out, and the unit was "burned in" over the next several days. By August 14, 1996, high pump pressures and flows were observed, and the test was discontinued. The pump problems resulted from a tolerance buildup design between the pump shaft assemblies and the pump cain (a sleeve that fits over the pump shaft). Pump design was corrected to include tighter tolerances, and the configuration was changed. Testing resumed, with the new configuration, on July 21, 1997.

All eight sample pumps in the MCA life test failed. A failure analyses report, Orbital Science Corporation (OSC) document design file memo No. 503, described sample pump Nos. 2, 4, and 8 failures as:

"...loss of lower pump bearing to rotor shaft attachment. This review further found the method of attachment by the manufacturer to be prone to variation. This loss of attachment resulted in relative motion of inner bearing race to shaft at operational speeds. This in turn led to abrasion of the shaft to the point where notching of the shaft caused wobbling of the rotor in a direction opposite to the offset displacement of the eccentric bearing driving the crankshaft. This effectively reduced the stroke of the crankshaft/yoke and the attached diaphragms, thereby resulting in reduced pumping efficiency and eventual out-of-specification performance."

Sample pump Nos. 2, 4, and 8 failure analyses resulted in a revision to the source control drawing to impose tighter controls on the pump vendor. This drawing explicitly calls out an interference fit between the bearing inner face and the rotor shaft. Table 51 shows the sample pump test durations. All pumps started a 12-day burn-in on July 4, 1997, and began operation on July 21, 1997.

Table 51. Sample pump test duration.

Sample Pump No.	Failure Date	Total Life (Days)	Operational Life (Days)
1	4/15/98	285	273
2	10/7/97	95	83
3	5/19/98	319	307
4	10/15/97	103	91
5	5/27/98	327	315
6	8/6/98	398	386
7	9/24/98	447	435
8	10/22/97	110	98

Results of the MSFC testing have caused the supplier of the MCA to place tighter controls on manufacturer tolerances for the sample pumps. Eight of the new pumps with design modifications are on order by ION Corporation and should be delivered in January 1999. They will then be placed on life testing.

The filament assembly contains four filaments mounted inside a vacuum chamber (with a sight glass provided for periodic observation), a roughing pump, an ion pump, a power supply, and other associated equipment. From past experience, the filaments are expected to last ≈2 yr.

The filament assembly test was started August 13, 1996. The test shut down on February 16, 1998, after ≈552 days of operation. In summary, because the sample pump was disconnected (inoperable), the system pressure increased above the acceptable level to operate the filaments. The increase in system pressure would have tripped the protection relay, however, the power supply was not connected properly into the protection relay and the filaments failed. The system is designed so when the system pressure increases, the protection relay disrupts power to prevent filament failure. In conclusion, the filament assembly life test failure resulted in improper test stand configuration.

Planing is underway to procure a replacement filament assembly. This new assembly should be delivered during 1999 and life testing resumed.

7.5 Vapor Compression Distillation Urine Processor Assembly Life Test[31]

The purpose of the VCD UPA life test was to provide for long-duration operation of the VCD at normal *ISS* operating conditions to determine the useful life of the hardware, specifically the flight-like components. The VCD design has evolved considerably over the past 20 yr. Since it was initially developed, improvements include changes in the peristaltic fluids pump, improved sensors, modifying the shape of the distillation centrifuge to a tapered drum, and improvements to the compressor. The materials have been upgraded to withstand the harsh environment inside the assembly, but long-term testing of a complete VCD/UPA (with flight-like components) to determine the life characteristics of mechanical components under simulated on-orbit conditions had not been done. The VCD/UPA contains mechanical design features which inherently have limited life, such as the peristaltic pumps. The life test was planned so that the VCD/UPA would be tested in the way that it will operate on orbit (with operation for a portion of each day) rather than running continuously, as the manufacturer, Life Systems, Inc., (LSI) had done during previous testing. The on-off operation presents a more severe condition for the mechanical components and, therefore, would reveal design problems not apparent during previous testing.

7.5.1 VCD/UPA Process and Hardware Description

The VCD/UPA is a phase-change H_2O recovery technology which will reclaim H_2O from urine and other *ISS* wastewaters. Two VCD/UPA's were tested, designated the VCD–5 and VCD–5A. The process and hardware are described in section 5.7.

The VCD–5 and VCD–5A were flight-like as indicated in table 52. Considering the components by *ISS* UPA ORU, the function, capacity, material, and final design aspects are compared with the *ISS* UPA. The controller for the VCD–5 and VCD–5A is a 400 series life systems controller. The controller for the *ISS* UPA is the next-generation controller, with a new design having additional capabilities, particularly with regard to self-diagnostics (e.g., fault detection and isolation).

Table 52. VCD–5 and VCD–5A flight-like characteristics.

ORU/Component	Flight-Like Characteristics[a]				ORU/Component	Flight-Like Characteristics[a]			
	Function	Capacity	Material	Design		Function	Capacity	Material	Design
Pressure Control Assembly					Disstillation Assembly				
Membrane separator	√	√	√		(cont.)				
Pressure sensors	√	√			Bearings	√	√	√	√
Valves	√	√			Pulleys	√	√		√
Check valve	√	√			Insulation	√			
Microbial filter	√				Heat exchanger	√			
QDs[b]					Plumbing	√			
Housing[b]					Speed sensor	√			
Fluids Control Assembly					Liquid level sensor	√	√	√	
Conductivity sensor	√	√			Compressor	√	√	√	√
Pressure sensor	√	√			Temperature sensor	√			
Relief valves	√	√			Demister	√	√		
Check valves	√	√			Shaft assembly	√	√		
Valves	√	√			End hub	√	√		
Microbial check valve					Stationary bowl	√	√		
(not on the 5A)	√	√	√		Front plate	√	√		
QDs[b]					QDs[b]				
Housing[b]					Fluids Pump Assembly				
Controller					Pump	√	√	√	√
Controller	√	√			Motor	√	√		
Wastewater Storage					Harmonic drive	√	√	√	√
Assembly					Shell	√	√		
Bellows	√	√			Tubing	√	√	√	√
Position indicator	√	√	√		Speed sensor (S2)	√	√		
Shell			√		Speed sensor[b]				
Check valve	√				QDs[b]				
Isolation valve[b]					Purge Pump Assembly				
QDs[b]					Pump	√	√	√	√
Recycle Filter Tank					Motor	√	√		
Valves	√	√			Harmonic drive	√	√	√	√
Filter	√				Shell	√	√		
Shell	√				Tubing	√	√	√	√
QDs[b]					Cooling jacket	√	√		
Distillation Assembly					Speed sensor (S2)	√	√		
Distillation unit	√	√			Speed sensor[b]				
Motor	√				QDs[b]				
Gear	√	√	√	√	Membrane gas/liquid				
Magnetic drive	√	√	√	√	separator	√	√	√	

[a]"√" indicates that the VCD–5 and VCD–5A component is like the ISS UPA design and is therefore "flight-like." If no √ is present then the component is not "flight-like."

[b]This component is not used by the VCD–5 or the VCD–5A.

7.5.2 Upgrades From Previous VCD's

The VCD–5 and VCD–5A are the designations given to refurbished earlier generation VCD's. During development of the *ISS* ECLSS design, the following additional requirements were levied on the UPA and incorporated in the VCD–5 and VCD–5A:

- Addition of a wastewater storage assembly (facility wastewater tank used for the VCD–5A)
- Addition of a coolant jacket to the purge pump assembly
- Change in software operational aspects (i.e., operating modes, mode transitions, and process control loops).

The VCD–5 is the designation given to the refurbished VCD used in the Boeing POST at MSFC. The POST VCD had previously been the VCD–4B, the first VCD to include a purge pump in the design and use a harmonic drive on the purge pump. The VCD–5 life test began on May 6, 1993. The VCD–5 was used in stages 9 (July 19, 1994 to December 21, 1994) and 10 (October 1, 1996 to March 27, 1997) of the WRT.

The VCD–5A is the designation given to the refurbished VCD used in the comparative test (designated the VCD–4) in 1990 to compare the VCD with the Thermoelectric Integrated Membrane Evaporation System (TIMES), previously baselined for use on the *ISS*. The VCD-4 was not the final flight configuration, but allowed performance characterization of the VCD components. The VCD–4 was upgraded to be functionally identical with the flight design; at which time it was redesignated VCD–5A. The hardware modifications included design improvements to meet the additional requirements. The VCD–5A was checked out in early 1993 in building 4755 at MSFC and life testing began on January 12, 1993. A purge gas test was conducted in 1996 using the VCD–5A.

As a result of information gained during fabrication and testing of the VCD–4, the following design improvements were made for the VCD–5A:

- Retrofit of the fluids pump to provide dual support (two bearings) for the shaft, rather than the previous cantilevered design.

- Replacement of the commercial vacuum pump with a dual support peristaltic purge pump.

- Change from truly tubular weld fittings to Parker weld fittings.

- Change from the commercial conductivity sensor to an LSI conductivity sensor.

- Replacement of the helicoil tube-in-shell recuperative HX with a tube-type HX.

- Addition of a static membrane gas/H_2O separator assembly.

- Addition of fluids pump tubing overpressurization protection.

The VCD/UPA life testing was performed at MSFC in building 4755, in the ECLS test facility. The test facility provided all necessary utilities and data collection and monitoring capabilities. The VCD–5 was located next to the EEF and the VCD–5A was located in the northwest corner of the north high bay. Urine was collected in the EEF and a restroom, and pretreated using Oxone® and H_2SO_4 (liquid form and, later, in solid tablet form as planned for use on the *ISS*) prior to processing in the VCD–5A. The EEF was designed, built, and integrated with the ECLSS WRT to provide wastewater typical of that expected to be produced on board the *ISS*.

7.5.3 Test Description and Performance

The VCD–5 life test began on May 6, 1993, and ran until February 16, 1994, for a total of 204 test days. A Gantt chart of the VCD–5 operation during this period is shown in figure 75. Additional testing was performed during stages 9 and 10 of the WRT. This testing revealed several problems that can be directly attributed to QC problems. Most anomalies were related to low centrifuge speed, high compressor temperatures, and high condenser pressures. Conditions that recurred but were not listed as "anomalies" are short-term, high product H_2O conductivity and blockage of the G/LS and pressure regulator with Norprene® particles.

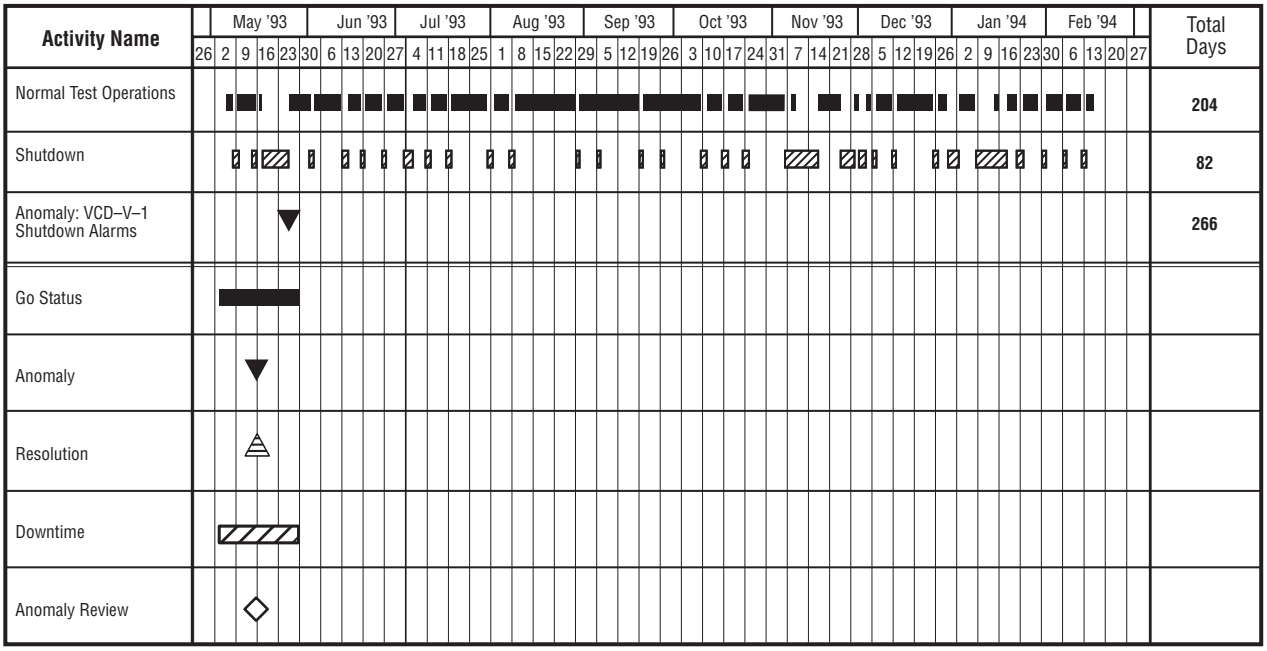

Figure 75. Gantt chart of VCD–5 operation.

The results of laboratory analyses of product H_2O and brine samples are listed in table 53. The product H_2O quality was within specification for all parameters for all of these samples (150 μmho/cm conductivity, pH of 3 to 8, and TOC <50). The brine analysis shows an increasing solids content, as expected. The exact percentage of solids is difficult to determine. The three methods used to calculate the percentage solids show significant variation in calculated percentage, but the trend is the same for each of the methods.

Table 53. VCD–5 significant events and anomalies.

Anomaly Number	Event/Anomaly Description	Date Occurred	Actionee	Date Closed	Notes/Action to Resolve Anomaly
	Life test began	5/7/93			
VCD–5–1*	Recurring shutdowns due to low centrifuge speed (S4), low gas/liquid differential pressures, and high compressor temperatures (T1)	5/19/93 1/11/94 recurring	Hutchens, Long, Salyer	1/13/94 5/25/94 7/19/94	LSI field service on 1/12/94 corrected drive belt that had been misaligned during assembly. LSI field service on 5/23/94 made adjustments, recalibrated sensors, fixed leaks, and cleaned components. LSI field service on 7/19/94 replaced faulty hardware and fixed leaks in the fluids pump.
	High product water conductivity alarms, recurring problem	5/26/93 recurring	Hutchens, Long, Salyer	–	The procedure was changed so that the conductivity sensor is disconnected at the beginning of a processing cycle until the timer resets for up to 15 min of additional reprocessing.
	Leak found in pump housings	6/4/93	Hutchens, Long, Salyer	6/4/93	Purge duration increased.
	Short in the DAS	8/2/93	Hutchens, Long, Salyer	8/2/93	Repaired.
	Blockage of pressure regulator and gas/water separator	N/A	Hutchens, Long, Salyer	1/13/94	Norprene® particles found in the pressure regulator and gas/water separator. These components were cleaned and reinstalled.
	High compressor temperature alarms	11/4/93 recurring	Hutchens, Long, Salyer	2/16/94	Facility vacuum used to assist the purge pump.
	Test stopped due to low S4, low P5, and high T1	11/9/93	–	11/16/93	Test restarted.
	Repairs made	1/13/94	–	–	Drive belt reinstalled correctly, gas/liquid separator and pressure regulator cleaned of Norprene® particles and reinstalled.
			WRT Stage 9		
VCD–5–2	CPU failure	9/11/94	Hutchens, Long	11/9/94	Multiplexer card replaced.
VCD–5–3*	High compressor outlet temperature (T1)	9/11/94	Hutchens, Long	12/22/94	High pressures caused by urinal interface.
			WRT Stage 10		
VCD–5–4	Motor speed controller malfunction	1/1/96	Hutchens, Long, Salyer	6/27/96	Motor speed controller replaced by LSI.
VCD–5–5*	Vespel® particles found in product water	10/30/96	Wieland, Long	11/6/96	Vespel® gear replaced.
VCD–5–6*	Continued high conductivity (K1) alarms	10/31/96 recurring	Hutchens, Long	10/31/96	Cleaned K1 sensor and sensor housing.
VCD–5–7	Compressor outlet temperature (T1) high, due to gas entering the still at the beginning of a cycle	11/4/96	Wieland, Long	12/9/96	Air was being injected into the still at the beginning of each cycle. A sample port was added at the outlet of the wastewater supply tank. During sample collection, free gas is released before wastewater enters the still.
VCD–5–8*	Purge pump failure	3/21/97	Wieland, Long	3/24/97	Facility vacuum was used until conclusion of the WRT stage 10. The pump was then disassembled, but no obvious failure was apparent. Upon reassembly, the pump worked properly.

*Indicates that a flight-like component is affected.

The significant events and anomalies that occurred during testing of the VCD–5 are summarized in table 53. The first anomaly related to difficulty at startup with reaching the normal drive speed for the centrifuge, high compressor temperatures, and low G/LS pressures. The low centrifuge speed was a particularly vexing problem and there were numerous efforts to correct this, including adjusting the software. When the other problems led to disassembling the VCD–5, it was found that the drive belt for the centrifuge had been incorrectly installed by the hardware supplier, resulting in the low speed.

A recurring event was high conductivity of the product H_2O. The procedure was changed to include disconnecting the conductivity sensor at the beginning of a processing cycle until the timer reset for up to 15 min of additional reprocessing. One effect of this is to reduce the performance by reprocessing H_2O that meets specification.

Leakage occurred which limited the ability of the purge pump to maintain a vacuum in the still. As a result, the pumping rate could not keep pace with the collection of noncondensable gases in the condenser. Increasing the duration of the purge helped, but eventually a facility vacuum pump was needed to ensure adequate vacuum. One source of leakage was the drive shaft of the pump.

The DAS was found to have a short, which was repaired the same day it was found. This did not involve flight-like components.

The pressure regulator and the G/LS were found to be blocked with particles of Norprene® spalling from the purge pump tubes. These components were cleaned and reinstalled. (Further investigation of the purge pump tubing problem showed that spalling had occurred in the VCD–5A as well.)

High compressor temperature alarms occurred repeatedly during the life test. This was also related to leakage. Use of facility vacuum to assist the purge pump helped to reduce these alarms, but the combination of problems led to stopping the test on November 9, 1993, until repairs could be made on January 13, 1994. Beginning on test day 20, a fan was used to cool the compressor motor from 66 to 42 °C (151 to 108 °F) which eliminated high-temperature shutdowns. Also, software changes were made to enable longer purge times since air in the wastewater feed was a factor. Compressor gear wear was also a factor and during the repairs, the compressor gear backlash was found to be 0.254 to 0.305 mm (0.010 to 0.012 in.) versus 0.076 to 0.102 mm (0.003 to 0.004 in.) when new. This is considered normal wear for a total running time of 7,400 hr, but near the maximum desired backlash. Particles of Vespel® from the compressor gear were also present in the product H_2O indicating gear wear.

To prepare the VCD–5 for the stage 9 WRT, the accelerated life test was discontinued on February 17, 1994, shortly after the repairs were made (January 13, 1994) that resolved some of the anomalies. Although the accelerated testing proved valuable, the decision to discontinue it was based upon the continuing problems with the VCD–5 resulting from poor QC by the hardware supplier. Repairs were made to correct the remaining problems before continuing the testing (stages 9 and 10 WRT's).

The second anomaly occurred during the stage 9 WRT, when the central processing unit (CPU) failed. (This was not a flight-like CPU.) The MUX card was replaced and testing continued.

The third anomaly, recurring high compressor outlet temperatures at the beginning of each processing cycle, also occurred during the stage 9 WRT, as well as during previous testing. The cause for this is gravity-related, since any free gas entrained in the wastewater collects at the top of the tank where the outlet is located. This would not happen on orbit due to more even distribution of free gas throughout the wastewater. Thus, at the beginning of a cycle, this gas is injected into the still before the wastewater. Since the gas does not provide evaporative cooling, as the wastewater does, the compressor temperature increases until wastewater reaches the still.

The fourth anomaly occurred during the stage 10 WRT, when the motor speed controller malfunctioned. The motor speed controller was replaced by LSI. (The cause of the malfunction was not identified. The controller was sent to the manufacturer for repair, but was apparently lost.)

The fifth anomaly was the presence of Vespel® particles in the product H_2O, indicating deterioration of the Vespel® gear, and the gear was replaced. The quantity of Vespel® particles found in the product H_2O then decreased as residual particles were swept from the H_2O lines.

The sixth anomaly was the recurring high conductivity of the product H_2O at the beginning of a processing cycle. The cause of the high conductivity readings was not specifically identified; although when the sensor was cleaned, particles of Vespel® were found in the sensor and housing. Another possible factor is gas bubbles in the product H_2O stream. The conductivity quickly decreased as processing proceeded.

The seventh anomaly was the recurring high temperatures at the compressor outlet (see also anomaly three).

At the beginning of a processing cycle, high temperatures occurred for ≈40 min before coming down to the desired range. The temperature was measured at the outlet of the compressor (vt1) and indicated the temperature close to the gears. The temperature spiked above the alarm setpoint of 93 °C (200 °F) due to the excessive load on the compressor and/or inadequate cooling of the gears. The high temperatures were eliminated after a sample port was added at the outlet of the wastewater supply tank, which enabled free gas to be removed during sample collection before the wastewater entered the still.

The eighth anomaly was failure of the purge pump, near the end of the stage 10 WRT. Facility vacuum was used for the completion of the test. The pump was then disassembled, but no obvious failure was apparent. Upon reassembly, the pump worked properly.

In 1998, when the VCD–5 was being prepared for subsequent integrated testing, the fluids pump was disassembled to investigate the problems with high conductivity at startup and occasionally at other times, and the difficulty maintaining sufficiently low purge pressures. The housing of the pump (made of anodized aluminum) was found to be corroded inside. None of the tubing had failed, but one of the clamps holding a recycle-loop tube (on the pressure side of the pump) was very loose, which could allow small amounts of brine to be pumped into the housing and then vacuumed out by the purge pump when the housings were evacuated. This would explain the high conductivity of the product H_2O and the pump housing leakage seen during stage 10. In addition, one of the O-rings fell apart when it was removed, and looked kinked like it had not been installed properly.

The VCD–5A life test began on January 12, 1993, and ran until November 9, 1995, (612 test days) with additional testing (purge gas test) after some repairs were made, until April 24, 1996, for a total of 665 test days. A Gantt chart of the VCD–5A operation is shown in figure 76. The total mass of wastewater/urine processed was 5,198 kg (11,449 lb) until November 9, 1995. The overall average production rate was, therefore, 1.76 kg/hr (3.87 lb/hr) for 2,960 hr in Normal, through November 9, 1995. The quality of the product H_2O measured by conductivity was well below the specified limit (150 μmho/cm) except for a few momentary spikes. The conductivity increased until the recycle filter tank was replaced, when it would drop to ≈25 μmho/cm.

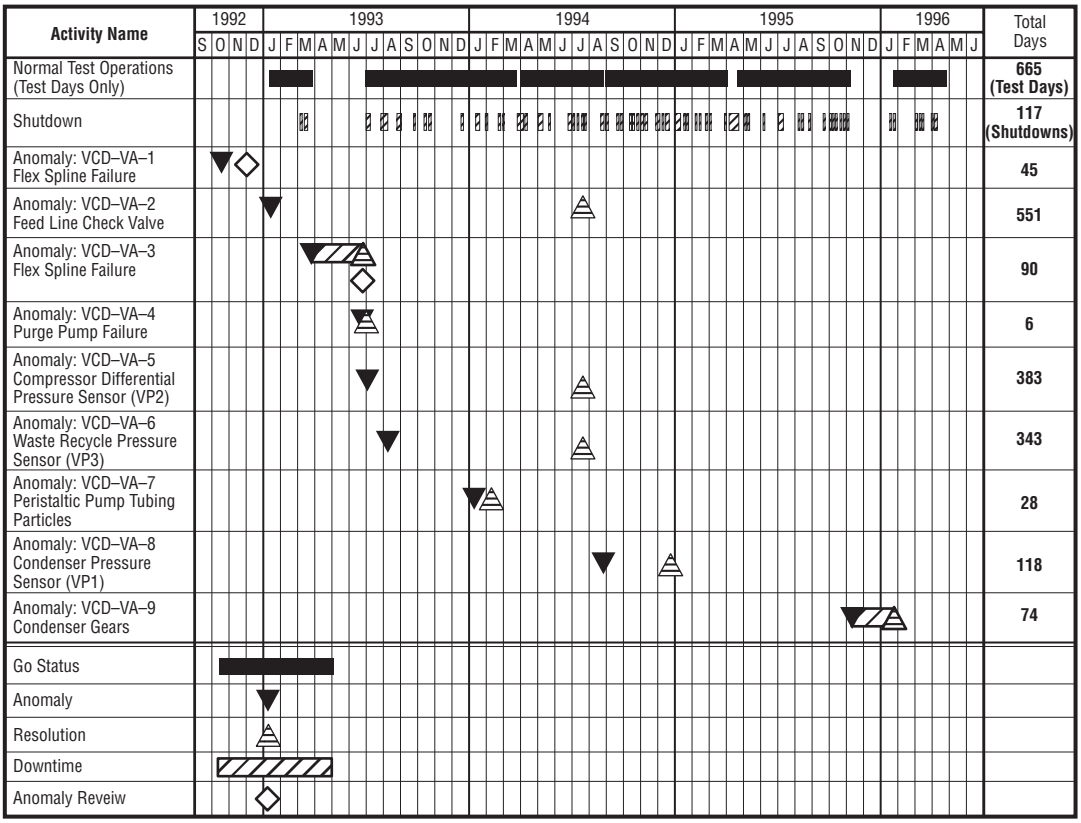

Figure 76. Gantt chart of VCD–5A operation.

The purge gas test was conducted for 3 wk to collect purge gas samples for analysis to ensure that the purge gases would not create a safety hazard during flight experiment operation. The test was halted on April 24, 1996, due to persistent high compressor motor current draws and high compressor temperatures. For the purge gas test, the amounts of wastewater processed and the distillate produced are summarized in table 54.

Table 54. Purge gas test wastewater processing.

Test Day	1 Batch 1	1 Batch 2	2	3	4	5	6	7
Urine processed (lb)	26.68	26.90	44.54	55.13	25.79	37.25	27.12	22.71
Distillate produced (lb)	27.65	25.05	41.60	52.20	23.77	35.00	25.16	20.99
Percent recovery	103.6	93.1	93.4	94.7	92.2	94.0	92.8	92.4
Test Day	**8**	**9**	**10**	**11**	**12**	**13**	**Total**	
Urine processed (lb)	20.06	13.85	12.35	13.23	12.57	13.01	351.19	
Distillate produced (lb)	17.56	13.64	11.20	12.10	11.14	11.93	328.99	
Percent recovery	87.5	98.5	90.7	91.5	88.6	91.7	93.7	

The significant events and anomalies that occurred during testing of the VCD–5A are listed in table 55.

Table 55. VCD–5A significant events and anomalies.

Anomaly Number	Event/Anomaly Description	Date Occurred	Actionee	Date Closed	Action to Resolve Anomaly
VCD–5A–1*	Fluids pump stopped due to harmonic drive failure	10/20/92	Hutchens, Long, Salyer	12/17/92	Harmonic drive replaced. Cause not determined.
	Test started	1/12/93			
VCD–5A–2	Feed line check valve allows into the external transfer tank backflow	1/14/93	Hutchens, Long, Salyer	7/19/94	Inspect valve and replace defective parts.
VCD–5A–3*	Harmonic drive failure	3/30/93	Hutchens, Long, Salyer	6/24/93	Determined misalignment caused failure.
VCD–5A–4	Purge pump failure	6/25/93	Hutchens, Long, Salyer	7/1/93	Failed electronics in the signal conditioner were replaced.
VCD–5A–5	Compressor differential pressure sensor (P2) failure	7/2/93	Hutchens, Long, Salyer	7/9/93	No action required since the sensor is not critical to data evaluation and is not included in the flight configuration.
VCD–5A–6	Waste recycle pressure sensor (P3) failure	8/9/93	Hutchens, Long, Salyer	7/19/94	Flight-like sensor installed. New material resistant to corrosive environment that caused initial failure.
VCD–5A–7*	Peristaltic purge pump tubing particles	1/11/94	Hutchens, Long, Salyer	2/8/94	An inspection will be made periodically to monitor buildup of material.
VCD–5A–8	Condensor pressure sensor (VP1) failure	8/26/94	Hutchens, Long, Salyer	12/21/94	Replaced with sensor made of Hastelloy C.
VCD–5A–9*	High T1, high T2, high K1, and water coming out purge line (Compressor gears worn out after 4,831 hr of operation)	11/9/95	Wieland, Long, Salyer	1/19/96	Replaced compressor gears and the drive O-ring.
	Facility vacuum used to assist the purge pump during purge gas testing				
VCD–5A–10	Compressor and still bearings will not rotate	6/27/96	Wieland, Long, Salyer	7/31/97	Compressor and still bearings rebuilt in-house by MSFC personnel.

*Indicates that a flight-like component is affected.

The first anomaly occurred during checkout testing of the VCD–5A at LSI when the flex spline failed in a gear speed reduction mechanism in the harmonic drive for the fluids pump (fig. 77). At that time the drive had operated for ≈400 hr. The failed part was analyzed at MSFC. However, a definite cause of the failure could not be determined because the failure surfaces were smeared by the assembly operating after the component had sheared (see the third anomaly for more information). The drive was replaced with a new one of the same design. Previously, the harmonic drives had operated for much longer without failure.

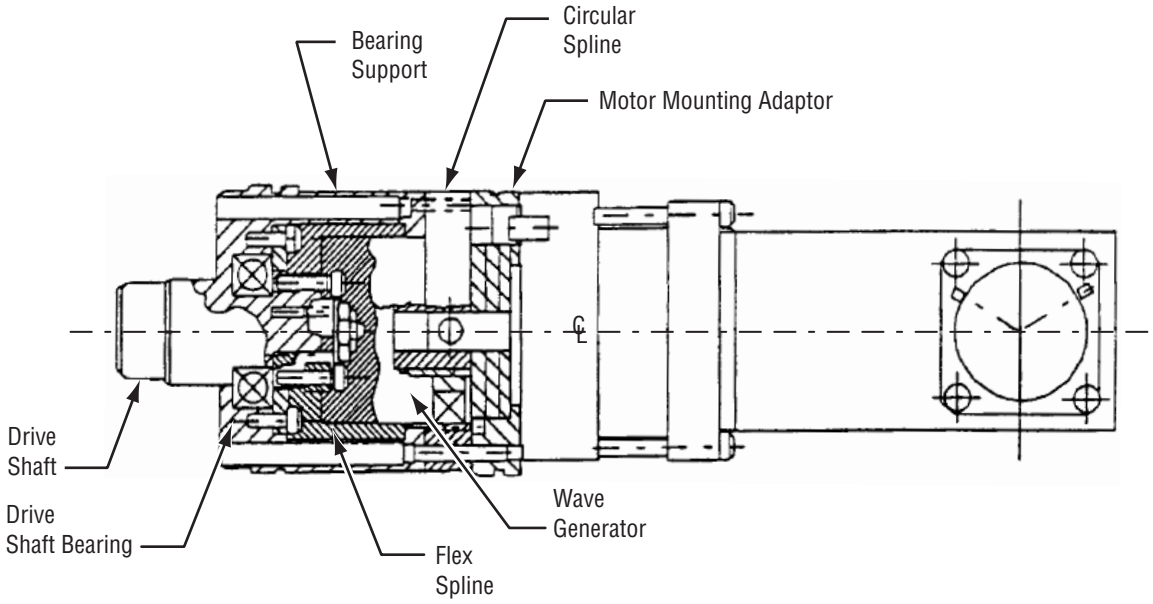

Figure 77. Harmonic drive.

The second anomaly was the failure of the wastewater feed-line check valve on January 14, 1993, which allowed wastewater to flow back into the external transfer tank. This did not adversely affect operation of the VCD and no immediate action was taken to replace the failed valve. The procedure was changed to include closing the manual valve at the VCD interface after transfers of wastewater from the facility supply.

The third anomaly was another failure of the fluids pump, after 51 days of testing at 362 hr of operation. The failure was similar to that which occurred during checkout at LSI. A flex spline in the harmonic drive of the fluids pump failed in both cases. The exhaustive 3-mo investigation which followed determined that the failures resulted from a slight horizontal misalignment (0.127 mm (0.005 in.)) introduced into the pump driveshaft during its assembly at the hardware supplier. The manufacturer (Harmonic Drive Technologies) said that misalignment of the spline could overstress it and lead to fatigue failure. The potential for this problem may have been introduced into the pump during retrofit at the hardware vendor (to support the drive shaft at both ends; see sec. 7.5.2 about the retrofit), since during previous testing when the pump drive shaft was a cantilever design, the harmonic drive operated for a much longer period of time. The vendor has implemented use of a new alignment jig during hardware assembly to ensure proper alignment. This jig will be used for flight hardware assembly. The pump was sent back to the supplier, the part replaced, and the misalignment corrected. Testing resumed on June 25, 1993, but the purge pump did not receive power, due to the fourth anomaly.

The fourth anomaly was failure of the purge pump electronics. This problem was traced to a failed power converter and capacitor on the purge pump controller card. These items were replaced and testing resumed on July 2, 1993. This failure did not affect any flight-like components.

The fifth anomaly occurred when the VCD–5A was restarted on July 2, 1993, and the compressor differential pressure sensor (P2) was nonfunctional. No actions were taken since the P2 sensor is not critical to data evaluation and not included in the flight configuration.

The sixth anomaly was failure of the waste recycle pressure sensor (P3) on August 9, 1993. This sensor is flight-like in function (although the flight sensor will be somewhat different). LSI provided a temporary replacement sensor so the failed sensor could be analyzed. The temporary sensor was installed on August 30, 1993. Even without the P3 sensor, system backup features would allow operation of the VCD–5A.

The seventh anomaly was related to the Norprene® tubing used in the peristaltic purge pump. This pump uses the same tubing as the fluids pump although it pumps a two-phase mixture, which is mostly gas. This application was found to cause spalling of the Norprene® which resulted in clogging of the G/LS with Norprene® particles. The initial resolution suggested by the hardware supplier was to add a filter downstream of the pump to prevent G/LS clogging. An inspection of the air/H_2O separator was made every 30 days to avoid buildup of particles.

The eighth anomaly was failure of the condenser pressure sensor (P1). This sensor was replaced with a sensor made of Hastelloy C, a high nickel, molybdenum, and chromium alloy that is more resistant to corrosion.

The ninth anomaly involved high-temperature alarms and liquid coming out of the purge line. The VCD–5A was deactivated until repairs could be made by LSI. The operating time on the compressor gears and the drive belt was estimated to be 4,831 hr, including time before the life test began. The compressor gears and the centrifuge drive belt were found to be worn and were replaced.

The tenth anomaly was the failure of the compressor and the centrifuge to rotate due to a worn compressor and still bearings. More torque was required than the motor generated. The compressor and still bearings were rebuilt by MSFC personnel.

Facility vacuum was used to assist the purge pump when leakage exceeded the pump capacity to adequately evacuate the pump housings and purge the condenser. The facility vacuum was connected as shown in figure 78.

During test days 613–665 the VCD–5A processed 460.0 kg (1,011.3 lb) of wastefeed, averaging ≈3.6 lb/hr. The recycle filter tank was replaced on test days 626 and 651.

The results of the life testing of the VCD–5 and VCD–5A have led to numerous improvements in the flight design. For example, lessons learned about the VCD relate to the critical nature of pump drive mechanism alignment and the impacts of QC on system performance. Although the problems have been

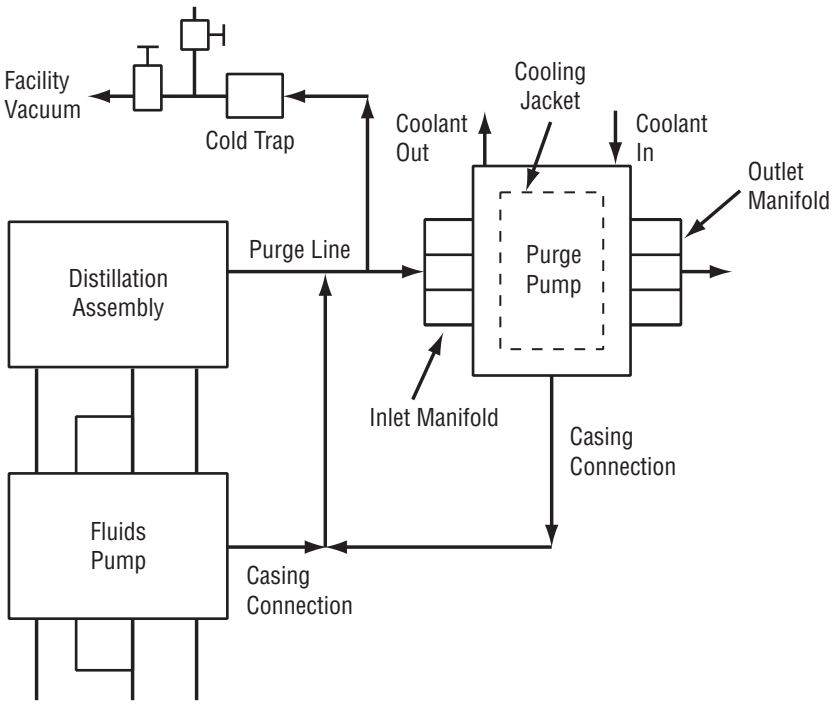

Figure 78. Facility vacuum connection to the purge and fluids pumps.

resolved, the number of problems relating to QC and the sensitivity of hardware performance are causes for concern.

The operating lifetimes of VCD components are listed in table 56. The lifetimes of most of the components are greater than the duration of the life test. The times indicate time of operation of that component, excluding standby and shutdown conditions, except where "operation" is continuous, such as the wastewater storage assembly and fluids control assembly.

Table 56. VCD component lifetimes.

Parameter	Units	Specified Values			Initial Samples (Batch 1)	
		Nominal	Maximum	Minimum	Tubes A&C	Tubes B&D
pH	pH units	7	6	8	8.2	7.5
Conductivity	µmho/cm	3.3			2.69	2.14
Turbidity	NTU		11		0.7	0.8
Iodine, residual	ppm	4.10			3.31	9.75
Iodide	ppm				2.43	2.35
Total Iodine	ppm				5.74	12.1
Chromium	mg/L		0.05		<0.010	<0.005
Iron	mg/L		0.3		<0.005	<0.005
Nickel	mg/L		0.05		<0.009	0.039
Molybdenum	mg/L					<0.020
Titanium	mg/L					<0.001
TOC	mg/L		1		<1	<1
TIC	mg/L					<1
Total carbon	mg/L					<1
R2A–7 day	CFU/100 mL		1		<1	<1
Total solids	mg/L		2		<10	<10
Color	Color units		15		<1	<1
Cadmium	mg/L		0.01		<0.001	<0.001
Copper	mg/L		1		<0.005	<0.005
Lead	mg/L		0.05		<0.010	<0.010
Manganese	mg/L		0.05		0.002	<0.001
Silver	mg/L		0.05		<0.002	<0.002
Zinc	mg/L		5		0.002	<0.001
Selenium	mg/L		0.01		<0.010	<0.010

7.6 Water Degradation Study

The original water degradation study (WDS) began in January 1993 and was completed in January 1996. Due to several unexpected results, follow-on testing began in January 1995 and was completed in January 22, 1998.

As stated in the report entitled "Interim Report on the Space Station Water Degradation Study Covering the First 24 Months of Exposure," the WDS is a Space Station-supporting development activity designed to demonstrate how H_2O quality changes during long-term, stagnant storage in distribution lines.

The need for the WDS originally stemmed from the 1991 Space Station restructure. The resulting design changes called for the H_2O lines to be launched wet, and to remain undisturbed until the activation of H_2O recovery systems, ≈3 yr later. This scenario raised concerns over whether the biocidal I_2 would break down during extended storage, leaving the distribution lines vulnerable to microbial growth, biofouling, and microbial-induced corrosion. Scientists and engineers at MSFC began investigating the change in H_2O quality under long-term storage conditions. As a result, the WDS was developed.

To assess the change in H_2O quality during long-term storage, the WDS was developed to demonstrate the effects of time, tube material, and initial I_2 concentration on H_2O quality. The WDS includes time as a parameter for two reasons: (1) To provide the intermediate data points within the 3-yr exposure period, and (2) to gain insight into the rate at which H_2O quality changes take place. Tube material was also included as a parameter since the Space Station baseline has, at various times, called for both titanium and SS as the material of construction for the H_2O recovery and management system. At the time the WDS test plans were in preparation, the baseline design called for SS, but a decision to change the material to titanium was pending. By varying the material of construction, the WDS was sought to identify any significant differences in H_2O quality changes stemming from material effects. In addition, the WDS has varied initial I_2 concentrations to determine the effectiveness of different concentrations of I_2 in the distribution lines prior to launch. The WDS was conducted at ambient temperature in building 4755 north high bay.

The WDS consists of 34 tubes configured as straight sections, 10 ft in length, with valves at each end (fig. 79). These tubes are grouped into two batches, designated as batch 1 (initial test batch) and batch 2 (the follow-on test batch). Within each batch, the tubes are grouped into sets according to exposure time. All tubes are stored vertically in a rack until their exposure time is complete.

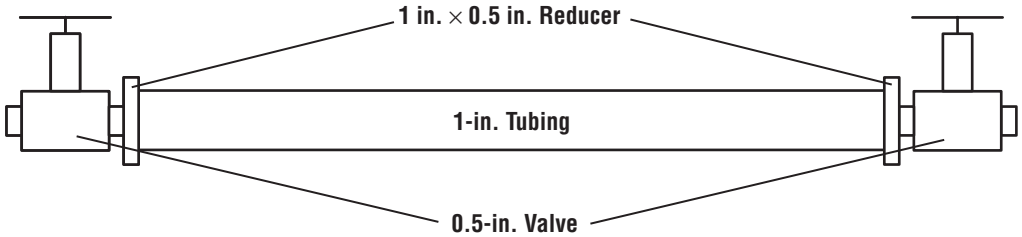

Note: Tubes are installed vertically in the test

Figure 79. WDS tube configuration.

Batch 1: The original batch of tubes used in the WDS contained seven sets of four tubes each. Each set of four tubes included two tubes made of SAE AMS 4942C titanium (equivalent to ASTM B338 grade 2 tubing) and two tubes made of corrosion-resistant steel (CRES) 316L SS. Initial I_2 concentrations are denoted in table 57.

Table 57. WDS test configuration.

	Batch 1 (Began January 1993)				Batch 2 (Began January 1995)		
Tube Designation	**A**	**B**	**C**	**D**	**E**	**F**	**G**
Tube Material	CRES 316L	CRES 316L	Titanium	Titanium	Titanium	Titanium	Titanium
Valve Material	CRES 316L	CRES 316L	CRES 316L	CRES 316L	Titanium	Titanium	Titanium
Initial Iodine (I2) Concentration (ppm)	4	10	4	10	4	10	0

Although the original WDS test requirements called for the titanium tubes to have titanium valves, concerns over cost and lead time led the investigators to substitute SS valves. The decision to use SS was based on two factors: (1) The prediction of minimal galvanic effects between SS and titanium, and (2) the apparent likelihood that the Space Station WRM system would include both SS and titanium components.

Batch 2: It was observed that dissolved nickel levels in batch 1 were above Space Station specifications in both the SS and the titanium tubes. Investigators concluded that either the SS valve bodies or a lubricant in the valves was donating nickel to the H_2O. Since all batch 1 test fixtures included these valves, the decision was made to add all titanium tube configurations to the test using titanium tubes and valves, and no nickel containing lubricants. These all-titanium fixtures constitute batch 2, and were placed into service in January 1995.

Batch 2 consists of two tube sets, each of which contains three tubes. These tube sets are designated as sets 4 and 7, because the exposure times are identical to sets 4 and 7 in batch 1. The tubes in the batch 2 tube sets are designated as tubes E, F, and G.

The H_2O used in the test is 18 Mohm/cm, filtered DI H_2O, sterilized within the tube at 250 °F for 1 hr. Iodination occurred after the H_2O returned to ambient temperature, following sterilization. Chemical and microbial parameters were analyzed prior to beginning the test (table 58).

Table 58. WDS initial H_2O quality.

Parameter	Units	Specified Values			Initial Samples (Batch 1)	
		Nominal	Maximum	Minimum	Tubes A&C	Tubes B&D
pH	pH units	7	6	8	8.2	7.5
Conductivity	µmho/cm	3.3			2.69	2.14
Turbidity	NTU		11		0.7	0.8
Iodine, residual	ppm	4.10			3.31	9.75
Iodide	ppm				2.43	2.35
Total Iodine	ppm				5.74	12.1
Chromium	mg/L		0.05		<0.010	<0.005
Iron	mg/L		0.3		<0.005	<0.005
Nickel	mg/L		0.05		<0.009	0.039
Molybdenum	mg/L					<0.020
Titanium	mg/L					<0.001
TOC	mg/L		1		<1	<1
TIC	mg/L					<1
Total carbon	mg/L					<1
R2A–7 day	CFU/100 mL		1		<1	<1
Total solids	mg/L		2		<10	<10
Color	Color units		15		<1	<1
Cadmium	mg/L		0.01		<0.001	<0.001
Copper	mg/L		1		<0.005	<0.005
Lead	mg/L		0.05		<0.010	<0.010
Manganese	mg/L		0.05		0.002	<0.001
Silver	mg/L		0.05		<0.002	<0.002
Zinc	mg/L		5		0.002	<0.001
Selenium	mg/L		0.01		<0.010	<0.010

Results from the WDS batch 1 demonstrated that it is possible to store H_2O in a SS or titanium distribution system for a period of 3 yr, without detectable microbial growth. The WDS has shown that the microbial integrity of the H_2O can be maintained even after I_2 depletion, if the initial H_2O quality is high, and the filling process is carefully controlled. Some chemical parameters such as pH, conductivity, I_2, iron, nickel, and TOC were outside the Space Station limits by tests end. Due to the lack of microbial/biofilm growth, however, a flushing of the distribution lines would resolve the problem once the system is brought on line. It was also demonstrated that initial I_2 levels of 10 ppm are insufficient to maintain I_2 levels above a 2-ppm minimum for extended periods. This intensifies the need for aseptic techniques in the filling of distribution lines.

Results from the WDS batch 2 are available for only the 15-mo test set. Tubes initially containing 10-ppm I_2 were shown to contain 6.15-ppm I_2. The tube initially containing 4-ppm I_2 was found to contain <0.5-ppm I_2. No microbial/biofilm growth was observed in either tube, and all chemical parameters other than I_2, were within Space Station specifications.

7.7 Biofilm

As stated in the document entitled "Test Plan for the Assessment of Biofilm Accumulation in the Water Distribution Lines and Storage Tanks of the *International Space Station*," the objective of the test is to provide information for use in assessing the extent of microbial growth and biofilm formation in the *ISS* WRM system distribution lines and storage tanks. The test is being used to identify the areas of concern and develop countermeasure plans if necessary.

The test is composed of two very similar system layouts (fig. 80). One system contains clean H_2O, and simulates the conditions in the postprocessor H_2O distribution lines. This is designated as the "clean" side (or processed H_2O) system. The other system is filled with wastewater, and simulates the conditions in the H_2O distribution lines and storage tanks prior to the WP Unibeds®. This is designated as the "dirty" side (or wastewater) system. Both systems are integrated into a single test stand, and are stacked in a horizontal plane. Access for the replacement and service parts are provided for in the layout of the test stand and the system layout.

Four titanium and four SS tubes of 0.25-in. outside diameter are arranged in parallel as alternating pairs. Each tube is 4-ft long (prior to bending), and bent at four equally spaced intervals. Each end of the sample tube assembly contains a SS quick disconnect so the tubes can be removed from the system easily.

The storage tank is 12.75 in. high and has an inner diameter of 15.75 in. The tank is constructed of Inconel 718. In the top of the tank, there are 33 tapped holes into which are placed titanium, SS, and Inconel coupons (11 of each material; e.g., titanium, SS, and Inconel). These are attached to 0.75-in. threaded bars. The bars are screwed into the tapped holes so that the attached coupons extend into the tank.

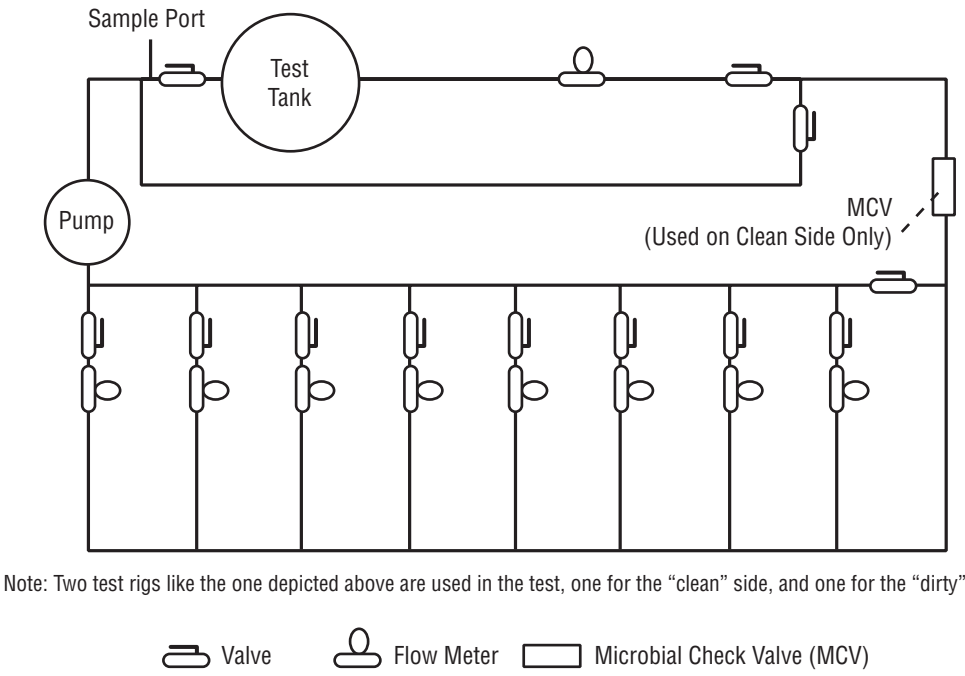

Figure 80. Biofilm life test.

The entire system was chemically cleaned, and steam sterilized prior to test initiation. Sterilization was accomplished by passing 195 °F H_2O through the system for 4 hr, followed by a cooling to 100 °F, and an additional 4 hr at 195 °F. After sterilization, the H_2O was drained from the system by purging with argon prior to filling with test H_2O (dirty in one circuit and clean in the other).

The biofilm life test processed H_2O (clean side) was initiated in January 1997 and completed ≈12 mo of testing, though not continuous. All major shutdowns are listed below for the processed H_2O loop:

1. June 13, 1997: Test stopped due to pump failure. Pump was rebuilt by manufacturer. New MCV installed and restart occurred July 3.

2. July 23, 1997: MCV removed and backflushed. Restart occurred the same day.

3. August 4, 1997: MCV removed and backflushed. Restart occurred August 5.

4. August 6, 1997: MCV removed and replaced with tube assembly. Restart occurred the same day.

5. August 8, 1997: Test stopped due to inadequate flow at maximum pump capacity. System was flushed and restart occurred August 10.

6. October 28, 1997: Test stopped due to pump failure. Pump head was replaced with an extra pump head. Restart occurred the same day.

7. January 26, 1998: Pump failed (S/N 332920) with 90 days of operation. Replaced pump with spare pump head (S/N 332590).

8. February 9, 1998: Pump failed after 13 days of operation.

Throughout the clean side testing, the conductivity, total I_2, and iodide values gradually increased. The pH values averaged 5 pH units with a slow decline as testing progressed. Microbial counts were relatively low; Bacillus cepacia and methylobacterium radiotolerans were isolated during testing. Tank coupons and the bent tubes also showed low microbial counts.

On June 13, 1997, the pump failed, causing the test to shut down. A significant amount of fine, black particles was present when the pump was removed from the system and examined. Pump wear and the MCV resin were two suspects for the source of the particles. An H_2O sample taken during this time period showed iron at 23.1 ppm and nickel at 4.41 ppm. The MCV was backflushed with H_2O and a substantial amount of "black" particles exited the MCV. After pump repair, a second MCV was installed, all H_2O in the storage tank was drained, and the test restarted. The first set of two bent tubes (SS and titanium) was then removed for sampling. When the H_2O was eliminated from the bent tubes, black particles were again observed. At this time, there was concern that the particles were throughout the system.

On July 29, 1997, a decrease in flow was noted in sample tube No. 8. On August 4, 1997, the pump ceased flowing and the MCV was removed on the theory that it was clogged. When the MCV was flushed, "black" particles were collected from the inlet and the outlet sides. Two days later, the system flow was restored without the MCV; however, there was still no flow observed through sample tube No. 8.

On August 8, 1997, there was inadequate flow through the system with the pump at maximum load and the test was stopped. After assessment of the clean side system test data, the MCV was removed from the system and the system was flushed thoroughly with DI H_2O to remove most of the particles. Hot H_2O (≈180 °F) was then flushed through the system using the sterilization cart to attempt removal of any particles that adhered to surface areas. Then, hotter H_2O (≈250 °F) was circulated through the system in an attempt to reach sterilization conditions. Sterile DI H_2O was placed in the storage tank (by pressure) for circulation throughout the system. A microbial sample was taken for analysis. After the microbial assay results were received, a combination of ersatz and processed H_2O was pumped into the storage tank and the clean side testing was restarted. Iodine was injected into the storage tank instead of using an MCV.

Pump failures occurred on October 28, 1997; January 28, 1998; and February 9, 1998. The clean side of the biofilm life test was terminated February 9, 1998, after 388 days of testing. The decision to terminate the test was based on inadequate flow of H_2O through the system for the following reasons: (1) The pump removed in January had been in operation for 2 mo and was removed from test due to inadequate flow. An examination of the pump showed erosion of the protective metal sheath around the rare Earth magnet. The particles of sheath, casing, and magnet were released into the tubing of the test apparatus, clogging the quick disconnects throughout the plumbing and disallowing H_2O flow. The clogging problem was not reversible. (2) The concentration of micro-organisms in the clean H_2O loop

was steadily increasing after the removal of the microbial check valve from the system in October 1997. The increase in microbial counts was traced to contamination in the concentrated I_2 solution used to maintain the I_2 concentration in the system.

The biofilm life test, dirty-side testing began in April 1997 and has operated 569 days as of October 31, 1998. The dirty-side system has not experienced any anomalies at this writing. The pH values average 6.7 pH units while the conductivity values average 556 μmhos/cm. The TOC values average 222 ppm with a minimum value of 168 ppm and a maximum value of 267 ppm. Microbial counts of the H_2O average 1.21E+08 CFU/100 mL showing a three-log fluctuation in sample results (the minimum count is 6.30E+05 CFU/100 mL and the maximum count is 6.2E+08 CFU/100 mL). Three sets of three coupons (SS, titanium, and Inconel 718) have been removed from the storage tank. The SS coupons had microbial counts averaging 7.55E+03 CFU/cm^2, the titanium coupons averaged 3.96E+04 CFU/cm^2, and the Inconel 718 coupons averaged 1.10E+04 CFU/cm^2.

7.8 Temperature and Humidity Control Condensing Heat Exchanger Surface

As stated in the document entitled "Test Plan to Evaluate Microbial Control Measures for the Temperature and Humidity Control Subsystem Condensing Heat Exchanger of the *International Space Station*, August 12, 1997," the microbial growth test will duplicate the conditions on the surface of the *ISS* THC CHX. In particular, the test will monitor the growth of micro-organisms on materials, simulating the surface of the *ISS* THC CHX. The primary objectives of this study are to evaluate (1) the extent of microbial growth which may occur on the CHX using "real" humidity condensate (as opposed to ersatz solution) in conjunction with the extent of microbial control with an antimicrobial additive (silver) in the hydrophilic coating; (2) the effectiveness, in terms of microbial control, of allowing the CHX to dry for a 2-hr period (dryout cycle), every 7 days; (3) the potential for hardware operational degradation (corrosion, biofilm accumulation) due to microbial activity, and to recommend for operation and maintenance of the THC hardware in flight, and (4) the data accumulated as it relates to the WP design effort.

The microbial growth test (fig. 81) included an insulated chamber, six-coated metal cascades, a multichannel peristaltic pump, portable chiller, vacuum pump, and a drying fixture (not shown in schematic). The microbial growth chamber (MGC) simulated the *ISS* CHX finstock material and slurper bar holes. The hardware was challenged with actual humidity condensate collected in the EEF located in building 4755. Feedwater was pumped from the chilled holding tank via the pump manifold. The H_2O was dispensed on each of the six-panel assemblies, which are arranged in a staired or cascaded configuration (fig. 82). H_2O was dispensed on the top panel, and flowed down the cascade, wetting all the panels before exiting into the collection flask at the end of the panel series.

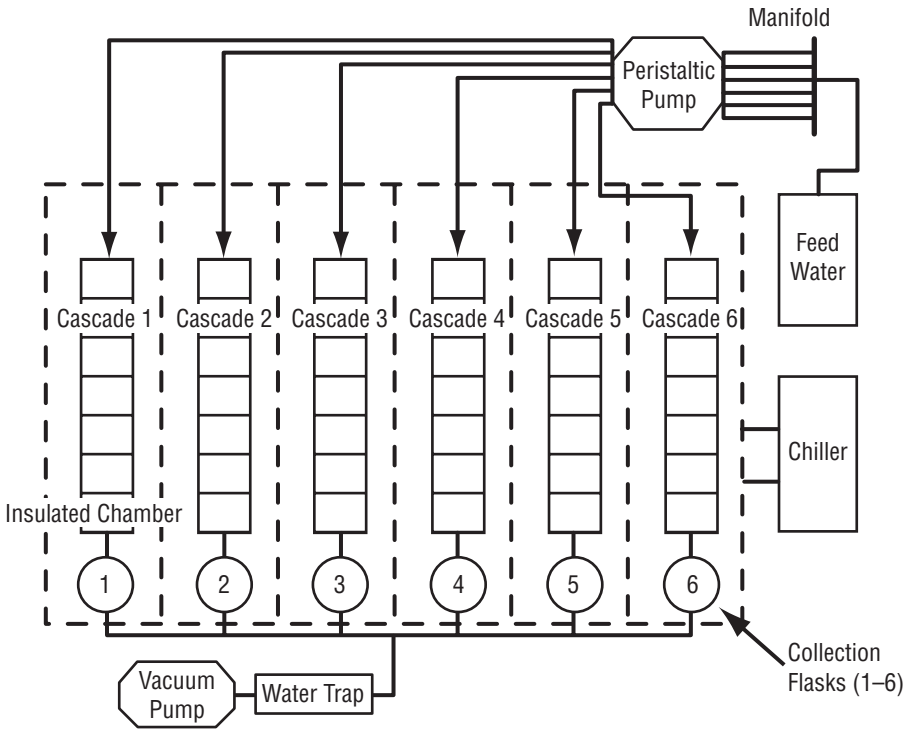

Figure 81. Microbial growth chamber.

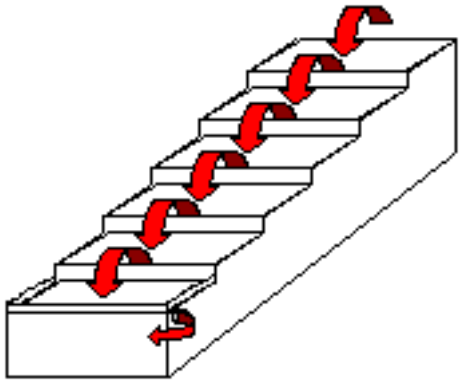

Figure 82. Cascade test arrangement.

The basic test rig used a panel set which includes a pan (2×3 in.) containing a piece of fin stock (2×2×0.25 in.) covered by a top plate. All the wetted surfaces were coated with a hydrophilic coating. The panel set was designed to represent the hydrophilic-coated air passages through the THC CHX. The construction materials were 316L SS. The cascades were coated to support the following test scheme:

Cascade Nos. 1 and 2: Both cascade panels were treated with a hydrophilic coating, and no biocidal silver. For the duration of the test, cascade #1 was operated with a drying cycle (2 hr after the hardware becomes dry, every 7 days). No drying cycle was incorporated in the test of cascade No. 2. Both panels were used as reference panels to evaluate the baseline microbial challenge to the test hardware.

Cascade Nos. 3 and 4: Both cascade panels were treated with a hydrophilic coating and silver biocide. These cascades were operated without a drying cycle for 361 days. During that time the microbial control of the antimicrobial coating only (in duplicate) was tested. On test day 362, biweekly dry cycles of cascade No. 4 were incorporated in the test to assess the effects of dry cycles on the surface of a panel with an established microbial population.

Cascade Nos. 5 and 6: Both cascade panels were treated with a hydrophilic coating and silver biocide. These cascades were operated with a drying cycle (2 hr, after the hardware becomes dry, every 7 days) for 361 test days. During that time microbial control from drying cycles on an antimicrobial coating (in duplicate) was assessed. On test day 362, the drying scheme of cascade No. 6 was changed from every week to once a month. The drying frequency of cascade No. 6 was increased to evaluate its effect on the panels.

Humidity condensate (feed H_2O) was stored inside the insulated chamber. A peristaltic pump delivered the cooled humidity condensate to the MGC at a flow rate of 0.12 mL/min, and this flow was split into six channels, each at 0.02 mL/min. The flow rate of 0.02 mL/min represents the average daily condensate formation rate (0.5 lb/hr) for a crew of two working at a moderate rate. H_2O samples (chemical and microbiological) were collected once per month. Surface samples (microbiological only) from panels 1 and 4 were collected twice per month.

The CHX microbial growth test concluded under nominal conditions, and test was completed the last week of September 1998. Microbial surface sample data, collected from panels Nos. 1 and 4 of each cascade, is shown in figure 83. Preliminary results clearly show effective microbial control with a drying cycle alone (cascade No. 1) if compared to cascade No. 2 with no drying cycle. A suppressed microbial growth environment was observed in the cascades with a silver coating and no dry cycle. Drying cycles and silver coating provided effective continuous control of microbial growth on surfaces.

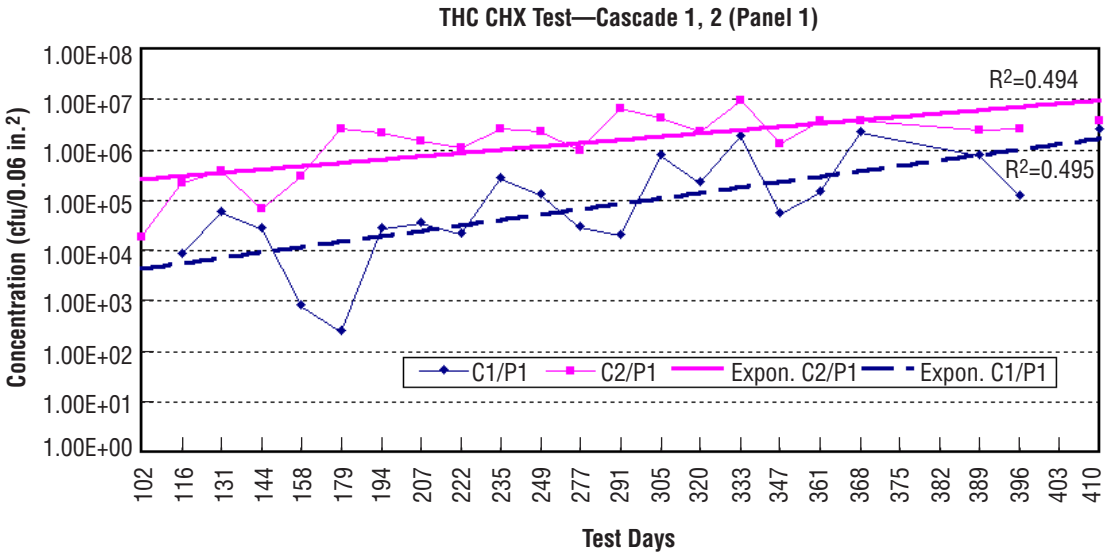

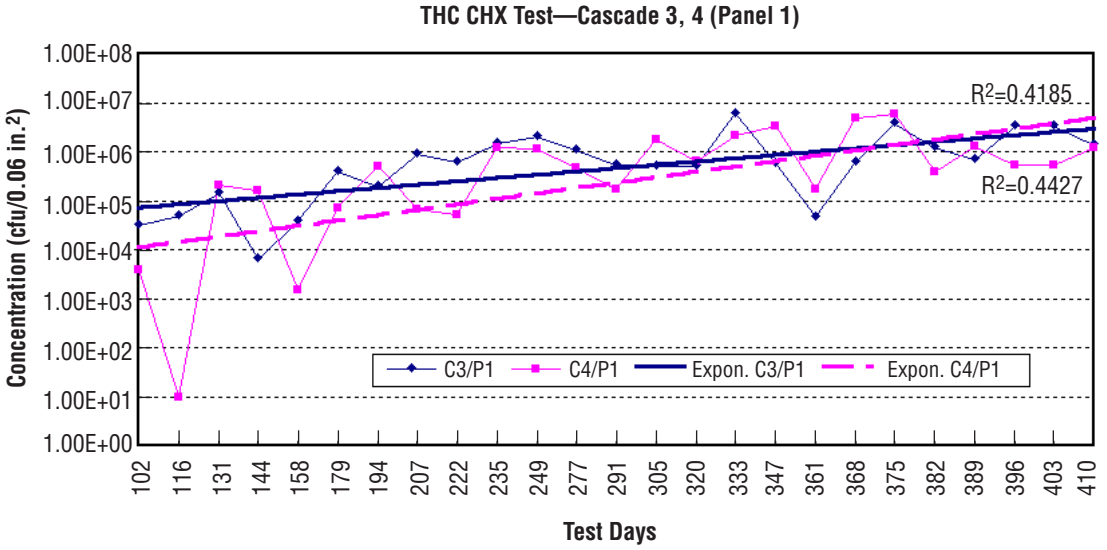

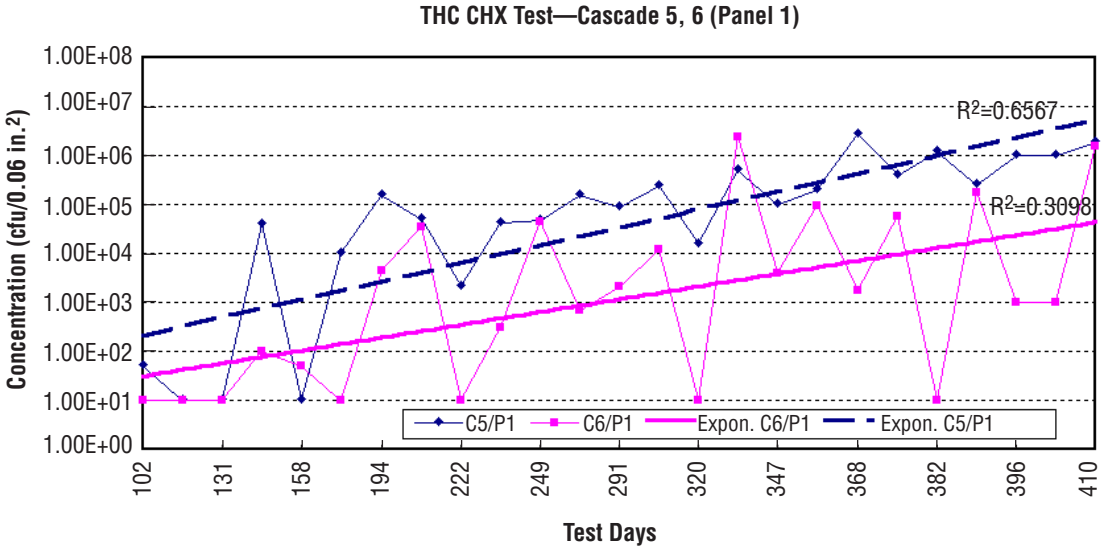

Figure 83. Microbial counts.

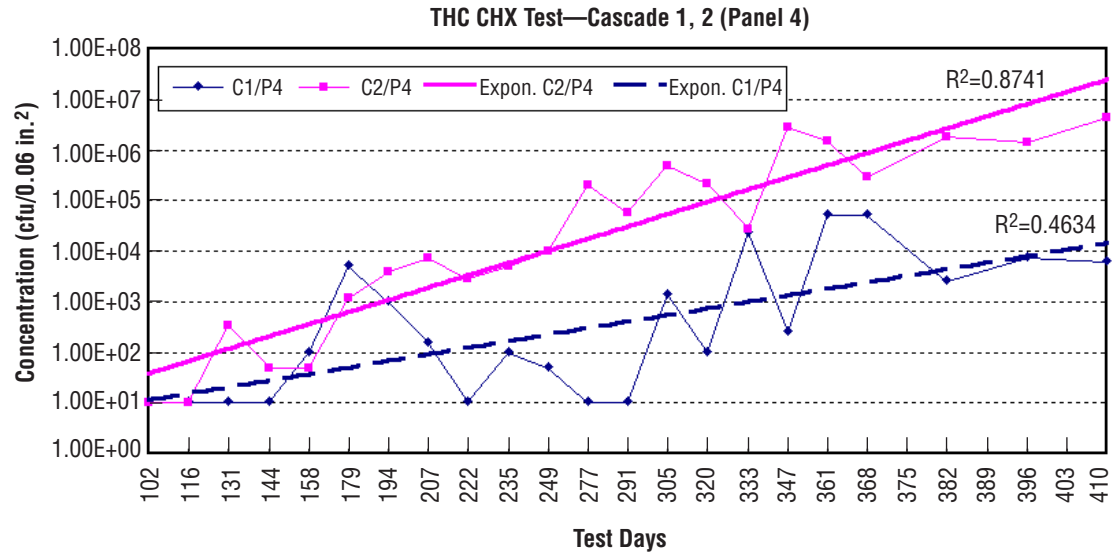

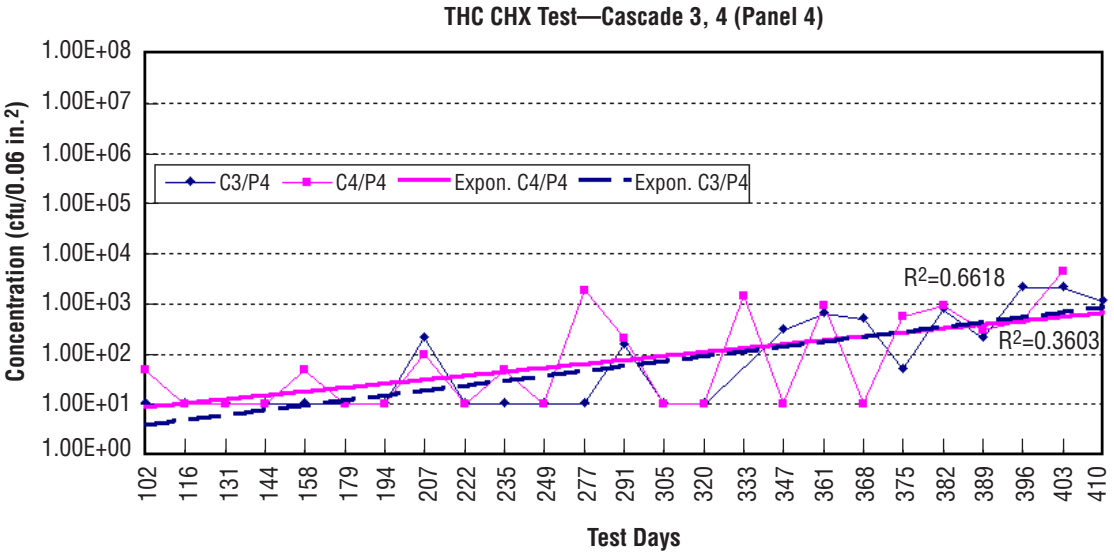

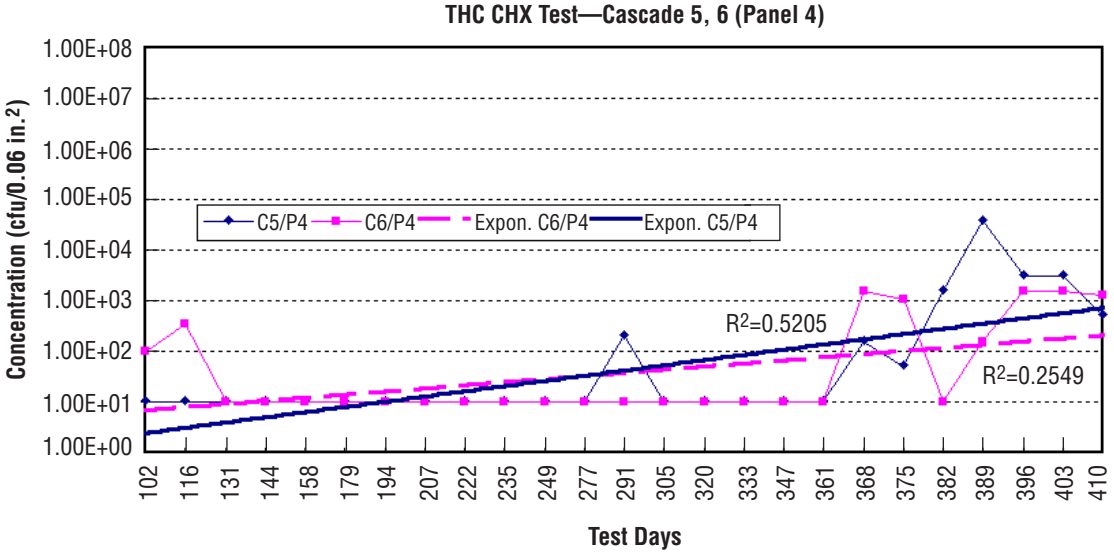

Figure 83. Microbial counts (Continued).

The test was extended 3 mo to assess (1) the results of incorporating a drying cycle after microbial growth was allowed to colonize the surface of the panels, and (2) the effect of increasing the time between drying cycles on panels that were dried weekly. Data obtained from the test extension are being evaluated and will be presented in the next interim report and also in a final test report.

The extended microbial growth chamber test was initiated after all panels of all cascades were sampled for surface heterotrophs. The test continued with no interruption, changeout, sterilization, or disinfection of H_2O, apparatus or assemblies. A 2-hr drying cycle was utilized, as in prior test. Table 59 summarizes the test extension parameters.

The data from this test will be used to determine the benefit(s) of incorporating dry cycles during the operation of the *ISS* THC assembly.

Table 59. MGC extension summary.

Cascade	Hydrophilic Coating	Drying Cycle	Comments	Rationale
1	Without silver biocide	Each week	A drying cycle each week as in previous test	This cascade serves as a control.
2	Without silver biocide	No	No drying cycle as in previous test	This cascade serves as a control.
3	With silver biocide	No	Control, no change from prior test scheme	This cascade serves as a control.
4	With silver biocide	Every 2 wk	Drying cycle effect on existing population, prior test had no drying cycle	Drying cycle was introduced to determine effects of drying on an established biofilm population.
5	With silver biocide	Each week	Control, same drying cycle as in previous test	The scheme was continued as in previous test to evaluate extended effects of the drying cycle.
6	With silver biocide	Every 4 wk	Variable dry cycle, prior test had a drying cycle each week	The drying frequency was increased from one drying event each week to one every 4 wk. Data will be evaluated to determine the effect of an extended duration between drying cycles.

8. TEST SUPPORT

8.1 Functional ECLSS Data System Database

The functional ECLSS data system (FEDS) was implemented in 1990, and served ECLSS testing through chemical, microbial, and electronic sensor data storage and retrieval. FEDS was established to track and maintain all sample schedules, analyses from independent labs for chemical and microbial parameters, predetermined parameter specifications to maintain H_2O quality, sensor data, and analytical control samples. Table 60 shows FEDS statistics. The database provides ECLSS engineers on-line access to analyze data and provides formatted reports, graphical, and statistical results. Menu-driven interfaces allow the user to retrieve data on line or extract test data to files. A rewrite of the FEDS General User's Manual was distributed in May 1996 by ION Corporation. This manual was the first revision since ION's May 1991 distribution.

Table 60. FEDS statistics.

Size	240 MB
Number of records	320,000
Number of tables	32

The FEDS operating platform was transferred from Oracle to FoxPro in 1998. In 1997, the MSFC Environmental Control and Life Support Branch (ED62) was informed that the MINS2 VAX, were FEDS had resided for 8 yr, was to be decommissioned due to operating costs. ED62 sought alternate platforms and recommended a pentium PC operating FoxPro. Transition from the VAX Oracle platform to PC FoxPro was initiated July 30, 1997. Programmers from ED62 and Computer Sciences Corporation (CSC) developed FoxPro FEDS and then converted the FEDS data from Oracle to FoxPro format. Accessibility to the MINS2 VAX terminated January 1998 with the transfer of FEDS to the PC platform. ED62, CSC, and ION continued development of FEDS through September 30, 1998. CSC responsibilities expired in September and were transferred to ION.

FEDS still stores data from all ECLSS testing performed since 1989 at MSFC, and has supported all test reports for ECLSS hardware produced since that time. FEDS has served as a powerful analysis tool for the ECLSS hardware design engineers. Other specific testing supported is described in table 61.

8.2 Analytical Laboratory Support

Analytical laboratory support was essential to perform MSFC's TTA's involving development testing of Space Station air and H_2O systems. Unique capabilities have been enhanced under NASA contract NAS8–50000, schedule F, and NAS8–38250 and NAS8–40369. Boeing provided test support for life testing, the IART, and stage 10 of the WRT.

Table 61. Testing supported by FEDS from 1996 to 1999.

Test	Stage	Description
ART	TCIT	Trace contaminant injection test—trace contaminant injection test of the THC CHX, the TCCS, and the CDRA at the system level.
LFT	SPE	Solid polymer electrolyze—life test of the SPE oxygen generator using archived water from WRT stages 9 and 10.
LFT	BIO	Biofilm life test—to assess the extent of microbial growth and biofilm formation in the *ISS* WRM system distribution lines and storage tanks.
LFT	MGC	Microbial growth chamber—assess the extent of microbial growth on the THC CHX. CHX performance assessed.
LFT	HCE	Humidity condensate evaluation—Evaluation of the condition of humidity condensate stored in the refrigerator for use in the Biofilm LFT or other tests.
LFT	VGP	VCD purge gas analysis—modify the VCD–VA life test to collect purge gas samples in support of a VCD flight experiment.
WRT	VFE	VRA flight experiment—functional test of the VRA flight experiment in conjunction with EMI, vibration, and toxicity tests in preparation for shuttle flight.
WRT	EGE	Ethylene glycol evaluation—evaluate the ability of the WP to remove ethylene glycol from wastewater. The ethylene glycol level is artificially high for evaluation purposes.
WRT	NUT	No-unibed test of WP—combine urine distillate and humidity condensate only. Process through prefilter, IRN–150 bed, VRA, IX bed, PCWQM, and then to the WP product tank.
WRT	S10	Stage 10—evaluation of the latest WRM system design for the USOS of the *ISS* for an extended duration in recipient mode.
WRT	UWP	WP with urine in feed—bench test of WP unibeds to determine if the WP can be used to process waste feed which includes pretreated urine.

Analysis and full characterization of H_2O and air samples for both organic and inorganic contaminants involves both standard environmental methods (EPA, Standard Methods, etc.). Unique methods developed by the Boeing Laboratory specifically for contaminants derived from human metabolic processes and equipment off-gassing are established by the MSFC's Analytical Control Test Plan and Microbiological Methods for Water Recovery Testing (ver. 3.2). High volume sampling, from several different simultaneous tests, requires analysis for numerous chemical and microbial parameters. Strict custody procedures and computerized sample and data management are in place to ensure and preserve sample identity, tractability, custody, tracking, and data reporting.

Boeing Analytical Services supported the IART and stage 10. Altran Materials Corporation supports chemical, microbial, scanning electron micrography assessments of the microbial growth chamber, and biofilm life tests. Specialized Assays, Inc. supported chemical evaluation of the SPE. The EET will utilize Specialized Assays, Inc.; Altran Materials, Corp.; and Wyle Laboratories for chemical and microbial analysis of the test's H_2O.

Lab analysis confirmed the acceptability of the facility tank H_2O for use by test subjects for hygiene purposes. To enhance Space Station waste inputs, the laboratories prepared ersatz to simulate animal condensate, equipment off-gassing contaminants, and CHeCS wastewater.

REFERENCES

1. Ray, C.D.; and Minton-Summers, S.: *International Space Station* ECLSS Technical Task Agreement Summary Report, *NASA TM 108508*, May 1996.

2. Space Station Processor Mostly Liquid Separator (MLS) Final Report, SVHSER 18272, Hamilton Standard, for Boeing Contract NAS8–50000–JC6104, July 30, 1997.

3. Hamilton Standard Process Pump Phase II, SVHSER 18280, Hamilton Standard, for Boeing Contract NAS8–50000–JC6104, July 31, 1997.

4. Gas/Liquid Separator Evaluation, HSPC 97T37, Hamilton Standard, for ION Corporation Contract NAS8–40369–4376, October 31, 1997.

5. *International Space Station* Water Processor Gas/Liquid Separator Item 8161 Phase I Trade Study Report, Hamilton Standard, for Ion Corporation Contract NAS8–40369–4376, May 15, 1998.

6. Particulate Filter Trade Study, (Draft), Michigan Technological University, for ION Corporation Contract NAS8–38250–4321, May 1998.

7. Final Test Report for Urine Pretreatment Study Phase III (UPS-III), SVHSER 18186, Hamilton Standard, for Boeing Contract NAS8–50000–JC6103, June 1997.

8. Final Test Report for Urine Pretreatment Injection System, SVHSER 17066, Rev. A, Hamilton Standard, for ION Corporation Contract NAS8–38250–28, August 1995.

9. Final Test Report for Urine Pretreatment Sulfuric Acid Injection Design Study Phase II (UPS–II), SVHSER 17575, Rev. A, Hamilton Standard, for Boeing Purchase Order JC6103 and NASA Contract NAS8–5000, June 1996.

10. Martin, C.E., ION Corporation; and Ogle K. MSFC: Assessment of Commercial and Aerospace Fan Technology for Application as Portable Air Movement Units on the *International Space Station*, Rev. 2, ION Corporation Contract NAS8–38250–28, March 5, 1997.

11. Pressurized Payloads Interface Requirements Document *International Space Station* Program, SSP 57000.

12. Design and Performance Specification Portable Fan Assembly for the *International Space Station*, MSFC–SPEC–2763, April 3, 1998.

13. *International Space Station* Portable Fan Assembly Interface Control Document, ICD–3–60073, April 3, 1998.

14. Sabatier Reactor Subsystem Final Report, SVHSER 19377, Hamilton Standard, for ION Corporation Contract NAS8–40369–4376, November 1998.

15. Oman, E.J.; Audeves, D.; Hand, D.W.; Huang, C.; Crittenden, J.C.; Hokanson, D.R.; and Rogers, T.N.: Development of the Volatile Reactor Assembly Model for the *International Space Station* Potable Water System Phase II Report, Michigan Technological University, for ION Corporation Contract NAS8–38250–3523, May 1998.

16. Hand, D.W.; Bulloch, J.L.; Hokanson, D.R.; Clancey, B.L.; and Crittenden, J.C.: Development of the Multifiltration Bed Model for the *International Space Station* Potable Water System—Phase I Report, Michigan Technological University, for ION Corporation Contract NAS8–38250–27, August 1995.

17. Perry, J.L.; Carrasquillo, R.L.; Franks, G.D.; Frederick, K.R.; Knox, J.C.; Long, D.A.; Ogle, K.Y.; and Parrish, K.J.: *International Space Station* Integrated Atmosphere Revitalization Subsystem Testing, NASA MSFC, Intersociety Conference on Environmental Systems (ICES) Paper 961519, July 1996.

18. Perry, J.L.; Franks, G.D.; and Knox, J.C.: *International Space Statio*n Program Phase III Integrated Atmosphere Revitalization Subsystem Test Final Report, NASA TM 108541, August 1997.

19. Tatara, J.D., ION Corporation; Perry, J.L. and Franks, G.D., NASA MSFC: Overview of the *International Space Station* System-Level Trace Contaminant Injection Test, ICES Paper 981665, July 1998.

20. Perry, J.L., MSFC; Curtis, R.E.; Alexandre, K.L.; Ruggiero, L.L.; and Sheets, N.: Boeing Defense and Space Group, Performance Testing of the Trace Contaminant Control Subassembly for the *International Space Station*, ICES Paper 981621, July 1998.

21. Alexandre, K.L.: Trace Contaminant Control Subassembly Performance Confirmation Test Preparation, Restoration, and Detailed Procedures, D495–51019–1, Boeing Defense and Space Group, Huntsville, AL, October 10, 1997.

22. Prime Item Development Specification for United States Laboratory, *International Space Station*, S683–29523D, Boeing Defense and Space Group, Huntsville, AL, 191, pp. 109–115, March 28, 1995.

23. Curtis, R.E., Boeing Defense and Space Group; Perry, J.L., MSFC; and Abramov, L.H., NIICHIMMASH, Performance Testing of a Russian *Mir Space Station* Trace Contaminant Control Assembly, ICES Paper 972267, July 1997.

24. Final Report: Test of the Russian Trace Contaminant Control System Filters, T495–51029–1, Boeing Contract NAS8–50055, June 1996.

25. Perry, J.L.; Carter, R.N.; Frederick, K.R., MSFC; and Tatara, J.D., ION Corporation: Performance Demonstration of a Metal Monolith Catalytic Converter for Trace Contaminant Control, NASA Test Report, November 1998.

26. Ray, C.D.; and Carrasquillo, R.L., MSFC; and Minton-Summers, S., ION Corporation: Summary of Current and Future MSFC *International Space Station* Environmental Control and Life Support System Activities, ICES Paper 972331, July 1997.

27. Carter, D.L.: Phase III Integrated Water Recovery Testing at MSFC: *International Space Station* Recipient Mode Test Results and Lessons Learned, ICES Paper 972375, July 1997.

28 Ray, C.D.; et al.: ICES Paper 972331, July 1997.

29. Callahan, D.; Chiu, C.; and Salyer, B.: Environmental Control and Life Support Systems Life Test Interim Report No. 14, ION Corporation Contract NAS8–40369, September 1998.

30. Callahan, D.; et al.: Environmental Control and Life Support Systems Life Test Interim Report No. 14, September 1998.

31. Wieland, P.; Hutchens, C.; Long, D., MSFC; and Salyer, B., ION Corporation: Final Report on Life Testing of the Vapor Compression Distillation/Urine Processing Assembly (VCD/UPA) at the Marshall Space Flight Center (1993 to 1997), NASA TM–1998–208539, August 1998.

REPORT DOCUMENTATION PAGE

Form Approved
OMB No. 0704-0188

1. AGENCY USE ONLY *(Leave Blank)*	2. REPORT DATE	3. REPORT TYPE AND DATES COVERED
	August 1999	Technical Memorandum

4. TITLE AND SUBTITLE

International Space Station ECLSS Technical Task Agreement Summary Report

5. FUNDING NUMBERS

6. AUTHORS

C.D. Ray and B.H. Salyer,* Compilers

7. PERFORMING ORGANIZATION NAMES(S) AND ADDRESS(ES)

George C. Marshall Space Flight Center
Marshall Space Flight Center, AL 35812

8. PERFORMING ORGANIZATION REPORT NUMBER

M–935

9. SPONSORING/MONITORING AGENCY NAME(S) AND ADDRESS(ES)

National Aeronautics and Space Administration
Washington, DC 20346–0001

10. SPONSORING/MONITORING AGENCY REPORT NUMBER

NASA/TM—1999–209573

11. SUPPLEMENTARY NOTES

Prepared by the Structures and Dynamics Laboratory, Science and Engineering Directorate
*ION Corporation

12a. DISTRIBUTION/AVAILABILITY STATEMENT

Unclassified-Unlimited
Subject Category 54
Nonstandard Distribution

12b. DISTRIBUTION CODE

13. ABSTRACT *(Maximum 200 words)*

This Technical Memorandum provides a summary of current work accomplished under Technical Task Agreement (TTA) by the Marshall Space Flight Center (MSFC) regarding the *International Space Station* (*ISS*) Environmental Control and Life Support System (ECLSS). Current activities include ECLSS component design and development, computer model development, subsystem/integrated system testing, life testing, and general test support provided to the *ISS* program.

Under ECLSS design, MSFC was responsible for the six major ECLSS functions, specifications and standard, component design and development, and was the architectural control agent for the *ISS* ECLSS. MSFC was responsible for ECLSS analytical model development. In-house subsystem and system level analysis and testing were conducted in support of the design process, including testing air revitalization, water reclamation and management hardware, and certain nonregenerative systems.

The activities described herein were approved in task agreements between MSFC and NASA Headquarters Space Station Program Management Office and their prime contractor for the ISS, Boeing. These MSFC activities are in-line to the designing, development, testing, and flight of ECLSS equipment planned by Boeing. MSFC's unique capabilities for performing integrated systems testing and analyses, and its ability to perform some tasks cheaper and faster to support *ISS* program needs, are the basis for the TTA activities.

14. SUBJECT TERMS

Space Station, environmental control, life support, technical task agreement, MSFC

15. NUMBER OF PAGES

198

16. PRICE CODE

A09

17. SECURITY CLASSIFICATION OF REPORT	18. SECURITY CLASSIFICATION OF THIS PAGE	19. SECURITY CLASSIFICATION OF ABSTRACT	20. LIMITATION OF ABSTRACT
Unclassified	Unclassified	Unclassified	Unlimited